UNIVERSIDAD NACIONAL AUTÓNOMA DE MÉXICO

PROGRAMA DE DOCTORADO EN CIENCIAS BIOMÉDICAS

INSTITUTO DE INVESTIGACIONES BIOMÉDICAS

IDENTIFICACIÓN DE NUEVOS FACTORES DE RIESGO PARA EL CÁNCER DE MAMA: LA INFECCIÓN POR *Toxocara canis* INCREMENTA EL TAMAÑO DEL TUMOR E INDUCE MAYOR METÁSTASIS EN UN MODELO MURINO

TESIS

QUE PARA OPTAR POR EL GRADO DE:

DOCTORA EN CIENCIAS

PRESENTA:

ROCÍO ALEJANDRA RUIZ MANZANO

TUTOR PRINCIPAL:

DR. JORGE MORALES MONTOR

INSTITUTO DE INVESTIGACIONES BIOMÉDICAS U.N.A.M.

COMITÉ TUTOR:

DR. PEDRO ULISES OSTOA SALOMA

INSTITUTO DE INVESTIGACIONES BIOMÉDICAS U.N.A.M.

DRA. SAMIRA MUÑOZ

UNIDAD DE INVESTIGACIÓN MÉDICA EN ENFERMEDADES INFECCIOSAS Y PARASITARIAS, I.M.S.S.

CIUDAD DE MÉXICO, SEPTIEMBRE, 2020

Agradecimientos Académicos

A la Universidad Nacional Autónoma de México, por permitir el desarrollo de mis estudios superiores.

Al Instituto de Investigaciones Biomédicas y al Programa de Doctorado en Ciencias Biomédicas.

Al Consejo Nacional de Ciencia y Desarrollo (CONACYT), por otorgarme la beca No. 421443 para la realización de este trabajo de Doctorado.

Al Dr. Jorge Morales Montor, por aceptarme para trabajar en su laboratorio, por todo el conocimiento que me compartió, por ser mentor y guía en este proceso. Por permitirme el desarrollo de diferentes trabajos en el laboratorio. Gracias.

A mi comité tutoral, Dr. Pedro Ostoa Saloma y Dra. Samira Muñoz.

Al jurado para examen de grado, por el tiempo que tomaron para la revisión y evaluación de este trabajo: Dr. Luis Ignacio Terrazas Valdés, Dr. Ezequiel Fuentes Pananá, Dr. Pedro Ostoa Saloma, Dra. Rocío Ángeles García Becerra, Dr. Armando Pérez Torres,

A la Dra. Karen Nava Castro, por su apoyo y guía técnica en las técnicas de cultivo celular primario (esplenocitos).

A la Dra. Magarita Isabel Palacios Arreola, por ensañarme algunos de los procedimientos técnicos realizados en esta Tesis (cultivo de células 4T1, inoculación de tumores, citometría de flujo).

A la Dra. Mariana Segovia Mendoza, por su asesoría técnica en el cultivo *in vitro* para la evaluación de la proliferación de células.

Al M. en C. Pablo Martínez Labat por proveer una parte de los huevos de *Toxocara canis* utilizados en este trabajo de Tesis.

A Azucena Pichardo por su paciencia y su atención. Sin ti no hubiera sido posible todo este proceso de entrada, permanencia y titulación. Gracias y más gracias por ser una persona tan amable, educada y atenta.

Al M. en C. Esteban Santacruz Martínez, por su asesoría en la estadística y técnicas realizadas en este trabajo.

Agradecimientos personales

A mi mamá y a mi papá, por ser mi soporte y ejemplo, por creer siempre en mí y por quererme como soy.

A Esteban, mi compañero en una buena parte de esta travesía. Gracias por todo el apoyo, el cariño, la comprensión, por tus atenciones y cuidados. "Detrás de un gran hombre, hay una gran mujer".

A mis compañeras(os) de laboratorio, por hacer este proceso llevadero y divertido además de formativo y por su ayuda en los procesos del laboratorio. Gracias Marisa, Rosalía, Tania, Víctor, Nashla, Ricardo, Mariana, Carmen, Chintia, Salvador, Lucio.

A todos los que de manera directa o indirecta colaboraron para que esto se hiciera realidad (Laura Soto, Aaron Rodríguez, Génesis Dehesa, Mariana Ruiz, Gonzalo Mendoza).

Dedicatorias

A Nicolás. Por ser lo más perfecto que hay. Por ser el futuro. Porque te amo con todo mi corazón hoy y siempre.

A María del Carmen Manzano Licea y Mariano Ruiz Aguirre, por todo el amor.

A Mariana Ruiz Manzano y Mariano Ruiz Manzano, por ser mis hermanos favoritos.

A Ximena Mendoza Ruiz, por ser mi sobrina favorita, la más lista y hermosa.

A Lourdes Ruiz Aguirre, José Guadalupe Serdán Delgado, Ximena Serdán Ruiz y Alba Serdán Ruiz, por adoptarme y quererme. Ahrr, ahrr.

A Esteban Santacruz Ruiz Martínez, por el cariño, por la vida juntos.

A mis amiguis, Miriam Hernández y Rogelio Azcárraga.

Índice

Índice de tablas

Índice de figuras

Resumen

A nivel mundial el cáncer de mama es el más importante en incidencia y prevalencia en mujeres. Diferentes factores de riesgo interactúan para incrementar la probabilidad de desarrollar cáncer de mama. Contaminantes ambientales biológicos como los agentes infecciosos, juegan un papel significativo en el desarrollo de tumores y los helmintos han sido reconocidos como inductores o promotores del cáncer, debido a su habilidad de regular la respuesta inmune del hospedero. *Toxocara canis* es un nematodo zoonótico y cosmopolita, con habilidades inmuno-reguladoras. La infección por *T. canis* ha sido relacionada con la presencia de linfocitos T (LT) cooperadores $CD4^+$ (Th2 o Tipo 2) y células T reguladoras (Treg). Las respuestas Tipo 2 y reguladora, pueden favorecer el desarrollo de comorbilidades que usualmente son controladas o eliminadas a través de una respuesta Tipo 1, como el cáncer. Si la infección por *T. canis* puede afectar el crecimiento de tumores mamarios aun no es conocida. Entonces, el primer objetivo de este estudio fue evaluar los diferentes componentes de la respuesta inmune sistémica del hospedero a la infección por *T. canis* y el segundo objetivo fue determinar si estos cambios pueden alterar el crecimiento tumoral a través de la modulación de la respuesta inmune. En los ratones infectados crónicamente con *T. canis* se confirmó una respuesta Tipo 2, caracterizada por niveles elevados de IgGs específicas, un incremento en el porcentaje de $CD4^+Foxp3^+$, linfocitos B $CD19^+$, macrófagos $F4/80^+$ esplénicos, y un aumento sistémico de IL-4, IL-10 y VEGF. De modo importante, los ratones infectados desarrollaron tumores más grandes. El análisis del microambiente tumoral inmune reveló que la infección redujo la proporción de linfocitos $TCD8^+$, e incrementó el porcentaje de macrófagos $F4/80^+$ y linfocitos B $CD19^+$, esto acompañado de una respuesta local Tipo 2 representada por el aumento en la cantidad de IL-4, VEGF y un microambiente regulador asociado al incremento en la expresión de IL-10. Por lo tanto, estos hallazgos mostraron que la infección por *T. canis* promueve la progresión del tumor y el desarrollo de éste a través de la modulación del microambiente tumoral inmune.

Abstract

Worldwide, breast cancer is the most important type of cancer in regard to incidence and prevalence in the woman. Several risk factors interact to increase the probability of breast cancer development. Biological environmental contaminants such as infectious agents play a significant role in tumor development and helminths have been recognized as cancer enhancers or inducers due to their ability to regulate the host immune response. *Toxocara canis* is a zoonotic and cosmopolite nematode, with immuno-regulatory abilities. *T. canis* infection has been related to a T helper type-2 cell (Th2 or Type 2) and regulatory response. Type 2 and regulatory immune responses may favor the development of comorbidities that are usually controlled or eliminated through a Type 1 response, such as cancer. Whether *T. canis* infection affects mammary tumor growth is not yet known. The first aim of this study was to evaluate different components of the systemic host immune response to *T. canis* infection, and the second aim was to determine if these changes may alter mammary tumor growth through modulation of the immune response. A Type 2 response was confirmed in chronic *T. canis* infected mice characterized by elevated levels of specific IgGs, an increase in the proportions of splenic $CD4^+Foxp3^+$, $CD19^+$ B lymphocyte, $F4/80^+$ macrophages, and higher levels of systemic IL-4, IL-10 and VEGF. Importantly, infected mice developed larger tumors. Tumor immune cell milieu analysis revealed that infection correlated with reduced infiltration of $CD8^+$ lymphocytes, increased $F4/80^+$ macrophages, and $CD19^+$ B cells proportions, accompanied by a Type 2 local response represented by increased amounts of IL-4, VEGF, and a regulatory microenvironment associated to higher IL-10 levels. Thus, study supports that *T. canis* infection enhances tumor development and suggests that this is done through the modulation of tumor immune microenvironment.

Abreviaturas empleadas

Breg: Linfocitos B reguladores.

CDc: Células Dendríticas Convencionales.

CDIS: Carcinoma Ductal *In Situ*.

CDt1: Células Dendríticas tipo 1.

CDt2: Células Dendríticas tipo 2.

DE: Desviación Estándar

d.p.i.: días post-inoculación.

ELISA: ensayo por inmunoabsorción ligado a enzimas (Enzyme-Linked Immunosorbent Assay).

FMO: fluorescencia menos uno (Fluoresce Minus One).

GLP: Ganglios Linfáticos Periféricos.

g: gravedades.

h: hora(s).

HL: Huevo Larvado.

HRP: peroxidasa de rábano (horse radish peroxidase).

IARC.: Agencia Internacional para la Investigación en Cáncer (International Agency for Research on Cancer).

IFN-γ: interferón gamma.

IL: Interleucina.

INEGI:

LT: Linfocitos T.

LB: Linfocitos B.

L1, L2, L3: Larva 1, Larva 2, Larva 3.

MAA: Macrófagos Activados Alternativamente.

MAT: Macrófagos Asociados a Tumor.

min: minutos.

NK: asesina natural (Natural Killer).

OMS: Organización Mundial de la Salud.

PBS: Solución buffer de fosfatos (Phosphates Buffer Solution).

RPMI: medio Roswell Park Memorial Institute (Roswell Park Memorial Institute medium).

SFB: Suero Fetal Bovino.

SSI: Solución Salina Isotónica.

TES: Productos/antígenos de excreción y secreción de *Toxocara canis* (*Toxocara* Excretory-Secretory products/antígens).

TGF-β : Factor de crecimiento transformante beta (Transforming Growth Factor-beta).

TNF-α: Factor de necrosis tumoral alfa (Tumor Necrosis Factor-alpha).

TNBC: Cáncer de mama triple negativo (Triple Negative Breast Cancer).

Th: Linfocitos T cooperadores (T helper).

Treg: Linfocitos T reguladores.

VEGF: Factor de crecimiento vascular endotelial (Vascular Endothelial Growth Factor).

I. ANTECENDENTES

1.1 Cáncer de mama

El cáncer es una de las principales causas de mortalidad a nivel mundial y es considerado un problema de salud pública. También, es el más importante en términos de incidencia y prevalencia en mujeres, además de que es el de mayor incidencia en mujeres en 154 países (GLOBOCAN IARC, 2018). El cáncer mamario en el hombre, representa aproximadamente el 0.5% del total de los casos de cáncer de mama (Edge and Compton, 2010). Se estima que 1 de cada 8 mujeres desarrollará cáncer de mama durante el curso de su vida (Jemal et al., 2009).

En México, el cáncer de mama es la primera causa de cáncer en mujeres. En el año 2018 la Organización Mundial de la Salud (O.M.S.) reportó 27,283 casos nuevos en mujeres y 6,884 muertes relacionadas (GLOBOCAN IARC, 2018). La incidencia de tumor maligno de mama en mujeres, ha ido en aumento en los últimos años (INEGI, 2015). Además de esta alta incidencia, en 2018 se presentaron 83,287 casos de prevalencia del cáncer de mama (GLOBOCAN IARC, 2018).

En la progresión del cáncer hay tres fases: benigna, no invasiva e invasiva. Por definición, en la fase benigna y la no invasiva las células transformadas no traspasan la membrana basal, pero estas etapas están diferenciadas por el grado histológico (Giuliano et al., 2017). En el cáncer invasivo, las células tumorales migran a través de la membrana basal al tejido aledaño y a otros órganos en la etapa de metástasis (Hanahan and Coussens, 2012).

1.1.1 Respuesta inmune en cáncer de mama

Las células inmunes detectan y destruyen células transformadas en un fenómeno llamado inmunovigilancia (Fig. 1.1). El tumor también puede permanecer en un estado de dormancia (inmunoequilibrio), debido de manera importante por el control

de las células inmunes y la inmunovigilancia (Fig. 1.2). Pero, cuando las células transformadas evaden los mecanismos de eliminación (inmunoescape), sobreviven y proliferan. En el microambiente tumoral interactúan células no neoplásicas (fibroblastos, células endoteliales, mesenquimales, de la respuesta inmune innata y adaptativa), con células tumorales para formar un microambiente tumoral dinámico. Cuando el balance entre las interacciones entre las células estromales, inmunes y tumorales, con sus productos de secreción lleva a una "inmunosupresión" local, las células no neoplásicas adquieren un fenotipo y actividad "pro-tumoral" (Fig 1.3) se establece y el tumor se desarrolla (Emens et al., 2012; Zitvogel et al., 2006).

En la inmunovigilancia (Fig. 1.1), los antígenos de las células transformadas son reconocidos por células dendríticas convencionales (CDc), que los presentan en los órganos linfoides secundarios como el bazo y los ganglios linfáticos periféricos (GLP) a células T *naïve* (Fig. 1.1.A) (Gardner and Ruffell, 2016; Mellman and Steinman, 2001; Steinman et al., 1999). Las células dendríticas tipo 1 (CDt1) presentan antígenos a través de MHC-I preferencialmente a linfocitos T (LT) $CD8^+$ citotóxicos, mientras que las CD tipo 2 (CDt2) lo hacen con el MHC-II a LT $CD4^+$ cooperadores (Fig. 1.1.B) (Gardner and Ruffell, 2016). Después de su activación, estos LT migran al sitio donde está la célula transformada, donde los LT $CD4^+$ secretan citocinas que ayudan a los linfocitos $CD8^+$con sus funciones citotóxicas (Fig. 1.1.D). Además, los LT $CD4^+$ en los órganos linfoides secundarios, activan a linfocitos B (LB) que proliferan y eventualmente se transforman en células plasmáticas productoras de anticuerpos específicos (Fig. 1.1.C) (Chen and Mellman, 2013; Palacios-Arreola et al., 2014; Zitvogel et al., 2006)

En la fase de equilibrio (Fig. 1.2), las células epiteliales transformadas que evadieron el reconocimiento inmune, proliferaron y se desarrollaron como un tumor benigno que eventualmente puede evolucionar como carcinoma ductal *in situ* (CDIS) (Fig. 1.2. A, B). Esta es la fase menos estudiada y suele pasar desapercibida. En estas fases células inmunes son reclutadas, entre ellas las NK, los LT $CD8^+$, neutrófilos, eosinófilos, macrófagos y mastocitos, que por sus características citotóxicas pueden reconocer y eliminar células transformadas limitando su proliferación (Zitvogel et al., 2006).

Cuando las células tumorales han evadido el reconocimiento inmune, se establece recambio de poblaciones inmunes en el estroma del tumor, con subtipo nuevos y otros cambiando a subtipo con funciónes inmunosupresoras y pro-tumorales (Fig. 1.3) (Zitvogel et al., 2006). Dentro de los cambios que pueden presentarse están las CDt2, que fallan en la presentación de antígenos tumorales, probablemente por el procesamiento inadecuado de los antígenos asociado a la naturaleza de estos. Estas CDt2 pueden ser tolerogénicas, al no generar una adecuada activación y estimulación (Gardner and Ruffell, 2016).

Como la mayoría de las poblaciones celulares inmunes en el inicio del desarrollo tumoral los macrófagos favorecen la eliminación de células transformadas, pero inmersos en el microambiente tumoral como macrófagos asociados a tumor (MAT), pueden adquirir características que favorecen el desarrollo tumoral. La presencia de una mayor cantidad de MAT en tumores de mama está asociada a un pronóstico reservado (Zhao et al., 2017). Así, dependiendo del microambiente que rodea a los macrófagos, éstos adquieren diferentes fenotipos específicos y en los tumores los MATs activos poseen características similares a los macrófagos activados alternativamente (MAA) o M2, pero estudios recientes mencionan que los MATs pueden tener características de M2, pero también de macrófagos activados de modo clásico (MAC) o M1 (Zhou et al., 2020). En general estos MATs tienen efectos en la angiogénesis, la invasión tumoral y la regulación de la respuesta inmune (Zhou et al., 2020).

Los MAA producen IL-4, IL-10, IL-13, TGF-β y VEGF (Fig. 1.3), expresan arginasa-1 y se han relacionado con la cicatrización de heridas y la respuesta humoral, lo que colabora con la inducción de la respuesta tipo Th2 y reguladora e inhibe la citotóxica mediada por la tipo Th1 (Qian and Pollard, 2010; Zhao et al., 2017). Mientras que se ha visto que los MAT producen IL-6, IL-8 e IL-10 y pueden expresar CD169 y TCR (Zhou et al., 2020).

Uno de los factores secretados por los MAA es el VEGF, cuya importancia radica en la inducción de angiogénesis (Fig. 1.3). El proceso angiogénico se ha vinculado a la propagación de nuevos vasos sanguíneos para incrementar la aportación de oxígeno y nutrientes al tumor, lo que permite la proliferación de las células tumorales. Por lo anterior, se han buscado terapias blanco encaminadas al bloqueo de la acción del VEGF, como una estrategia para limitar el aporte de nutrientes al tumor (Alameddine et al., 2013). Así, el anticuerpo monoclonal Bevacizumab ha sido empleado en el tratamiento de cáncer de mama (Aalders et al., 2017). Lo anterior respaldado en el hallazgo de niveles elevados de VEGF en los tumores mamarios triple negativos (TNBCs), que se correlaciona con peor pronóstico, recurrencia y supervivencia de los pacientes (Linderholm et al., 2009).

Otra subpoblación reguladora implicada en el desarrollo de cáncer son los linfocitos B reguladores (Breg). Dentro de los mecanismos de regulación de estas células en el tumor se ha observado que el co-cultivo de Breg purificados de tumor mamario suprime la proliferación de $CD4^+$, $CD8^+$ o células NK (Zhang et al., 2016). Además, las Breg en el tumor pueden inducir la formación de MAT y con ello contribuir a la supresión de la respuesta antitumoral (Schwartz et al., 2016). Otra característica reguladora de los Bregs es la secreción de IL-10 (Shen et al., 2014). Esta interleucina suprime las respuestas tipo Th1 y Th17, al mismo tiempo que promueve las respuestas Th2 y Treg e inhibe la liberación de citocinas proinflamatorias por los macrófagos (Carter et al., 2012).

Además de las células Breg, otra subpoblación celular que produce IL-10 son las Treg, en las cuales esta interleucina tiene funciones paracrinas y autócrinas, ya que junto con TGF-β induce la generación de Treg y tiene un efecto en células adyacentes, como los LT $CD8^+$, en quienes suprimen sus funciones efectoras (Fig. 1.3) (Jarnicki et al., 2014). En cuanto a cáncer de mama se ha observado una correlación entre grandes cantidades de Tregs infiltrados y un peor grado del tumor y pronóstico de alto riesgo y recaída tardía (Bates et al., 2006; Gao et al., 2014).

En resumen, el desarrollo tumoral estimula una respuesta inmune dependiente del grado del progreso de la enfermedad. En las fases tempranas la respuesta citotóxica controla la proliferación de las células transformadas, pero en las fases de inmunosubversión el microambiente tumoral induce un fenotipo regulador en las subpoblaciones de células inmunes en el tumor. Entonces, la progresión y crecimiento del tumor va de la mano con el fenotipo de las células inmunes y en los factores solubles que producen, en una interacción multidireccional con los elementos que conforman el tumor.

1.1.2 Factores de riesgo asociados a cáncer de mama

Hay muchos factores de riesgo asociados al desarrollo de tumores de mama. El primero y más importante es el sexo, las mujeres adquieren mucho más la enfermedad que los hombres. Otros factores de riesgo son una menarca temprana, primer parto después de los 30 años de edad, menopausia tardía, nuliparidad, sobrepeso u obesidad, historia personal o familiar de cáncer de mama, alcoholismo, fumar, el tratamiento de reemplazo hormonal en la menopausia y el uso de anticonceptivos hormonales (Barnard et al., 2015; Esquivel-Velázquez et al., 2015; Palacios-Arreola et al., 2017).

A pesar de los factores de riesgo antes mencionados, en la mayoría de las mujeres con cáncer de mama no es posible identificar factores de riesgo específicos (IARC, 2008). Por lo que es preciso tomar en cuenta a factores de riesgo relacionados con el ambiente, por ejemplo los contaminantes ambientales químicos, físicos y biológicos. Dentro de los estos últimos están los agentes infecciosos que incluyen virus, hongos, bacterias y parásitos.

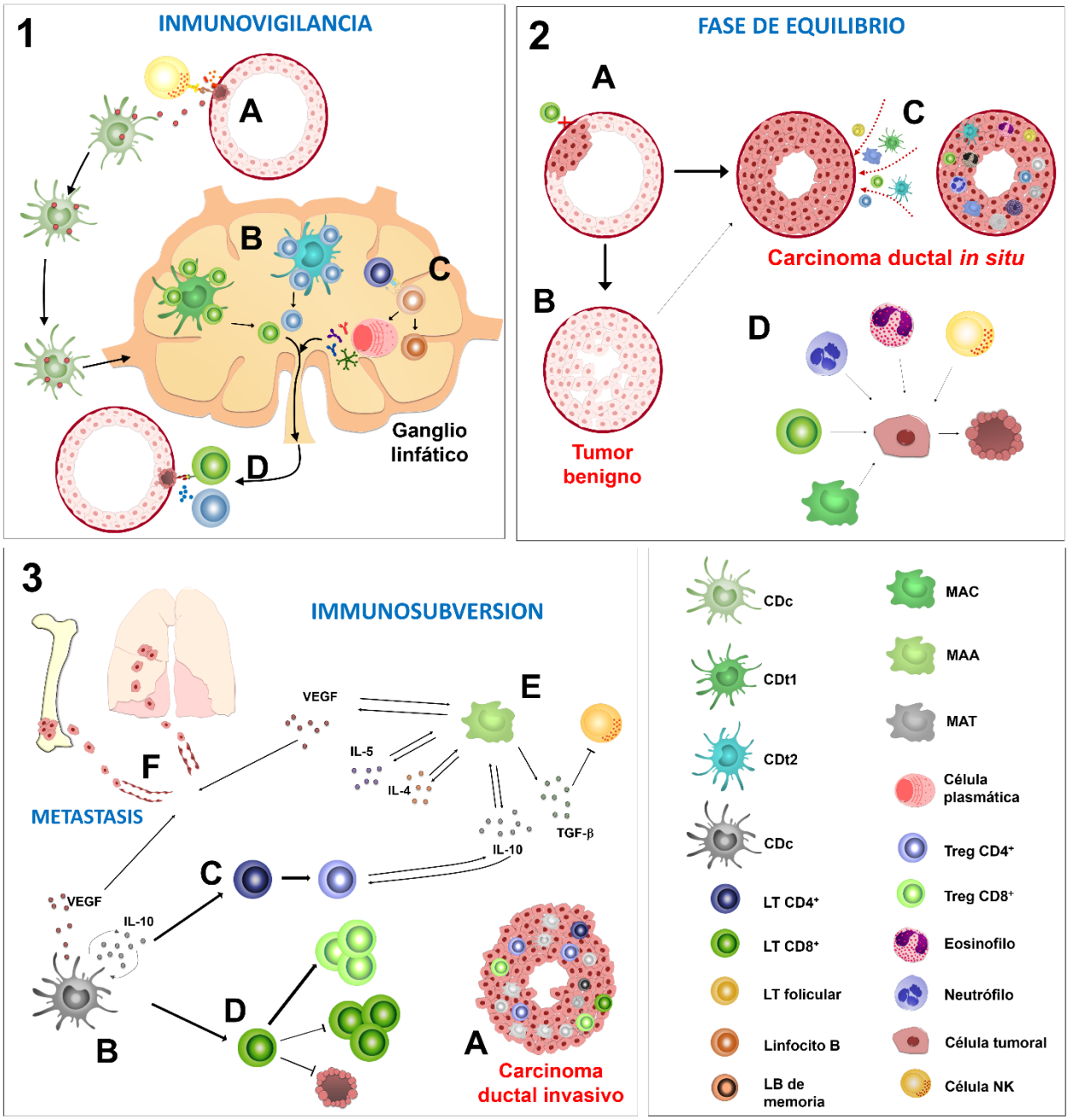

Figura 1. Respuesta inmune en el desarrollo del tumor mamario. 1. *Inmunovigilancia.* **A.** Las células dendríticas (CD) convencionales (CDc) en el tejido mamario, capturan antígenos de las células transformadas destruidas por células NK. Las CDc migran a los ganglios linfáticos periféricos (GLP). **B.** Las CD tipo 1 (CDt1) presentan antígenos a linfocitos T (LT) $CD8^+$, y las tipo 2 (CDt2) a LT $CD4^+$. **C.** En los GLP los LT foliculares activan linfocitos B (LB) que proliferan y se diferencian en células plasmáticas o LB de memoria. **D.** Los LT $CD8^+$ y los $CD4^+$ activados migran al tejido mamario donde se encuentran células transformadas y las destruyen. **2. *Fase de eliminación y equilibrio*. A.** Las células

transformadas evaden el reconocimiento inmune. **B.** Se da la proliferación de estas células e inicia el desarrollo de un tumor benigno. **C.** Se desarrolla el Carcinoma ductal *in situ* (CDIS). **D.** En la fase de equilibrio los LT $CD8^+$, neutrófilos, eosinófilos, macrófagos, células NK pueden destruir células tumorales controlando la proliferación y crecimiento tumoral **3. *Inmunosubversión y metástasis*. A.** Cuando se establece el carcinoma ductal invasivo, las CD se pueden convertir en reguladoras (CDr) productoras de IL-10. **B.** La IL-10 induce la generación de más CDrs y la expansión de LT reguladores (Treg) $CD4^+$ (**C**) y $CD8^+$ (**D**), inhibe la proliferación de LT $CD8^+$ (**E**) y sus funciones citotóxicas (**F**). **G.** Los MAA también producen IL-10 y (**H)** TGF-β (que inhibe las funciones citotóxicas de las células NK), IL-4 e IL-5. **I.** El VEGF producido por los MAA favorece la angiogénesis y la metástasis a GLP, pulmón y hueso.

1.1.3 Parásitos como factores de riesgo para el desarrollo de cáncer

Aunque los agentes biológicos son ubicuos, la relación entre la presencia de estos y el desarrollo de diferentes tipos de cáncer ha sido medianamente abordada, a pesar de que se ha reportado que el 15% de los diferentes tipos de cáncer están ligados a infecciones por virus, bacterias o parásitos (Plummer et al., 2016). Los agentes infecciosos de importancia médica, implican un problema de salud no solo por su impacto al inducir enfermedad, sino porque se han asociado con el cáncer debido a la activación de los procesos inmunológicos en su hospedero. Existe evidencia de que agentes patógenos o componentes de los mismos pueden tener una función pro-cancerígenica. Por ejemplo, la bacteria *Helicobacter pylori*, puede inducir cáncer gástrico (Botelho et al., 2013).

Entre los parásitos asociados al cáncer, los helmintos juegan un papel importante en el progreso tumoral, debido a su habilidad de modificar la respuesta inmune del hospedero y su ubiquidad en el ambiente. Diferentes trematodos son descritos como carcinogénicos para el cáncer de vejiga (*Schistosoma haematobium*) y colangiosarcoma (*Chlonorchis sinensis* y *Opisthorchis viverrini*) (Botelho et al., 2013; Machicado and Marcos, 2016).

En ese sentido, se han descrito diferentes mecanismos por los cuales los helmintos promueven el crecimiento tumoral. La mayoría asociados a infecciones crónicas, que estos parásitos suelen producir y que están mediadas por sus productos de excreción y secreción (ES). La inflamación crónica conduce a inestabilidad y mutaciones genómicas, regulación a la baja de genes supresores, inhibición de la apoptosis y modulación de la respuesta inmune, por lo que puede beneficiar la progresión de tumores (Botelho et al., 2013; Machicado and Marcos, 2016).

En relación al desarrollo de tumores y la co-infección con parásitos, ya se ha documentado el efecto *in situ* del nematodo murino *Heligmosomoides polygyrus* en el desarrollo de tumores colorectales, asociado a la expansión de células Treg en el colon y ganglios linfáticos mesentérico (Pastille et al., 2017).

La importancia de la infección por helmintos está relacionada no solo con las funciones reguladoras de éstos, sino con su ubiquidad y distribución geográfica. Un nematodo que posee características inmunomoduladoras, infecta a humanos y otros hospederos a nivel mundial es *Toxocara canis* (Maizels, 2013).

1.2 *Toxocara canis*

La infección por *Toxocara canis* (Werner, 1982) es una enfermedad cosmopolita, zoonótica y desatendida. Los cánidos domésticos y silvestres, incluyendo a los perros, son sus hospederos definitivos, afectando principalmente a cachorros menores de 3 meses debido a la transmisión perinatal (Archielli and Kozubsky, 2008; Magnaval et al., 2001).

La frecuencia de *T. canis* en perros puede ser tan alta como el 100%, especialmente en cachorros, aunque varía dependiendo del lugar donde se realizó el estudio, la técnica diagnóstica y el tamaño de la muestra (Ma et al., 2018). La alta frecuencia de las fases adultas en los canidos está asociado con un potencial riesgo de exposición para los hospederos, principalmente en lugares donde hay poblaciones

de perros no controladas, como perros callejeros o ferales, o bien cánidos de vida libre.

1.2.1 Ciclo biológico

Toxocara spp. presenta un ciclo biológico directo (Webster 1958), en el que la hembra adulta oviposita en el intestino delgado del cánido y consecuentemente los huevos salen en heces (Schantz and Glickman, 1983; Schnieder et al., 2011). La larva se desarrolla dentro del huevo y la rapidez de este desarrollo depende de las condiciones del medio. En un ambiente con una humedad relativa del 85-95% (Schnieder et al., 2011) temperatura de 15-30°C (Azam et al., 2012), la larva 1 (L1) aparece a los 6 días y la larva 2 (L2) al 12º día aproximadamente (Webster, 1958). Un punto de discusión es la etapa larvaria en la que *T. canis* se convierte en infectante. De un modo clásico, se menciona a la L2 como la infectante (Webster, 1958), pero diferentes autores reportan dos mudas dentro del huevo y consideran a la larva tres (L3) como la fase infectante (Bruñaská et al., 1995; Schantz and Glickman, 1983), pero no hay un consenso en este sentido, por lo que en este texto se mencionará a la fase infectante como el huevo larvado (HL), sin hacer mención al estado larvario que contiene (Fig. 2).

1.2.1.1 Hospederos definitivos

Los perros adultos se infectan por consumo de HL, de larvas en tejidos o en la etapa perinatal. Además se han reportado que perras que ingirieron larvas del cuarto o quinto estadio de desarrollo en heces o vómito de sus cachorros pueden desarrollar parásitos adultos intestinales (Schantz and Glickman, 1983). Las fases adultas intestinales también se pueden desarrollar si el canido consumió tejidos de hospederos infectados con larvas encapsuladas, que son liberadas en el aparato digestivo (Overgaauw, 1997).

Los cachorros se infectan vía transplacentaria (intrauterina) (Schantz and Glickman, 1983) y vía lactogénica (transmamaria) por calostro y/o leche (Burke and Roberson,

1985) (Fig 2). Si las larvas fueron transmitidas vía transplacentaria, atraviesan el sincitio trofoblasto, llegan al hígado y pulmones fetales, donde permanecen hasta el nacimiento. Entonces, migran a intestino y se convierten en adultos. En la transmisión lactogénica, las larvas que vía sanguínea llegaron a la glándula mamaria de la madre llegan al calostro y/o leche (Schnieder et al., 2011; Webster, 1958), el cachorro las ingiere y en el intestino delgado se desarrollan a adultos (Fig. 2) (Burke and Roberson, 1985).

Si la infección es debida a la ingestión de HL, las larvas se liberan en el tracto digestivo y ayudadas por proteasas (Robertson et al., 1989) atraviesan la pared intestinal y migran al hígado por capilares venosos. En el parénquima hepático llegan a la vena cava, donde son transportadas y llegan a la aurícula y ventrículo derecho cardiacos, posteriormente van a arteria pulmonar y capilares arteriales por donde llegan a los alveolos pulmonares (Schnieder et al., 2011; Webster, 1958). En el pulmón las larvas pueden atravesar los alveolos y dirigirse cranealmente hacia los bronquiolos, bronquios y tráquea, pasar al tracto digestivo para terminar su desarrollo como nematodos adultos intestinales (Webster, 1958). Esto pasa comúnmente en cachorros, pero en perros adultos, sobre todo las hembras lo común es que continúen una migración somática (*larva migrans*), donde las larvas alcanzan capilares venosos pulmonares y vía vena pulmonar regresan al corazón izquierdo, donde impulsadas por el ventrículo se distribuyen en diferentes órganos a través de la aorta (Schnieder et al., 2011; Webster, 1958).

1.2.1.2 Hospederos paraténicos

Los hospederos no cánidos que son infectados por larvas de *T. canis*, son los hospederos paraténicos. Pueden ser vertebrados (humanos, bovinos, ovinos, ratones, ratas, conejos, aves, cerdos, etc.) o invertebrados (moscas, cucarachas, etc.) (de Oliveira et al., 2002; González-García et al., 2017; Lopes Rassier et al., 2013; Strube et al., 2013). En los hospederos paraténicos la larva no se desarrolla a adulto, por lo que estos no son indispensables para que el ciclo biológico se complete, pero facilitan la

infección, debido a que *T. canis* puede infectar a otros hospederos mediante canibalismo o depredación, (Schnieder et al., 2011; Taira et al., 2003).

En los hospederos paraténicos se desarrolla la migración somática o *larva migrans* antes descrita para los cánidos (Strube et al., 2013), por lo que las larvas pueden encontrarse en tejidos como el hígado, pulmones, riñones, músculo esquelético corazón, ojos y cerebro (Fig. 3). Debido a la respuesta inmune que estimulan, se forman granulomas eosinofílicos que encapsulan a las larvas en estos diferentes tejidos (Archielli and Kozubsky, 2008; Magnaval et al., 2001; Schnieder et al., 2011).

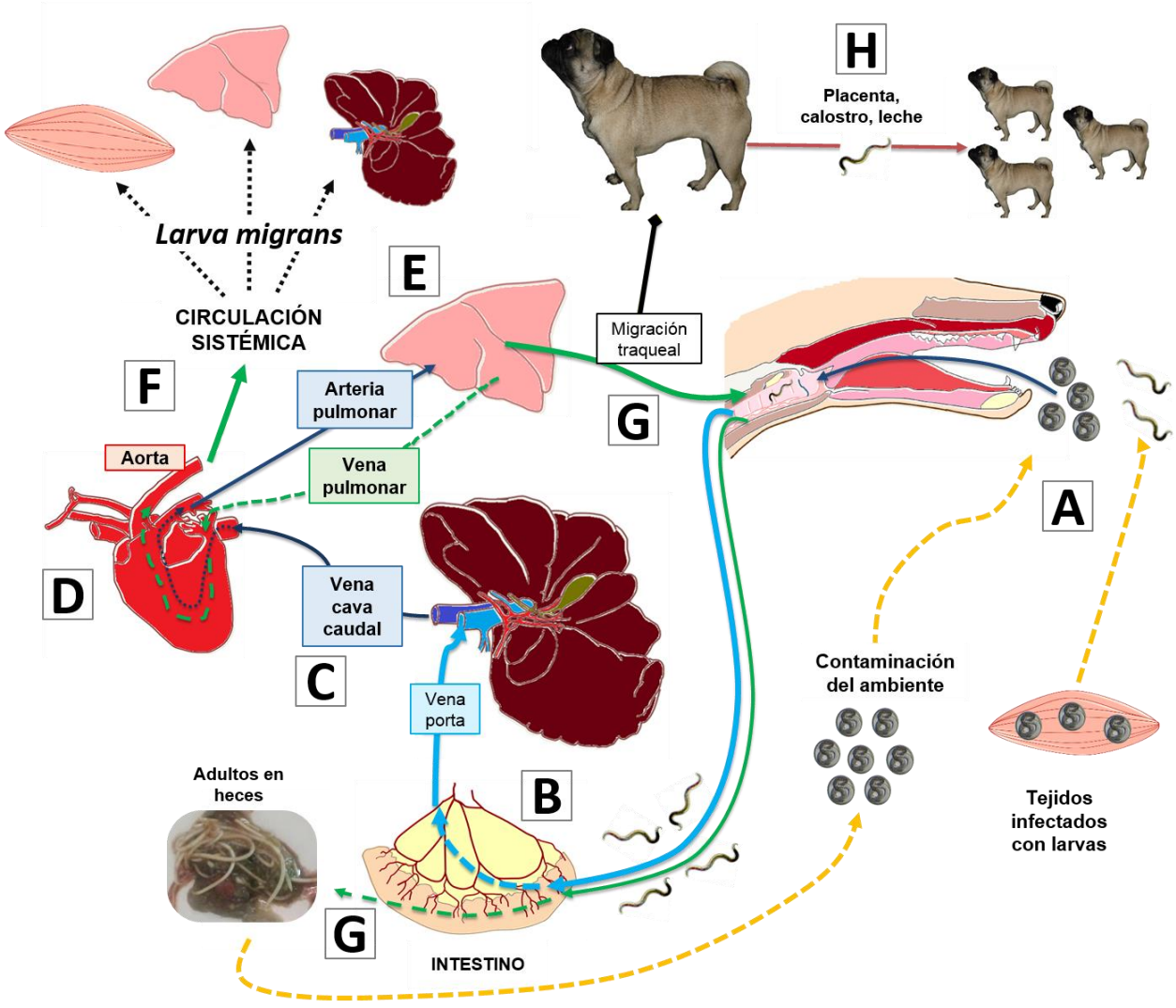

Figura 2. Ciclo biológico del *T. canis* en el hospedero definitivo. A. Infección vía oral por la ingestión de huevos larvados o tejidos con larvas. Después de la liberación de

las larvas en el tracto digestivo llegan al intestino. **B.** Las larvas atraviesan la pared intestinal y vía porta llegan al hígado. **C.** Por vena cava caudal van al corazón. **D.** De corazón derecho migran por la arteria pulmonar a pulmones (**E**)**.** De los pulmones pueden ir a corazón izquierdo y se distribuyen por la aorta a circulación sistémica (**F**)**,** o migrar a tráquea, ser deglutidas y convertirse en adultos intestinales que liberan huevos en las heces que contaminan el ambiente (**G**). **H.** Los cachorros se infectan principalmente vía transplacentaria y lactogénica.

En humanos la infección por *T. canis*, es una enfermedad prevalente y desatendida, aún en países industrializados (Chen et al., 2012). Se han caracterizado cuatro conjuntos de signos y síntomas en humanos, estos son *larva migrans* visceral, ocular, encubierta y neurotoxocariosis (Finsterer and Auer, 2007; Overgaauw and van Knapen, 2013).

Los humanos pueden infectarse al consumir HL o tejidos de otros hospederos infectados (Fig. 3). Los HL que se encuentran en las heces de perros con adultos intestinales contaminan el ambiente y se han encontrado en la tierra y arena que a su vez pueden contaminar agua y frutas y vegetales, donde pueden permanecer infectivas por meses o años (Kozan et al., 2007; Ma et al., 2018; Tefera et al., 2014).

En México no hay cifras oficiales respecto al número de perros y la contaminación ambiental por sus heces. Pero, según datos de la Secretaría de Salud existen alrededor de 22 millones de perros y de acuerdo con la Facultad de Medicina Veterinaria y Zootecnia, se calcula que el 30% tiene propietario, el 30% es comunitario y el 40% vive en la calle. Así, a nivel nacional se recogen aproximadamente 696 toneladas de excremento al día (Morán-Rodríguez, 2012).

A pesar del alto potencial de exposición, la incidencia de la infección por *T. canis* en humanos no ha sido establecida y las encuestas locales no reflejan la prevalencia real en México y en otros países. Un ejemplo de esto, es la variabilidad en la detección de anticuerpos anti-*T. canis* en rangos que van del 1.6% en personas de 0 a 40 años, en los que originalmente se buscaba detectar toxoplasmosis en Dinamarca, a un

86.75% en niños de primaria de 7 a 12 años en la capital de la República de las Islas Marshall (Fu et al., 2014; Stensvold et al., 2009). Por lo anterior, es esencial instaurar encuestas nacionales para el diagnóstico de esta enfermedad, con el fin de mostrar el problema de salud pública que representa esta enfermedad desatendida, asociada al alto riesgo de infección por *T. canis*.

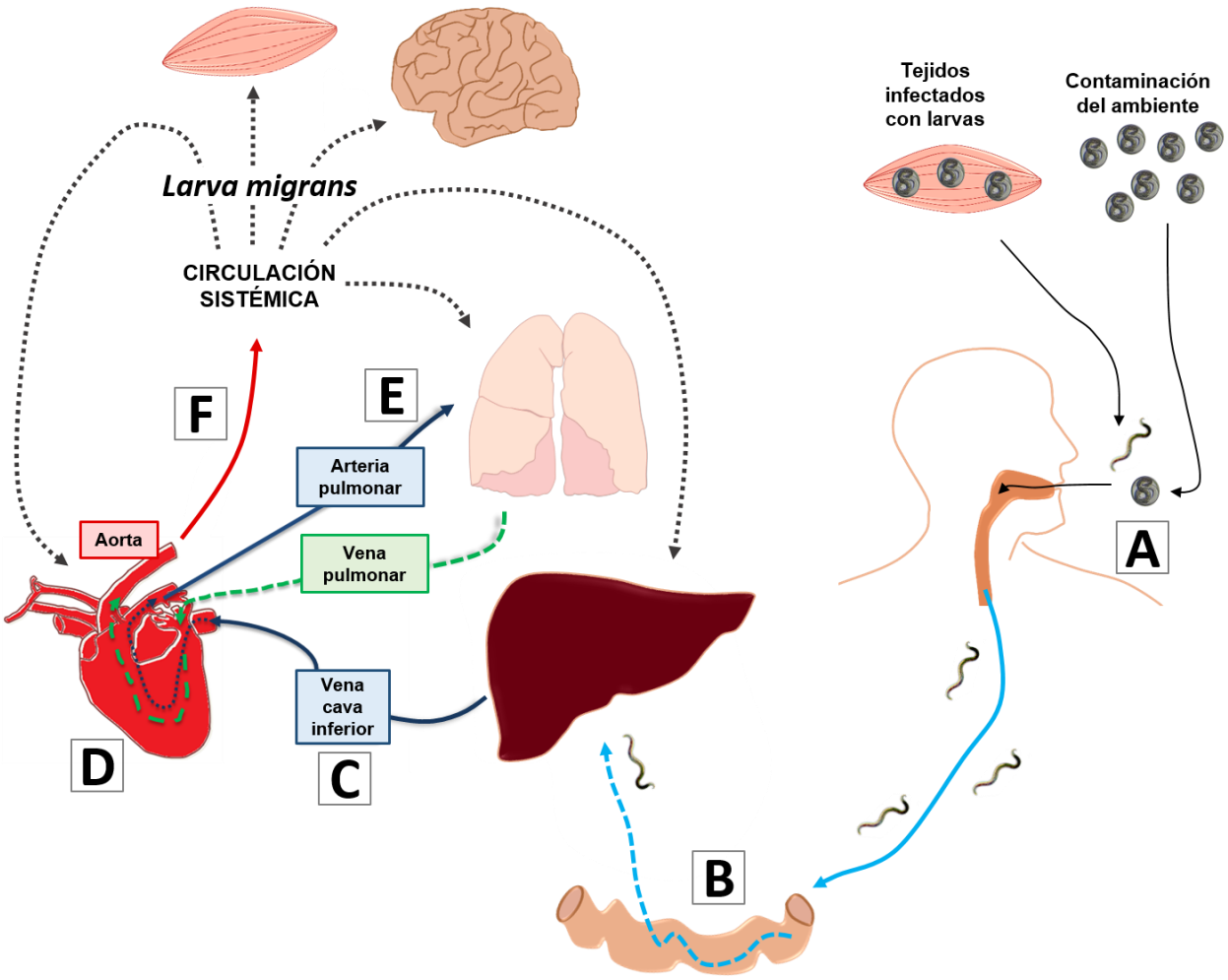

Figura 3. Ciclo biológico del *T. canis* en el hospedero paraténico. A. En humanos, la infección vía oral es a través de la ingestión de huevos larvados o tejidos de otros hospederos infectados con larvas. Después de su liberación en el tracto digestivo llegan al intestino. **B.** Atraviesan la pared intestinal, vía porta llegan al hígado. **C.** Por la vena cava inferior van al corazón. **D.** Del corazón derecho van por arteria pulmonar a pulmones. **E.** Después de atravesar el tejido alveolar regresan a corazón. **F.** Se distribuyen por circulación sistémica por la aorta a tejidos como músculo cardiaco, esquelético, cerebro, hígado, pulmones, entre otros (*larva migrans*).

1.2.2. Respuesta inmune a *T. canis*

Tanto la supervivencia como la acción patogénica de las larvas de *T. canis* en sus hospederos está mediada por sus productos de excreción y secreción (TES). Los cuales promueven y modulan la respuesta inmune del hospedero al mismo tiempo que la evaden para que el parásito pueda vivir, incluso por años en los tejidos de sus hospederos (Maizels, 2013).

En los hospederos paraténicos como los humanos y murinos, la respuesta inmune a *T. canis* ha sido asociada a una eosinofilia sanguínea y tisular en los sitios de migración de la larva o alrededor de ella. Además de la respuesta eosinofílica, se han detectado niveles elevados de anticuerpos IgG e IgE específicos de *T. canis*. Debido a esto, se ha asociado a la *larva migrans* por *T. canis* con una respuesta de linfocitos T cooperadores $CD4^+$ tipo 2 (Th2) (Maizels, 2013; Resende et al., 2015). En este sentido, la asociación de la respuesta tipo Th2 a helmintos está estrechamente ligada a la producción de anticuerpos y eosinofilia, pero muchas de las consideraciones generales entre parásitos, frecuentemente se extrapolan a otros. En la infección con *T. canis*, la repuesta tipo Th2 ha sido parcialmente dilucidada por la detección de citocinas séricas como IL-4, IL-5 e IL-10. Por ejemplo, en humanos con títulos elevados de anticuerpos anti-*T. canis*, se detectó un incremento en los niveles séricos de IL-4 e IL-10, comparados con los donadores controles (Mazur-Melewska et al., 2016). Este fenómeno se observó también en ratones infectados con *T. canis*, en los que la concentración de IL-5 e IL-4 aumentaron a los 7 y 14 d.p.i., respectivamente (Resende et al., 2015). Adicionalmente, en el sobrenadante del cultivo *in vitro* de linfocitos T obtenidos de células humanas sanguíneas periféricas de donadores positivos a *T. canis*, que fueron estimuladas con TES, se detectó un incremento en IL-4 e IL-5 (Del Prete et al., 1991).

Aunque los eosinófilos son las células innatas más relacionadas con la respuesta inmune a la infección por nematodos, los macrófagos, también juegan un papel importante en la defensa del hospedero. Se ha descrito que los MAA están involucrados con funciones anti-inflamatorias mediadas por la secreción de IL-4, IL-10,

IL-13, TGF-β, y VEGF, además de la respuesta humoral y de reparación de heridas, también participan en la protección a o contra? nematodos (Jenkins and Allen, 2010; Maizels, 2013; Qian and Pollard, 2010).

Tanto los eosinófilos, como los linfocitos Th2 y los MAA, han sido asociados con una respuesta del Tipo 2, en contra de los helmintos. Sin embargo, con el paso del tiempo y la cronicidad de la infección, la atenuación de la inflamación es importante para la supervivencia del hospedero, debido a que el daño está asociado a la inflamación constante y la liberación de productos celulares que afectan a células adyacentes. Los responsables de la regulación del sistema inmune son los productos de secreción y excreción de los helmintos, debido a que inducen la formación de células Treg y Breg (Nutman, 2015). La expansión de linfocitos reguladores se ha comprobado en ratones infectados con *T. canis*, en los que se detectó el aumento en la células positivas al factor de transcripción $Foxp3^+$ en el hígado de animales infectados, así como incremento en el RNAm de *Foxp3* en el bazo de estos, este marcador es característico de las células Treg (Othman et al., 2011).

Incluso si la respuesta inmune del hospedero a los diferentes helmintos es similar, la extrapolación de estudios en otros nematodos no debe ser asumida como una conjetura de lo que pasa en todos los parásitos. En el caso de *T. canis*, la larva migra y eventualmente entra en hipobiosis en diferentes tejidos. La respuesta inmune celular se localiza alrededor de la larva, pero es también sistémica por la estimulación durante la migración. La mayoría de la evidencia que liga la infección por *T. canis* a la respuesta tipo Th2, está basada en reportes que midieron células de la respuesta inmune y citocinas en varios compartimientos como vasos sanguíneos, aunque la mayoría la estudia en los tejidos adyacentes, donde la larva se establece o migra. Por lo que la caracterización integrada de la respuesta inmune es necesaria, para validar las asociaciones y los hallazgos dispersos en los diferentes reportes.

Tomando en cuenta que *T. canis* potencialmente puede inducir una respuesta reguladora en sus hospederos, es importante considerar la asociación de otras

enfermedades que puedan verse favorecidas por estas condiciones que establece la infección en el sistema inmune del hospedero, como es el caso del cáncer. Como se mencionó anteriormente en la inmunosubversión las principales poblaciones celulares que favorecen el crecimiento tumoral son las mismas que la infección por *T. canis* induce (Treg, Breg, MAA). Por lo que el siguiente trabajo se encaminó a caracterizar la respuesta inmune del hospedero a *T. canis* y posteriormente analizar la interacción de esta con el desarrollo de tumores mamarios y la respuesta inmune al tumor.

II. JUSTIFICACIÓN

El cáncer de mama, que es el más importante en términos de incidencia y prevalencia en mujeres, puede verse favorecido por la inducción de un microambiente inmune regulador. Por otro lado, la infección con *Toxocara canis* es una zoonosis prevalente que provoca una respuesta de este tipo en sus hospederos paraténicos. Por lo que, es necesario evaluar la influencia de la infección con *T. canis* en el crecimiento de tumores mamarios.

III. HIPÓTESIS

La infección con *Toxocara canis* en el modelo murino de tumores mamarios, ejercerá un aumento en el crecimiento de tumores inducidos *in vivo* y este crecimiento estará modulado por la respuesta inmune polarizada por el nematodo.

IV.OBJETIVOS

4.1 Objetivo general

- Determinar el efecto de la infección por *Toxocara canis* sobre el desarrollo de tumores, el microambiente tumoral y la respuesta inmune sistémica, en el modelo murino.

4.2 Objetivos particulares

- Caracterizar la respuesta inmune en contra de la infección por *T. canis* en ratones de la cepa BALB/c.

- Estudiar la progresión de los tumores en los ratones BALB/c con y sin infección con *T. canis*.

- Analizar el efecto de la infección por *T. canis*, sobre el tamaño y peso de las masas tumorales inducidas por la inyección de células 4T1 en ratones hembras de la cepa BALB/c.

- Determinar por citometría de flujo los porcentajes de las sub-poblaciones celulares involucradas en la respuesta inmune al cáncer de mama (células NK, linfocitos T citotóxicos $CD8^+$, linfocitos T cooperadores $CD4^+$, linfocitos T reguladores $CD4^+$ y $CD8^+$ y macrófagos), en el bazo, ganglios linfáticos periféricos y masas tumorales de ratones controles e infectados con *T. canis*.

- Observar los efectos de la infección por *T. canis* sobre la expresión proteica de las citocinas IFN-γ, TNF-α, IL-4, IL-5, IL-10, y VEGF en el suero, bazo y masas tumorales de ratones controles e infectados con *T. canis*.

V. MATERIALES Y MÉTODOS

5.1 Declaración ética

Los procedimientos experimentales y de cuidado animal se realizaron en el Instituto de Investigaciones Biomédicas (I.I.B.), Universidad Nacional Autónoma de México (U.N.A.M.) en la Unidad de Modelos Biológicos (U.M.B.). El Comité Institucional de Cuidado en el Uso de Animales de Laboratorio (C.I.C.U.A.L.) evaluó y aprobó los procedimientos experimentales (permiso número 2017-208), en adhesión a la norma Mexicana (NOM-062-ZOO-1999).

5.2 Animales

Para los experimentos se emplearon ratones hembras de la cepa singénica BALB/c que se mantuvieron en la U.M.B., U.N.A.M. en las siguientes condiciones estándar: temperatura controlada de 22°C y 12 horas de ciclos de luz y oscuridad. Se les administró agua y alimento Purina LabDiet 5015 (Purina, St. Louis MO), ambos en condiciones estériles.

La sangre se colectó a través de una punción cardiaca de los ratones profundamente anestesiados con Sevofluorano 5%, (Abbot). Posteriormente, la eutanasia de los animales se realizó a través de la dislocación cervical. Las muestras de suero se obtuvieron por centrifugación de la sangre (3250 *g*/10 min, HERMLE Z400K) y se guardaron a -70°C, hasta su uso.

5.3 *Toxocara canis*

5.3.1 Colección de adultos y obtención de huevos de *T. canis*

Los adultos de *T. canis*, se obtuvieron de perros naturalmente infectados, por eliminación espontánea o recuperación en heces por administración de piperacina (100-200 mg/kg) vía oral. Los parásitos adultos se colocaron en recipientes con PBS

estéril pH 7.4 (PBS), posteriormente se realizaron tres ciclos de lavados con PBS y PBS/formaldehído al 2% (PBS/F 2%) y se colocaron en PBS/F 2%.

En la cutícula en la sección anterior del cuerpo de las hembras adultas de *T. canis* se realizó una incisión, se obtuvo el útero y se extrajeron los huevos sin larvar. Los restos del nematodo se eliminaron con un colador fino. La suspensión de huevos se centrifugó a 3250 *g*/5 min (HERMLE Z400K) y se resuspendieron con PBS estéril, donde se mantuvieron a temperatura ambiente en un tubo Falcon de 50 ml cerrado, durante 21-28 días, revisando la presencia de larvas dentro de los huevos cada semana, hasta que el 80% de los huevos estuvieran larvados.

Además de los huevos obtenidos con esta metodología, el M. C. Juan Pablo Martínez Labat, de la Facultad de Estudios Superiores Cuautitlán, U.N.A.M., amablemente donó una suspensión de huevos para realizar las infecciones de los ratones.

5.3.2 Infección

Cuando el 80% de los huevos estuvieron larvados, se contaron y se administraron 500 huevos larvados vía oral con una cánula a los ratones.

5.3.3 Obtención y cuantificación de TES

Los TES se obtuvieron en base a las metodologías descritas por De Savigny y Bowman, con modificaciones. Primero, la suspensión de huevos larvados se centrifugó (3250 *g*/5 min) en un tubo Eppendorf de 1.5 ml. En una campana de flujo laminar, el sobrenadante se decantó y se le añadió 1 ml de hipoclorito de sodio 1%, para disgregar la membrana externa de los huevos, lo que se estimuló mediante la agitación gentil del tubo durante no más de 10 minutos. Los huevos se trasladaron a un tubo Falcon de 15 ml con 10 ml de agua bidestilada estéril y se centrifugaron a 3250 *g*/5 min. El sobrenadante se decantó y se realizaron 3 lavados con PBS, al final el pellet se resuspendió en 1 ml de medio de cultivo RPMI 1640 sin rojo fenol (Sigma, St.

Louis MO) con Antibiotic-Antimycotic 1% (GIBCO). La suspensión de larvas se trasladó a una caja para cultivo Falcon® 12.5 cm^2 con 20 ml de medio RPMI y se mantuvo en movimiento durante 20 min con un agitador magnético para promover la eclosión de las larvas. Posteriormente se colocó a 37°C, en una atmósfera humidificada conteniendo 5% CO_2 (v/v), durante toda la noche.

Mediante un aparato de Baerman modificado, las larvas se separaron de los cascarones, huevos sin larvar y detritus. Las larvas se mantuvieron en medio RPMI 1640, en cajas de cultivo a 37°C, 5% CO_2, una concentración de 10^4 larvas por ml de medio. Se recolectaron 10 ml semanalmente el sobrenadante del medio de cultivo con larvas y se restituyó con la misma cantidad de medio tibio. El medio recolectado se filtró con un filtro para jeringa de 20 μm (Millipore), y se precipitó con acetona (Herschi Trading, High Purity, 99.5%), a -20°C, en una dilución 1:8 durante toda la noche. Posteriormente se centrifugó a 8450 *g*/0°C/15 minutos. El sobrenadante se decantó y el sedimento de cada tubo se reunió y se dejó secar en la campana de flujo laminar. Se agregaron 50-100 μl de PBS y se almacenó a -20°C hasta su uso.

La concentración de proteína se determinó en microplaca con Bradford Protein Assay Bio Rad® usando la interpolación de una curva estándar con diferentes concentraciones de albúmina.

5.3.4 Recuperación de larvas de tejidos murinos y obtención del índice esplénico

Después de 49 d.p.i., se obtuvieron los pulmones, el hígado, los riñones, el corazón, el cerebro, el músculo del diafragma y los miembros torácicos y pélvicos de los ratones infectados. Los músculos recuperados de los miembros torácicos y pélvicos, así como el diafragma se combinaron y pesaron. Después, 1g de esta masa muscular se procesó para su digestión y el número de larvas obtenido se multiplicó por el peso del conjunto de músculos. Todos los tejidos fueron finamente cortados con bisturí y se realizó la digestión con 10 ml de jugo gástrico artificial (1% pepsin SIGMA (250 units/mg)/1% HCl, pH 2.0) por gramo de tejido, durante 4 horas a 37°C. Los tejidos digeridos se centrifugaron a 791 *g* durante 5 min y se les agregó 1 ml de solución de

paraformaldehído al 1% diluido en PBS para la fijación de las larvas. Todo el contenido de las larvas se examinó con microscopio óptico (M280LED, UNICO) y se contaron las larvas en cada tejido digerido.

El índice esplénico se calculó como lo describe Kayes y colaboradores (Kayes et al., 1985).

5.4 Línea celular 4T1

La línea celular 4T1 es derivada de un carcinoma mamario espontáneo de un ratón BALB/c MMTV^{+}. Estas células se pueden trasplantar a ratones BALB/c, en los que se crece rápidamente un tumor que es altamente invasivo y que puede migrar a GLP, sangre, hígado, pulmón, cerebro y hueso (Pulaski and Ostrand-Rosenberg, 2000).

El modelo de tumores de células 4T1 en ratones de la cepa BALB/c, se emplea porque semeja el cáncer de mama de estadio IV (Tabla 1) y porque permite medir la respuesta inmune intacta del animal. Tanto en el cáncer de mama estadio IV, como en el modelo de tumores 4T1, hay presencia de edema, ulceraciones cutáneas, extensión del tumor primario a la cavidad torácica (peritoneal en ratones, por el lugar de inyección) y la metástasis a diferentes órganos, preferentemente a pulmones (Tabla 1) (Harris et al., 1997).

5.4.1 Cultivo celular

La línea celular 4T1 de carcinoma de células mamarias (ATCC® CRL-2539) fue amablemente donada por la Dra. Karen Nava Castro. Un vial con células 4T1 se descongeló en hielo y las células se lavaron con 10 mL RPMI 1640 (Sigma, St. Louis MO) sin suplementar, posteriormente se centrifugaron a 791 *g*/5 min, se decantó el sobrenadante y el pellet se resuspendió con 1 ml de medio RPMI 1640 (Sigma, St. Louis, MO) suplementado con 10% de suero fetal bovino (ByProducts, Guadalajara, México), (RPMI 10% SFB), con 1.0 mM de piruvato de sodio, 100 U/ml de penicilina, 100 mg /ml de estreptomicina. Las células se incubaron a 37°C/5% de CO_2 (v/v) en una caja

Falcon® de 12.5 cm^2. Una vez que la monocapa de células adherentes alcanzó el 80% de confluencia se realizó el pase, con tres lavados con 5 ml de PBS y se despegaron las células con 200 µl de tripsina 0.25%/EDTA 1x.

Tabla 1. Comparación entre las características del cáncer de mama de estadio IV y los tumores 4T1.

Cáncer de mama (estadio IV)	Tumores 4T1
Edema/ulceraciones cutáneas	
Extensión del tumor primario a la cavidad	
Metástasis a diferentes órganos	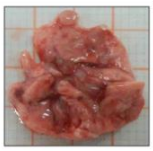

Después de realizar 2 pases, se cosecharon las células para inocularlas. Las células se deprendieron según la metodología arriba descrita, y se les agregaron 500 µl de SFB y 500 µl de PBS. La suspensión celular se transfirió a un tubo Eppendorf de 1.5 ml. Posteriormente, las células se centrifugaron a 791 *g*/5 min, el sobrenadante se decantó y el pellet se lavó con solución salina isotónica NaCl 0.9% estéril (SSI 0.9%), cuidando de no resuspender el botón y el sobrenadante se decantó. El botón se resuspendió en 1 ml de SSI 0.9%, se mantuvo en hielo y el conteo se realizó. Para efectuar el conteo de las células, en una cámara de Neubauer, se tomaron 10 µL de la suspensión celular, 20 µL de azul tripano y 70 µl de SSI 0.9%. Se realizaron los cálculos necesarios para obtener 10^4 células 4T1, en un volumen de 40 µl (250,000 células/ml).

5.4.2 Inducción de tumores 4T1

Los ratones fueron anestesiados (Sevofluorano 5%, Abbot, México) y la región mamaria caudal derecha se preparó asépticamente con EtOH al 70%. Se inyectaron 10^4 células 4T1 vivas, en un volumen de 40 μl de SSI 0.9%, en el tejido subcutáneo adiposo de la penúltima glándula mamaria caudal derecha, por debajo del pezón. La recuperación de los ratones se supervisó y se les regresó a su caja respectiva.

5.4.3 Esquema de infección e inducción de tumor

Para este estudio se emplearon 4 grupos experimentales (Tabla 2). Al grupo de ratones intactos (Intacto), no se les realizó ningún procedimiento, mientras que al grupo de animales infectados (*T. canis*), se infectaron como se menciona en el apartado 5.3.2. Los dos grupos restantes se les indujo el crecimiento tumoral (apartado 5.4.2), siendo el grupo 4T1 el que fungió como control del desarrollo tumoral (grupo 4T1) para compararlo con el grupo de animales infectados y con tumor (4T1+*T. canis*).

Tabla 2. Grupos experimentales (infección con *T. canis* y desarrollo de tumores 4T1).

Grupo	Infección con *T. canis*	Inducción de tumor
Intacto	Ausente	Ausente
T. canis	Presente	Ausente
4T1	Ausente	Presente
4T1+*T. canis*	Presente	Presente

La infección de ratonas se realizó con 500 HL y después de 21 días se realizó la inducción de tumor como previamente se describió y 49 d.p.i. se efectuó la eutanasia. En la figura 4 se muestra este esquema experimental de infección e inducción de tumor.

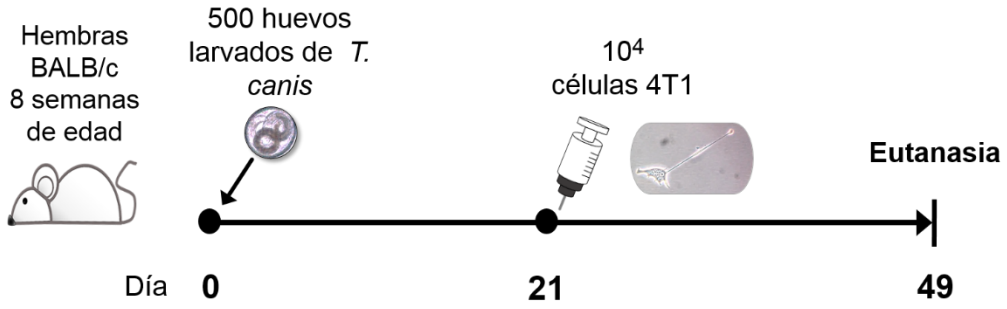

Figura 4. Esquema experimental de infección e inducción de tumores 4T1. Ratonas BALB/c de 8 semanas de edad se infectaron con 500 huevos larvados y después de 21 días se inocularon 10,000 células 4T1. La eutanasia se efectúo a los 49 d.p.i.

Después de la eutanasia, la sangre, el bazo, el hígado, los pulmones, los GLP (inguinales) y el tumor de los ratones se extrajeron. El bazo y el tumor se pesaron. La mitad del bazo y una cuarta parte del tumor, así como los nódulos linfáticos inguinales se disgregaron para ser evaluados por medio de citometría de flujo. La otra mitad del bazo y otra cuarta parte del tumor se congelaron en TRIzol™ (Invitrogen) para la posterior medición de citocinas.

5.4.4 Inyección intratumoral con TES

Las ratonas se inocularon con 10^4 células 4T1 y 14 días post-inoculación se inyectaron intratumoralmente. A cada ratona se anestesió con Sevorano inhalado y cuando no presentaron respuesta al dolor se tomó el tumor firmemente y se le inyectaron 20 μg de TES o PBS (vehículos) con una jeringa insulínica (Fig. 5).

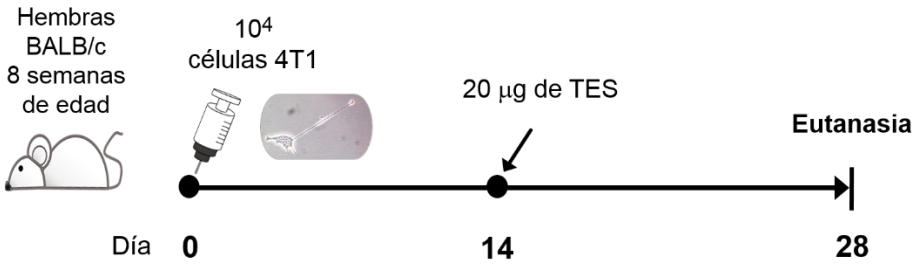

Figura 5. Esquema experimental de inducción de tumores 4T1 e inyección de TES. Ratonas BALB/c de 8 semanas de edad se inocularon con 10^4 células 4T1. A los 14 días

se inyectó cada tumor con 20 μg de TES o PBS (vehículo). La eutanasia se efectúo 49 días post-inoculación.

5.5 Citometría de flujo

5.5.1 Obtención de las suspensiones celulares

El bazo y los GLP se disgregaron mecánicamente entre dos mallas de nylon de 50 μm. Los eritrocitos de la suspensión de esplenocitos se lisaron con buffer ACK (apéndice 8.1.9) durante 10 min a temperatura ambiente. Ambas suspensiones celulares se centrifugaron a 791 *g*/5 min /4°C, y se lavaron con PBS y se centrifugaron de nuevo. Los pellets de células se resuspendieron con 200 μl de buffer de FACS (apéndice 8.1.10).

Por otro lado los tumores se cortaron finamente con una hoja de bisturí y se colocaron en 500 μl de solución de digestión (apéndice 8.1.11). La reacción se detuvo con 50 μl de SFB y se disgregaron entre 2 mallas de nylon de 50 μm, la suspensión de células se recolectó, se centrifugó a 1250 rpm/5 min/4°C y se resuspendió en 200 μl de buffer de FACS.

5.5.2 Marcaje celular

Aproximadamente $1x10^6$ células se incubaron (20 minutos a 4°C) con anti-CD16/CD32 (TruStain®, BioLegend, San Diego CA) y se lavaron con Buffer de FACS. Después se marcaron con los paneles de tinción que se muestran en la Tabla 3.

El kit Foxp3/Transcription Factor Staining Buffer (Tonbo biosciences, San Diego CA) se empleó para la tinción intracelular de Foxp3, de acuerdo al protocolo del proveedor. Después de la permeabilización de las células se realizó la tinción intracelular con anti-Foxp3, para la detección de células Treg.

Tabla 3. Paneles de tinción, moléculas y anticuerpos acoplados a fluoróforos empleados para el análisis por citometría de flujo.

Panel	Población	Blanco	Fluoróforo	Dilución	Clona
1	Linfocitos T	CD3ε	AlexaFluor® 488	1:100	145-2C11
	Linfocitos T cooperadores	CD4	PE	1:300	GK1.5
	Linfocitos T citotóxicos	CD8	PerCP	1:100	53-6.7
	Linfocitos Treg	Foxp3	AlexaFluor®647	1:100	150D
2	Células NK	NKp46	PE	1:200	29A1.4
	Macrófagos	F4/80	AlexaFluor® 647	1:200	BM8
3	Linfocitos B	CD19	PE	1:200	6D5

Los paneles de células NK/macrófagos y linfocitos B se fijaron con 100 μl de paraformaldehído 4%/PBS y 100 μl de buffer de FACS durante 20 min, se centrifugaron, decantaron y resuspendieron en 200 μl de buffer de FACS.

Todos los anticuerpos empleados para el marcaje en la citometría de flujo son de BioLegend, San Diego CA. Se realizaron los controles de compensación de las tinciones individuales para los cuatro fluorocromos y los tres tejidos. El análisis celular se realizó usando el citómetro de flujo FACSCalibur™ (BD Biosciences). Los datos se analizaron con el programa BD CellQuest™. La compensación se llevó a cabo en el citómetro FACSCalibur™ y con el software FlowJo (Treestar Inc.), empleando muestras sin teñir, tinciones simples como controles y FMO para Foxp3 ($CD3^+/CD4^+$; $CD3^+/CD8^+$).

5.5.3 Selección de poblaciones

En la figura 6 se observa la estrategia empleada para la selección de las diferentes subpoblaciones para la fenotipificación por citometría de flujo.

Las células se seleccionaron por tamaño y granularidad a través de un gate de complejidad (SSC) y tamaño (FSC) celulares. De este gate (FSC vs SSC) se eligieron de las células más grandes y complejas (Fig. 6A) las $F4/80^+$ (Fig. 6B) y de un gate de linfocitos (células pequeñas y poco complejas) ampliado las células $NKp46^+$ (Fig. 6C y D)

Los linfocitos T $CD3^+$ (Fig. 6F) y los linfocitos B $CD19^+$ (Fig. 6G), se obtuvieron del gate de linfocitos (FSC vs SSC) (Fig. 6E). Del gate de linfocitos T $CD3^+$ (Fig. 6F), se eligieron los linfocitos T $CD4^+$ y T $CD8^+$ (Fig. 6H). Y por último, de los LT $CD4^+$ se adquirieron las células $CD4^+$Treg como $Foxp3^+$ (Fig. 6I), y de los LT $CD8^+$, se seleccionaron los $CD8^+$Treg como $Foxp3^+$ (Fig. 6J).

Todos los gates de FSC vs SSC se obtuvieron después de la exclusión del *debris*. En los gates provenientes de la región de linfocitos se adquirieron colectando 10,000 eventos.

5.6 ELISA indirecto para la determinación de IgG anti-*T. canis*

Los pozos se sensibilizaron (Placa de poliestireno de 96 pozos Maxisorp Nunc) con 50 µl of TES (1 µg/ml) en buffer de bicarbonatos y se incubaron a 4°C durante la noche. Posteriormente, la placa se decantó y se lavó con la solución de lavado (apéndice 8.1.3). Todos los lavados para las ELISAs se hicieron por triplicado con esta solución. La solución de bloqueo al 3% se adicionó (apéndice 8.1.4) y se incubó durante 30 minutos a 37°C y se lavó. Después del bloqueo, el suero de cada ratón se agregó por duplicado en una dilución de 1:200, en solución de dilución y se incubó 1 h a temperatura ambiente. A continuación se agregaron 50 µl a cada pozo de anti-IgG de ratón conjugado con peroxidasa (HRP) anti-mouse IgG, IgG1 e IgG2 (Jackson),

diluidos 1:10,000 en solución de dilución (apéndice 8.1.5). La placa se mantuvo 90 min a temperatura ambiente. Finalmente el lavado y la reacción enzima-sustrato se realizaron con la adición de 50 µl de solución cromógeno recién preparada (apéndice 8.1.6). La reacción se detuvo a los 10 min con 50 µl de ácido sulfúrico 2N. La lectura de las absorbancias se efectuó a 492 nm en el lector de microplacas Stat Fax 4200 (Awareness Technology).

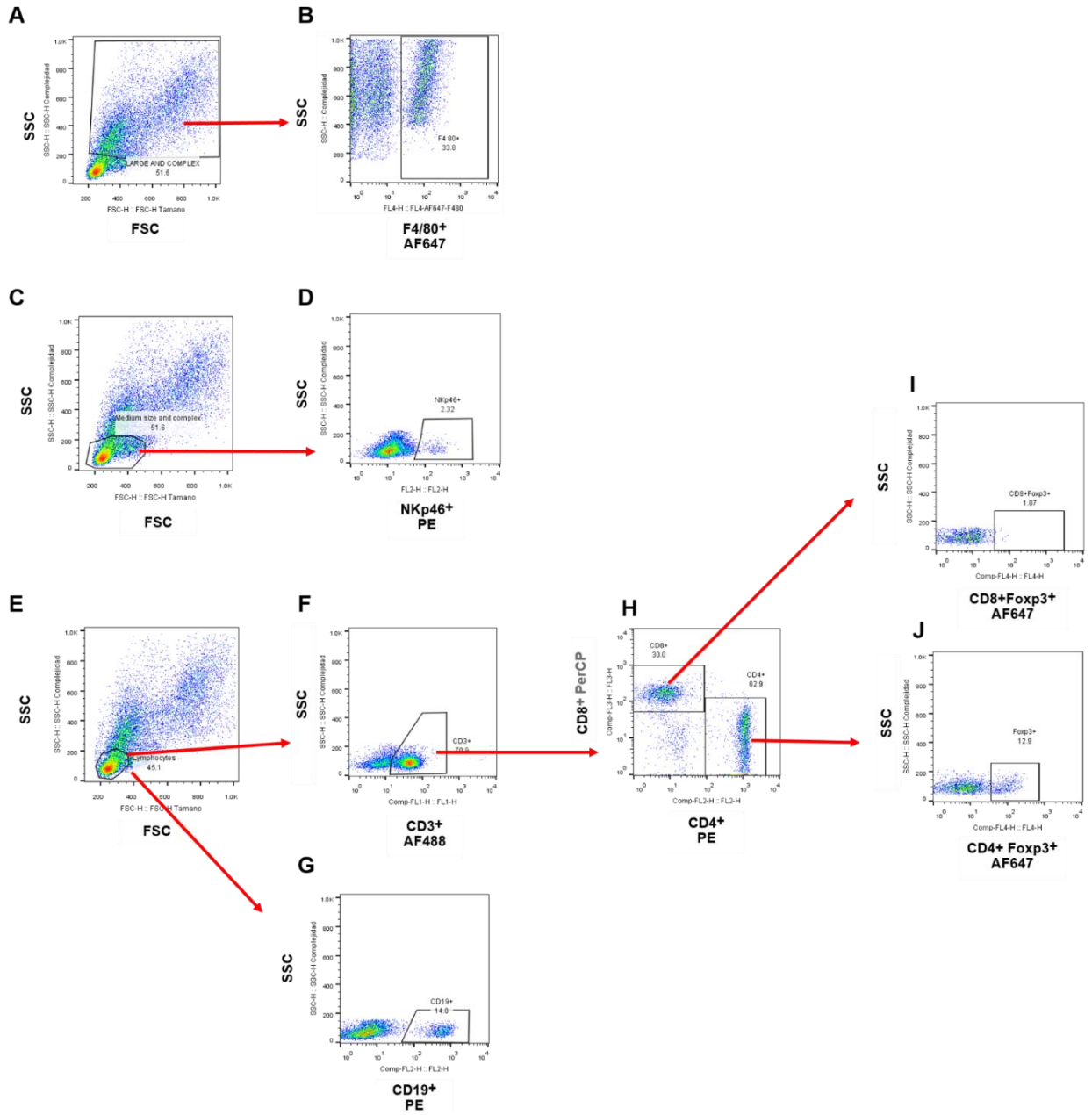

Figura 6. Estrategia de selección de las diferentes subpoblaciones de células inmunes. Dot plots representativos del análisis que pertenecen a esplenocitos murinos.

5.7 Determinación de citocinas

5.7.1 Extracción de proteína de bazo y tumor

El bazo y el tumor de los ratones se obtuvieron y se guardaron en TRIzol™ (Ambion) a -70°C hasta su uso. La separación de proteínas se realizó mediante los lineamentos del procedimiento del TRIzol™ (Ambion), con modificaciones. En breve: el tejido se homogeneizó en TRizol con el Polytron (Kinematica), se le adicionó cloroformo y se agitó por 20 minutos. Posteriormente se incubó 2-3 min y se centrifugó (8450 *g*, 4°C). La fase orgánica se separó y se añadió EtOH 100%. Cada tubo se agitó brevemente, incubó por 2-3 min y se centrifugó (8450 *g*, 4°C). Al sobrenadante se le añadió isopropanol frío, dejándolo 10 min y se centrifugó, para tomar el sobrenadante con pipeta y se lavó el pellet 3 veces con tiocinato de guanidinio (0.3 M). Se agregó de nuevo EtOH 100%, se centrifugó y se dejó secar. Las proteínas se solubilizaron con dodecil sulfato de sodio (SDS) 0.01% y se cuantificaron con el espectrofotómetro Nano Drop 1000 (Thermo Scientific). Se emplearon 10 µg de proteína para determinar los niveles de citocinas tisulares.

5.7.2 ELISA sándwich para la detección de citocinas

Las citocinas séricas y esplénicas se midieron con los kits de ELISA ABTS (PeproTech), de acuerdo a las indicaciones del protocolo de Peprotech. Los siguientes anticuerpos se emplearon: TNF-α (500-P64), IFN-γ (500-P119), IL-4 (500-P54), IL-5 (500-P55) and IL-10 (500-P60), empleando las mismas clonas sin y acopladas a Biotina como anticuerpos de captura y detección respectivamente, para elaborar el ELISA sándwich. La reacción enzima-sustrato de desarrolló con el sustrato líquido ABTS (PeproTech) y las placas se leyeron a una longitud de onda de 405 nm con un corrección de 650 nm, a diferentes tiempos de lectura, en el lector de microplacas Stat Fax 4200 (Awareness Technology).

5.7.3 ELISA indirecto para la cuantificación de VEGF

Los pozos de las placas de poliestireno de 96 pozos se sensibilizaron (Maxisorp Nunc) con 50 µl de proteína (10 µg), suero (dilución 1:2), el estándar de VEGF (Santa Cruz Biotechnology) para la curva (0.001 ng-1ng), todos en buffer de bicarbonatos (por duplicado) y se incubaron a 4°C durante la noche. Posteriormente, la placa se decantó y se lavó con la solución de lavado (todos los lavados se hicieron por triplicado). Se agregaron 200 µl de la solución de bloqueo (1%) y se mantuvo a 4°C por 1 h y se lavó. A continuación, se agregaron 50 µl de anticuerpo anti-VEGF C-1 (sc-7269, Santa Cruz Biotechnology) diluido 1:200, a cada pozo. La placa se mantuvo 1 h a 4°C. Para el reconocimiento de la IgG anti VEGF se adicionaron 50 µl de m-IgGκ BP-HRP (sc-516102 Santa Cruz Biotechnology) a una dilución 1:400, durante 2 h a temperatura ambiente. Por último, el lavado y la reacción enzima-sustrato se realizaron con 50 µl de la solución cromógeno. La reacción se detuvo a los 20 min con 50 µl de ácido sulfúrico 2N. La lectura de las absorbancias se efectuó a 492 nm en el lector de microplacas Stat Fax 4200 (Awareness Technology). Los anticuerpos se diluyeron en solución de dilución.

Todas las concentraciones de citocinas y VEGF se calcularon con la interpolación de una curva estándar. La determinación concentración de TES, de diluciones de sueros y anticuerpos se desarrolló después de la estandarización de las respectivas ELISAs.

5.8 Determinación del volumen tumoral

Para evaluar el desarrollo tumoral se midió el tamaño de los tumores con un Vernier (Fig. 7A-3) el día de la eutanasia. Estas mediciones se realizaron por encima de la piel, midiendo el diámetro mayor y el menor de cada masa tumoral (Fig. 7A-2,3). Aunado a esto el día de la eutanasia se extrajeron los tumores y se fotografiaron los tumores sobre una cuadrícula milimétrica (Fig. 7B-2, C-2), se pesaron y se determinó el volumen real mediante el desplazamiento de líquido producido por la masa en una probeta graduada.

Para obtener el volumen de un elipsoide se emplearon 2 fórmulas (Fig. 7A/B y C), y se compararon con el volumen real obtenido por desplazamiento de líquido. En total se midieron 31 tumores.

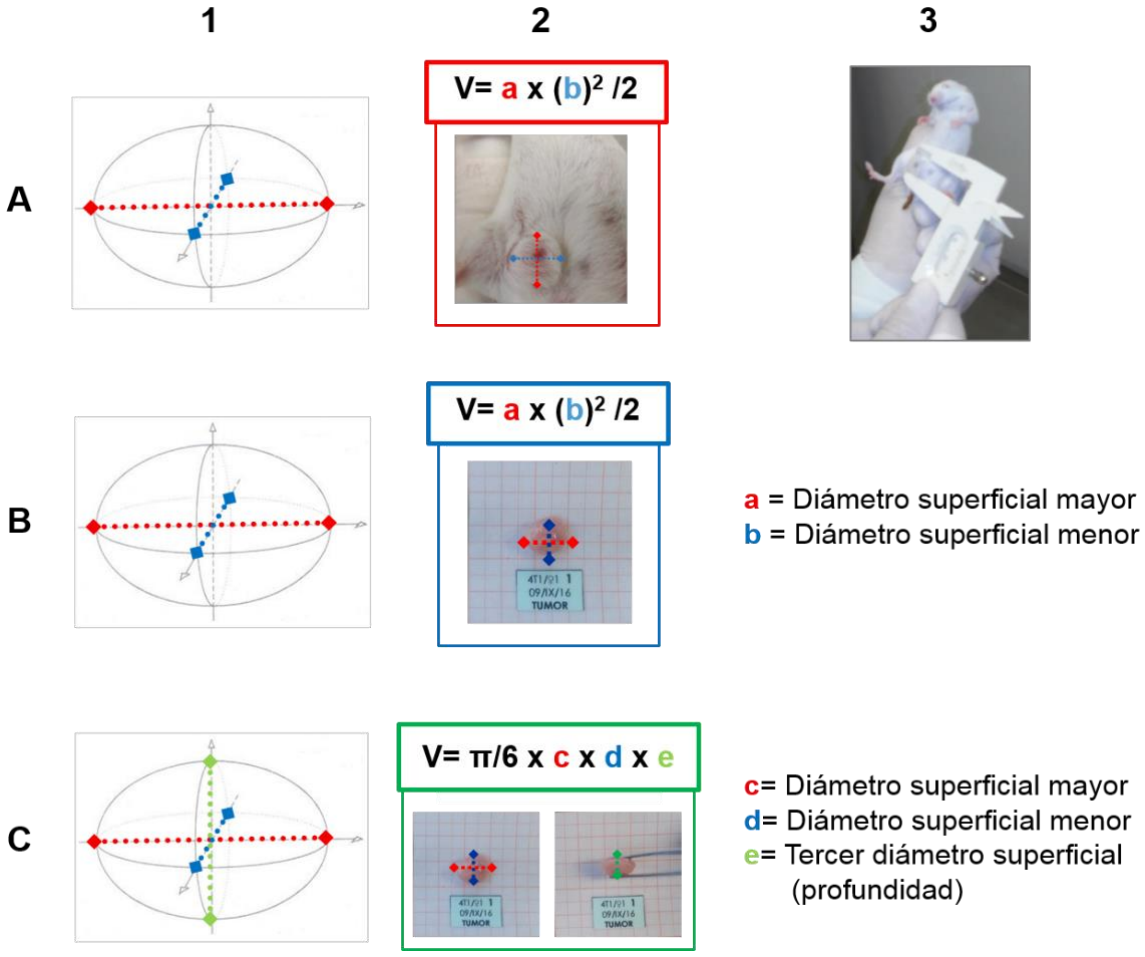

Figura 7. Medición del volumen de los tumores 4T1. A. Primer método empleado para la determinación del volumen tumoral en el que se realizaron las mediciones por encima de la piel del animal. **B.** Segundo método en el que se determinó cada diámetro (φ) del tumor extirpado. **C.** Tercer método que se realizó en los tumores extirpados e incluye φ mayor, el menor y el de profundidad. **1.** Representación esquemática de los elipsoides. Diámetros medidos: rojo= φ superficial mayor, azul= φ superficial menor; verde: profundidad. **2.** Fórmulas y representación de los diámetros medidos a los tumores. **3.** Fotografía que representa la medición con Vernier (**A**) y las equivalencias de los diámetros para la sustitución en las fórmulas.

5.9 Análisis estadístico

Los datos obtenidos de los experimentos se graficaron como el promedio±DE. Para analizar las diferencias entre el número de larvas en los tejidos de los ratones infectados, se usó una prueba de ANOVA, seguida de una prueba de Tukey. Mientras que, para comparar las diferencias entre los animales intacto (Int) vs infectado (*T. canis*) y entre los ratones con tumor (4T1) y con tumor e infectados (*T. canis*+4T1), se empleó la prueba de t de Student. La corrección de Welch se aplicó en los grupos en los que las varianzas fueron diferentes, esto determinado a través de la prueba de Fisher (F). En todos los casos las diferencias se consideraron significativas cuando $p \leq 0.05$.

La regresión lineal y correlación se realizaron para determinar si los valores de los diferentes métodos son cercanos al volumen real de los tumores.

Todos los análisis se calcularon usando Prism 6 ® software (GraphPad Sofware Inc.).

VI. Resultados

6.1 Respuesta inmune a *T. canis*

6.1.1 Las larvas de *T. canis* se establecen predominantemente en el músculo esquelético y el cerebro durante la infección crónica

Debido a que las larvas de *T. canis* migran a través de diferentes órganos que incluyen hígado, pulmones, riñones, corazón, músculo esquelético y cerebro, la recuperación de las larvas se realizó mediante la digestión del tejido para determinar cuáles son los más afectados por el establecimiento larvario.

Aunque en todos los tejidos antes mencionados se detectó la presencia de larvas, el mayor número se encontró en músculo esquelético y en cerebro (p≤0.001) (Fig. 8).

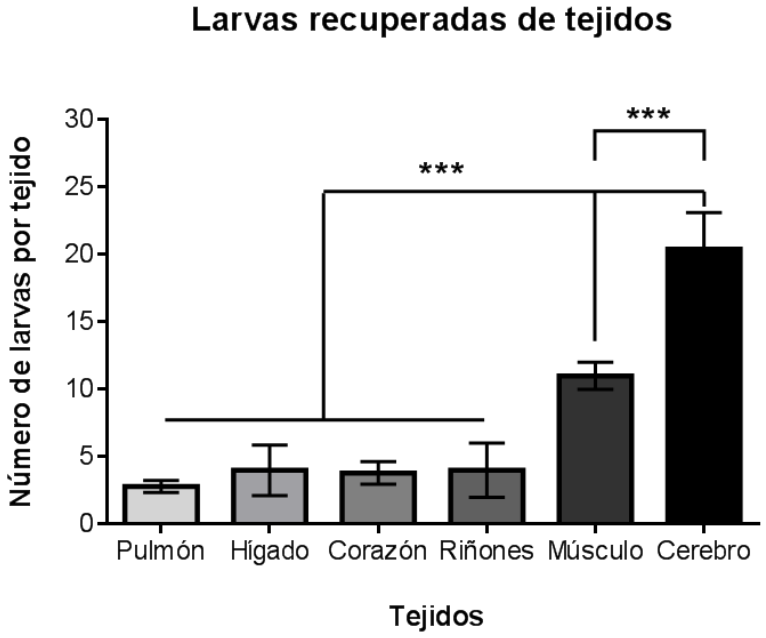

Figura 8. Larvas de *T. canis* recuperadas de tejidos de ratones infectados con el nematodo. Número de larvas recuperadas de pulmones, hígado, corazón, riñones, músculo esquelético y cerebro de ratones BALB/c después de 49 días post-infección con 500 huevos larvados de *T. canis*. Las gráficas representan el promedio±DE de los datos de 5 animales infectados. La significancia estadística se calculó usando una ANOVA seguida por la prueba de Tukey (***, p≤0.001).

6.1.2 La infección por *Toxocara canis* induce una respuesta humoral

El incremento en el peso y tamaño se observó en los bazos de los animales infectados traducido como el aumento del índice esplénico (p=0.0010) (Fig. 9A). También en los animales infectados se encontró elevada proporción de linfocitos B CD19⁺ en bazo (p=0.0064) y en los GLP (p=0.0006), comparada con los animales intactos (Fig. 9C). Para determinar la respuesta inmune humoral específica, se detectaron anticuerpos anti-*T. canis* IgG, en suero de los animales de ambos grupos y como se esperaba los niveles de IgG1 and IgG2a específicas para el nematodo fueron mayores en los animales infectados (p<0.0001, p<0.0001, respectivamente) (Fig. 9B).

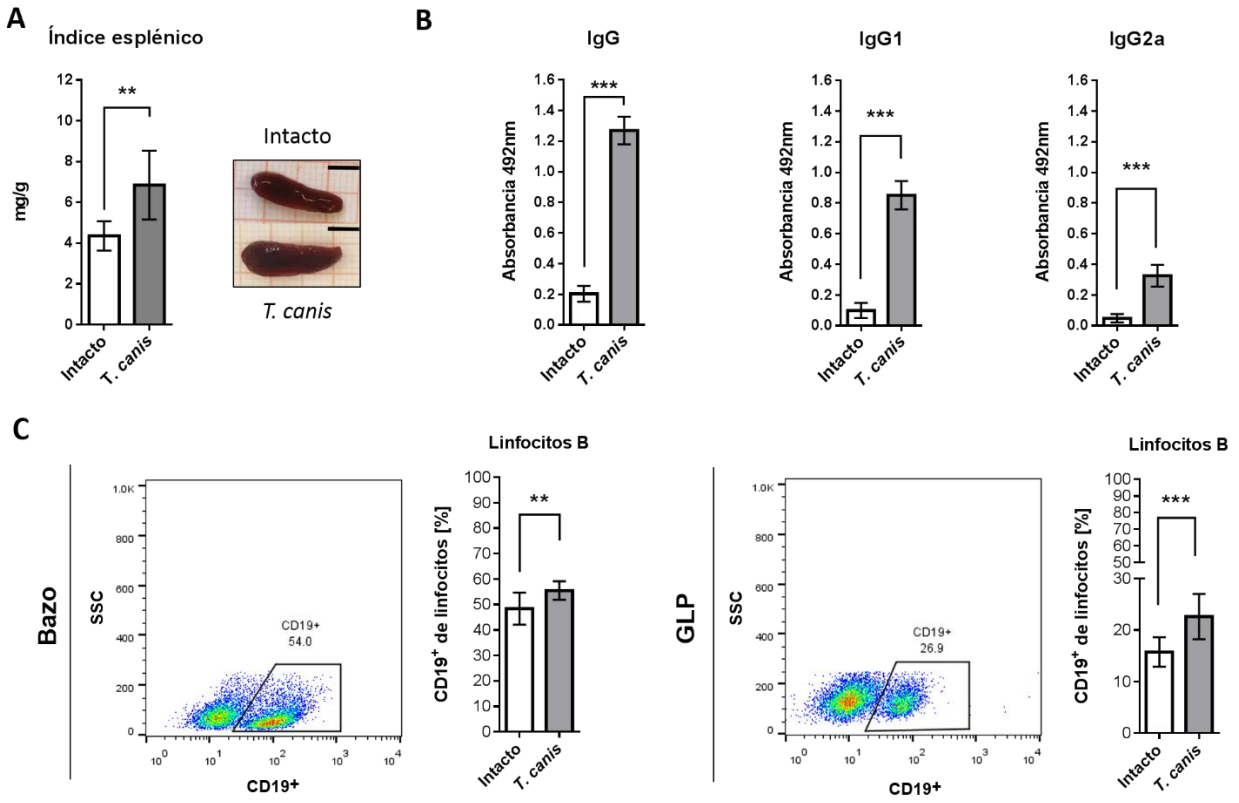

Figura 9. Respuesta humoral a la infección crónica con *T. canis*. A. Índice esplénico (izquierda) y fotografías representativas de los bazos (derecha) de los animales intactos e infectados (*T. canis*). La barra negra equivale a 0.5 cm. **B.** Niveles de IgG, IgG1 e IgG2a anti-*T. canis*. **C.** Dot plots representativos de los análisis de citometría de flujo de los porcentajes de LB (izquierda). Frecuencias de LB en bazo y GLP (derecha). Las gráficas representan el promedio ±DE de dos experimentos (intactos, n=10; *T.*

canis, n=10). La significancia estadística se realizó con una prueba de t (**, p≤0.01; ***, p≤0.001).

6.1.3 La infección modifica las proporciones de macrófagos en órganos linfoides secundarios

Debido a que las larvas de *T. canis* migran y se establecen en diferentes órganos, la respuesta inmune se evaluó en órganos linfoides secundarios. Para esto, los porcentajes de células NK y macrófagos (respuesta innata) y LT (respuesta adaptativa) se determinaron en bazo y en GLP después de 49 d.p.i. (Fig. 10, 11, 12).

Respecto a las células innatas en bazo, solamente la proporción de macrófagos se incrementó (p= 0.0228) debido a la infección (Fig. 10A). En los GLP, el porcentaje de éstas células fue menor (p=0.0117) que en los animales intactos. Por otro lado, no se detectaron células NK en los GLP (Fig. 10B).

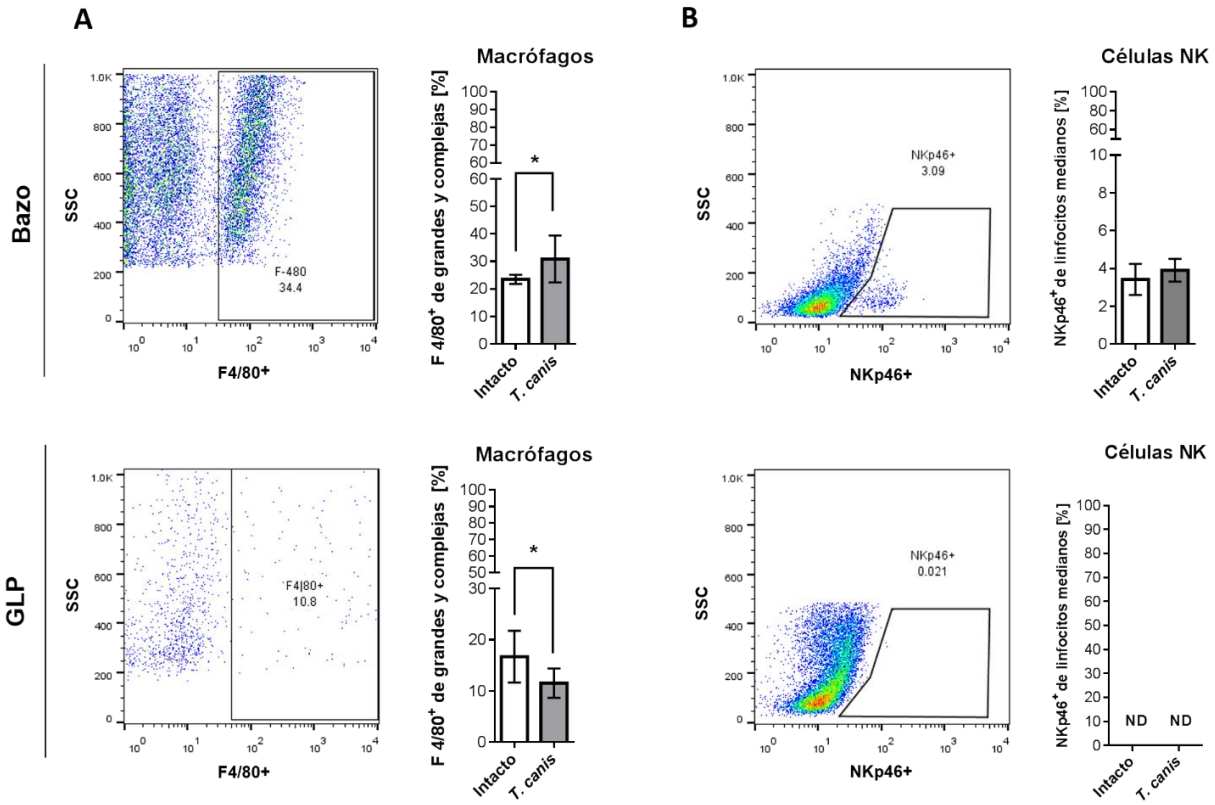

Figura 10. Cambios en las proporciones de células de la respuesta inmune innata en bazo y GLP con infección crónica. A. Frecuencias de macrófagos (F4/80+ de células

grandes y complejas). **B.** Frecuencias de células NK (NKp46$^+$ de células de tamaño y complejidad medianas). Las gráficas representan el promedio±DE de datos de dos experimentos (intactas, n=10; *T. canis*, n=10). La significancia estadística se calculó usando una Prueba de t (*, p≤0.05). ND, no hay datos porque esta población estuvo ausente en GLP.

6.1.4 La infección con el nematodo *T. canis* incrementa la proporción de linfocitos CD8$^+$ y células Treg CD4$^+$/Foxp3$^+$ en bazo y GLP

Cuarenta y nueve días después de la infección se evaluaron las subpoblaciones de los linfocitos T en bazo y GLP. Asociado a un incremento en las proporciones de linfocitos B CD19$^+$, el porcentaje de células T CD3$^+$ disminuyó en bazo (p=0.0155) y GLP (p=0.0331) (Fig. 11A, 12A) comparado con las mismas células de los ratones intactos.

Por otro lado, la infección indujo la expansión de células Treg CD4$^+$/FoxP3$^+$ en bazo (p<0.0001), y GLP (p=0.0077), como se esperaba (Fig. 11C, 12C). Un dato interesante fue el incremento en la proporción de linfocitos CD8$^+$ en bazo y GLP (p=0.0006; p=0.0001, respectivamente) en los animales infectados (Fig. 11B, 12B). La otra población de células que se determinó fueron las células T CD8$^+$/FoxP3$^+$, de las cuales a pesar de ser una población muy escasa, se observó un aumento (p=0.0002) solo en GLP de los ratones positivos a *T. canis*. En las proporciones de las células T CD4+ no se observaron cambios ni en bazo ni en GLP.

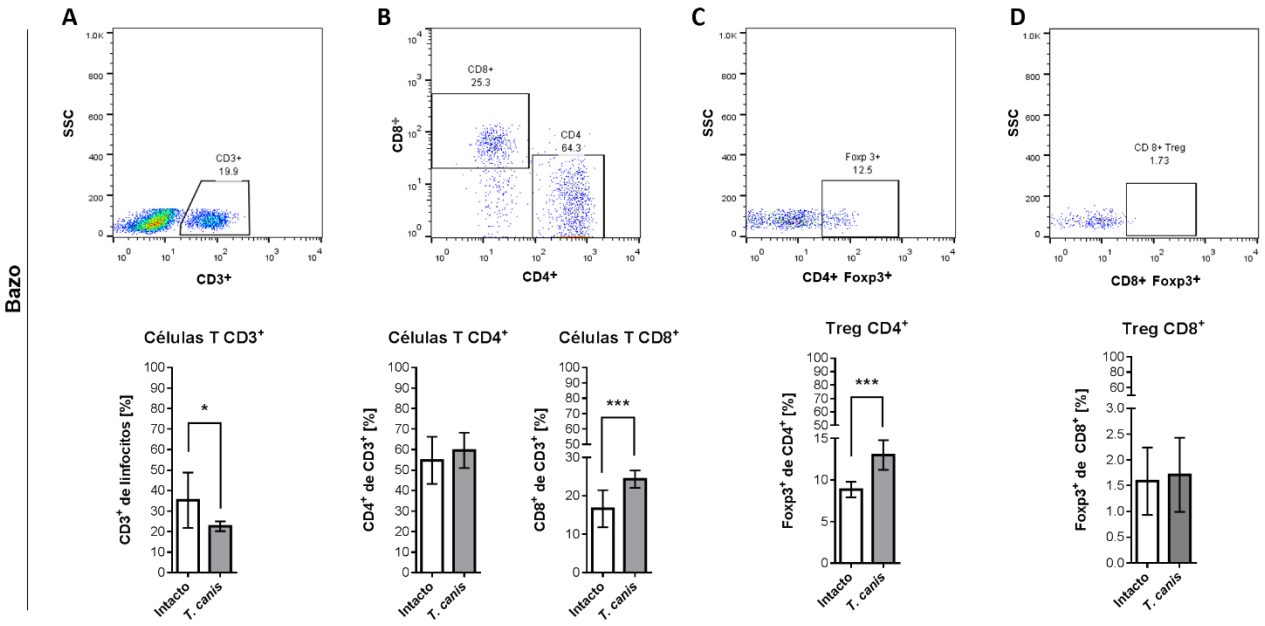

Figura 11. Proporciones de linfocitos T esplénicos en la infección crónica a *T. canis*. A. LT (CD3⁺). **B.** LT cooperadores (CD4⁺) y T citotóxicos (CD8⁺). **C.** Treg CD4⁺Foxp3⁺. **D.** Treg CD8⁺Foxp3⁺. En la parte superior se muestran los dot plots representativos de las poblaciones correspondientes. Las gráficas representan el promedio±DE de datos de dos experimentos (intacto, n=10; *T. canis*, n=10). La significancia estadística se calculó usando una Prueba de t (*, p≤0.05; ***, p≤0.001).

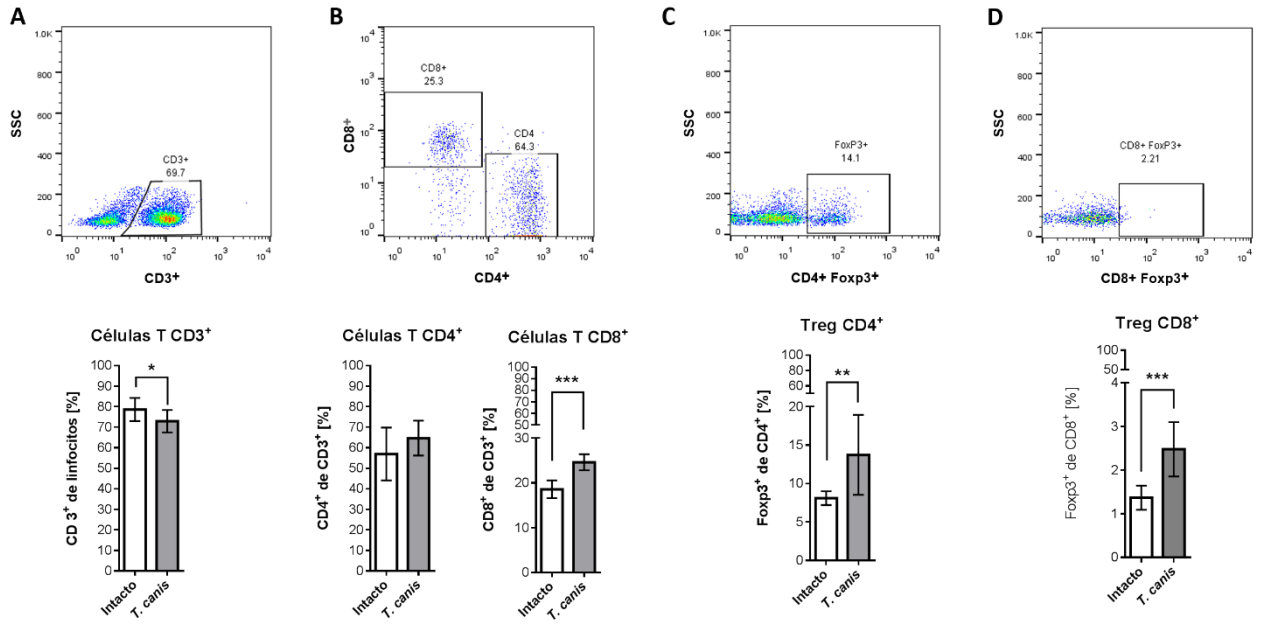

Figura 12. Proporciones de linfocitos T en GLP en la infección crónica con *T. canis*. A. LT (CD3⁺). **B.** LT cooperadores (CD4⁺) y T citotóxicos (CD8⁺). **C.** Treg CD4⁺Foxp3⁺. **D.** Treg

$CD8^+Foxp3^+$. En la parte superior se muestran los dot plots representativos de las poblaciones correspondientes. Las gráficas representan el promedio±DE de datos de dos experimentos (intacto, n=10; *T. canis*, n=10). La significancia estadística se calculó usando una Prueba de t (*, p≤0.05; **, p≤0.01; ***, p≤0.001).

6.1.5 La infección crónica por *T. canis* en ratones induce una respuesta sistémica de Tipo 2, una reguladora y una angiogénica

Para caracterizar la respuesta inmune sistémica en la infección crónica por *T. canis*, se midieron los niveles de citocinas de la respuesta Tipo 1 (TNF-α e IFN-γ), y Tipo 2 (IL-4, IL-5), la citocina reguladora IL-10 y el factor angiogénico VEGF.

Es de resaltar que en los animales infectados con *T. canis*, los niveles séricos de IFN-γ fueron menores (p=0.0128), mientras que las citocinas como IL-4, IL-5, IL-10 y VEGF tuvieron un incremento (p=0.0018; p=0.0035; p=0.0304; p=0.0110; respectivamente), comparado como los ratones intactos (Fig. 13). Por otro lado, no se observaron cambios significativos en los niveles de TNF-α.

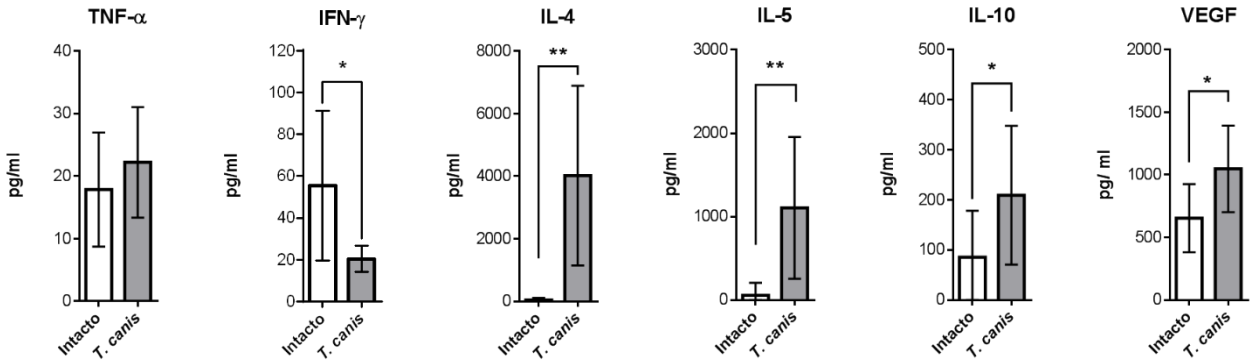

Figura 13. Análisis de citocinas séricas. La determinación de citocinas de la respuesta Tipo 1 (TNF-α e IFN-γ) y Tipo 2 (IL-4, IL-5, IL-10 y VEGF) se realizó mediante ELISA sándwich. Las gráficas indican datos de sueros obtenidos en dos experimentos independientes (intacto, n=10; *T. canis*, n=10). Las barras representan el promedio±DE de los niveles de citocinas (pg/ml de suero). La significancia estadística se calculó con una Prueba t (*, p≤0.05; **, p≤0.01; ***, p≤0.001).

En cuanto a los niveles de las citocinas esplénicas, en los animales infectados se detectó decremento de la citocina de la respuesta Tipo 1TNF-α (p=0.0060),. Al mismo tiempo, los niveles de las citocinas de la respuesta Tipo 2 como IL-4 y VEGF estuvieron incrementados (p=0.0369; p=0.0226), al igual que la citocina reguladora IL-10 (p=0.0102). De manera inesperada, la cantidad de IL-5 detectada en el bazo de los animales infectados fue menor (p=0.0019) a la que se detectó en los controles intactos (Fig. 14).

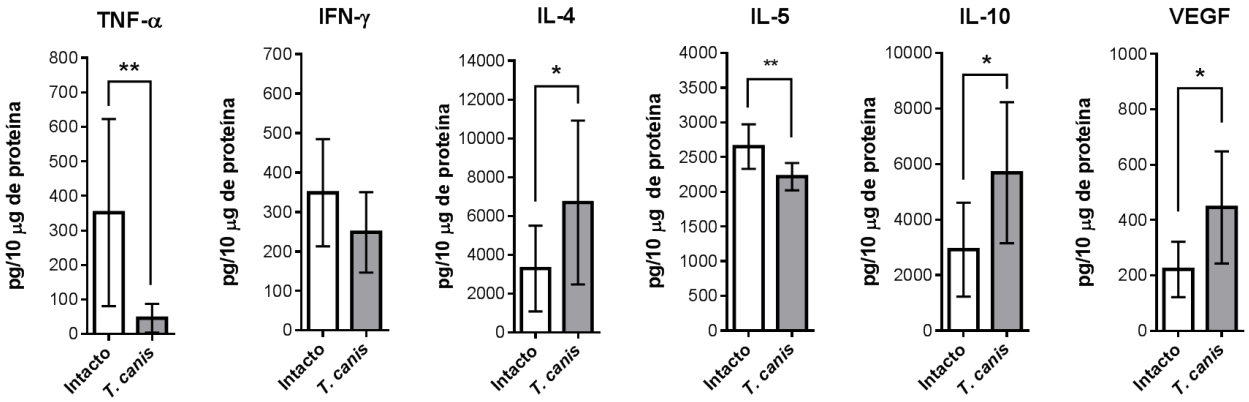

Figura 14. Análisls de citocinas esplénicas. La determinación de citocinas de la respuesta Tipo 1 (TNF-α e IFN-γ), Tipo 2 (IL-4, IL-5, VEGF) y reguladora (IL-10) se realizó mediante ELISA sándwich. Las gráficas indican datos de sueros obtenidos en dos experimentos independientes (intacto, n=10; *T. canis*, n=10). Las barras representan el promedio±DE de los niveles de citocinas (pg/ml de suero). La significancia estadística se calculó con una Prueba t (*, p≤0.05; **, p≤0.01).

6.1.5 Respuesta inmune sistémica a la infección crónica con *T. canis*

A pesar de que las larvas de *T. canis* se encontraron en todos los tejidos muestreados (pulmones, hígado, corazón, riñones, músculo esquelético y cerebro), la cantidad más grande de larvas se encontró en musculo y cerebro a los 49 d.p.i. (Fig. 15A).

La respuesta humoral característica asociada a la infección por *T. canis*, se evidenció a través de niveles elevados de IgG, IgG1 específicas, acompañado de la

expansión de LB en bazo y GLP, y el incremento de IL-4 en bazo y suero (Fig. 15B, C, D).

Por otro lado, en ambos órganos linfoides secundarios el porcentaje de LT citotóxicos $CD8^+$ y Treg fue mayor en los ratones infectados, no así las células NK o LT cooperadores en los que no se observaron cambios. Las dos poblaciones celulares que fueron diferentes entre los órganos linfoides fueron los macrófagos y los LTreg $CD8^+/FoxP3^+$. En bazo, la proporción de macrófagos se incrementó y los LTreg $CD8^+/FoxP3^+$ no cambiaron, mientras que en GLP los primeros disminuyeron y los segundos aumentaron (Fig. 15B, C).

Respecto al microambiente de citocinas esplénicas, se observó una respuesta Tipo 2, debido al aumento de IL-4, VEGF, acompañado por la disminución de la citocina Tipo 1, TNF-α y el incremento de IL-10. A pesar del incremento de otras citocinas Tipo 2 en bazo, la concentración de IL-5 fue menor en los animales infectados (Fig. 15B). Notablemente, los niveles séricos de todas las citocinas Tipo 2 fueron elevados en los ratones con *T. canis*, comparados con los intactos y solo en IFN-γ se detectó una disminución sérica (Fig. 15D).

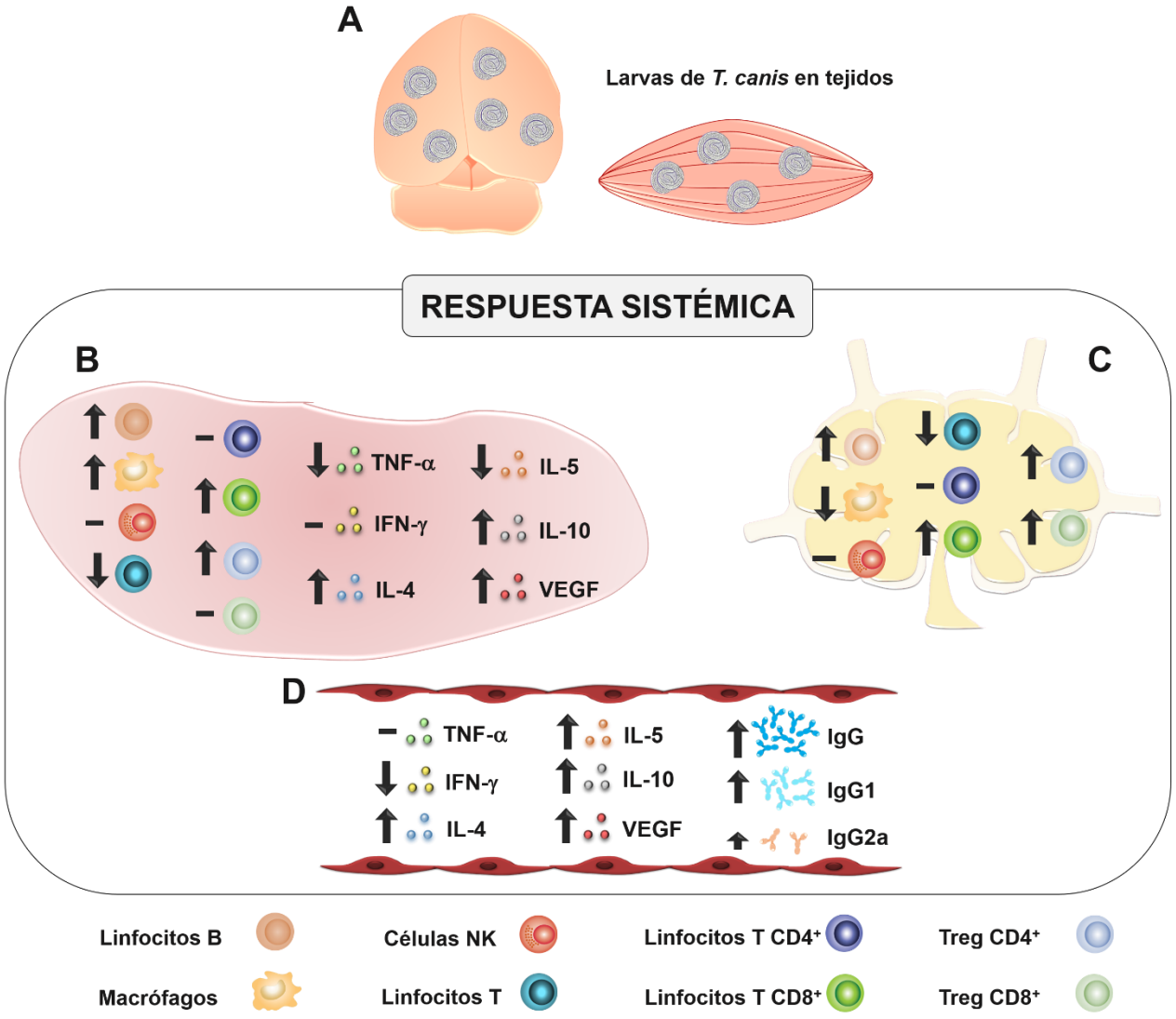

Figura 15. Respuesta inmune sistémica crónica a *T. canis*. **A.** Las larvas de T. *canis* migran a través de diferentes tejidos y se establecen principalmente en el cerebro y el músculo esquelético a los 49 d.p.i. **B.** En ratones infectados las proporciones esplénicas de LB, macrófagos, LT citotóxicos $CD8^+$, y $CD4^+$Treg aumentaron, mientras que los LT disminuyeron y las NK y LT cooperadores $CD4^+$ no cambiaron. Además en el bazo de los animales infectados, los niveles de TNF-α e IFN-γ (citocinas de la respuesta tipo 1) fueron menores que en los intactos, al mismo tiempo que IL-4, IL-10 y VEGF (citocinas de la respuesta tipo 2) se incrementaron, con excepción de la IL-5, que disminuyó. **C.** En los GLP los cambios en las proporciones de células fueron los mismos que en el bazo, con excepción de los macrófagos (que fue menor) y $CD8^+$Treg (que aumentó), ambos en ratones infectados. **D.** En el suero de los ratones infectados se

detectó una disminución en la cantidad de IFN-γ y un aumento de IL-4, IL-5, IL-10, VEGF, IgG, IgG1 e IgG2a anti-*T. canis*.

6.2 El patrón de distribución de las larvas de *T. canis* se modifica en ratones con tumor

La distribución de larvas se analizó en los diferentes tejidos de ratones infectados con *T. canis* y con tumor de células 4T1 (Fig. 16) y se observó una diferencia en la distribución de las larvas comparado con los animales infectados y sin tumor (Fig. 8). La mayor discrepancia fue el aumento en el número de larvas en músculo cardiaco, que en los animales con tumor no fue significativamente diferente al músculo esquelético y al cerebro, en comparación con los infectados (Fig. 16).

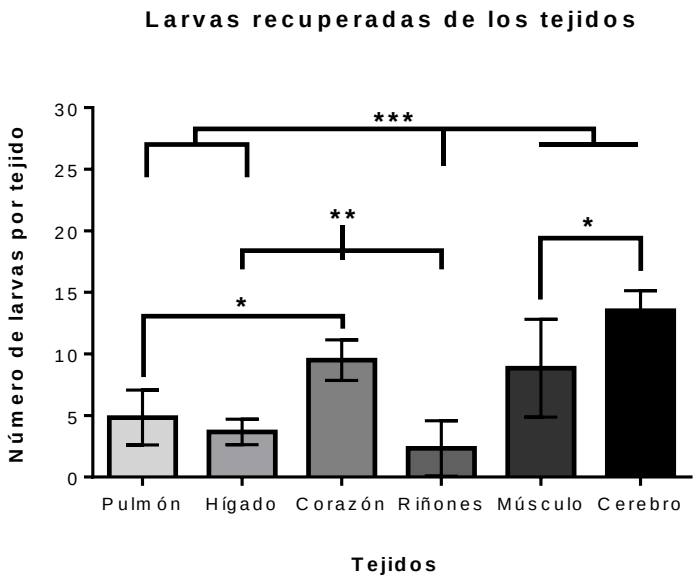

Figura 16. Larvas de *T. canis* recuperadas de tejidos de ratones infectados y con tumor. Número de larvas recuperadas de pulmones, hígado, corazón, riñones, músculo esquelético y cerebro de ratones BALB/c después de 49 días post-infección con 500 huevos larvados de *T. canis* y a los que se les indujo tumor de células 4T1. Las gráficas representan el promedio±DE de los datos de 5 animales infectados. La significancia estadística se calculó usando una ANOVA seguida por la prueba de Tukey (*, p≤0.05; **, p≤0.01; ***, p≤0.001).

6.3 La medición externa del tumor no refleja su volumen y peso real

Al inicio, se planteó el análisis de la progresión de los tumores 4T1, esto midiendo el diámetro mayor y menor de los tumores durante su crecimiento en los ratones. La medición se realizó por encima de la piel del ratón y una vez que el tumor se extrajo se midió también, con estas medidas se compararon diferentes fórmulas para obtener el volumen. Al final se realizó una correlación de los volúmenes obtenidos y el volumen real por desplazamiento de líquido (principio de Arquímedes) (Fig. 17).

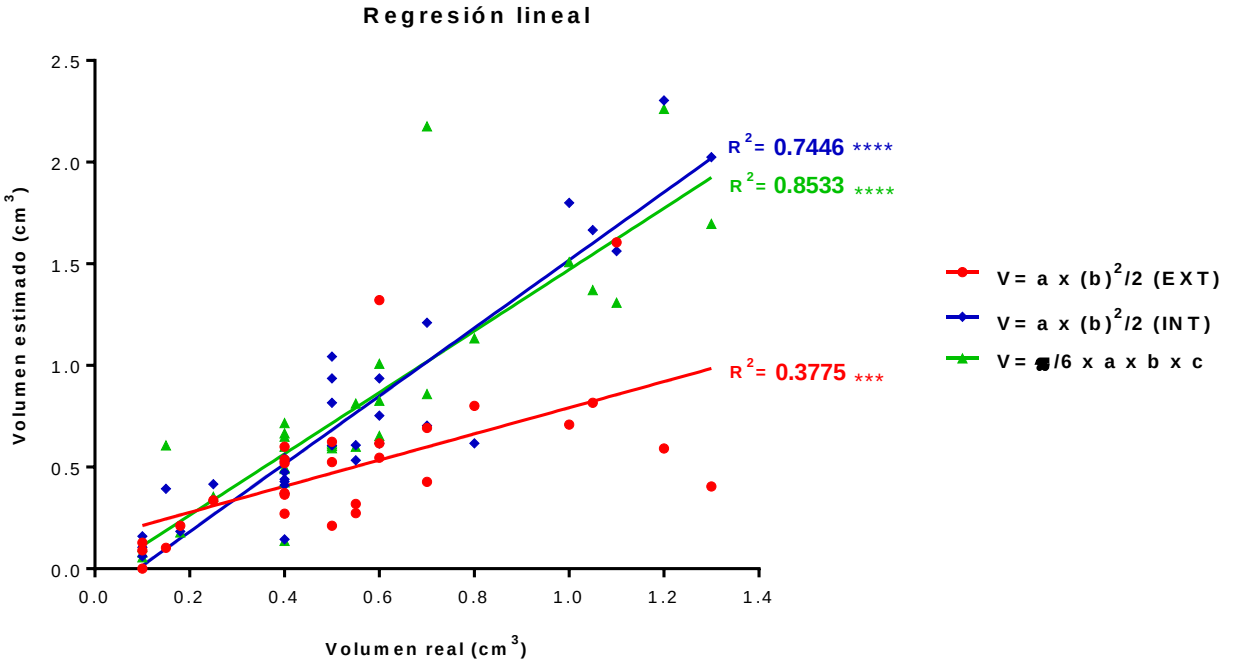

	Volumen real vs. V= a x (b)^2/2 (EXT)	Volumen real vs. V= a x (b)^2/2 (INT)	Volumen real vs. V= π/6 x a x b x c
P value			
P (two-tailed)	0.0002	< 0.0001	< 0.0001
P value summary	***	****	****
Significant? (alpha = 0.05)	Yes	Yes	Yes

Figura 17. Regresión lineal y correlación de los métodos para la medición del volumen tumoral. Los diferentes métodos de obtención del volumen de un cuerpo elipsoide se compararon, es decir, la fórmula que se incluye la medición del diámetro mayor y menor medidos antes de retirar el tumor (EXT, rojo) y al extirparlo (INT, azul), y la fórmula que contiene el diámetro mayor, el menor y la profundidad (verde), y su correlación con el volumen real.

Como se puede observar en la Figura 17, los volúmenes obtenidos de la medición sobre la piel del tumor empleando solo 2 diámetros y la fórmula V= a x (b)2/2, tienen un bajo coeficiente de determinación (R^2) comparados con el volumen real, por lo que aproximadamente 37% de las mediciones son iguales al volumen real. Esto concuerda con la detección del crecimiento de tumores que no conservan su forma elipsoide y que invaden tejidos adyacentes (Fig. 18). Por lo que el seguimiento del desarrollo tumoral con éste método se descartó debido a su baja exactitud de lo que ocurría con el verdadero tamaño tumoral.

Por otro lado, aunque no existen relaciones lineales exactas, los coeficientes de determinación de los otros dos métodos en los que se midió el tumor extirpado, fueron moderadamente representativos del volumen real. Empleando dos diámetros y la fórmula V= a x (b)2/2, aproximadamente 74% de las mediciones eran representativas, mientras que usando los tres diámetros y la fórmula V= π/6 x a x b x c, la fiabilidad de que sean iguales aumentó a 85% (Fig. 17).

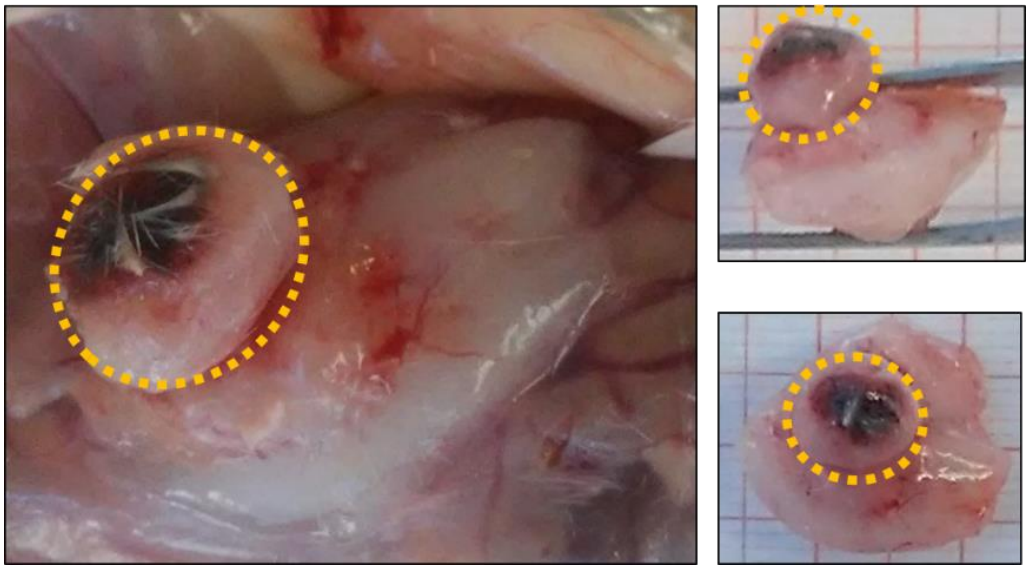

Figura 18. Fotografías representativas de un tumor con forma irregular. Se muestra la invasión a la cavidad peritoneal (derecha) de un tumor. Inicialmente se palpaba por encima de la piel como una masa elipsoide (líneas naranjas), pero al extirparlo se observó que crecía muy por debajo de la masa detectada inicialmente.

Adicionalmente, se realizó un análisis de regresión para determinar si la medición del peso (g) y el volumen real (cm^3) tienen una relación lineal y una correlación (Fig. 19). Y se determinó que el coeficiente de determinación es mayor al 95% por lo que, el volumen real es altamente representativo del peso. Después de los análisis anteriores, se decidió usar el peso como medida para comparar a los tumores de los animales intactos e infectados.

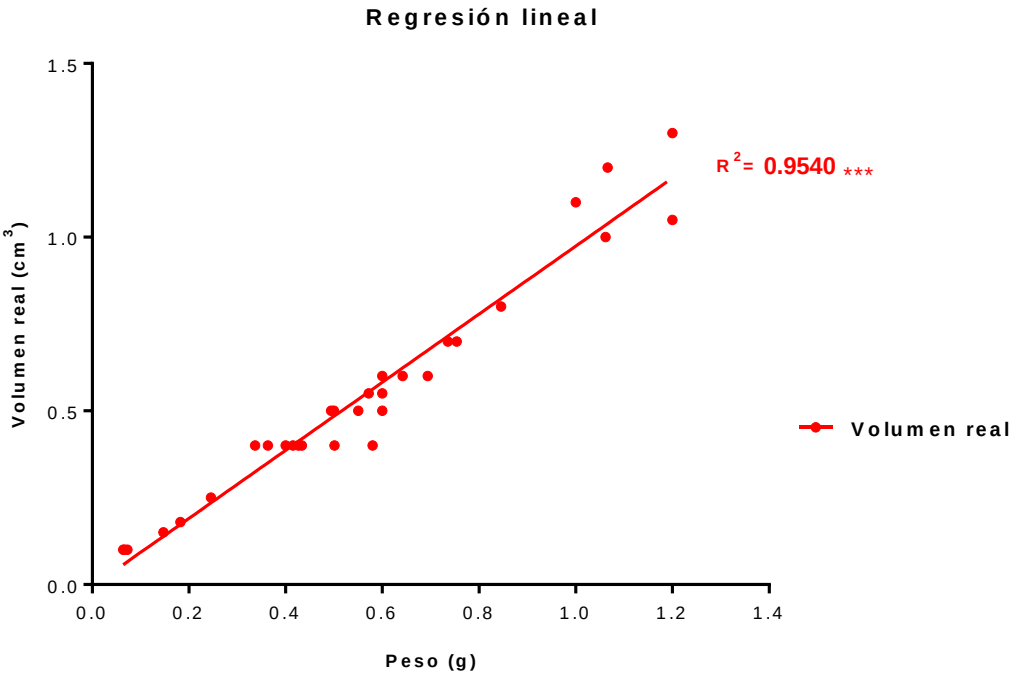

	Peso vs. Volumen real
P value	
P (two-tailed)	< 0.0001
P value summary	****
Significant? (alpha = 0.05)	Yes

Figura 19. Regresión lineal y correlación entre el volumen real y el peso de los tumores 4T1. Se determinaron las correlaciones entre el volumen real y el peso de los tumores.

6.4 Efecto de la infección por *T. canis* en el tamaño y microambiente inmune de los tumores mamarios

6.4.1 El desarrollo de tumores mamarios 4T1 se potencia por la infección

Un aumento significativo (p=0.0035) se observó en el tamaño y peso de los tumores obtenidos después de 28 días de la inyección de las células tumorales asociado a la infección crónica (Fig. 20). Los tumores fueron en promedio, de casi el doble de tamaño en los ratones infectados.

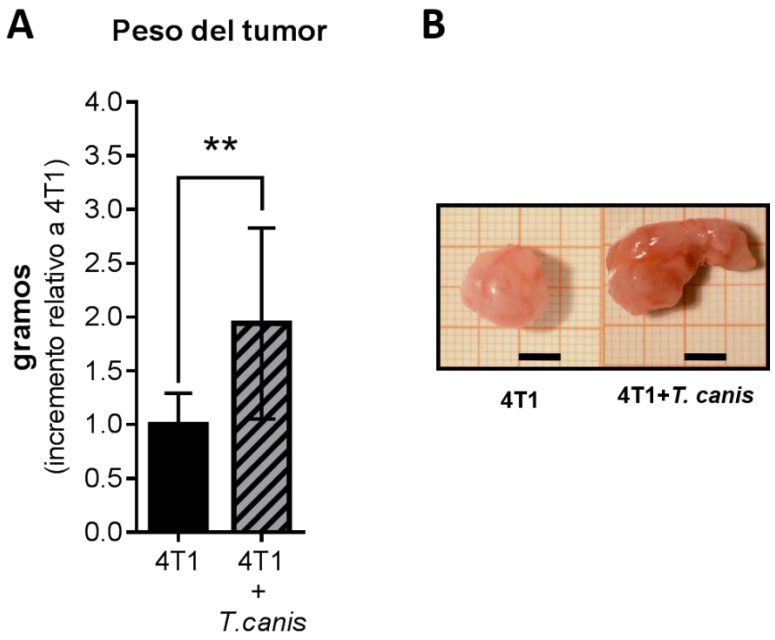

Figura 20. Tamaño y peso de tumores en animales controles e infectados. Peso de los tumores (izquierda). Fotografías representativas de los tumores de los ratones sin (4T1) y con infección (4T1+*T. canis*) (derecha). La barra negra equivale a 0.5 cm. Las gráficas representan el promedio ±DE de datos de los experimentos (4T1, n = 10; 4T1+*T. canis*, n = 10). La significancia estadística se realizó con una prueba de t (**, p≤0.01).

6.4.2 La infección aumenta la proporción de macrófagos en el tumor

La determinación de los porcentajes de macrófagos y células NK se realizó en el tumor. Como se observa en la Figura 21A, la proporción de macrófagos F4/80$^+$

aumentó en los ratones del grupo 4T1+*T. canis* (p=0.0004), en comparación de los controles sin infección (4T1). No se observaron diferencias significativas en las células NK (Fig. 21B) que estuvieron presentes en bajas proporciones en los tumores de ambos grupos.

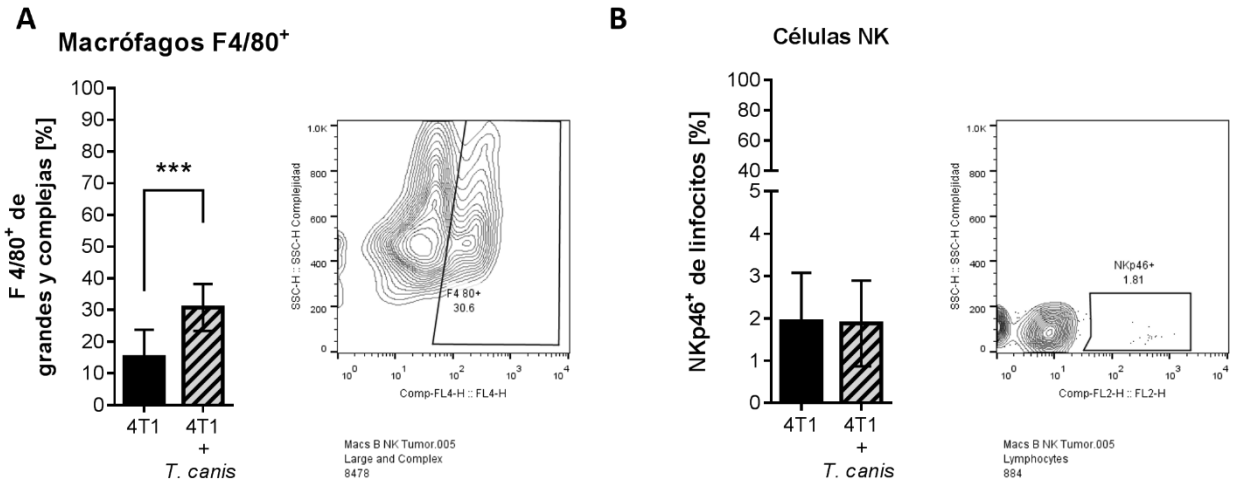

Figura 21. Cambios en las proporciones de células de la respuesta inmune innata en tumor. A. Frecuencias de macrófagos F4/80+ de células grandes y complejas. **B.** Frecuencias de células NK (NKp46+ de células de tamaño y complejidad medianas). Las gráficas representan el promedio±DE de datos de dos experimentos (4T1, n=10; 4T1+*T. canis*, n=10). A la izquierda se muestran los contour plots representativos de cada población. La significancia estadística se calculó usando una prueba de t (***, p≤0.001).

6.4.3 La proporción de células CD8+ citotóxicas se reduce en los tumores de los ratones infectados.

La determinación de las proporciones de LT (CD3+), LT cooperadores (CD4+), LT citotóxicos (CD8+), Treg CD4+ y Treg (CD8+) se realizó en el tumor (Fig. 22). Un aumento en el porcentaje de LT CD3+ (p=0.0334) (Fig. 22A) y una disminución en las proporciones de LT citotóxicos (p= 0.0279) se observaron en el grupo 4T1+*T. canis* (Fig. 22C), mientras que en las otras subpoblaciones no se detectaron diferencias significativas.

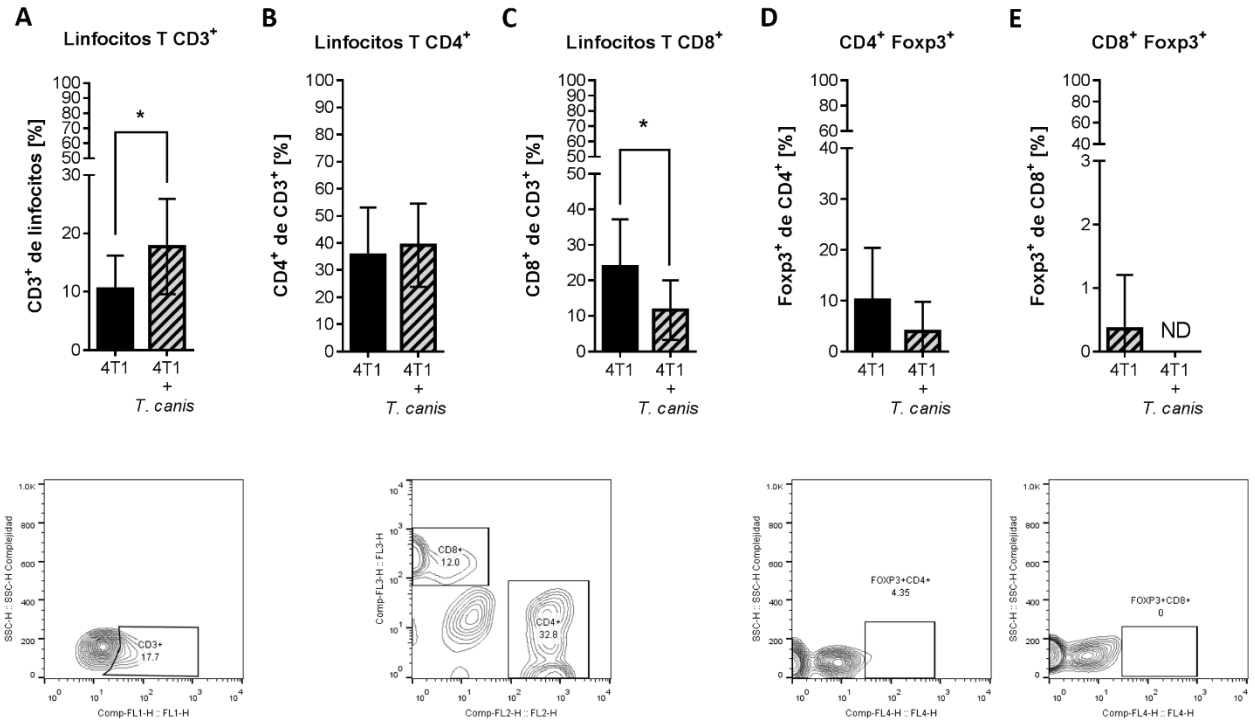

Figura 22. Proporciones de linfocitos T tumorales. **A.** LT ($CD3^+$). **B.** LT cooperadores ($CD4^+$). **C.** LT T citotóxicos ($CD8^+$). **D.** Treg $CD4^+Foxp3^+$. **E.** Treg $CD8^+Foxp3^+$. En la parte inferior se muestran los dot plots representativos de las poblaciones correspondientes. Las gráficas representan el promedio±DE de datos de los experimentos (4T1, n=10; 4T1+*T. canis*, n=10). La significancia estadística se calculó usando una Prueba de t (*, p≤0.05).

6.4.4 La proporción de linfocitos B $CD19^+$ tumorales aumenta en los ratones infectados.

El análisis de los linfocitos B tumorales se realizó (Fig. 23), a pesar de que es una población escasa en los tumores de células 4T1, en los animales con infección con *T. canis*, se detectó incremento significativo (p=0.0042).

6.4.5 El microambiente tumoral está enriquecido con citocinas de la respuestas tipo 2, reguladora y angiogénica, debido a la infección crónica con *T. canis*.

La citocinas en el microambiente tumoral son importantes reguladores de la respuesta inmune local. Por esto, se determinó la expresión intratumoral de citocinas

de la respuesta Tipo 1 (TNF-α and IFN-γ), Tipo 2 (IL-4, IL-5), reguladora (IL-10) y angiogénica (VEGF) (Fig. 24). El ambiente de citocinas en el tumor de los ratones infectados está polarizado a una respuesta tipo 2, debido al aumento en la IL-4 (p= 0.0111), además del factor angiogénico, VEGF (p= 0.0003), aunque la expresión de IL-5 no presentó cambios significativos estadísticamente. El aumento en las citocinas Tipo 2 estuvo acompañado con la disminución en los niveles de TNF-α (p= 0.0006). Así mismo, se detectó aumento en IL-10 (p= 0.0456) (Fig. 24), lo que sugiere un microambiente tumoral regulador.

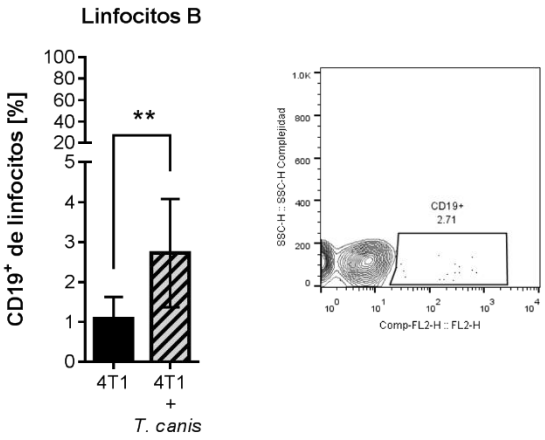

Figura 23. Proporciones de linfocitos B tumorales. A la derecha se muestra el contour plot representativo de los linfocitos B CD19+ en tumor. La gráfica representa el promedio±DE de datos de los experimentos (4T1, n=10; 4T1+*T. canis*, n=10). La significancia estadística se calculó usando una Prueba de t (*, p≤0.05; ***, p≤0.001).

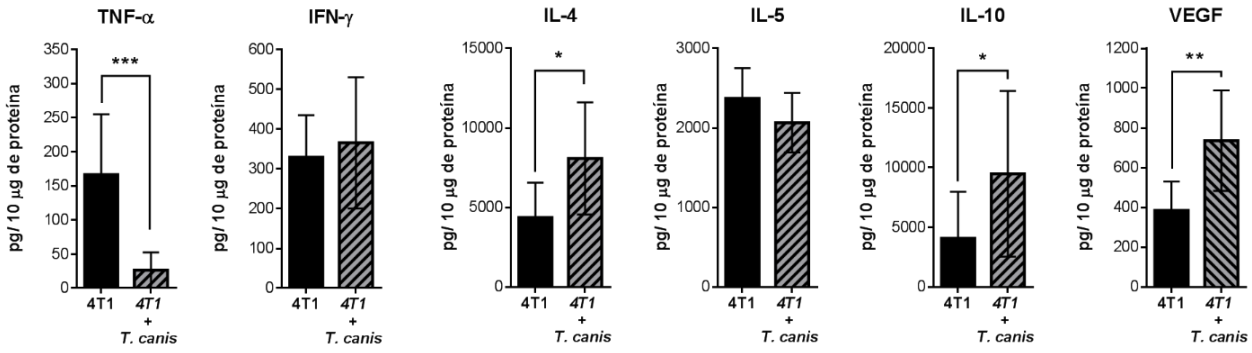

Figura 24. Análisis de la expresión de citocinas en el microambiente tumoral. Determinación por ELISA sándwich de las citocinas TNF-α, IFN-γ, IL-4, IL-5, IL-10 y VEGF).

La gráfica representa el promedio±DE de datos de los experimentos (4T1, n=10; 4T1+*T. canis*, n=10). La significancia estadística se calculó usando una prueba t (*, p≤0.05; **, p 0.01; ***, p≤0.001).

6.5 Efecto de la infección por *T. canis* y la inducción de los tumores mamarios en la respuesta inmune sistémica

6.5.1 La respuesta humoral en contra de *T. canis* se mantiene en los ratones con tumor.

Respecto a la respuesta inmune humoral, además de la esplenomegalia característica asociada a la inducción del tumor, se detectó aumento en el peso de los bazos de los animales infectados en comparación con los no infectados (p<0.0001) (Fig. 25A).

Por otro lado, al igual que en los animales infectados sin tumor (grupo *T. canis*), se presentó aumento en los niveles de anticuerpos específicos (IgG) en el grupo 4T1+*T. canis*, comparado con el grupo 4T1 (p<0.0001) (Fig. 25B). Por último, en el grupo 4T1+*T. canis*, la proporción de LB CD19⁺ en bazo, fue mayor que en el grupo 4T1 (p=0.0002) (Fig. 25C). No se detectaron diferencias significativas en el porcentaje de las células B de los GLP (Fig. 25D). En conjunto, estos resultados demostraron que la respuesta inmune humoral se conservó aun con la inducción del tumor.

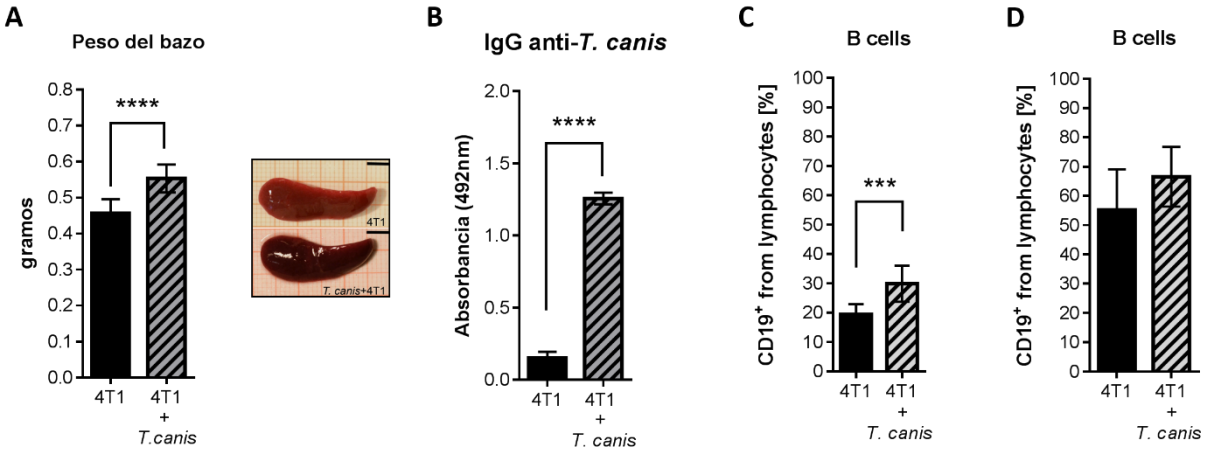

Figura 25. Respuesta humoral sistémica en ratones con tumor e infectados con *T. canis*. **A.** Peso del bazo (izquierda) y fotografías representativas del bazo (derecha) de los animales con tumor (4T1) e infectados y con tumor (4T1+*T. canis*). La barra negra equivale a 0.5 cm. **B.** Niveles de IgG anti-*T. canis.* Análisis de citometría de flujo de los

porcentajes de LB CD19+ del bazo (**C**) y GLP (**D**). Las gráficas representan el promedio ±DE de datos de dos experimentos (4T1, n=10; 4T1+*T. canis*, n=10). La significancia estadística se realizó con una prueba de t (***, p≤0.001; ****, p≤0.0001).

6.5.2 En los ratones con tumor, la infección no modifica las proporciones de células innatas en órganos linfoides secundarios

Para determinar si las modificaciones en las proporciones esplénicas y en los GLP inducidas por la infección con *T. canis* están presentes en los ratones con tumor, se realizó el análisis de las diferentes poblaciones celulares innatas y adaptativas. En ambos casos la composición de las proporciones de estas células fue similar entre grupos (Fig. 26 y 27).

En el estudio de los porcentajes de macrófagos F4/80+ y células NK en el bazo y los GLP de los ratones con tumor e infección (Fig. 26), no se observaron diferencias estadísticamente significativas en ninguno de los órganos linfoides secundarios que se analizaron.

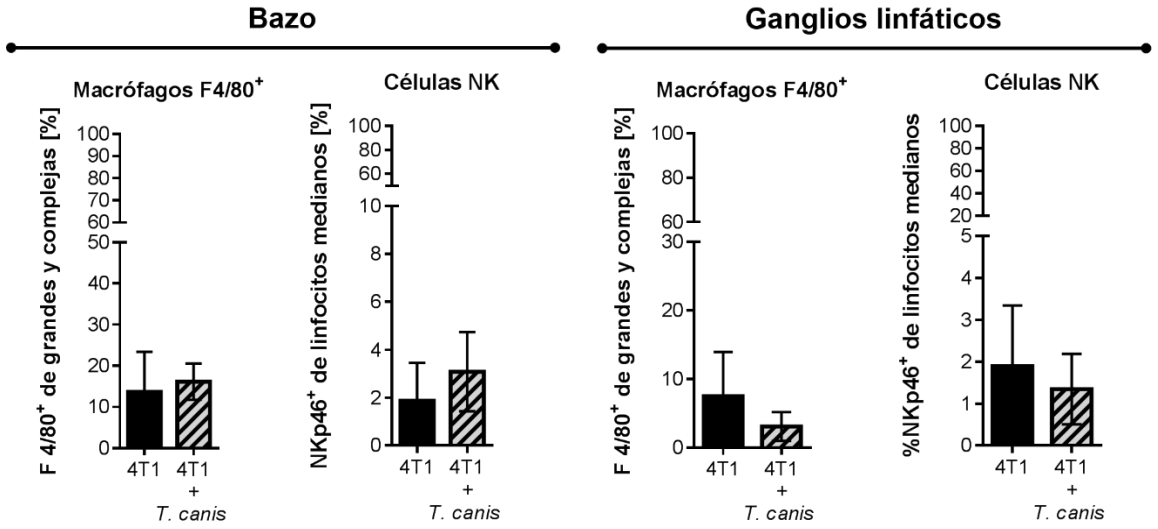

Figura 26. Proporciones de células de la respuesta inmune innata en bazo y GLP. Frecuencias de macrófagos (F4/80+ de células grandes y complejas) y de células NK (NKp46+ de células de tamaño y complejidad medianas). Las gráficas representan el promedio±DE de datos de los experimentos (4T1, n=10; 4T1+*T. canis*, n=10). La significancia estadística se calculó usando una Prueba de t.

6.5.3 La infección modifica las proporciones de algunas poblaciones celulares en bazo y GLP en ratones con tumor

Debido a que la infección alteró diferentes poblaciones de células adaptativas en el bazo y los GLP, los porcentajes de linfocitos T, linfocitos T cooperadores CD4+T, citotóxicos CD8+ y Treg Foxp3+ se evaluaron en los animales a los que también se les indujo el tumor mamario (Fig. 27). No se observaron cambios significativos en las células esplénicas (Fig. 27 panel superior) y en los GLP de ratones infectados con *T. canis*, la proporción de Treg Foxp3+CD4+ (p=0.0162) se incrementó comparado con el grupo que solo tenía tumor. La infección indujo aumento en el porcentaje de LT CD8+ (Fig. 12) en GLP de los ratones del grupo 4T1+*T. canis,* esta población tuvo decremento (p=0.0137) en comparación del grupo control (4T1) (Fig. 27 panel inferior).

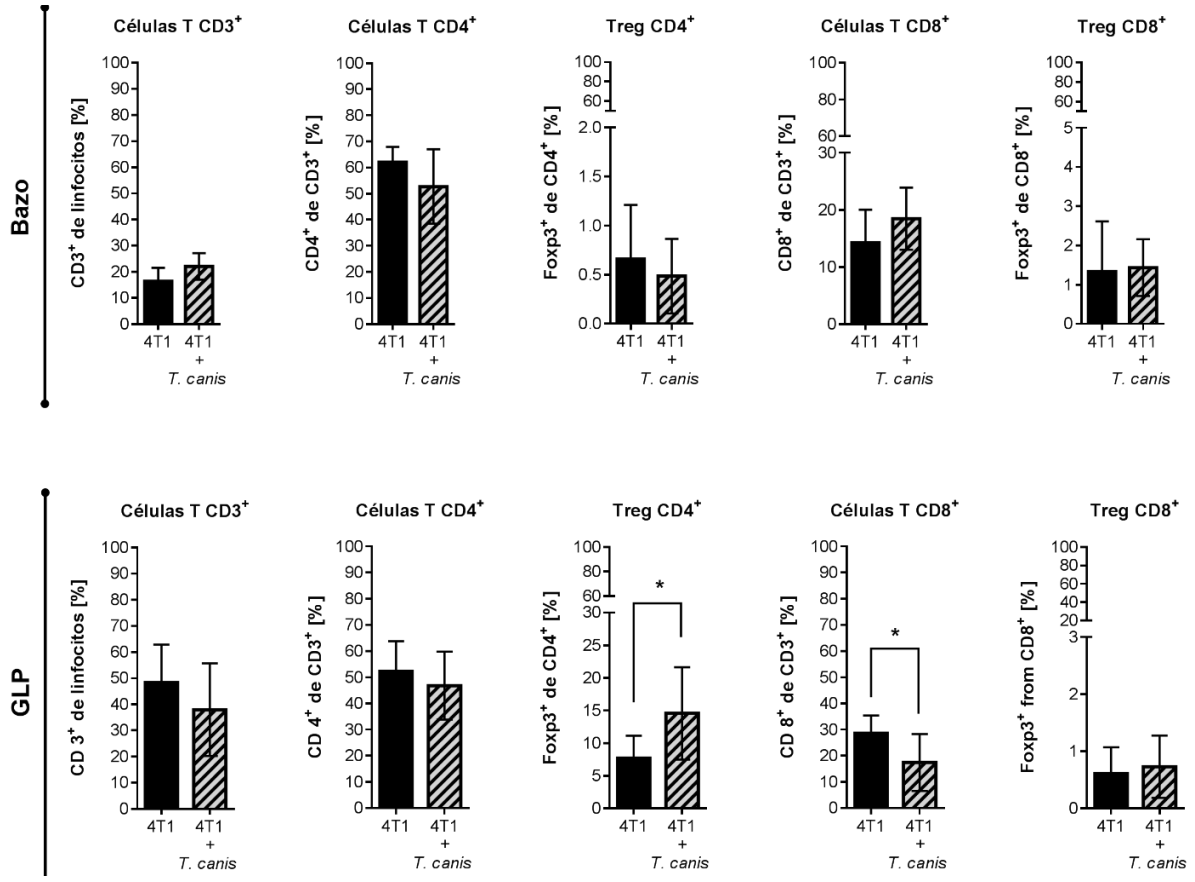

Figura 27. Proporciones de linfocitos T en bazo y GLP. Se muestran los porcentajes de linfocitos T (CD3+), LT cooperadores (CD4+), T citotóxicos (CD8+), LT reguladores (Treg CD4+Foxp3+ y CD8+Foxp3+) en bazo (panel superior) y GLP (panel inferior) de los ratones con tumor (4T1) y con tumor e infectados (4T1+*T. canis*). Las gráficas

representan el promedio±DE de datos de los experimentos (4T1, n=10; 4T1+*T. canis*, n=10). La significancia estadística se calculó usando una Prueba de t (*, p≤0.05).

6.5.4 El VEGF sistémico aumenta en los animales con tumor e infectados

La expresión sistémica de factores solubles se evaluó para determinar si los cambios en el microambiente tumoral están relacionados con la respuesta sistémica (Fig. 28). En el bazo la citocina de la respuesta Tipo 1, TNF-α, disminuyó en los animales infectados (p=0.0311) (Fig. 28 panel superior). Respecto a las citocinas de la respuesta inmune Tipo 2, aunque la IL-4 aumentó en los ratones infectados, este cambio no fue estadísticamente significativo, a diferencia de la disminución en los niveles de IL-5 (p = 0.0002) y el incremento en VEGF (p < 0.0001) (Figura 28 panel superior). Los factores solubles medidos en el suero de los ratones con tumor tuvieron un comportamiento similar cuando lo animales fueron infectados, con excepción del incremento en VEGF sérico en el grupo 4T1+*T.canis* (p=0.0030) (Fig. 28 panel inferior).

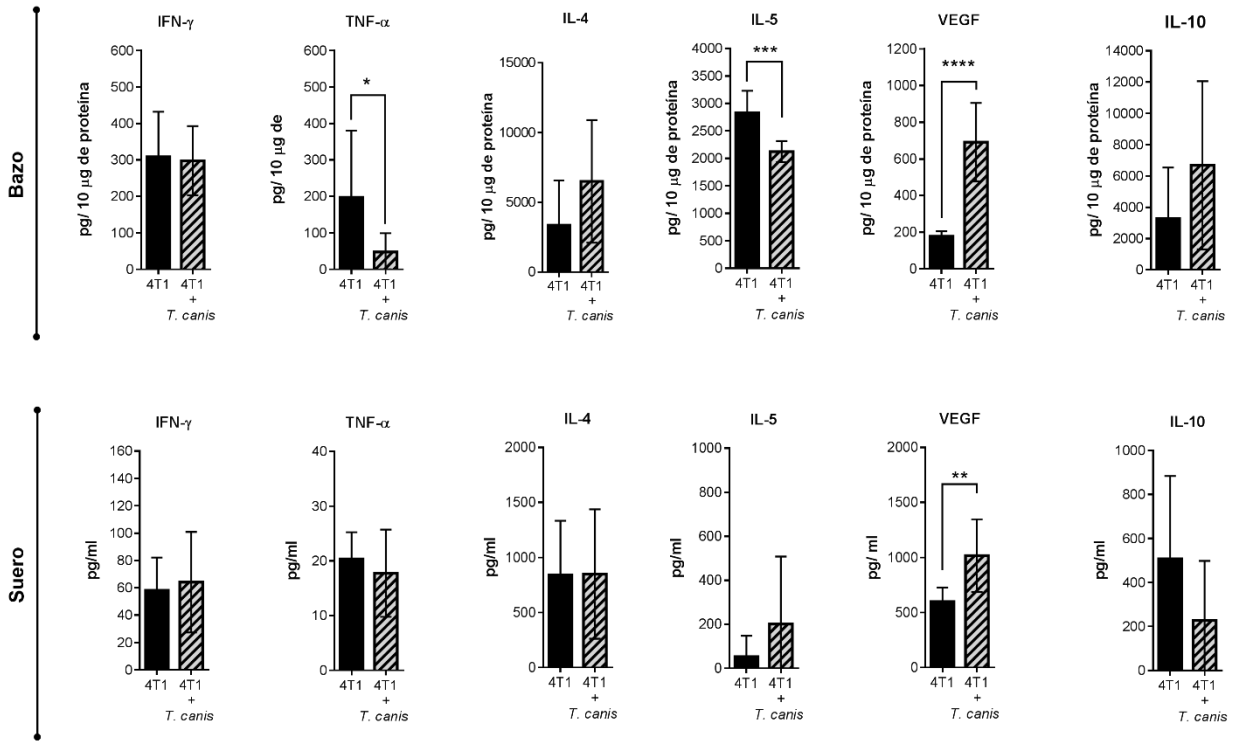

Figura 28. Análisis de la expresión sistémica de citocinas séricas y esplénicas. Determinación de citocinas de la respuesta Tipo 1 (TNF-α e IFN-γ), Tipo 2 (IL-4 e IL-5), reguladora (IL-10) y angiogénica (VEGF). Las gráficas indican datos de sueros y

proteína esplénica (4T1, n=10; 4T1+*T. canis*, n=10). Las barras representan el promedio±DE de los niveles de citocinas (pg/ml de suero o pg/10 μg de proteína esplénica). La significancia estadística se calculó con una Prueba t (*, p≤0.05; **, p≤0.01; ***, p≤0.001; ****, p≤0.001).

6.5.5 Respuesta inmune a la infección crónica con *T. canis* y la inducción de tumor mamario

En el tumor, las proporciones de macrófagos y LB aumentaron y las de LT CD8⁺ disminuyeron (Fig. 29). Además, se evidenció un claro microambiente con aumento de IL-4, asociado a la disminución de TNF-α y un medio local regulador por el incremento de IL-10. La respuesta humoral asociada a la infección por *T. canis*, se conservó después de la inducción del tumor mamario, representada por la expansión de LB CD19⁺ en bazo y esplenomegalia. En el bazo incrementó el VEGF y el TNF-α e IL-5 disminuyeron (Fig. 29).

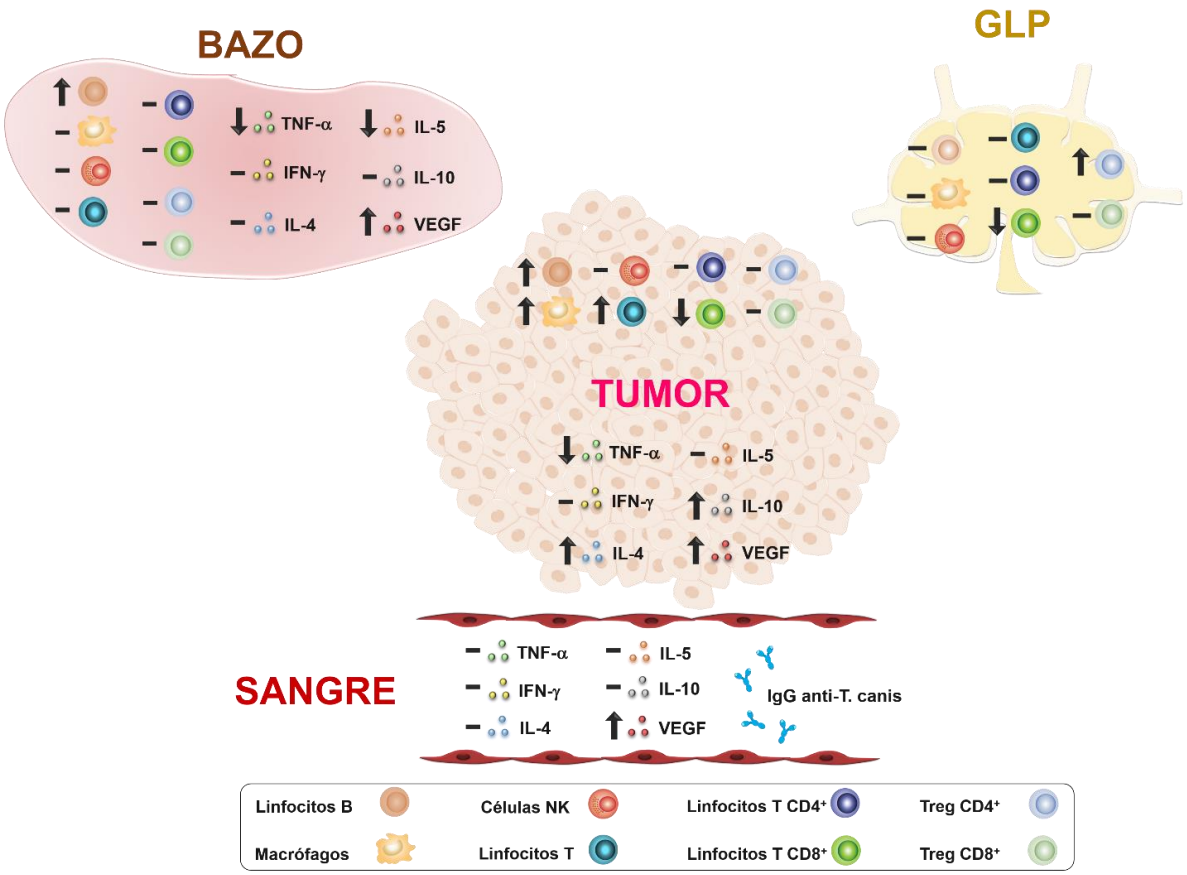

Figura 29. Respuesta inmune local y sistémica en animales con tumor e infectados con *T. canis*.

6.6 Efecto de la infección por *T. canis* en la metástasis de tumores mamarios

6.6.1 La metástasis pulmonar se ve aumentada en los animales infectados

En los pulmones se observaron más lesiones macroscópicas sugerentes de metástasis en los ratones 4T1+*T. canis*, mientras que en hígado no se observaron lesiones macroscópicas hepáticas en los animales con tumor e infección (Fig. 30).

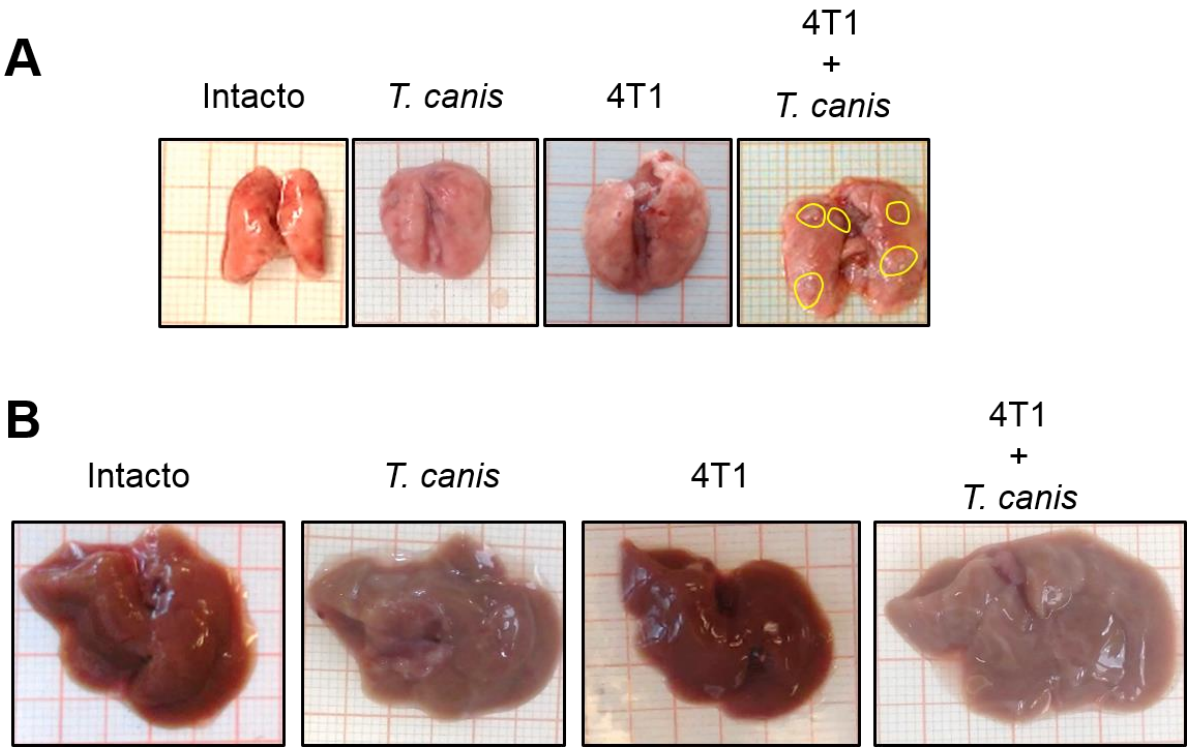

Figura 30. Metástasis macroscópica en pulmones de los animales infectados. Imágenes representativas de pulmones de animales con tumor (4T1) y con tumor e infectados (4T1+*T. canis*), de pulmones (**A**) e hígado (**B**). Las líneas amarillas delimitan las lesiones sugerentes de tumor.

6.7 Efecto de la inyección de TES en el tamaño del tumor, el microambiente inmune local, la respuesta inmune sistémica y la metástasis

6.7.1 La inyección intratumoral de TES no aumenta el tamaño del tumor

Debido a que la respuesta inmune del hospedero a las larvas de *T. canis* está mediada por los TES, se incluyeron los grupos de animales a los que se les inyectaron TES intratumoralmente y su vehículo (PBS 1x). Aunque visualmente los tumores parecían más grandes (Fig. 31 derecha), no se obtuvieron diferencias significativas entre el peso de los tumores de los grupos de animales inyectados con TES y con vehículo (Vh) (Fig. 31 izquierda).

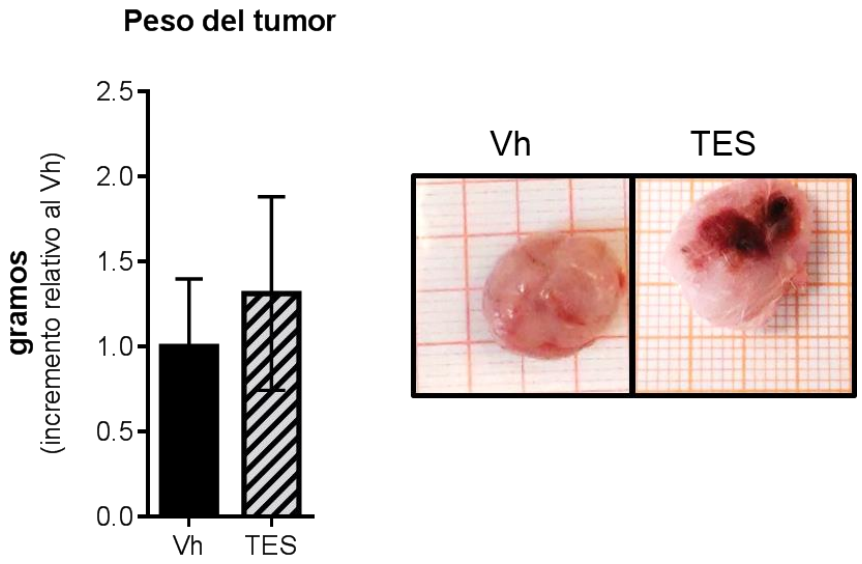

Figura 31. Peso y tamaño de las masas tumorales con inyección intratumoral de TES. A la izquierda se muestra el peso promedio de los tumores, y a la derecha se muestran las fotografías demostrativas de los grupos intacto y a los que se les inyectó intratumoralmente, el vehículo (Vh) y los antígenos de secreción y excreción (TES). Las barras representan el promedio±DE (Vh, n = 5; TE, n= 8).

6.7.2 La inyección intratumoral de TES no modifica la respuesta inmune, pero aumenta las metástasis macroscópicas

La medición de las subpoblaciones se realizó en tumor, bazo y GLP de los animales a los que se les administró intratumoralmente el vehículo y los TES. En ninguna de las subpoblaciones medidas, macrófagos (F4/80$^+$), NK, LT (CD3$^+$), LT cooperadores (CD4$^+$), LT citotóxicos (CD8$^+$), TregCD4$^+$, Treg CD8$^+$ y LB (CD19$^+$), de los tres tejidos analizados se encontraron diferencias significativas entre las proporciones de células (Fig. 32).

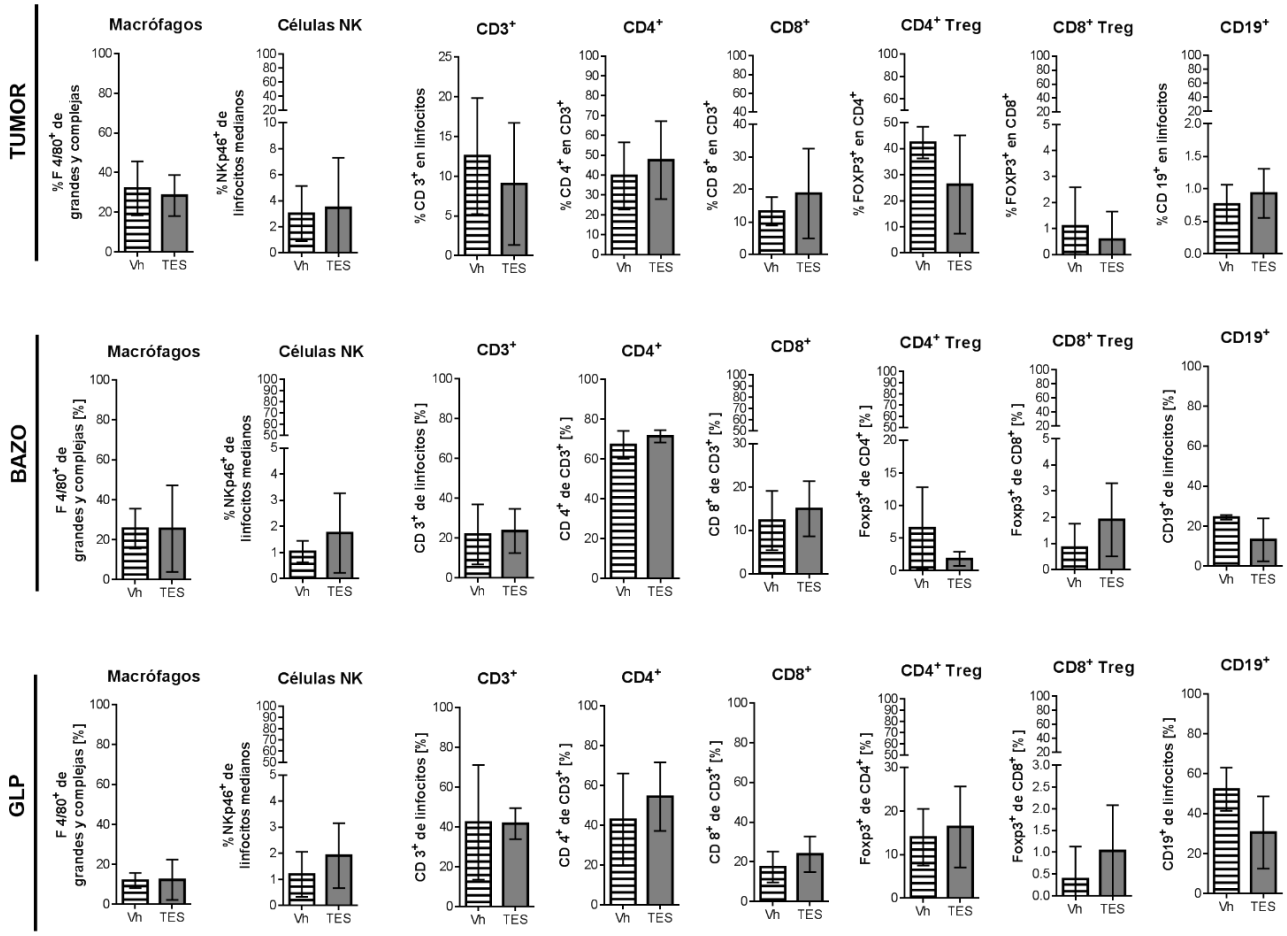

Figura 32. Subpoblaciones de células en tumor, bazo y GLP de animales con inyección intratumoral con TES. Determinación de la frecuencias de macrófagos (F4/80$^+$), células NK (NKp46$^+$) LT (CD3$^+$), LT cooperadores (CD4$^+$), LT citotóxicos (CD8$^+$), TregCD4$^+$, Treg CD8$^+$ y LB (CD19$^+$). Las barras representan el promedio±DE (Vh, n = 5; TES, n= 8).

A pesar de que la diferencia en el tamaño de los tumores a los que se les inyectaron los TES no fue significativa, se detectaron lesiones macroscópicas pulmonares sugerentes de metástasis en los pulmones de los animales del grupo TES (Fig. 33). Macroscópicamente en el hígado de los animales de los dos grupos con tumor (4T1 y 4T1+*T. canis*), no se observaron lesiones.

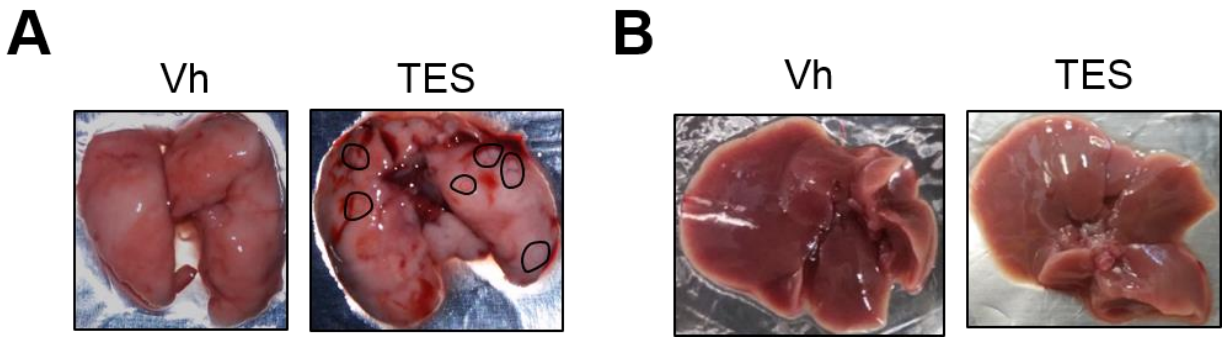

Figura 33. Metástasis macroscópica en pulmón de los animales a los que se les inyectaron los TES. Fotografías representativas de pulmones (A) e hígado (B) de animales de los grupos vehículo (Vh) y los antígenos de secreción y excreción de *T. canis* (TES). Las líneas delimitan las lesiones sugerentes de metástasis.

6.8 Interacciones inmunes asociadas a la promoción del desarrollo tumoral debido a la infección crónica con *T. canis* en ratones

En el microambiente del tumor de los ratones infectados con *T. canis* (Fig. 34A) las poblaciones encontradas en mayor proporción como los macrófagos y los linfocitos B pueden promover su crecimiento. Por ejemplo, los macrófagos como MAA pueden producir IL-4, IL-10 y VEGF (Fig. 34B). Estos factores solubles a su vez tienen efectos sobre otras células, así, la IL-4 (Fig. 34C) puede inhibir la generación de LTh1 productores de TNF-α e INF-γ, citocinas que promueven citotoxicidad de los LT $CD8^+$. Conjuntamente, la IL-4 fomenta el cambio de fenotipo a LTh2, que producen más IL-4 e IL-10, además de IL-5, la cual es característica de la respuesta inmune sistémica a la infección por *T. canis* (Fig. 13 y 14). Otra de la citocinas producidas por los MAA, la IL-10 (Fig. 34D) fomenta el cambio de fenotipo de LB a Breg y la generación de células Treg, ambas productoras de IL-10. Además esta interleucina inhibe la actividad citotóxica y la proliferación de los LT $CD8^+$. Finalmente, el VEFG (Fig. 34E) fomenta la formación de vasos sanguíneos que alimentan al tumor y promueven la metástasis a órganos como hígado y/o pulmones. Así, en el microambiente tumoral el aumento de macrófagos y LB puede favorecer el aumento su tamaño y debido al incremento de IL-4, IL-10 y VEGF tumoral y la disminución local de TNF-α, éstas poblaciones pueden poseer un fenotipo de MAA y Breg (Fig. 34A).

Por otro lado, los LT $CD8^+$ pueden tener capacidad citotóxica para eliminar células tumorales, y el porcentaje reducido en el tumor de los animales infectados (Fig. 34A) posiblemente influyó también en el desarrollo de éste. Aunado a la disminución de los LT $CD8^+$ en el tumor, se observó decremento en esta población en los GLP que puede estar asociada con el aumento de LTreg, que inhiben localmente la generación de los LT $CD8^+$ (Fig. 34F).

A nivel sistémico el incremento en suero sanguíneo de IgG específica contra *T. canis* se mantuvo en los animales con tumor (Fig. 34G), así como de VEGF sérica y esplénica. También en bazo se observaron cambios asociados a la infección como la disminución de IL-5 y TNF-α (Fig. 34H).

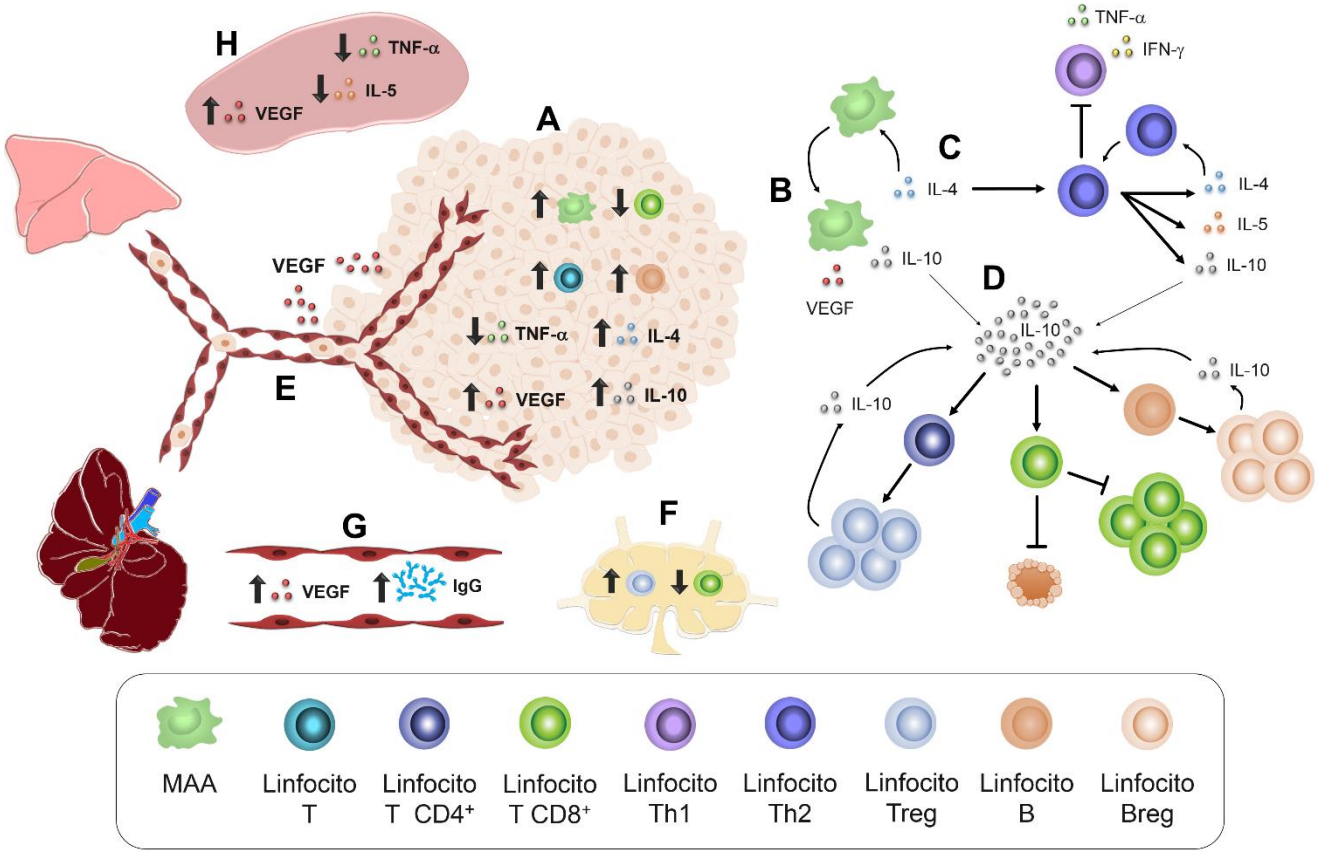

Figura 34. Interacciones inmunes asociadas a la promoción del desarrollo tumoral asociado a la infección crónica con *T. canis* en ratones. A. En el microambiente tumoral, el aumento en la proporción de macrófagos F4/80$^+$ (**B**) que pueden tener un fenotipo de MAA producen IL-4 (**C**) que influye en la generación de LTh2 y la inhibición del cambio de fenotipo a Th1. **D**. La IL-10 puede fomentar aumento en Breg, Treg y disminuir la capacidad citotóxica y proliferativa de los LT CD8$^+$. **E**. El incremento tumoral y sistémico de VEGF puede fomentar la formación de vasos sanguíneos y a la vez la metástasis a hígado y/o pulmones. **F**. Aumento de Treg y la disminución de LT CD8$^+$ en los GLP. **G**. A nivel sérico, se observó incremento de IgG anti-*T. canis* y de VEGF. **H**. En el bazo solamente se detectó un aumento de VEGF y disminución de TNF-α e IL-5.

V. Discusión

Durante años la investigación del cáncer se ha concentrado en una aproximación centrada en las células, basada en las vías de señalización y los cambios en el DNA (Law et al., 2017). Todo esto, con el principal objetivo de encontrar la "cura para el cáncer" y proporcionar tratamientos más personalizados. Este tipo de investigación ha arrojado diferentes avances en la biología celular y tratamiento del de esta enfermedad, pero no se ha prestado la misma atención a otros aspectos del desarrollo del cáncer, como lo son sus factores de riesgo. Estos involucran las interacciones entre células, su microambiente e incluso con otros organismos. Dentro de estas interacciones el sistema inmune posee un papel primordial en el desarrollo tumoral que puede ser controlado si los mecanismos de inmunovigilancia funcionan adecuadamente. Tanto las células tumorales, las inmunes y otros organismos patógenos co-evolucionaron mediante interacciones que pueden o no favorecer el desarrollo de morbilidades.

Los organismos parásitos regulan la respuesta inmune del hospedero para favorecer la supervivencia de estos. Esta regulación ha sido documentada y es mediada por los productos de excreción y secreción de los helmintos, que promueven que poblaciones como los MAA, Tregs, Bregs y factores solubles sean producidos por estas células, para dirigir esta respuesta (McSorley and Maizels, 2012). Por un lado, la regulación de la respuesta inmune permite la supervivencia de los helmintos, pero también puede favorecer la progresión del tumor. En el presente trabajo se estudió el efecto de la infección crónica con *T. canis* en el desarrollo de tumores mamarios murinos inducidos con células 4T1, debido a que el sistema inmune de los ratones BALB/c no está comprometido como en otros modelos, lo que permitió la evaluación de la respuesta inmune local (tumor) y la sistémica.

Para estudiar la fase crónica sistémica de la infección se seleccionó como tiempo final los 49 d.p.i., debido a que en este punto la fase miotrópica-neurotrópica se ha establecido (Abo-Shehada and Herbert, 1984; Epe et al., 1994; Strube et al., 2013) y porque entre 42-54 d.p.i. las larvas están produciendo más activamente TES (Rodríguez-Caballero et al., 2017). Se ha demostrado que la línea singénica de ratones BALB/c es altamente susceptible a la infección con *T. canis*. En estos animales las larvas migran al cerebro desde el tercer día post-infección y se pueden encontrar en el cerebro y en la musculatura (Epe et al., 1994; Resende et al., 2015). Como se esperaba a los 49 d.p.i. la mayoría de las larvas se establecieron en el cerebro y el músculo esquelético. Sin embargo, también se encontraron en los otros órganos como pulmones, hígado, riñones y corazón.

La respuesta humoral a la infección con *T. canis* es el resultado de interacciones complejas entre las células inmunes, citocinas y el parásito. Trabajos previos reportan esplenomegalia dependiente de la dosis de HL administrada (Kayes et al., 1985) e incremento en los niveles de anticuerpos anti-*T. canis* en ratones con infección crónica (Bowman et al., 1987; Pinelli et al., 2007). Diferentes estudios reportan el uso de 500 HL como única dosis de administración (Bowman et al., 1987; Oshima, 1961; Pinelli et al., 2005). Y aunque en el presente estudio solo determinamos un punto temporal (49 d.p.i.), la esplenomegalia y los títulos elevados de IgG anti-*T. canis* se detectaron al administrar 500 HL, lo cual a pesar de esta limitación de una sola medición en el tiempo y dosis, los datos obtenidos contribuyen al entendimiento de la respuesta inmune en la infección crónica por *T. canis* en ratones.

Respecto a la producción de anticuerpos específicos, se ha descrito la asociación entre la secreción aumentada de IgG2a con la respuesta Th1, y entre elevados niveles de IgG1 y la respuesta Th2 (Mosmann, 1989). Por lo tanto, títulos elevados de IgG1 anti-*T.canis* pueden estar asociados a la respuesta tipo 2 ligada a citocinas Th2 (Fan et al., 2003). También, la IgG1 es considerada un marcador en la infección por *T. canis*, que, ligada al gradual incremento en niveles de IgG2a pueden ayudar en la

determinación del curso de la infección (Novák et al., 2017). Estudios previos en ratones infectados crónicamente con *T. canis* mostraron que los niveles séricos de IgG1 se incrementaron significativamente con dosis de 100 y 1000 HL y con dosis de 1000 huevos, las respuestas específica de IgG1 e IgG2a se incrementaron, pero el aumento de IgG1 fue mayor que el de IgG2a (Pinelli et al., 2007). Esto concuerda con los resultados de nuestro estudio, ya que los niveles de IgG1 e IgG2a se incrementaron, pero en el grupo intacto el incremento relativo de IgG1 fue 2.6 veces mayor que el de IgG2a ($p<0.0001$) (Fig. 9B). Por lo tanto, la respuesta en la infección crónica a *T. canis*, es predominantemente a través de IgG1, relacionada a la respuesta Tipo 2.

Otra característica relacionada con la respuesta inmune humoral es el aumento en la proporción de LB en bazo y GLP, una característica previamente reportada en ratas infectadas con *T. canis* (Del Rio-Araiza et al., 2018). La expansión de LB, el incremento de IL-4 en bazo y los elevados niveles séricos de anticuerpos tipo IgG1 específicos a *T. canis*, sugieren una respuesta Tipo 2. Esto puede ser explicado por la habilidad de la IL-4 de inducir un cambio en la recombinación de IgG1 e IgG4 en los LB, los cuales originarán células plasmáticas especializadas en la producción de anticuerpos (Moens and Tangye, 2014; Pracht et al., 2017). Por otro lado, LB $CD19^+$ esplénicos, llamados Breg poseen la habilidad de secretar IL-10, que suprime a los LT $CD4^+$ y $CD8^+$ e induce la formación de Treg (Rosser and Mauri, 2015).

Como se ha mencionado, los helmintos poseen la capacidad de sobrevivir en sus hospederos por largos periodos de tiempo, induciendo respuesta inmune crónica. En la fase temprana de la infección por *T. canis* se establece la respuesta tipo 2 asociada a niveles elevados de IL-4, IL-5, IL-13, IgE y eosinofilia periférica, pero con el tiempo el continuo daño tisular es debido a la respuesta inmune por sí misma, más que por el parásito (Resende et al., 2015). Por lo tanto, el balance inmunológico entre las respuestas Tipo 1 y Tipo 2 y su regulación, es importante para la supervivencia del hospedero y es diferente entre parásitos (McSorley and Maizels, 2012). Como ya se mencionó, *T. canis* induce la respuesta Tipo 2, la reguladora y disminuye la producción

de citocinas Tipo 1. (Del Prete et al., 1991; Othman et al., 2011; Resende et al., 2015). En el caso de nuestro estudio, la respuesta Tipo 2 quedó evidenciada por el aumento de IL-4 sistémica (Bazo y suero) y el aumento sérico de IL-5, en contraste con la reducción de citocinas Tipo 1, como TNF-α esplénico. Mientras que la respuesta reguladora a la infección estuvo representada por de la expansión de LT $CD4^+/FoxP3^+$ en órganos linfoides secundarios (bazo y GLP) y por el incremento de LT $CD8^+/FoxP3^+$ en GLP, junto con los niveles elevados de IL-10 en bazo y suero de los animales infectados.

La respuesta de células Treg en la infección por *T. canis* se ha reportado en bazo, donde se detectaron niveles elevados del RNAm de *Foxp3* desde la 2-16 semana post-infección, pero la caracterización de LT $CD4^+Foxp3^+$ no se realizó en este estudio (Othman et al., 2011). En nuestro trabajo, la expresión del factor de transcripción Foxp3 en LT $CD4^+$ se identificó en bazo, además de los GLP, donde las proporciones de ambas poblaciones de Treg ($CD4^+/FoxP3^+$ y $CD8^+/FoxP3^+$) estaban elevadas. En este sentido, la infección con el nematodo murino *H. polygyrus* indujo la expansión de Treg $Foxp3^+CD4^+$ en ganglios linfáticos mesentéricos de ratones con infección entérica (Pastille et al., 2017). A diferencia de *T. canis*, *H. polygyrus* se localiza solo en el intestino y la proximidad de ganglios linfáticos mesentéricos a este órgano, puede explicar la expansión de Treg en los ganglio regionales. Pero en el caso del incremento de LT $CD4^+/FoxP3^+$ en GLP (inguinales) causada por la infección por *T. canis*, refleja una respuesta sistémica debido a que las larvas realizan una la migración a través de diferentes órganos y tejidos. En cuanto a la función de los LT $CD8^+/FoxP3^+$ en la respuesta a helmintos, se ha reportado que los LT $CD8^+/FoxP3^+$ aislados de la lámina propia intestinal de ratones infectados con *H. polygyrus*, pueden suprimir la proliferación de esplenocitos a través del contacto directo, e independiente de IL-10 (Metwali et al., 2006).

Adicionalmente a la presencia de células Treg, los helmintos inducen otros tipos de células con funciones reguladoras, como Breg y MAA (Allen and Maizels, 2011).

Aunque se necesita de una futura caracterización para determinar el fenotipo de LB y macrófagos F4/80$^+$ en este estudio, el incremento en las proporciones de estas dos poblaciones en bazo aunado al microambiente rico en IL-4, IL-10, VEGF, y los niveles disminuidos de TNF-α e IFN-γ, sugieren un fenotipo regulador de ambos tipos celulares. Esto se fundamenta a través de reportes de estudios *in vitro*, donde se cultivaron macrófagos de ratones infectados con *T. canis*, los cuales producían cantidades mayores de IL-10 y menores de TNF-α, que los de los ratones sin infección (Kuroda et al., 2001).

En la primera parte del presente trabajo se integraron diferentes componentes de la respuesta inmune a la infección crónica por *T. canis* en ratones. Estos resultados sugieren una respuesta Tipo 2 caracterizada por niveles elevados de IL-4, IL-5 y VEGF, una respuesta humoral y una reguladora asociada a IL-10, CD4$^+$Treg y CD8$^+$Treg.

Pero el papel de estas células y citocinas en los mecanismos inflamatorios y reguladores necesita estudiarse en el futuro. El entendimiento de la respuesta inmune a la infección crónica a *T. canis* es esencial para comprender la interacción que esta infección puede tener con otras comorbilidades. En algunas de éstas puede ayudar al control de la enfermedad (autoinmunes) o a promoverla (cáncer o alergias). Por lo que conocer la respuesta inmune a *T. canis* puede ayudar al tratamiento o el establecimiento de medidas preventivas asociadas a otras enfermedades. En este sentido se realizó el estudio del efecto de la infección en el desarrollo de un tumor mamario en ratones.

En los animales con tumor se detectó la redistribución de las larvas en tejidos, comparada con los animales sin tumor. Aunque en ambos casos la mayoría se encontraron en músculo esquelético y cerebro, en los animales con tumor se observó aumento en el número de larvas en el músculo cardiaco, lo que es consistente con la proposición de Othman, que menciona la acumulación de larvas en el cerebro, al

mismo tiempo que algunas migran constantemente y se distribuyen en diferentes tejidos (Othman, 2012).

Respecto a la determinación del volumen tumoral mediante la medición de sus diámetros, ya sea por encima de la piel o una vez extraído, nuestros datos demostraron que no refleja significativamente el volumen real del tumor. Por lo que a pesar de que este método de aproximación al tamaño del tumor se ha usado desde hace años (Carlsson et al., 1983), no debería de ser tomado como la medida más cercana al tamaño del tumor. Al contrario, el volumen real medido por desplazamiento de líquido es muy cercano (95%) al valor del peso del tumor. Por lo tanto, de manera indistinta podrían usarse ya sea el peso o el volumen real por desplazamiento de líquido.

Además de la infección, la inducción tumoral modifica la respuesta inmune sistémica en el hospedero. Se destaca el decremento significativo en la proporción de Treg en bazo de los animales con tumor comparado con los animales intactos, lo cual se ha reportado previamente (Palacios-Arreola et al., 2017). Además, la inducción del tumor de células 4T1 provoca marcados cambios en el bazo, como esplenomegalia característica de este modelo (Gregório et al., 2016). Ambas anormalidades están asociadas a una respuesta leucemoide y a una hematopoyesis extramedular (esplénica), documentada en el modelo de tumores 4T1. Debido a la eritropoyesis extramedular se presenta el incremento en la proporción de granulocitos y la disminución en la de linfocitos (DuPre and Hunter, 2007).

Como ya se mencionó, el modelo experimental empleado en nuestro estudio, el sistema inmune de los ratones se presenta sin alteraciones previas a la inducción del tumor o la infección, por lo que pudimos determinar los cambios en la respuesta a ambos fenómenos. De manera notable, se observó que 21 días después de la inyección de las células 4T1 de tumor mamario, el crecimiento de los tumores

aumentó. Además a los 49 d.p.i., el microambiente tumoral se modificó, lo que puede explicar el incremento en el desarrollo del tumor.

La infección por *T. canis* aumentó el tamaño y peso promedio de los tumores hasta el doble, comparado con los tumores de animales sin infección. Este incremento está asociado a las modificaciones del microambiente tumoral inmune. Por ejemplo, la expansión de macrófagos $F480^{+}$, LB $CD19^{+}$, el aumento en IL-4, IL-10 y VEGF y la reducción en los niveles de TNF-α, en el grupo 4T1+*T.canis*. Se ha reportado que el aumento de macrófagos en el tumor de mama está asociado con un mal pronóstico, sobre todo si estos son del tipo MAA (Zhao et al., 2017). Aunque aún se necesita hacer la caracterización de macrófagos y LB en este modelo de infección, el incremento de IL-4, IL-10 y VEGF en el tumor, sugieren fuertemente que estos macrófagos pueden ser del tipo MAA. Así mismo, a pesar de que el porcentaje de LB detectados en tumor fue bajo, estos podrían también tener un fenotipo regulador, que necesita caracterización, ya que linfocitos Breg $CD19^{+}$ también producen IL-10 (Rosser and Mauri, 2015), por lo que diferentes poblaciones de células inmunes pueden estar contribuyendo al microambiente tumoral supresor.

Hay evidencia de que algunos helmintos son inductores de diferentes tipos de tumores (Machicado and Marcos, 2016) y la coexistencia de enfermedades causadas por infecciones helmínticas y la promoción del crecimiento tumoral se han descrito recientemente. En un modelo de cáncer de colon asociado a colitis en ratones, la infección intestinal con el nematodo *H. polygyrus* promovió el desarrollo de tumores colónicos (Pastille et al., 2017). En otro modelo, la infección intestinal por el nematodo *Trichuris muris* aceleró el desarrollo de adenomas intestinales en ratones APC min/+ (Hayes et al., 2017). En estos dos estudios, el nematodo y los tumores están en la misma localización anatómica. Pero en nuestro estudio, las larvas de *T. canis* migran a través de diferentes órganos (Schnieder et al., 2011) y la respuesta reguladora estimulada por el parásito se encuentra diseminada a través de diferentes compartimentos corporales.

Contrario a nuestra hipótesis inicial, el incremento en el tamaño de los tumores en los animales infectados, no estuvo asociado con la elevación de la proporción local de Treg ($CD4^+/Foxp3^+$ y/o $CD8^+/Foxp3^+$). A pesar de que la proporción de Treg en el tumor no aumentó por la infección, en los GLP de los ratones del grupo 4T1+*T. canis* si hubo incremento de $CD4^+/Foxp3^+$. La inducción de Treg en los tumores puede ser menor a la generación de éstas células en los ganglios linfáticos centinelas, tal vez porque la conversión a Treg es más activa aquí, que en los tumores (Wang et al., 2012).

El microambiente en los ganglios linfáticos centinelas del tumor (GLCT) es importante en la progresión de la respuesta inmune tumoral (Deng et al., 2010). Por ejemplo, las células Treg $Foxp3^+$ en los GLCT modulan la función de LT $CD8^+$, a través de la supresión de la secreción de IFN-γ por LT $CD8^+$ (Deng et al., 2010). Otro mecanismo por el cual las células Treg regulan la expansión y afectan la diferenciación de los LT $CD8^+$ es por competencia de IL-2, al mismo tiempo que esta citocina puede promover la expansión de las células Treg (Mcnally et al., 2011). Esto puede explicar lo observado en los ratones del grupo 4T1+*T. canis*, en los que aunque el porcentaje de LT $CD4^+Foxp3^+$ fue menor que en los tumores de los no infectados (grupo 4T1), en los GLP la proporción de Treg $CD4^+Foxp3^+$ fue mayor y de $CD8^+$ menor.

La importancia en la disminución en el porcentaje de LT $CD8_+$ en el tumor, radica en la función de éstas célula en el control del desarrollo tumoral. Una infiltración aumentada de LT $CD8^+$ en el modelo de tumores murinos 4T1, mostró que los LTC $D8^+$ pueden inducir apoptosis directamente sobre las células tumorales, a través de la producción de IFN-γ (Yang et al., 2016). Por lo anterior, la disminución en ésta población de LT en tumor puede estar relacionada con el incremento en el tamaño del tumor de los ratones infectados.

Además de la asociación con la respuesta Tipo 2 y el crecimiento tumoral, la angiogénesis también está relacionada con este tipo de respuesta (Hanahan and

Weinberg, 2000). La angiogénesis juega un papel importante en el desarrollo del tumor y la diseminación de células tumorales a través de los vasos sanguíneos (Joyce and Pollard, 2009). Por lo que el incremento de VEGF tumoral y sistémico (sérico y esplénico) en los animales infectados con *T. canis*, y asociado a una respuesta inmune de Tipo 2, posiblemente promovió el crecimiento del tumor y la metástasis.

Por otro lado, la respuesta humoral de los ratones infectados se preservó después de la inducción del tumor, ya que los niveles de IgG específicos a *T. canis* a los 49 días fueron similares en los ratones infectados y sin tumor, esto acompañado de la expansión de LB $CD19^+$ en el bazo y la esplenomegalia en estos ratones. Por lo que a pesar de que en la respuesta sistémica no se observaron diferencias entre los grupos 4T1 y 4T1+*T. canis*, respecto a las poblaciones de células innatas y adaptativas, y las citocinas (IL-4, IL-5, IL-10, TNF-α, IFN-γ), la infección fue evidenciada por la conservación de la respuesta humoral.

En referencia a las metástasis macroscópicas pulmonares, en el grupo de ratones con *T. canis* y con tumor, se observó mayor número de lesiones macroscópicas sugerentes de metástasis pulmonares. Este fenómeno puede ser explicado por los elevados niveles de VEGF asociados a la infección. En este sentido, se ha reportado la relación positiva en la expresión de VEGF en los tumores de pacientes con cáncer de mama y la metástasis en ganglios linfáticos centinelas (Eroğlu et al., 2017).

Además, del aumento local y sistémico de VEGF, en los TES se ha caracterizado la presencia de proteasas de serina, que pueden degradar componentes de la matriz extracelular como laminina y fibronectina, además de albúmina e incluso IgG caprina (González-Páez et al., 2014; Maizels, 2013). Estas proteasas son un mecanismo de invasión importante para la larva (Maizels, 2013), lo que de manera similar podría estar funcionando para la invasión y metástasis de las células neoplásicas que necesitan penetrar a través de la membrana basal y remover la matriz extracelular de los tejidos, lo que llevan a cabo con proteasas que degradan o procesan los componentes de

la matriz extracelular (Kumar and Weaver, 2009). A pesar de que no determinamos la presencia de los TES en el microambiente tumoral, se ha reportado que estos productos pueden ser detectados en suero de los ratones infectados (Rodríguez-Caballero et al., 2015), por lo que los TES podrían estar llegando al tumor vía sanguínea. Para evaluar el efecto de los TES en el microambiente tumoral y la metástasis, se inyectaron los TES dentro del tumor y se observó que no se presentó incremento significativo en el tamaño de los tumores o diferencias en las subpoblaciones tumorales o en órganos linfáticos secundarios. Esto contrario a lo que está reportado en otro modelo de tumores, ya que la inyección de antígenos obtenidos por sonicación de huevos larvados de *T. canis* antes de la inoculación de la línea WEHI-164 de fibrosarcoma, puede disminuir el tamaño de estos tumores (Darani et al., 2009). Con la inyección intratumoral de TES, se detectó que el aumento de las metástasis pulmonares macroscópicas en estos animales fue más evidente que en los ratones a los que se les inyectó solo el vehículo.

En conjunto los resultados obtenidos en este trabajo muestran el efecto de la infección con *T. canis* sobre el aumento del tamaño de los tumores y la modificación de su microambiente inmune y la metástasis pulmonar. Por lo que medidas de prevención y control deben de llevarse a cabo para la prevención de la infección por este nematodo a fin de disminuir el riesgo de contraer esta morbilidad, que puede modificar la respuesta inmune del hospedero y promover el desarrollo de tumores mamarios.

VI. Conclusiones

- La infección crónica con el nematodo *T. canis* en ratones BALB/c está caracterizada por una respuesta inmune Tipo 2, asociada a una respuesta humoral, una reguladora y una angiogénica.

- La infección con *T. canis* incrementa los niveles séricos y esplénicos de VEGF.

- La determinación del volumen tumoral mediante la medición de sus diámetros no refleja significativamente el volumen real del tumor. Y el volumen real medido por desplazamiento de líquido es muy cercano (95%) al valor del peso del tumor.

- Los tumores de los ratones infectados con *T. canis* fueron hasta dos veces más grandes que los de los no infectados.

- El microambiente tumoral en los animales infectados se ve modificado ligado a una respuesta Tipo 2, reguladora y angiogénica, asociada al incremento de IL-4, IL-10, VEGF.

- En los animales infectados se detectaron más lesiones macroscópicas pulmonares sugerentes de metástasis que en los no infectados.

VII. Referencias bibliográficas

- Aalders, K.C., Tryfonidis, K., Senkus, E., Cardoso, F., 2017. Anti-angiogenic treatment in breast cancer: Facts, successes, failures and future perspectives. Cancer Treat. Rev. 53, 98–110. https://doi.org/10.1016/j.ctrv.2016.12.009
- Abo-Shehada, M.N., Herbert, I. V., 1984. The migration of larval *Toxocara canis* in mice II. Post-intestinal migration in primary infections. Vet. Parasitol. 17, 75–83. https://doi.org/10.1016/0304-4017(84)90066-9
- Alameddine, R.S., Otrock, Z.K., Awada, A., Shamseddine, A., 2013. Crosstalk between HER2 signaling and angiogenesis in breast cancer: molecular basis, clinical applications and challenges. Curr. Opin. Oncol. 25, 313–324. https://doi.org/10.1097/CCO.0b013e32835ff362
- Allen, J.E., Maizels, R.M., 2011. Diversity and dialogue in immunity to helminths. Nat. Rev. Immunol. 11, 375–388.
- Archielli, S., Kozubsky, L., 2008. *Toxocara* and toxocariosis. Acta Bioquímica Clínica Latinoam. 42, 379–384.
- Barnard, M.E., Boeke, C.E., Tamimi, R.M., 2015. Established breast cancer risk factors and risk of intrinsic tumor subtypes. Biochim. Biophys. Acta - Rev. Cancer 1856, 73–85. https://doi.org/10.1016/j.bbcan.2015.06.002
- Bates, G.J., Fox, S.B., Han, C., Leek, R.D., Garcia, J.F., Harris, A.L., Banham, A.H., 2006. Quantification of regulatory T cells enables the identification of high-risk breast cancer patients and those at risk of late relapse. J. Clin. Oncol. 24, 5373–5380. https://doi.org/10.1200/JCO.2006.05.9584
- Botelho, M.C., Veiga, I., Oliveira, P.A., Lopes, C., Teixeira, M., da Costa, J.M.C., Machado, J.C., 2013. Carcinogenic ability of Schistosoma haematobium possibly through oncogenic mutation of KRAS gene. Adv. cancer Res. Treat. 2013, 1–8.
- Bowman, D.D., Mika-Grieve, M., Grieve, R.B., 1987. Circulating Excretory-Secretory Antigen Levels and Specific Antibody Responses in Mice Infected with *Toxocara canis*. Am. J. Trop. Med. Hyg. 36, 75–82. https://doi.org/10.4269/ajtmh.1987.36.75
- Burke, T.M., Roberson, E.L., 1985. Prenatal and lactational transmission of *Toxocara canis* and *Ancylostoma caninum*: experimental infection of the bitch before pregnancy. Int. J. Parasitol. 15, 71–75.
- Carlsson, G., Gullberg, B., Hafström, L., 1983. Estimation of liver tumor volume using different formulas -an experimental study in rats. J. Cancer Res. Clin. Oncol. 105, 20–3.
- Carter, N.A., Rosser, E.C., Mauri, C., 2012. Interleukin-10 produced by B cells is crucial for the suppression of Th17/Th1 responses, induction of T regulatory type 1 cells and

reduction of collagen-induced arthritis. Arthritis Res. Ther. 14, R32. https://doi.org/10.1186/ar3736

- Chen, D.S., Mellman, I., 2013. Oncology meets immunology: The cancer-immunity cycle. Immunity 39, 1–10. https://doi.org/10.1016/j.immuni.2013.07.012
- Chen, J., Zhou, D.-H., Nisbet, A.J., Xu, M.-J., Huang, S.-Y., Li, M.-W., Wang, C.-R., Zhu, X.-Q., 2012. Advances in molecular identification, taxonomy, genetic variation and diagnosis of *Toxocara* spp. Infect. Genet. Evol. 12, 1344–1348. https://doi.org/10.1016/j.meegid.2012.04.019
- Darani, H.Y., Shirzad, H., Mansoori, F., Zabardast, N., Mahmoodzadeh, M., 2009. Effects of *Toxoplasma gondii* and *Toxocara canis* antigens on WEHI-164 fibrosarcoma growth in a mouse model. Korean J. Parasitol. 47, 175–177. https://doi.org/10.3347/kjp.2009.47.2.175
- de Oliveira, V.C., de Mello, R.P., D'Almeida, J.M., 2002. [Muscoid dipterans as helminth eggs mechanical vectors at the zoological garden, Brazil]. Rev Saude Publica 36, 614–620. https://doi.org/10.1590/S0034-89102002000600011
- Del Prete, G.F., De Carli, M., Mastromauro, C., Biagiotti, R., Macchia, D., Falagiani, P., Ricci, M., Romagnani, S., 1991. Purified protein derivative of Mycobacterium tuberculosis and excretory-secretory antigen(s) of *Toxocara canis* expand in vitro human T cells with stable and opposite (type 1 T helper or type 2 T helper) profile of cytokine production. J. Clin. Invest. 88, 346–350. https://doi.org/10.1172/JCI115300
- Del Rio-Araiza, V.H., Nava-Castro, K.E., Alba-Hurtado, F., Quintanar-Stephano, A., Aguilar-Díaz, H., Muñoz-Guzmán, M.A., Ostoa-Saloma, P., Ponce-Regalado, M.D., Morales-Montor, J., 2018. Prolactin as immune cell regulator in *Toxocara canis* somatic larvae chronic infection. Biosci. Rep. BSR20180305. https://doi.org/10.1042/BSR20180305
- Deng, L., Zhang, H., Luan, Y., Zhang, J., Xing, Q., Dong, S., 2010. Accumulation of Foxp3+ T regulatory cells in draining lymph nodes correlates with disease progression and immune suppression in colorectal cancer patients. Clin. Cancer Res. 16, 4105–4112. https://doi.org/10.1158/1078-0432.CCR-10-1073
- DuPre, S.A., Hunter, K.W., 2007. Murine mammary carcinoma 4T1 induces a leukemoid reaction with splenomegaly: Association with tumor-derived growth factors. Exp. Mol. Pathol. 82, 12–24. https://doi.org/10.1016/j.yexmp.2006.06.007
- Edge, S.B., Compton, C.C., 2010. The American Joint Committee on Cancer: the 7th Edition of the AJCC Cancer Staging Manual and the Future of TNM. Ann. Surg. Oncol. 17, 1471–1474. https://doi.org/10.1245/s10434-010-0985-4
- Emens, L.A., Silverstein, S.C., Khleif, S., Marincola, F.M., Galon, J., 2012. Toward integrative cancer immunotherapy: targeting the tumor microenvironment. J.Transl.Med. 10, 70. https://doi.org/10.1186/1479-5876-10-70

- Epe, C., Sabel, T., Schnieder, T., Stoye, M., 1994. The behavior and pathogenicity of Toxacara canis larvae in mice of different strains. Parasitol. Res. 80, 691–695. https://doi.org/10.1007/BF00932955
- Eroğlu, A., Ersöz, C., Karasoy, D., Sak, S., 2017. Vascular endothelial growth factor (VEGF)-C, VEGF-D, VEGFR-3 and D2-40 expressions in primary breast cancer: Association with lymph node metastasis. Adv. Clin. Exp. Med. 26, 245–249. https://doi.org/10.17219/acem/58784
- Esquivel-Velázquez, M., Ostoa-Saloma, P., Palacios-Arreola, M.I., Nava-Castro, K.E., Castro, J.I., Morales-Montor, J., 2015. The Role of Cytokines in Breast Cancer Development and Progression. J. Interf. Cytokine Res. 35, 1–16. https://doi.org/10.1089/jir.2014.0026
- Fan, C., Lin, Y., Du, W., Su, K., 2003. Infectivity and pathogenicity of 14-month-cultured embryonated eggs of *Toxocara canis* in mice 113, 145–155. https://doi.org/10.1016/S0304-4017(03)00046-3
- Finsterer, J., Auer, H., 2007. Neurotoxocariasis. Rev. Inst. Med. trop. S. Paulo 49, 279–287. https://doi.org/10.1590/S0036-46652007000500002
- Fu, C.-J., Chuang, T.-W., Lin, H.-S., Wu, C.-H., Liu, Y.-C., Langinlur, M.K., Lu, M.-Y., Hsiao, W.W.-W., Fan, C.-K., 2014. Seroepidemiology of *Toxocara canis* infection among primary schoolchildren in the capital area of the Republic of the Marshall Islands. BMC Infect. Dis. 14, 261. https://doi.org/10.1186/1471-2334-14-261
- Gao, D., Liu, S., Leung, S., Kos, Z., Nielsen, T.O., Foulkes, W.D., Lau, S., 2014. Prognostic significance of FOXP3+ tumor-infiltrating lymphocytes in breast cancer depends on estrogen receptor and human epidermal growth factor receptor-2 expression status and concurrent cytotoxic T-cell infiltration. Breast Cancer Res. 16, 1–12.
- Gardner, A., Ruffell, B., 2016. Dendritic Cells and Cancer Immunity. Trends Immunol. 37, 855–865. https://doi.org/10.1016/j.it.2016.09.006
- Giuliano, A.E., Connolly, J.L., Edge, S.B., Mittendorf, E.A., 2017. Breast Cancer — Major Changes in the American Joint Committee on Cancer Eighth Edition Cancer Staging Manual. A Cancer Journals Clin. 67, 290–303. https://doi.org/10.3322/caac.21393.
- González-García, T., Muñoz-Guzmán, M.A., Sánchez-Arroyo, H., Prado-Ochoa, M.G., Cuéllar-Ordaz, J.A., Alba-Hurtado, F., 2017. Experimental transmission of *Toxocara canis* from *Blattella germanica* and *Periplaneta americana* cockroaches to a paratenic host. Vet. Parasitol. 246, 5–10. https://doi.org/10.1016/j.vetpar.2017.08.025
- González-Páez, G.E., Alba-Hurtado, F., García-Tovar, C.G., Argüello-García, R., 2014. Proteinases in Excretory-Secretory Products of T*oxocara canis* Second-Stage Larvae:

Zymography and Modeling Insights. Biomed Res. Int. 2014, 1–9. https://doi.org/10.1155/2014/418708

- Gregório, A.C., Fonseca, N.A., Moura, V., Lacerda, M., Figueiredo, P., Simões, S., Dias, S., Moreira, J.N., 2016. Inoculated cell density as a determinant factor of the growth dynamics and metastatic efficiency of a breast cancer murine model. PLoS One 11, 1–19. https://doi.org/10.1371/journal.pone.0165817
- Hanahan, D., Coussens, L.M., 2012. Accessories to the Crime: Functions of Cells Recruited to the Tumor Microenvironment. Cancer Cell 21, 309–322. https://doi.org/10.1016/j.ccr.2012.02.022
- Hanahan, D., Weinberg, R.A., 2000. The Hallmarks of Cancer Review 100, 57–70.
- Harris, J., Morrow, M., Norton, L., 1997. Malignant tumors of the breast. Cancer Princ. Pract. Oncol. 1557–1616.
- Hayes, K.S., Cliffe, L.J., Bancroft, A.J., Forman, S.P., Thompson, S., Booth, C., Grencis, R.K., 2017. Chronic Trichuris muris infection causes neoplastic change in the intestine and exacerbates tumour formation in APC min /+ mice. PLoS Negl. Trop. Dis. 11, 1–19.
- Jarnicki, A.G., Lysaght, J., Todryk, S., Mills, K.H.G., 2014. Suppression of Antitumor Immunity by IL-10 and TGF- -Producing T Cells Infiltrating the Growing Tumor: Influence of Tumor Environment on the Induction of CD4+ and CD8+ Regulatory T Cells. J. Immunol. 177, 896–904. https://doi.org/10.4049/jimmunol.177.2.896
- Jemal, A., Siegel, R., Ward, E., Hao, Y., Xu, J., Thun, M.J., 2009. Cancer Statistics. CA. Cancer J. Clin. 59, 225–249. https://doi.org/10.3322/caac.20006.Available
- Jenkins, S.J., Allen, J.E., 2010. Similarity and Diversity in Macrophage Activation by Nematodes, Trematodes, and Cestodes. J. Biomed. Biotechnol. 2010, 1–14. https://doi.org/10.1155/2010/262609
- Joyce, J.A., Pollard, J.W., 2009. Microenvironmental regulation of metastasis. Nat Rev Cancer 9, 239–252. https://doi.org/10.3892/ol.2018.8378
- Kayes, S.G., Omholt, P.E., Grieve, R.B., 1985. Immune Responses of CBA/J Mice to Graded Infections with. Infect. Immun. 48, 697–703.
- Kozan, E., Kircali, F., Ml, S.E.V.İ., Köse, M., Eser, M., Çek, H.Ç.İ., 2007. Examination of Helminth Contaminated Wastewaters Used for Agricultural Purposes in Afyonkarahisar. Türkiye Parazitol Derg 31, 197–200.
- Kumar, S., Weaver, V.M., 2009. Mechanics, malignancy, and metastasis: The force journey of a tumor cell. Cancer Metastasis 28, 113–127. https://doi.org/10.1007/s10555-008-9173-4.Mechanics
- Kuroda, E., Yoshida, Y., Shan, B.E., Yamashita, U., 2001. Suppression of macrophage interleukin-12 and tumour necrosis factor-alpha production in mice infected with

Toxocara canis. Parasite Immunol. 23, 305–311. https://doi.org/10.1046/j.1365-3024.2001.00387.x

- Law, A.M.K., Lim, E., Ormandy, C.J., Gallego-Ortega, D., 2017. The innate and adaptive infiltrating immune systems as targets for breast cancer immunotherapy. Endocr. Relat. Cancer 24, R123–R144. https://doi.org/10.1530/ERC-16-0404
- Linderholm, B.K., Hellborg, H., Johansson, U., Elmberger, G., Skoog, L., Lehtiö, J., Lewensohn, R., 2009. Significantly higher levels of vascular endothelial growth factor (VEGF) and shorter survival times for patients with primary operable triple-negative breast cancer. Ann. Oncol. 20, 1639–1646. https://doi.org/10.1093/annonc/mdp062
- Lopes Rassier, G., Borsuk, S., Pappen, F., Scaini, C.J., Gallina, T., Villela, M.M., Da Rosa Farias, N.A., Benavides, M.V., Berne, M.E.A., 2013. *Toxocara* spp. seroprevalence in sheep from southern Brazil. Parasitol. Res. 112, 3181–3186. https://doi.org/10.1007/s00436-013-3499-8
- Ma, G., Holland, C. V., Wang, T., Hofmann, A., Fan, C.K., Maizels, R.M., Hotez, P.J., Gasser, R.B., 2018. Human toxocariasis. Lancet Infect. Dis. 18, e14–e24. https://doi.org/10.1016/S1473-3099(17)30331-6
- Machicado, C., Marcos, L.A., 2016. Carcinogenesis associated with parasites other than Schistosoma, Opisthorchis and Clonorchis: A systematic review. Int. J. Cancer 138, 2915–2921. https://doi.org/10.1002/ijc.30028
- Magnaval, J.F., Glickman, L.T., Dorchies, P., Morassin, B., 2001. Highlights of human toxocariasis. Korean J. Parasitol. 39, 1–11. https://doi.org/10.3347/kjp.2001.39.1.1
- Maizels, R.M., 2013. *Toxocara canis*: Molecular basis of immune recognition and evasion. Vet. Parasitol. 193, 365–374. https://doi.org/10.1016/j.vetpar.2012.12.032
- Mazur-Melewska, K., Figlerowicz, M., Cwalińska, A., Mikoś, H., Jończyk-Potoczna, K., Lewandowska-Stachowiak, M., Służewski, W., 2016. Production of interleukins 4 and 10 in children with hepatic involvement in the course of *Toxocara* spp. infection. Parasite Immunol. 38, 101–107. https://doi.org/10.1111/pim.12303
- Mcnally, A., Hill, G.R., Sparwasser, T., Thomas, R., Steptoe, R.J., 2011. CD4+CD25+ regulatory T cells control CD8+ T-cell effector differentiation by modulating IL-2 homeostasis. PNAS 108, 7529–7534.
- McSorley, H.J., Maizels, R.M., 2012. Helminth infections and host immune regulation. Clin. Microbiol. Rev. 25, 585–608. https://doi.org/10.1128/CMR.05040-11
- Mellman, I., Steinman, R.M., 2001. Dendritic cells: Specialized and regulated antigen processing machines. Cell 106, 255–258. https://doi.org/10.1016/S0092-8674(01)00449-4
- Metwali, A., Setiawan, T., Blum, A.M., Urban, J., Elliott, D.E., Hang, L., Weinstock, J. V., 2006. Induction of CD8+ regulatory T cells in the intestine by Heligmosomoides

polygyrus infection. Am. J. Physiol. Liver Physiol. 291, G253–G259. https://doi.org/10.1152/ajpgi.00409.2005

- Moens, L., Tangye, S.G., 2014. Cytokine-mediated regulation of plasma cell generation: IL-21 takes center stage. Front. Immunol. 5, 1–13. https://doi.org/10.3389/fimmu.2014.00065
- Mosmann, T., 1989. Th1 And Th2 Cells: Different Patterns Of Lymphokine Secretion Lead To Different Functional Properties. Annu. Rev. Immunol. 7, 145–173. https://doi.org/10.1146/annurev.immunol.7.1.145
- Novák, J., Panská, L., Macháček, T., Kolářová, L., Horák, P., 2017. Humoral response of mice infected with *Toxocara canis* following different infection schemes 62, 823–824. https://doi.org/10.1515/ap-2017-0099
- Nutman, T.B., 2015. Looking beyond the induction of Th2 responses to explain immunomodulation by helminths. Parasite Immunol. 37, 304–313.
- Oshima, T., 1961. Standardization of Techniques for Infecting Mice with *Toxocara canis* and Observations on the Normal Migration Routes of the Larvae. J. Parasitol. 47, 652–656.
- Othman, A.A., 2012. Therapeutic battle against larval toxocariasis: Are we still far behind? Acta Trop. 124, 171–178.
- Othman, A.A., El-Shourbagy, S.H., Soliman, R.H., 2011. Kinetics of Foxp3-expressing regulatory cells in experimental *Toxocara canis* infection. Exp. Parasitol. 127, 454–459. https://doi.org/10.1016/j.exppara.2010.10.005
- Overgaauw, P.A.M., 1997. Aspects of *Toxocara* epidemiology: Human toxocarosis. Crit. Rev. Microbiol. 23, 215–231. https://doi.org/10.3109/10408419709115137
- Overgaauw, P.A.M., van Knapen, F., 2013. Veterinary and public health aspects of *Toxocara* spp. Vet. Parasitol. 193, 398–403. https://doi.org/10.1016/j.vetpar.2012.12.035
- Palacios-Arreola, M.I., Nava-Castro, K.E., Castro, J.I., García-Zepeda, E., Carrero, J.C., Morales-Montor, J., 2014. The role of chemokines in breast cancer pathology and its possible use as therapeutic targets. J. Immunol. Res. 2014. https://doi.org/10.1155/2014/849720
- Palacios-Arreola, M.I., Nava-Castro, K.E., Río-Araiza, V.H. Del, Pérez-Sánchez, N.Y., Morales-Montor, J., 2017. A single neonatal administration of Bisphenol A induces higher tumour weight associated to changes in tumour microenvironment in the adulthood. Sci. Rep. 7, 1–11.
- Pastille, E., Frede, A., McSorley, H.J., Gräb, J., Adamczyk, A., Kollenda, S., Hansen, W., Epple, M., Buer, J., Maizels, R.M., Klopfleisch, R., Westendorf, A.M., 2017. Intestinal helminth infection drives carcinogenesis in colitis-associated colon cancer. PLoS

Pathog. 13, 1–22.

- Pinelli, E., Brandes, S., Dormans, J., Fonville, M., Hamilton, C.M., der Giessen, J. van, 2007. Toxocara canis: Effect of inoculum size on pulmonary pathology and cytokine expression in BALB/c mice. Exp. Parasitol. 115, 76–82. https://doi.org/10.1016/j.exppara.2006.06.002
- Pinelli, E., Withagen, C., Fonville, M., Verlaan, A., Dormans, J., Van Loveren, H., Nicoll, G., Maizels, R.M., Van Der Giessen, J., 2005. Persistent airway hyper-responsiveness and inflammation in *Toxocara canis*-infected BALB/c mice. Clin. Exp. Allergy 35, 826–832. https://doi.org/10.1111/j.1365-2222.2005.02250.x
- Plummer, M., de Martel, C., Vignat, J., Ferlay, J., Bray, F., Franceschi, S., 2016. Global burden of cancers attributable to infections in 2012: a synthetic analysis. Lancet Glob. Heal. 4, e609–e616.
- Pracht, K., Meinzinger, J., Daum, P., Schulz, S.R., Reimer, D., Hauke, M., Roth, E., Mielenz, D., Berek, C., Côrte-Real, J., Jäck, H.-M., Schuh, W., 2017. A new staining protocol for detection of murine antibody-secreting plasma cell subsets by flow cytometry. Eur. J. Immunol. 47, 1389–1392. https://doi.org/10.1002/eji.201747019
- Qian, B.Z., Pollard, J.W., 2010. Macrophage Diversity Enhances Tumor Progression and Metastasis. Cell 141, 39–51. https://doi.org/10.1016/j.cell.2010.03.014
- Resende, N.M., Gazzinelli-Guimarães, P.H., Barbosa, F.S., Oliveira, L.M., Nogueira, D.S., Gazzinelli-Guimarães, A.C., Gonçalves, M.T.P., Amorim, C.C.O., Oliveira, F.M.S., Caliari, M. V., Rachid, M.A., Volpato, G.T., Bueno, L.L., Geiger, S.M., Fujiwara, R.T., 2015. New insights into the immunopathology of early *Toxocara canis* infection in mice. Parasit. Vectors 8, 354.
- Robertson, B.D., Bianco, A.T., McKerrow, J.H., Maizels, R.M., 1989. *Toxocara canis*: proteolytic enzymes secreted by the infective larvae in vitro. Exp. Parasitol. 69, 30–36.
- Rodríguez-Caballero, A., Martínez-Gordillo, M.N., Caballero-Salazar, S., Rufino-González, Y., Ponce-Macotela, M., 2017. *Toxocara canis*: Analysis of the kinetics of antigen release and antibody production in an in vivo model for the detection of past or present infection. Vet. Parasitol. 243, 183–187. https://doi.org/10.1016/j.vetpar.2017.06.027
- Rodríguez-Caballero, A., Martínez-Gordillo, M.N., Medina-Flores, Y., Medina Escutia, M.E., Meza-Lucas, A., Correa, D., Caballero-Salazar, S., Ponce-Macotela, M., 2015. Successful capture of *Toxocara canis* larva antigens from human serum samples. Parasit. Vectors 8. https://doi.org/10.1186/s13071-015-0875-5
- Rosser, E.C., Mauri, C., 2015. Perspective Regulatory B Cells : Origin , Phenotype , and Function. Immunity 42, 607–612. https://doi.org/10.1016/j.immuni.2015.04.005

- Schantz, P., Glickman, L., 1983. Ascáridos de perros y gatos: un problema de salud pública y de medicina veterinaria. Boletín la Of. Sanit. Panam. 94, 571–586. https://doi.org/10.1007/BF00746189
- Schnieder, T., Laabs, E.M., Welz, C., 2011. Larval development of *Toxocara canis* in dogs. Vet. Parasitol. 175, 193–206. https://doi.org/10.1016/j.vetpar.2010.10.027
- Schwartz, M., Zhang, Y., Rosenblatt, J.D., 2016. B cell regulation of the anti-tumor response and role in carcinogenesis. J. Immunother. Cancer 4, 1–15. https://doi.org/10.1186/s40425-016-0145-x
- Shen, M., Hu, P., Donskov, F., Wang, G., Liu, Q., Du, J., 2014. Tumor-associated neutrophils as a new prognostic factor in cancer: A systematic review and meta-analysis. PLoS One 9, 1–10. https://doi.org/10.1371/journal.pone.0098259
- Steinman, R.M., Inaba, K., Turley, S., Pierre, P., Mellman, I., 1999. Antigen capture, processing, and presentation by dendritic cells: Recent cell biological studies. Hum. Immunol. 60, 562–567. https://doi.org/10.1016/S0198-8859(99)00030-0
- Stensvold, C.R., Skov, J., Møller, L.N., Jensen, P.M., Kapel, C.M.O., Petersen, E., Nielsen, H. V., 2009. Seroprevalence of human toxocariasis in Denmark. Clin. Vaccine Immunol. 16, 1372–1373. https://doi.org/10.1128/CVI.00234-09
- Strube, C., Heuer, L., Janecek, E., 2013. *Toxocara* spp. infections in paratenic hosts. Vet. Parasitol. 193, 375–389. https://doi.org/10.1016/j.vetpar.2012.12.033
- Taira, K., Saeed, I., Lind, P., Murrell, K.D., Kapel, C.M.O., 2003. Population dynamics of *Toxocara canis* in pigs receiving a single or multiple infection. Parasitology 127, 593–602.
- Tefera, T., Biruksew, A., Mekonnen, Z., Eshetu, T., 2014. Parasitic Contamination of Fruits and Vegetables Collected from Selected Local Markets of Jimma Town , Southwest Ethiopia. Int. Sch. Res. Not. 2014, 1–7. https://doi.org/10.1155/2014/382715
- Wang, C., Lee, J.H., Kim, C.H., 2012. Optimal population of Foxp3+ T cells in tumors requires an antigen priming-dependent trafficking receptor switch. PLoS One 7, e30793.
- Webster, G.A., 1958. A Report on *Toxocara canis* Werner, 1782. Can. J. Comp. Med. Vet. Sci. 22, 272–279.
- Yang, S.X., Wei, W.S., Ouyan, Q.W., Jiang, Q.H., Zou, Y.F., Qu, W., Tu, J.H., Zhou, Z.B., Ding, H.L., Xie, C.W., Lei, Q.M., Zhong, C.R., 2016. Interleukin-12 activated CD8+T cells induces apoptosis in breast cancer cells and reduces tumor growth. Biomed. Pharmacother. 84, 1466–1471. https://doi.org/10.1016/j.biopha.2016.10.046
- Zhang, Y., Morgan, R., Chen, C., Cai, Y., Clark, E., Khan, W.N., Shin, S.U., Cho, H.M., Bayati, A. Al, Pimentel, A., Rosenblatt, J.D., 2016. Mammary-tumor-educated b cells acquire lap/tgf-β and pd-l1 expression and suppress antitumor immune responses.

Int. Immunol. 28, 423–433. https://doi.org/10.1093/intimm/dxw007

- Zhao, X., Qu, J., Sun, Y., Wang, J., Liu, X., Wang, F., Zhang, H., Wang, W., Ma, X., Gao, X., Zhang, S., 2017. Prognostic significance of tumor-associated macrophages in breast cancer: a meta-analysis of the literature. Oncotarget 8, 30576–30586. https://doi.org/10.18632/oncotarget.15736
- Zhou, J., Tang, Z., Gao, S., Li, C., Feng, Y., Zhou, X., 2020. Tumor-Associated Macrophages : Recent Insights and Therapies. Front. Oncol. 10, 1–13. https://doi.org/10.3389/fonc.2020.00188
- Zitvogel, L., Tesniere, A., Kroemer, G., 2006. Cancer despite immunosurveillance: immunoselection and immunosubversion. Nat. Rev. Immunol. 6, 715–727. https://doi.org/10.1038/nri1936

VIII. Apéndice

8.1 Soluciones empleadas

8.1.1 Solución de carbonatos (0.1 M, pH 9.6):

- 3.18 g de Na_2CO_3 (carbonato de sodio).
- 5.68 g de $NaHCO_3$ (bicarbonato de sodio).

I) Los reactivos se mezclaron en 800 ml de agua destilada grado II (H_2O DD).

II) La solución se ajustó a pH 9.6 y se aforó a 1.0 L. Se almacenó a 4°C hasta su uso.

8.1.2 Solución salina de fosfatos (PBS 10x y 1x).

- 80.06 g de NaCl (cloruro de sodio).
- 2.0 g de KCl (cloruro de potasio).
- 6.12 g de Na_2HPO_4 (fosfato disódico anhidro).
- 1.9 g de KH_2PO_4 (fosfato de potasio monobásico).

I) Los reactivos se mezclaron en 800 ml de H2O DD.

II) La solución se ajustó a pH 7.2 y se aforó a 1.0 L.

III) Se almacenó a temperatura ambiente hasta su uso.

IV) La solución PBS empleada en este trabajo fue 1x, por lo que se agregaron 100 ml de PBS 10x y se aforó con H2O DD a 1 L. la solución se ajustó a pH 7.4 y se guardó a temperatura ambiente hasta su uso.

8.1.3 Solución de lavado (PBS Tween 20 al 0.05%).

- 500 µl de Tween 20 (BioRad).
- 100 ml de PBS 10x pH 7.2.

I) Los reactivos se aforaron a 1 L de H2O DD.

II) Se almacenó a 4° C hasta su uso.

8.1.4 Solución de bloqueo (para una placa de ELISA).

- 1 g (1%) o 3 g (3%) de albúmina sérica bovina (Sigma).
- 100 ml de solución PBS Tween 20 al 0.05% (BioRad).

I) Se mezclaron los reactivos y se usó en el momento que se realizó el ensayo.

8.1.5 Solución de dilución.

- 0.1 g de albúmina sérica bovina (Sigma).
- 100 ml de solución PBS Tween 20 al 0.05% (BioRad).

I) Se mezclaron los reactivos y se usó en el momento que se realizó el ensayo.

8.1.6 Solución de cromógeno (para una placa de ELISA).

- 5 ml de citrato de sodio 0.1 M.
- 5 ml de ácido cítrico 0.1 M.
- 5 mg de ortofenildiamina (OPD).

- 5 µl de H_2O_2 30%.

I) Se preparó la solución agregando el H_2O_2 30% al final y se usó inmediatamente después de su preparación.

8.1.7 Medio de cultivo RPMI 1640 (GIBCO ®).

I) Se colocó el medio en polvo con 2g de NaHCO3 en vaso de precipitado de 1L.
II) Se agregaron 800 ml de H2O DD y se disolvió.
III) Se ajustó el pH a 7.2-7.4 y se aforó a 1L con H2O DD.
IV) Se filtró al vacío con una membrana de 0.22µm.
VI) Se agregaron los antibióticos (penicilina/estreptomicina), se homogeneizó y se hicieron alícuotas de 250 ml.
VII) Se dejó a prueba de esterilidad a por una noche y se guardó a 4°C hasta su uso.

8.1.8 Jugo gástrico artificial

- 1% pepsina SIGMA (250 unidades/mg).
- 1% HCl 37%.

I) Se añadieron los ingredientes y se disolvieron en 100 ml de PBS 1x.
II) Se ajustó el pH a 2 y se usó en el momento.

8.1.9 Buffer ACK

- 150 mM NH_4Cl.
- 10 mM $KHCO_3$.
- 0.1 mM Na_2.
- EDTA.

I) Se añadieron los ingredientes y se disolvieron en 100 ml H2O DD.
II) Se ajustó el pH a 7.3.

8.1.10 Buffer de FACS

- 2% SFB.
- 0.02% NaN_3.
- 100 ml PBS 1x estéril.

I) Se añadieron los ingredientes y se disolvieron en 100 ml de PBS 1x.
II) Se guardó a 4°C hasta su uso.

8.1.11 Solución de digestión de tumores

- Colagenasa.
- DNAsa.
- Medio RPMI 1640 (500 µl/tumor).

I) Se añadieron los ingredientes y se usó en el momento.

8.2 Artículos originales publicados derivados de la Tesis.

Ruiz-Manzano Rocío Alejandra, Hernández-Cervantes Rosalía, Del Río-Araiza Víctor Hugo, Palacios-Arreola Margarita Isabel, Nava-Castro Karen Elizabeth, Morales-Montor Jorge. (**2019**).Immune response to chronic *Toxocara canis* infection in a mice model. *Parasite Immunology*; 00:e12672.
https ://doi.org/10.1111/pim.12672

Ruiz-Manzano Rocío Alejandra, Palacios-Arreola Margarita Isabel, Hernández-Cervantes Rosalía, Del Río-Araiza Víctor Hugo, Nava-Castro Karen Elizabeth, Ostoa-Saloma Pedro, Muñoz-Cruz Samira and Morales-Montor Jorge. (**2020**). Potential Novel Risk Factor for Breast Cancer: *Toxocara canis* infection increases tumor size due to modulation of the tumor immune microenvironment. Frontiers in Oncology; 10:736.
https://doi: 10.3389/fonc.2020.00736

Received: 23 April 2019 | Revised: 18 September 2019 | Accepted: 23 September 2019

DOI: 10.1111/pim.12672

ORIGINAL ARTICLE

Parasite Immunology WILEY

Immune response to chronic *Toxocara canis* infection in a mice model

Rocío Alejandra Ruiz-Manzano[1] | Rosalía Hernández-Cervantes[1] | Víctor Hugo Del Río-Araiza[2] | Margarita Isabel Palacios-Arreola[3] | Karen Elizabeth Nava-Castro[3] | Jorge Morales-Montor[1]

[1]Departamento de Inmunología, Instituto de Investigaciones Biomédicas, Universidad Nacional Autónoma de México, Ciudad de México, México

[2]Departamento de Parasitología, Facultad de Medicina Veterinaria y Zootecnia, Universidad Nacional Autónoma de México, Ciudad de México, México

[3]Departamento de Genotoxicología, Centro de Ciencias de la Atmósfera, Universidad Nacional Autónoma de México, Ciudad de México, México

Correspondence
Jorge Morales-Montor, Departamento de Inmunología, Instituto de Investigaciones Biomédicas, Universidad Nacional Autónoma de México; Circuito Mario de la Cueva s/n, Ciudad Universitaria, AP 70228, Ciudad de México, México 04510.
Emails: jmontor66@biomedicas.unam.mx; jmontor66@hotmail.com

Funding information
This study was supported by grants from Programa de Apoyo a Proyectos de Investigación e Innovación Tecnológica (PAPIIT); Dirección General de Asuntos del Personal Académico (DGAPA); Universidad Nacional Autónoma de México (UNAM), Grant/Award Number IN-209719; and Fronteras en la Ciencia, Consejo Nacional de Ciencia y Tecnología (CONACYT), Grant Number FC 2016 2125 (both to J. Morales-Montor). Grant from PAPIIT, DGAPA, UNAM and IA 20219 was awarded to Karen E. Nava-Castro.

Abstract

Aims: The zoonotic nematode *Toxocara canis* causes larva migrans syndrome that induces an immune response characterized by the production of antibodies and eosinophilia. A Th2 polarization has been associated with the infection, but there are still details of the cellular and humoral immune response that need to be described. Thus, the aim of this study was to describe the systemic host immune response to *T canis* chronic infection in a mouse model.

Methods and Results: BALB/c mice were inoculated once with 500 *T canis* embryonated eggs, *per os*. After 49 days, the amounts of larval found in brain and muscle tissues were statistically two and four times higher, respectively, than the amounts found in lung, liver, kidney or heart tissues. Splenic proportions of $F4/80^+$ cells, as well as B, cytotoxic T and $CD4^+Foxp3^+$ lymphocytes, were statistically higher ($P \leq .05$, $P \leq .01$, $P \leq .001$ and $P \leq .001$, respectively) as compared with control mice. In lymph nodes, some of these proportions changed, with the exception of $F4/80^+$ cells. IgG1 levels in infected mice sera were increased. IL-4, IL-10 and VEGF levels were statistically higher in spleen ($P \leq .05$, all) and sera ($P \leq .01$, $P \leq .05$ and $P \leq .05$, respectively) in the infected mice. Also, in infected animals, IL-5 serum levels were increased ($P \leq .01$).

Conclusion: These results suggest that *T canis* chronic infection in BALB/c mice results in a type 2 response with an incipient regulatory response.

KEYWORDS

adaptive immunity, cellular immunity, humoral immune response, innate immunity, larva migrans, Th1-Th2 cytokine balance, *Toxocara canis*

1 | INTRODUCTION

Toxocara canis infection is a worldwide neglected zoonosis. Canids, including domestic dogs, are the definitive hosts. Meanwhile, paratenic hosts include humans, mice, rats, lambs, poultry, pigs, flies and cockroaches.[1-4] In these paratenic hosts, *T canis* larval migrate through different organs and tissues including liver, lungs, kidney, eye, heart, skeletal muscle and brain and do not develop into the adult form.[5] Four types of larva migrans manifestations have been characterized in humans: visceral, ocular, covert and neurotoxocarosis.[6,7]

The survival and pathogenic action of larval in their hosts are associated with *T canis* excretory-secretory (TES) products. TES also

promote and modulate the host immune response. The evasion of this response allows the larval to survive for several years in the host tissues.[8]

The immune response to chronic *T canis* infection in paratenic hosts is associated with peripheral blood eosinophilia, eosinophilic infiltration around larval sites of migration, specific antibody production (IgG and IgE) and a T helper type 2 (Th2) response.[9] This Th2 response has been demonstrated through serum cytokine detection and in vitro assays. For example, in human serum with anti-*T canis* antibodies, IL-4 and IL-10 levels were increased compared with control donors.[10] Also, in *T canis*-infected mice, IL-5 and IL-4 levels were increased at 7 and 14 days post-inoculation (d.p.i.), respectively.[9] Additionally, in human peripheral T cells specific for TES, IL-4 and IL-5 production was induced when cells were exposed to TES.[11]

Although eosinophils are related to the host response to nematode infection, other innate immune cells such as the macrophages also play an important role.[12] Depending on their surrounding milieu, macrophages acquire a classical or alternative activation in order to contribute to physiologic homeostasis.[13] Alternatively activated macrophages (AAMs), which possess wound-healing and humoral responses, have anti-inflammatory functions in helminth infection which are mediated through the secretion of IL-4, IL-10, IL-13, TGF-β and VEGF.[14,15] A previous study reported that macrophages from *T canis*-infected mice cultured in vitro produced higher quantities of IL-10 and lower quantities of TNF-α and IL-12; therefore, this infection may also be related to the generation of AAM.[16]

Together, eosinophils, Th2 cells and AAMs are traditionally associated with a protective host immune type 2 response to helminths. Nevertheless, when infection becomes chronic, the attenuation of this response ameliorates the damage to the host. Helminth excretory-secretory products (ES) are also responsible for host immune regulation by inducing T regulatory (Treg) cells and B regulatory (Breg) cells which also produce IL-10.[12] In this sense, *T canis* infection in mice induces the expansion of Foxp3$^+$ Treg in the liver and an increase of Foxp3 mRNA in the spleen.[17]

Even if host immune response to helminths is similar, extrapolation based on studies from other nematodes cannot be assumed due to the differences among parasites. For example, *T canis* larval migrate and eventually undergo hypobiosis in many tissues.[5] The immune cell response is thus focused on the larva, but it is also systemic, associated with the migration of the parasite. Most of the evidence that links *T canis* infection and a type 2 response is based on reports that measure immune cell populations and cytokines in various compartments such as blood vessels (sera) and the spleen, and most of the studied response is localized to adjacent tissues where larval migrate and establish themselves. Therefore, the aim of this study was to develop a descriptive study of the immune response to *Toxocara canis* chronic infection so as to integrate the findings from this and other associated reports in order to further unveil additional elements, mechanisms and interactions of this response.

2 | MATERIALS AND METHODS

2.1 | Ethics statement

Experimental procedures and animal care were performed at the Instituto de Investigaciones Biomédicas (IIB), Universidad Nacional Autónoma de México (UNAM) in the Biologic Models Unit (Unidad de Modelos Biológicos—UMB). The Institutional Care and Animal Use Committee (CICUAL) evaluated and approved experimental procedures (permit number 2017-208) adhering to Mexican regulation (NOM-062-ZOO-1999) and in strict accordance with National Institute of Health (NIH) of the US Guide for the Care and Use of Laboratory Animals. Blood was collected through cardiac puncture from deeply anaesthetized animals with sevoflurane 5% (Abbot, Mexico), and then, the mice were euthanized by cervical dislocation. Serum samples were obtained by blood centrifugation and stored at −70°C until use.

2.2 | Animals

Twenty-eight-week-old, BALB/c AnN strain, syngeneic female mice were purchased from Envigo México (Facultad de Química, UNAM) and kept at the UMB IIB, UNAM, in standard conditions: controlled temperature of 22°C and 12-hour light-dark cycles. Ad libitum water and Purina LabDiet 5015 (Purina) were delivered in sterile conditions.

2.3 | *Toxocara canis* infection

Adult *T canis* females were obtained from dog faeces after natural defecation. After three wash cycles with phosphate-buffered saline solution (PBS, pH 7.4) and PBS/2% formaldehyde solution, uteri were obtained through cuticle incision of the anterior section. Eggs were then passed through a fine mesh to eliminate debris. Egg suspension was centrifuged at 3250 g/5 min (HERMLE Z400K) and resuspended in PBS, where they were maintained at room temperature over 28 days. Larval development was supervised weekly. To induce infection, 500 larvated eggs were inoculated once with an oral feeding needle.

2.4 | larval recovery and splenic index

After 49 d.p.i., the lungs, livers, kidneys, hearts, brains and muscles from the diaphragm and thoracic and pelvic limbs from five infected mice were excised and minced finely with scalpel. The muscles recovered from the thoracic and pelvic limbs and diaphragm were pooled together and weighted. Then, 1 g of this pooled muscular mass was processed for digestion, and the number of larval obtained was multiplied for the weight of the pooled muscles. Tissues were digested in artificial gastric juice that contained 1% pepsin Sigma (250 units/mg)/1% HCl, pH 2.0, at 10 mL of artificial gastric juice per gram of tissue (4 h/37°C). Digested tissues were centrifuged at 791 g/5 min. For larval fixation, 1 mL of 4% paraformaldehyde/PBS was added.

Sample content was examined under a light microscope (M280LED, UNICO). Splenic index was obtained as described elsewhere.[18]

2.5 | *Toxocara canis* larval culture and TES collection

Toxocara canis excretory-secretory was obtained based on De Savigny[19] and Bowman[20] methods, with modifications. Briefly, embryonated egg suspension was centrifuged at 3250 g/5 min. To disaggregate the outer egg layer, 1 mL of sodium hypochlorite was added. After 10 minutes in continuous gentle agitation, eggs were washed with 10 mL of bi-distillate sterile water, centrifuged at 3250 g/5 min and washed three times with PBS. Eggs were resuspended in RPMI 1640 (Sigma) with 1% antibiotic-antimycotic (Gibco). larval hatching was stimulated with magnetic stirrer for 20 minutes, and egg suspension was maintained at 37°C in a humidified atmosphere containing 5% (v/v) CO_2 overnight. larval were cleaned from eggshells through a modified Baermann technique and maintained in a 10^4 larval/mL. The supernatant was recollected weekly and filtered with a 20-μm syringe filter (Millipore), from which the medium was replaced. Protein was precipitated with acetone (Herschi Trading, High Purity, 99.5%) at −20°C, resuspended in PBS and stored at −20°C until use. Protein concentration was calculated using the Bradford Protein Assay Bio-Rad® technique.

2.6 | Anti-*Toxocara canis* IgG detection

Polystyrene wells (96-well plate, MaxiSorp Nunc) were coated with 50 μL of TES (1 μg/mL) in bicarbonate buffer (pH 9.6) and incubated overnight at 4°C. The plate was washed with washing solution (PBS/Tween 20 0.05%) and blocked with 200 μL of 3% bovine serum albumin (BSA) (Sigma)/washing solution for 30 minutes at 37°C. After washing, 50 μL of sera (1:200 in PBS/1% BSA/Tween 20 0.05%) was added in duplicate and incubated for 1 hour at room temperature. The plate was washed, and 50 μL of a 1:10 000 dilution of peroxidase goat anti-mouse IgG, IgG1 and IgG2 (Jackson) was added and incubated for 90 minutes at room temperature. Enzyme-substrate reaction was developed by the addition of 50 μL of substrate solution (0.05% o-Phenylenediamine/0.01% H_2O_2/0.1 mol/L sodium citrate/0.1 mol/L citric acid) and stopped after 10 minutes with 50 μL of 2N sulphuric acid. Plates were read at a wavelength of 492 nm in a Stat Fax 4200 Microplate Reader (Awareness Technology).

2.7 | Flow cytometry

Left and right peripheral (inguinal) lymph nodes (PLN) and spleen were excised and mechanically disaggregated through a 50 μm nylon mesh with PBS. Erythrocytes in splenic suspension were lysed with ACK buffer (150 mmol/L NH_4Cl/10 mmol/L $KHCO_3$/0.1 mmol/L Na_2EDTA, pH 7.3) for 10 minutes. Both cell suspensions were washed with PBS and resuspended in FACS buffer (PBS/foetal bovine serum 2%/NaN_3 0.02%). Approximately $1x10^6$ cells were incubated (20 minutes at 4°C) with anti-CD16/CD32 (TruStain®, BioLegend), washed and then stained with three panels: (a) T lymphocyte: Alexa Fluor® 488-conjugated anti-CD3ε (145-2C11) 1:100, PE-conjugated anti-CD4 (GK1.5) 1:300, PerCP-conjugated anti-CD8 (53-6.7) 1:100 and Alexa Fluor® 647-conjugated anti-Foxp3 (150D) 1:100; (b) macrophage and NK mix: Alexa Fluor® 647-conjugated anti-F4/80 (BM8) and PE-conjugated anti-NKp46 (29A1.4); and (c) B lymphocyte: PE-conjugated anti-CD19 (6D5), 1:200. All antibodies were obtained from BioLegend. The Foxp3/Transcription Factor Staining Buffer Kit (Tonbo Biosciences) was used for intracellular Foxp3 staining according to manufacturer protocol. Gating strategy is described in Figure S1.

Cell analysis was performed with the BD FACSCalibur™ (BD Biosciences) flow cytometer. Data were analysed with FlowJo software (Treestar Inc). Compensation was assessed using BD FACSCalibur™ and FlowJo software with unstained samples, single stain controls and FMO for $Foxp3^+$ ($CD3^+/CD4^+$; $CD3^+/CD8^+$).

2.8 | Cytokine determination

Mice spleen was stored in TRIzol™ reagent (Ambion) at −70°C until use. Protein isolation was performed through procedural guidelines for TRIzol™ (Ambion). Protein quantification was done with the NanoDrop 1000 Spectrophotometer (Thermo Scientific). 10 μg of protein per well was used to determine cytokine tissue levels.

Sera and splenic cytokines were measured with ABTS ELISA Kits (PeproTech) with the following antibodies: TNF-α (500-P64), IFN-γ (500-P119), IL-4 (500-P54), IL-5 (500-P55) and IL-10 (500-P60). Biotinylated antibodies were used for antigen detection. Enzyme-substrate reaction was developed with ABTS liquid substrate (PeproTech). Plates were read at a wavelength of 405 nm with wavelength correction set at 650 nm in a Stat Fax 4200 Microplate Reader (Awareness Technology).

2.9 | VEGF quantification

Polystyrene wells (96-well plate, MaxiSorp Nunc) were coated with 50 μL of splenic protein (10 μg), sera (dilution 1:2) or standard curve (0.001 ng-1 ng) in bicarbonate buffer (pH 9.6) per duplicate and incubated at 4°C overnight. Plates were washed and blocked with 200 μL of PBS/BSA 1%/Tween 20 0.05% for 1 hour at 4°C. After washing, 50 μL of anti-VEGF/C-1 antibody (sc-7269, Santa Cruz Biotechnology) in a 1:200 dilution was added and incubated for 1 hour at 4°C. After washing, 50 μL of m-IgGκ/BP-HRP (sc-516102, Santa Cruz Biotechnology) (1:400) was added and maintained for 2 hours at room temperature. Enzyme-substrate reaction was developed with of 50 μL of substrate solution and stopped after 15 minutes with 50 μL 2N sulphuric acid. Plates were read at a wavelength of 492 nm in a Stat Fax 4200 Microplate Reader (Awareness Technology). Cytokine and VEGF concentrations were calculated by interpolation from a standard curve.

Cytokine and antibody determinations were performed after appropriate ELISA standardization.

2.10 | Statistical analysis

Data obtained from 2 independent experiments were charted as mean ± standard deviation. To analyse differences among numbers of larval in tissues from infected mice, an ANOVA test was used. Meanwhile to compare the differences between intact and infected animals, the Student *t* test was used. Welch's correction was applied in the groups where variances were different, as determined through an F test. The differences were considered significant when $P \leq .05$. All analyses were calculated using Prism 6® software (GraphPad Software Inc).

3 | RESULTS

3.1 | larval in chronic *Toxocara canis* infection establishes predominantly in musculature and brain

We assessed larval recovery from tissues to determine those most affected by the presence of *T canis* larval. Although in all sampled tissues larval were found, the highest numbers were found in skeletal muscle and brain ($P < .0001$) (Figure 1).

3.2 | *Toxocara canis* infection induces humoral response

An increase in spleen index from infected animals was observed ($P = .0010$) (Figure 2A). Also, in *T canis*-infected animals, a higher proportion of B cells CD19$^+$ was found in spleen ($P = .0064$) and PLN ($P = .0006$) compared with controls (Figure 2C). To determine specific humoral response, we detected anti-*T canis* IgG, IgG1 and IgG2a in serum, and specific IgG and IgG1 levels were higher ($P < .0001$ and $P < .0001$) in infected animals (Figure 2B).

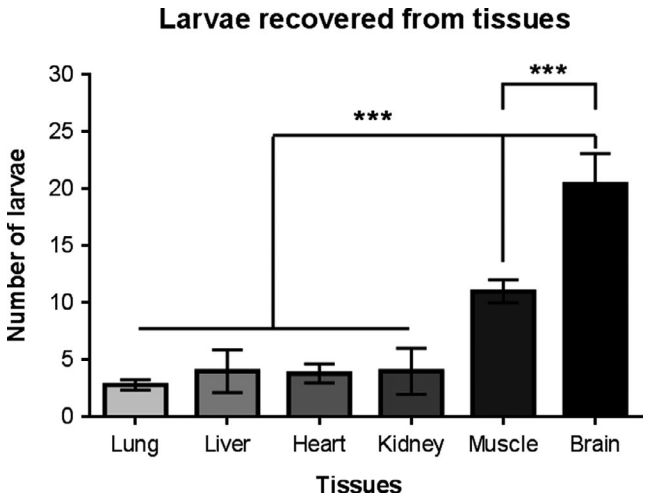

FIGURE 1 *Toxocara canis* larval recovery from BALB/c-infected mice. Number of larval recovered after 49 d.p.i. from lung, liver, heart, kidney, skeletal muscle and brain from *T canis*-infected mice with 500 larvated eggs. Graphs represent the mean ± SD of data from five infected animals. Statistical significance was calculated using one-way ANOVA followed by Tukey's multiple test (***$P \leq .001$)

3.3 | Infection modifies F4/80 + cell proportions in secondary lymphoid organs

Since *T canis* larval migrate and establish itself in different organs, immune response in secondary lymphoid organs was assessed. Flow cytometry analysis of natural killer (NK) cells and F4/80$^+$ macrophages (innate response) and immune T cells (adaptive response) in PLN and in spleen after 49 d.p.i. was performed (Figures 3, 4, 5). In spleen, the F4/80$^+$ cell proportion was increased ($P = .0228$) because of the infection (Figure 3A). In PLN, the F4/80$^+$ cell percentage was lower ($P = .0117$) in the *T canis*-infected group. NK cells were absent in PLN (Figure 3B).

3.4 | *Toxocara canis* infection increases the proportion of CD8$^+$ T lymphocytes and CD4$^+$/Foxp3$^+$ Treg cells in spleen and PLN

At 49 d.p.i., the T lymphocyte subpopulations were evaluated in spleen (Figure 4A–D) and PLN (Figure 5A–D). The infection induced a decrease in CD3$^+$ cells in the spleen (Figure 4A), an expansion of CD4$^+$/FoxP3$^+$ Treg cells in spleen (Figure 4C $P < .0001$) and PLN (Figure 5C $P = .0077$) as expected, and an unexpected increase in CD8$^+$T-cell proportion in both compartments ($P = .0006$ and $P = .0001$, respectively) (Figures 4B and 5B). The other regulatory cells measured were the CD8$^+$/FoxP3$^+$ Treg cells, whose amount was increased only in PLN (Figure 5D $P = .002$). The CD4$^+$ T cells (Figure 4B) and CD8$^+$/FoxP3$^+$ Treg splenic cells (Figure 4D) did not change. In PLN, there was a slight decrease in CD3$^+$ cells (Figure 5A).

3.5 | *Toxocara canis* chronic infection in mice induces a systemic type 2 towards a regulatory immune response

To characterize the immune response to *T canis* chronic infection, serum (Figure 6) and splenic (Figure 7) levels of type 1 response (TNF-α and IFN-γ) and type 2 response (IL-4, IL-5, IL-10 and VEGF) were measured.

Levels of IFN-γ in sera (Figure 6) were lower ($P = .0128$), while splenic levels did not change (Figure 7). In contrast, no statistical difference was seen in TNF-α serum levels (Figure 6). Type 2 cytokines such as IL-4, IL-5, IL-10 and VEGF were higher in sera from infected animals ($P = .0018$, $P = .0035$, $P = .0304$ and $P = .0110$, respectively) (Figure 6). Surprisingly, serum levels of IL-5, also a type 2 response cytokine, were decreased in infected animals ($P = .0019$) (Figure 6).

Concerning splenic levels of cytokines, type 1 response cytokine TNF-α was lower in infected animals ($P = .0060$) (Figure 7). At the same time, type 2 cytokines IL-4 and VEGF ($P = .0369$ and $P = .0226$, respectively) and the regulatory cytokine IL-10 ($P = .0102$) were all increased (Figure 7).

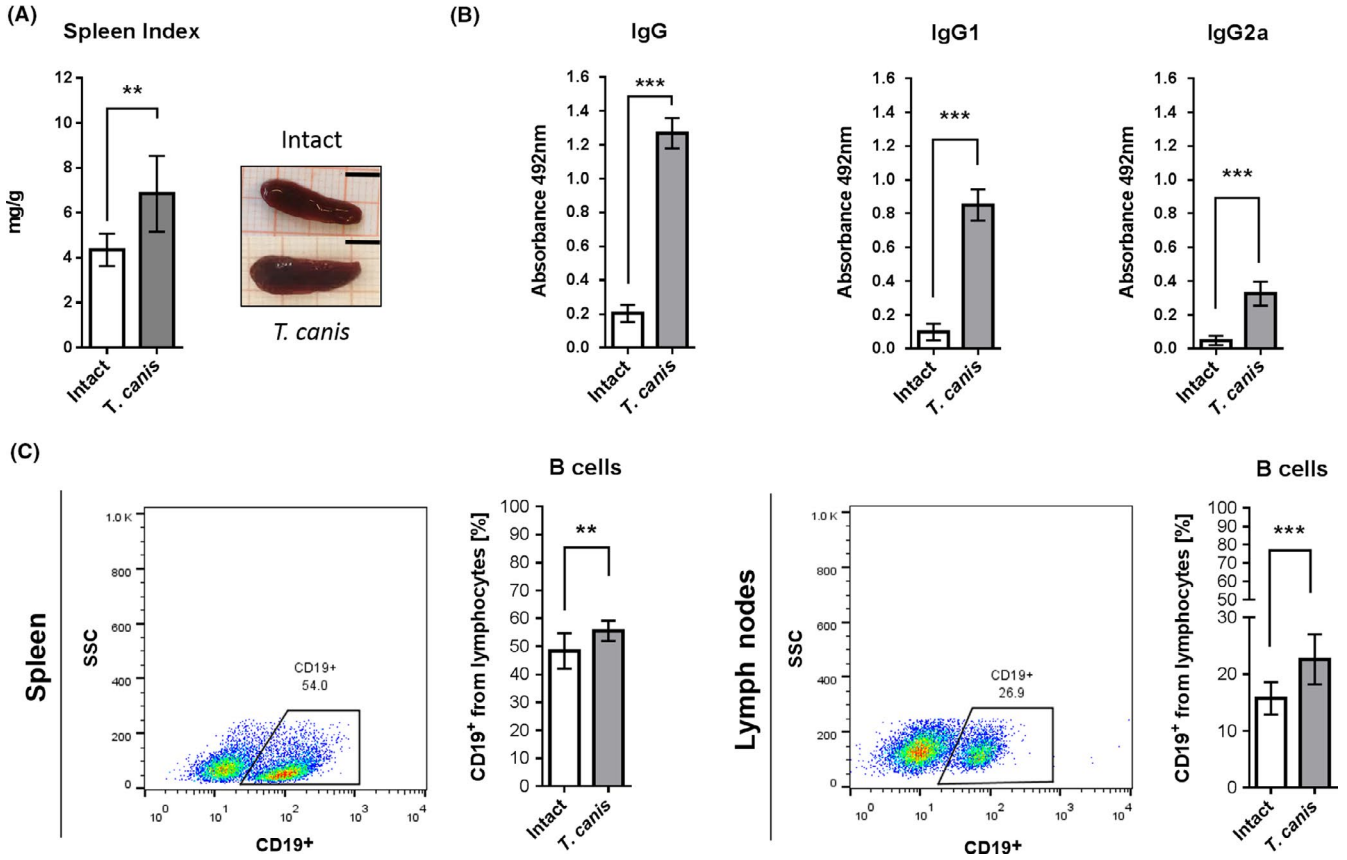

FIGURE 2 Humoral response to *Toxocara canis* infection in BALB/c mice. A, Spleen index and representative images of spleen (right) from intact and infected mice (*T canis*). Black bar = 0.5 cm. B, Anti-*T canis* IgG, IgG1 and IgG2a serum levels measured by indirect ELISA. C, Representative dot plots of cytometric analysis of B-cell percentage; gate from 10 000 lymphocytes collected. Frequencies of B lymphocytes ($CD19^+$) in spleen and PLN. Graphs represent the mean ± SD of data from two experiments (intact, n = 10; *T canis*, n = 10). Statistical significance was calculated using *t* test (**$P \leq .01$; ***$P \leq .001$)

4 | DISCUSSION

The migration of *T canis* larval throughout different tissues, as well as its establishment and immune response, depends on the paratenic host species, the number of larvated eggs administrated and the d.p.i.[4,21] In this sense, BALB/c mice have proven to be a highly susceptible mice strain in that larval migrate to the brain as early as the 3 d.p.i., the majority of the larval are established in the brain and musculature, and no death related to the infection has been reported.[9,22] To study the systemic chronic phase of the infection, 49 d.p.i. was selected because by this point, the myotropic-neurotropic phase has been established[4,22,23] and by 42-54 d.p.i. larval are actively shedding TES.[24] As expected, at 49 d.p.i. brain and musculature contained the highest number of larval among all the tissues sampled following infection with 500 larvated eggs. Nevertheless, larval were also identified in other organs (lungs, liver, kidneys and heart), which is consistent with the proposal from Othman, which mentioned the accumulation of larval in the brain and stated that some larval continuously migrate and are redistributed in different tissues.[25]

The humoral response to *T canis* infection is the result of complex interactions between immune cells, cytokines and parasites. This fact has been well studied and is the basis of diagnostic immunologic techniques (ELISA and Western blot). Previous reports have described an egg-dose–dependent splenomegaly[18] and also reported increased levels of anti-TES antibodies in mice chronically infected with *T canis*.[20,21] In different studies, 500 larva doses have been used.[20,26,27] Although we used only one time point (49 d.p.i.), splenomegaly and higher anti-*T canis* IgG levels were detected with one dose of 500 larvated eggs; therefore, despite this one time-point limitation, the obtained data enhance the understanding of the immune response to *T canis* chronic infection in mice.

There is an association between IgG2a secretion with a T helper (Th1) response and increased IgG1 levels with a Th2 response.[28] Therefore, higher levels of anti-*T canis* IgG1 may be associated with a type 2 response linked to Th2 cytokines.[29] Also, IgG1 is considered a marker in *T canis* infection and is associated with a gradual increase in IgG2a levels, which may aid in the determination of the infection course.[30] Previous studies of chronically *T canis*-infected mice showed that IgG1 serum levels were increased significantly at doses of 100 and 1000 larvated eggs.[21] Meanwhile, with a 1000 larvated egg dose, specific *T canis* IgG2a and IgG1 serum levels were significantly increased, but the augmentation of IgG1 levels was greater than IgG2a.[21] Results from our study correlate with these findings,

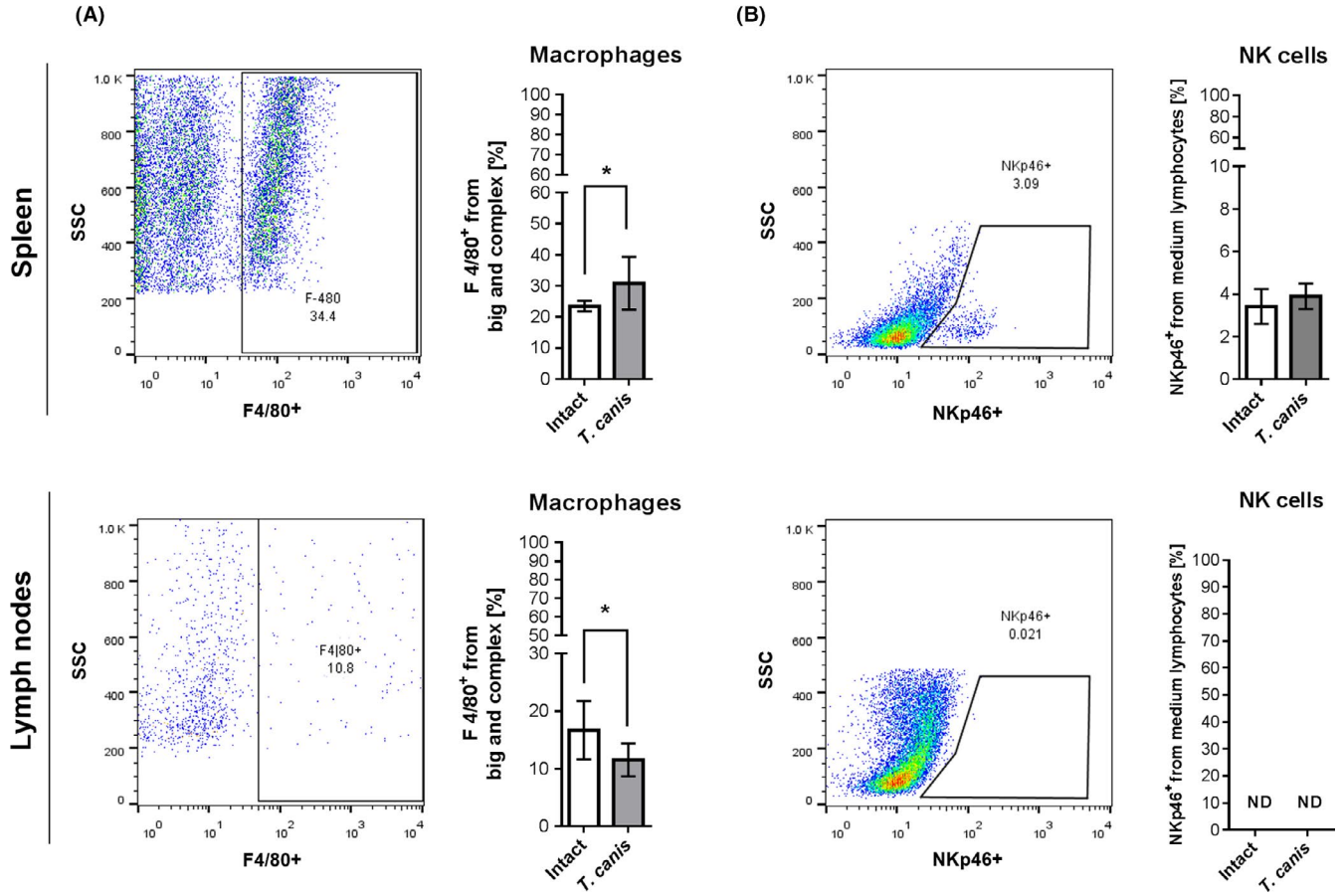

FIGURE 3 Innate immune cell proportion changes due to *Toxocara canis* infection in spleen and PLN. A., Representative dot plots of cytometric analysis of F4/80$^+$ macrophages; gate from 10 000 large and complex cells collected (left). Frequencies of F4/80$^+$ cells (right). B, Representative dot plots of cytometric analysis of NK cell percentage; gate from 10 000 from medium-size and complex cells collected (left). Frequencies of NK cells (NKp46$^+$) (right). Graphs represent the mean ± SD of data from two experiments (intact, n = 10; *T canis*, n = 10). Statistical significance was calculated using *t* test (*$P \leq .05$). ND, no data because this subpopulation was absent from the PLN

since IgG1 and IgG2a serum levels were increased. Although in the intact group the fold change was twice as much for IgG1 in comparison with IgG2 levels, in infected animals the fold change in IgG1 levels was 2.6 higher in the infected mice compared with the IgG2a levels ($P < .0001$) (Figure 2B). Thus, the response to *T canis* chronic infection is predominantly through an IgG1 response related to a type 2 response.

Another feature related to humoral response is the augmented proportion of B lymphocytes in spleen and PLN reported in *T canis*-infected rats.[31] Despite the fact that in our study only one time point was measured, the B-cell expansion, increased level of splenic IL-4 and higher levels of specific IgG with predominance of IgG1 in sera suggested a type 2 response. This can be explained by the ability of IL-4 to induce switch recombination to IgG1 and IgG4 in B cells, which originates plasmatic cells specialized in antibody production.[32,33] On the other hand, splenic CD19$^+$ B lymphocytes (Bregs) possess the ability to secrete IL-10, which suppress CD4$^+$ and CD8$^+$ T cells and induce Treg formation.[34]

Some helminths possess the capacity to survive in their hosts for long periods of time, inducing a chronic immune response. In the early phase of the infection, a type 2 response associated with higher levels of IL-4, IL-5, IL-13, IgE and peripheral eosinophilia is established, and with time, the continuous tissue damage is primarily due to the immune response itself rather than the parasite.[12] Therefore, the immune balance among Th1, Th2 and their regulation is important for host survival and is different among parasites.[35] As mentioned before, *T canis* infection induces both a type 2 and regulatory response but decreases type 1 cytokine production.[9,11,17] Type 2 response was suggested in this study, associated with the augmentation of IL-4 and the increased amount of serum IL-5, in contrast to the reduction in type 1 response represented by diminished TNF-α levels in spleen. Meanwhile, the regulatory response to the infection was supported through the expansion of CD4$^+$/FoxP3$^+$ cells in secondary lymphoid organs and an increase in CD8$^+$/FoxP3$^+$ cells in PLN, together with higher IL-10 levels in spleen and sera, that were found in infected animals.

The Treg response to *T canis* infection was reported in spleen, where *Foxp3* mRNA expression significantly increased from 2 to 16 weeks post-inoculation.[17] But Treg cell presence was not assessed. In the present work, we identified Foxp3 expression in

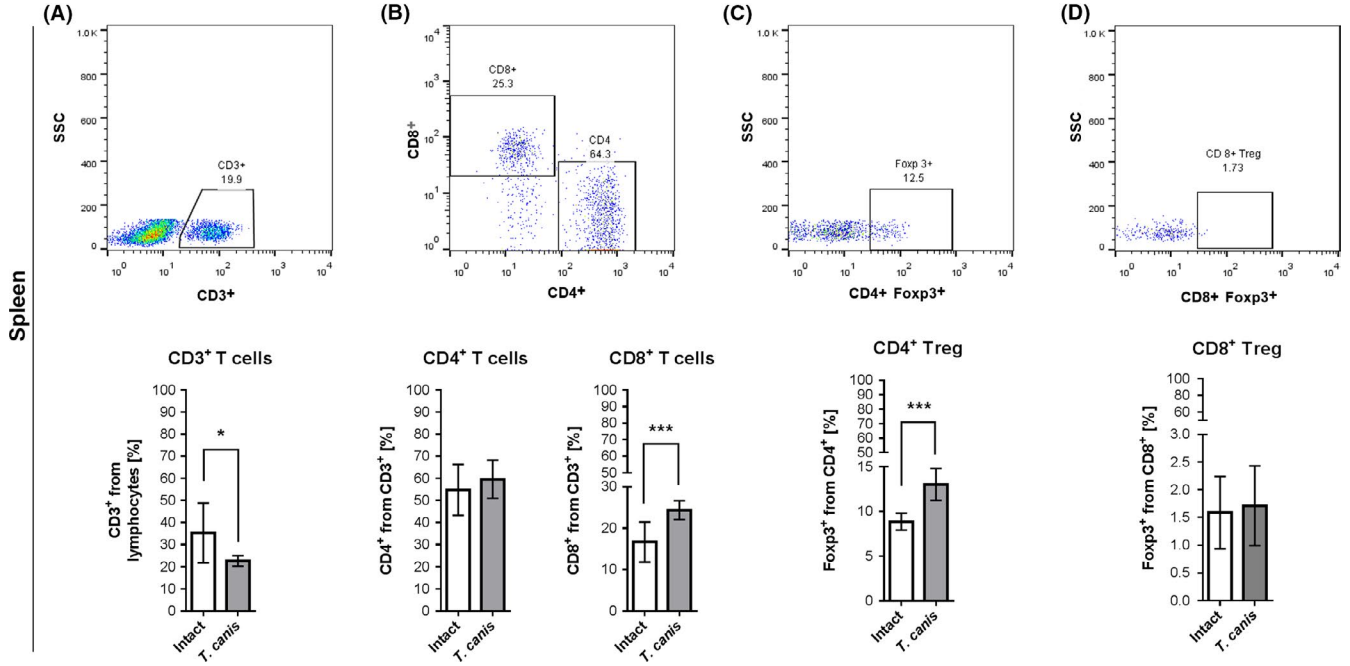

FIGURE 4 Splenic T-cell proportion changes due to *Toxocara canis* infection. Representative dot plots of cytometric analysis of T-cell percentage; gate from 10 000 lymphocytes collected (Upper panel). A, T lymphocytes ($CD3^+$). B, T helper ($CD4^+$) and T cytotoxic cells ($CD8^+$). C, T regulatory cells ($CD4^+Foxp3^+$). D, T regulatory cells ($CD8^+Foxp3^+$). Graphs represent the mean ± SD of data from two experiments (intact, n = 10; *T canis*, n = 10). Statistical significance was calculated using *t* test (*$P \leq .05$; ***$P \leq .001$)

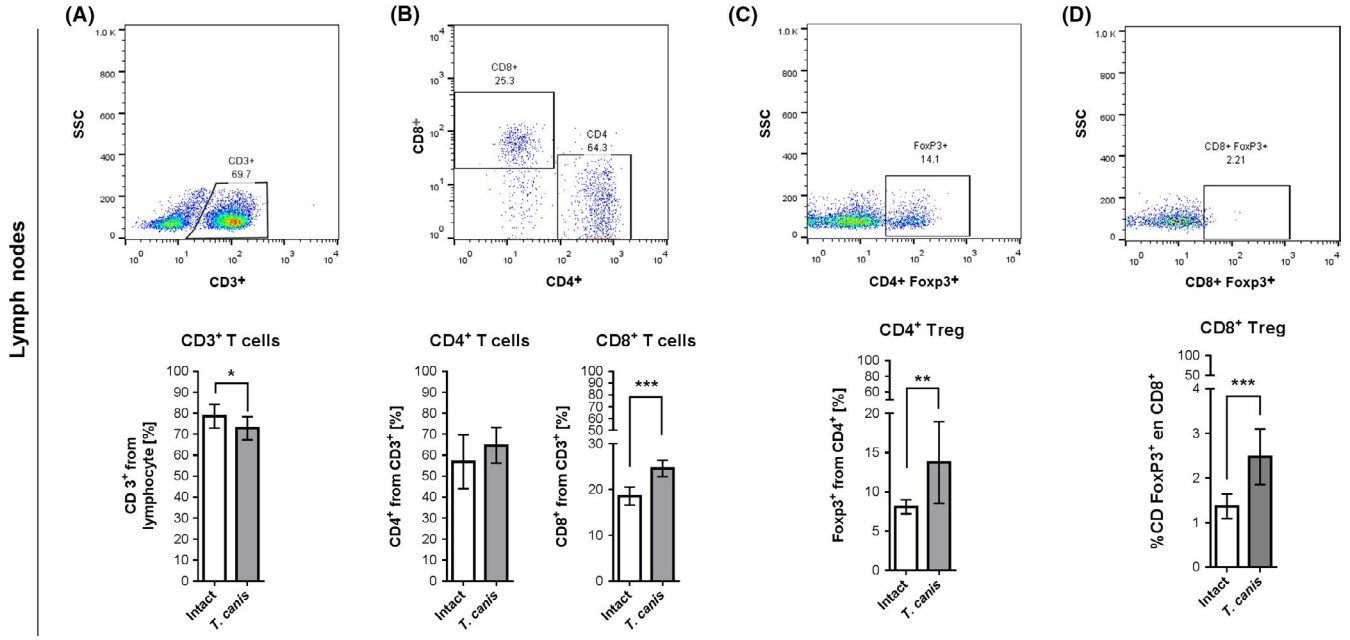

FIGURE 5 T-cell proportions in PLN from *Toxocara canis*-infected mice. Representative dot plots of cytometric analysis of T-cell percentage; gate from 10 000 lymphocytes collected (upper panel). A, T lymphocytes ($CD3^+$). B, T helper ($CD4^+$) and T cytotoxic cells ($CD8^+$). C, T regulatory cells ($CD4^+Foxp3^+$). D, T regulatory cells ($CD8^+Foxp3^+$). Graphs represent the mean ± SD of data from two experiments (intact, n = 10; *T canis*, n = 10). Statistical significance was calculated using *t* test (*$P \leq .05$; **$P \leq .01$; ***$P \leq .001$)

$CD4^+$ T cells in spleen. Furthermore, the presence of Treg cells was not limited to spleen but was also noted in PLN, where both $CD4^+$/$FoxP3^+$ and $CD8^+$/$FoxP3^+$ population proportions were increased. In this sense, infection by another nematode, *Heligmosomoides polygyrus*, induced the expansion of $CD4^+$/$Foxp3^+$ Treg cells in PLN (mesenteric) from infected mice.[36] Unlike *T canis*, *H polygyrus* is found only in intestine, and the proximity with mesenteric lymph nodes may explain Treg expansion. Conversely, the increase

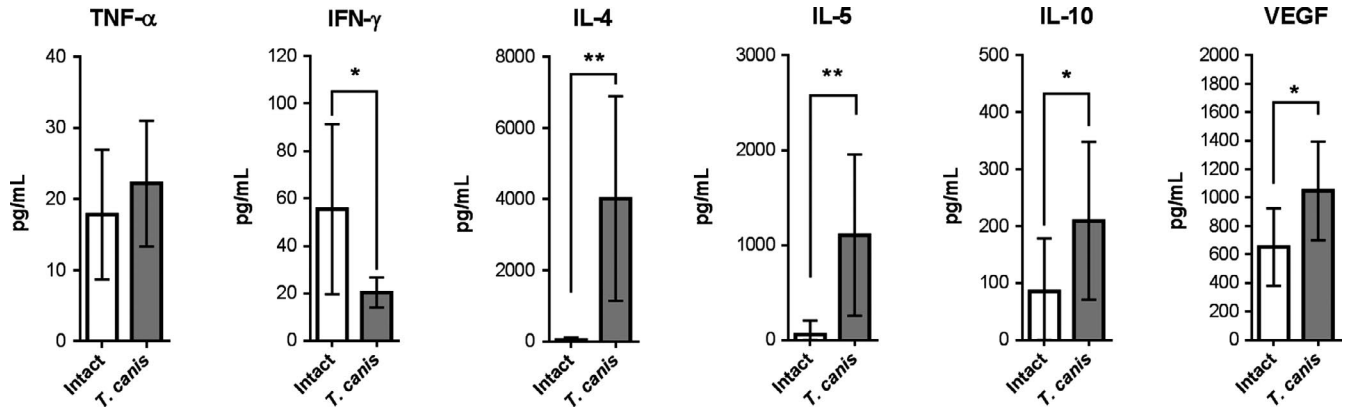

FIGURE 6 Serum cytokines from *Toxocara canis*-infected mice. Determination through sandwich ELISA of type 1 response (TNF-α and IFN-γ) and type 2 (IL-4, IL-5, IL-10 and VEGF) cytokines. Graphs indicate data from sera obtained from two independent experiments (intact, n = 10; *T canis*, n = 10). Bars represent the mean ± SD of cytokine levels (pg/mL from sera). Statistical significance was calculated using *t* test (**P* ≤ .05; ***P* ≤ .01)

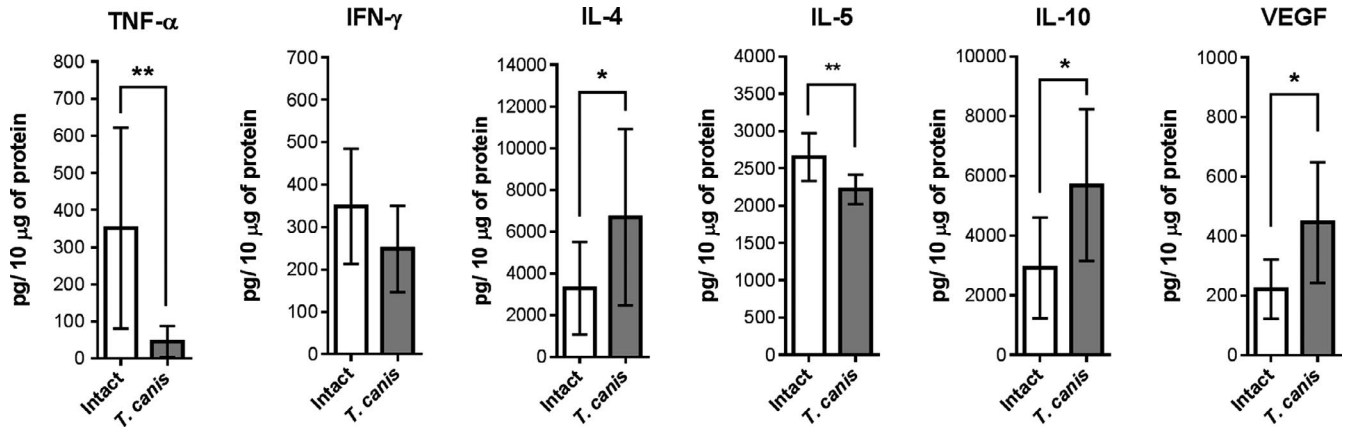

FIGURE 7 Splenic cytokines from *Toxocara canis*-infected mice. Determination through sandwich ELISA of pro-inflammatory (TNF-α and IFN-γ) and Th2 (IL-4, IL-5, IL-10 and VEGF) cytokines. Graphs indicate data from splenic protein obtained from two independent experiments (intact, n = 10; *T canis*, n = 10). Bars represent the mean ± SD of cytokine levels (pg/10 μg of splenic protein). Statistical significance was calculated using *t* test (**P* ≤ .05; ***P* ≤ .01)

in $CD4^+$/$FoxP3^+$ cells in PLN in *T canis* infection is associated with a systemic regulatory response. Moreover, the presence of $CD8^+$/$FoxP3^+$ has also been reported in *H polygyrus* infection, localized in lamina propria from infected mice; thus, the presence of these regulatory cells is induced not only for *T canis* but also for other nematodes.[37] With regard to $CD8^+$/$FoxP3^+$ function in helminth infection, these $CD8^+$ Tregs isolated from the lamina propria may suppress splenocyte proliferation in a contact-dependent way independently of IL-10.[37]

In addition to Treg cell presence, helminths induce other cells—namely Breg and AAM—with regulatory functions.[38] Although further characterization is needed to determine the phenotype of B cells and $F4/80^+$ macrophages in this study, the increased proportions of these cells in spleen, and the microenvironment constituted by increased amounts of IL-4, IL-10 and VEGF, along with decreased levels of TNF-α and IFN-γ, suggest a regulatory phenotype. This can be supported through the in vitro findings, in which cultured macrophages from *T canis*-infected mice produced higher amounts of IL-10 and decreased levels of TNF-α, which suggests that macrophages underwent an alternative activation associated with the infection.[16]

In summary, the systemic immune response to *T canis* chronic infection is characterized as a type 2 and regulatory response. Regardless, *T canis* larval were found in lungs, liver, heart and kidneys, and the highest numbers of larval were detected in musculature and brain at 49 d.p.i. The characteristic humoral response associated with *T canis* infection was evidenced by increased levels of specific IgG and IgG1, B-cell expansion in spleen and PLN, and increased IL-4 levels in spleen and sera (Figure 8).

In secondary lymphoid organs (spleen and PLN) from infected animals, the percentages of T cytotoxic $CD8^+$ and $CD4^+$/$FoxP3^+$ cells were increased, but no changes were observed in the proportions of NK cells or T helper lymphocytes (Figure 8). Splenic expansion of macrophages and a decreased percentage of these cells in the PLN contrasted with the increased proportion of $CD8^+$/$FoxP3^+$ in PLN (Figure 8).

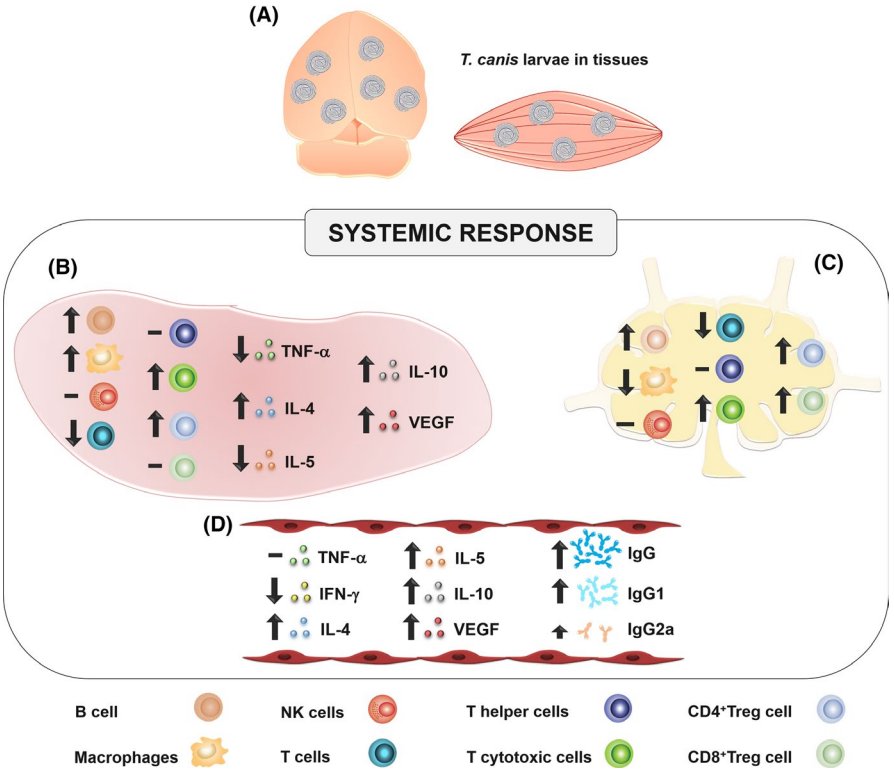

FIGURE 8 Systemic immune response to *Toxocara canis*. A, *T canis* larval migrate through different tissues and establish themselves mainly in brain and skeletal muscle at 49 d.p.i. B, In infected mice, splenic proportion of B cells, F4/80$^+$ cells, T cytotoxic CD8$^+$ and CD4$^+$/FoxP3$^+$ cells were increased; meanwhile, T cells were decreased and NK and T helper cell proportions did not change. Also in spleen from infected mice, TNF-α (type 1 response cytokine) was diminished, and IL-4, IL-10 and VEGF (type 2 response cytokines) were increased with the exception of IL-5, which was decreased. C, In PLN, immune cell proportions were similar to those in the spleen, with the exception of F4/80$^+$, whose proportion was lower, and CD8$^+$/FoxP3$^+$, whose proportion was higher, both in infected mice. D, In sera from infected animals, there was a reduction in IFN-γ levels and an augmentation of IL-4, IL-5, IL-10 and VEGF, and the levels of anti-*T canis* IgG and IgG1 were 2.6 times higher than the levels of IgG2a

As for the cytokine splenic microenvironment, a type 2 response was detected that was associated with the augmentation of IL-4 and VEGF and the diminution of the type 1 response cytokine (TNF-α) in infected mice, while at the same time levels of the regulatory cytokine IL-10 were increased. Also, in *T canis*-infected mice sera, type 2 response cytokines were elevated (IL-4, IL-5 and VEGF), type 1 cytokine IFN-γ was decreased, and the regulatory cytokine IL-10 was elevated (Figure 8).

These cytokine levels, combined with the Foxp3 regulatory response, suggest that in mice infected with *T canis* at 49 d.p.i., although there is a type 2 response, a regulatory response is evident in the host.

In conclusion, this descriptive study integrates different components of host immune response to murine *T canis* chronic infection. The results suggested a type 2 response characterized by IL-4, IL-5, a humoral response and a regulatory response associated with IL-10, VEGF, CD4$^+$/FoxP3$^+$ and CD8$^+$/FoxP3$^+$ cells. However, the role of these cells and cytokines in the inflammatory and regulatory mechanisms needs further research. The understanding of host immune response to chronic *T canis* infection is essential for comprehending the interactions that this infection may have with other comorbidities, some of which may be controlled (autoimmune diseases) or enhanced (cancer or allergic diseases) with a systemic regulatory response. Thus, understanding of the *T canis* immune response may make available the development of treatments or the establishment of preventable measures associated with other diseases.

ACKNOWLEDGEMENTS

We are very grateful to MsC. Juan Pablo Martínez Labat, Facultad de Estudios Superiores Cuautitlán, México, for providing *Toxocara canis* eggs. Margarita Isabel Palacios-Arreola has a postdoctoral fellowship from DGAPA, UNAM. Rocío Alejandra Ruiz-Manzano and Rosalía Hernández-Cervantes are recipients of CONACyT PhD scholarship numbers 421443 (RARM) and 293845 (RHC). Both are students from the Programa de Doctorado en Ciencias Biomédicas, UNAM.

CONFLICT OF INTEREST

The authors declare no competing conflicts of interest.

DATA AVAILABILITY STATEMENT

The data that support the findings of this study are available from the corresponding author upon reasonable request.

ORCID

Rocío Alejandra Ruiz-Manzano https://orcid.org/0000-0002-8507-6447

Rosalía Hernández-Cervantes https://orcid.org/0000-0003-4667-5225

Víctor Hugo Del Río-Araiza https://orcid.org/0000-0002-7868-6407

Margarita Isabel Palacios-Arreola https://orcid.org/0000-0001-8882-7544

Karen Elizabeth Nava-Castro https://orcid.org/0000-0003-2223-6703

Jorge Morales-Montor https://orcid.org/0000-0002-9461-610X

REFERENCES

1. de Oliveira VC, de Mello RP, D'Almeida JM. Muscoid dipterans as helminth eggs mechanical vectors at the zoological garden, Brazil. *Rev Saude Publica*. 2002;36(5):614-620.
2. González-García T, Muñoz-Guzmán MA, Sánchez-Arroyo H, Prado-Ochoa MG, Cuéllar-Ordaz JA, Alba-Hurtado F. Experimental transmission of *Toxocara canis* from *Blattella germanica* and *Periplaneta americana* cockroaches to a paratenic host. *Vet Parasitol*. 2017;246:5-10.
3. Lopes Rassier G, Borsuk S, Pappen F, et al. *Toxocara* spp. seroprevalence in sheep from southern Brazil. *Parasitol Res*. 2013;112(9):3181-3186.
4. Strube C, Heuer L, Janecek E *Toxocara* spp. infections in paratenic hosts. *Vet Parasitol*. 2013;193(4):375-389.
5. Schnieder T, Laabs EM, Welz C. Larval development of *Toxocara canis* in dogs. *Vet Parasitol*. 2011;175(3–4):193-206.
6. Finsterer J, Auer H. Neurotoxocariasis. *Rev Inst Med trop S Paulo*. 2007;49(5):279-287.
7. Overgaauw P, van Knapen F. Veterinary and public health aspects of *Toxocara* spp. *Vet Parasitol*. 2013;193(4):398-403.
8. Maizels RMT. oxocara canis : Molecular basis of immune recognition and evasion. *Vet Parasitol*. 2013;193(4):365–374.
9. Resende NM, Gazzinelli-Guimarães PH, Barbosa FS, et al. New insights into the immunopathology of early *Toxocara canis* infection in mice. *Parasit Vectors*. 2015;8(1):354.
10. Mazur-Melewska K, Figlerowicz M, Cwalińska A, et al. Production of interleukins 4 and 10 in children with hepatic involvement in the course of *Toxocara* spp. infection. *Parasite Immunol*. 2016;38(2):101-107.
11. Del Prete GF, De Carli M, Mastromauro C, et al. Purified protein derivative of *Mycobacterium tuberculosis* and excretory-secretory antigen(s) of *Toxocara canis* expand in vitro human T cells with stable and opposite (type 1 T helper or type 2 T helper) profile of cytokine production. *J Clin Invest*. 1991;88(1):346-350.
12. Nutman TB. Looking beyond the induction of Th2 responses to explain immunomodulation by helminths. *Parasite Immunol*. 2015;37(6):304-313.
13. Gordon S, Martinez-Pomares L. Physiological roles of macrophages. *Pflugers Arch Eur J Physiol*. 2017;469(3–4):365-374.
14. Jenkins SJ, Allen JE. Similarity and diversity in macrophage activation by nematodes, trematodes, and cestodes. *J Biomed Biotechnol*. 2010;2010:1-14.
15. Qian BZ, Pollard JW. Macrophage diversity enhances tumor progression and metastasis. *Cell*. 2010;141(1):39-51.
16. Kuroda E, Yoshida Y, Shan BE, Yamashita U. Suppression of macrophage interleukin-12 and tumour necrosis factor-alpha production in mice infected with *Toxocara canis*. *Parasite Immunol*. 2001;23(6):305-311.
17. Othman AA, El-Shourbagy SH, Soliman RH. Kinetics of Foxp3-expressing regulatory cells in experimental *Toxocara canis* infection. *Exp Parasitol*. 2011;127(2):454-459.
18. Kayes SG, Omholt PE, Grieve RB. Immune responses of CBA / J mice to graded infections with Toxocara canis. *Infect Immun*. 1985;48(3):697-703.
19. De Savigny H. In vitro maintenance of *Toxocara canis* larvae and a simple method for the production of *Toxocara* ES antigen for use in serodiagnostic tests for visceral larva migrans. *J Parasitol*. 1975;61(4):781-782.
20. Bowman DD, Mika-Grieve M, Grieve RB. Circulating excretory-secretory antigen levels and specific antibody responses in mice infected with *Toxocara canis*. *Am J Trop Med Hyg*. 1987;36(1):75-82.
21. Pinelli E, Brandes S, Dormans J, et al. *Toxocara canis*: Effect of inoculum size on pulmonary pathology and cytokine expression in BALB/c mice. *Exp Parasitol*. 2007;115(1):76-82.
22. Epe C, Sabel T, Schnieder T, Stoye M. The behavior and pathogenicity of *Toxacara canis* larvae in mice of different strains. *Parasitol Res*. 1994;80(8):691-695.
23. Abo-Shehada MN, Herbert IV. The migration of larval *Toxocara canis* in mice II. Post-intestinal migration in primary infections. *Vet Parasitol*. 1984;17(1):75-83.
24. Rodríguez-Caballero A, Martínez-Gordillo MN, Caballero-Salazar S, Rufino-González Y, Ponce-Macotela M *Toxocara canis*: analysis of the kinetics of antigen release and antibody production in an in vivo model for the detection of past or present infection. *Vet Parasitol*. 2017;243(3700):183-187.
25. Othman AA. Therapeutic battle against larval toxocariasis: are we still far behind? *Acta Trop*. 2012;124(3):171-178.
26. Oshima T. Standardization of techniques for infecting mice with *Toxocara canis* and observations on the normal migration routes of the larvae. *J Parasitol*. 1961;47(4):652-656.
27. Pinelli E, Withagen C, Fonville M, et al. Persistent airway hyper-responsiveness and inflammation in *Toxocara canis*-infected BALB/c mice. *Clin Exp Allergy*. 2005;35(6):826-832.
28. Mosmann T. Th1 And Th2 cells: different patterns of lymphokine secretion lead to different functional properties. *Annu Rev Immunol*. 1989;7(1):145-173.
29. Fan C, Lin Y, Du W, Su K. Infectivity and pathogenicity of 14-month-cultured embryonated eggs of Toxocara canis in mice. *Vet Parasitol*. 2003;113:145-155.
30. Novák J, Panská L, Macháček T, Kolářová L, Horák P. Humoral response of mice infected with Toxocara canis following different infection schemes. *Acta Parasitol*. 2017;62(4):823-824.
31. Del Rio-Araiza VH, Nava-Castro KE, Alba-Hurtado F, et al. Prolactin as immune cell regulator in *Toxocara canis* somatic larvae chronic infection. *Biosci Rep*. 2018;38(4):BSR20180305.
32. Moens L, Tangye SG. Cytokine-mediated regulation of plasma cell generation: IL-21 takes center stage. *Front Immunol*. 2014;5:1-13.
33. Pracht K, Meinzinger J, Daum P, et al. A new staining protocol for detection of murine antibody-secreting plasma cell subsets by flow cytometry. *Eur J Immunol*. 2017;47(8):1389-1392.
34. Rosser EC, Mauri C. Perspective regulatory B cells: origin, phenotype, and function. *Immunity*. 2015;42(4):607-612.
35. McSorley HJ, Maizels RM. Helminth infections and host immune regulation. *Clin Microbiol Rev*. 2012;25(4):585-608.

36. Pastille E, Frede A, McSorley HJ, et al. Intestinal helminth infection drives carcinogenesis in colitis-associated colon cancer. *PLoS Pathog*. 2017;13(9):1-22.
37. Metwali A, Setiawan T, Blum AM, et al. Induction of $CD8^+$ regulatory T cells in the intestine by *Heligmosomoides polygyrus* infection. *Am J Physiol Liver Physiol*. 2006;291(2):G253-G259.
38. Allen JE, Maizels RM. Diversity and dialogue in immunity to helminths. *Nat Rev Immunol*. 2011;11(6):375-388.

SUPPORTING INFORMATION

Additional supporting information may be found online in the Supporting Information section at the end of the article.

How to cite this article: Ruiz-Manzano RA, Hernández-Cervantes R, Del Río-Araiza VH, Palacios-Arreola MI, Nava-Castro KE, Morales-Montor J. Immune response to chronic *Toxocara canis* infection in a mice model. *Parasite Immunol*. 2019;00:e12672. https://doi.org/10.1111/pim.12672

frontiers in Oncology

ORIGINAL RESEARCH
published: 29 May 2020
doi: 10.3389/fonc.2020.00736

Potential Novel Risk Factor for Breast Cancer: *Toxocara canis* Infection Increases Tumor Size Due to Modulation of the Tumor Immune Microenvironment

Rocío Alejandra Ruiz-Manzano[1], *Margarita Isabel Palacios-Arreola*[2], *Rosalía Hernández-Cervantes*[1], *Víctor Hugo Del Río-Araiza*[3], *Karen Elizabeth Nava-Castro*[2], *Pedro Ostoa-Saloma*[1], *Samira Muñoz-Cruz*[4] *and Jorge Morales-Montor*[1]*

[1] *Departamento de Inmunología, Instituto de Investigaciones Biomédicas, Universidad Nacional Autónoma de México, Ciudad de México, Mexico,* [2] *Departamento de Genotoxicología y Mutagénesis Ambiental, Centro de Ciencias de la Atmósfera, Universidad Nacional Autónoma de México, Ciudad de México, Mexico,* [3] *Laboratorio de Inmunología y Biología Molecular de Parásitos, Facultad de Medicina Veterinaria y Zootecnia, Departamento de Parasitología, Universidad Nacional Autónoma de México, Ciudad de México, Mexico,* [4] *Unidad de Investigación Médica en Enfermedades Infecciosas y Parasitarias, Instituto Mexicano del Seguro Social, Ciudad de México, Mexico*

OPEN ACCESS

Edited by:
Laurence Gluch, The Strathfield Breast Centre, Australia

Reviewed by:
Stanley Ching-Cheng Huang, Case Western Reserve University, United States
Carlos Martinez-Perez, Medical Research Council Institute of Genetics and Molecular Medicine (MRC), United Kingdom

***Correspondence:**
Jorge Morales-Montor
jmontor66@biomedicas.unam.mx

Specialty section:
This article was submitted to Women's Cancer, a section of the journal Frontiers in Oncology

Received: *14 January 2020*
Accepted: *17 April 2020*
Published: *29 May 2020*

Citation:
Ruiz-Manzano RA, Palacios-Arreola MI, Hernández-Cervantes R, Del Río-Araiza VH, Nava-Castro KE, Ostoa-Saloma P, Muñoz-Cruz S and Morales-Montor J (2020) Potential Novel Risk Factor for Breast Cancer: Toxocara canis Infection Increases Tumor Size Due to Modulation of the Tumor Immune Microenvironment. Front. Oncol. 10:736. doi: 10.3389/fonc.2020.00736

Worldwide, breast cancer is the most important type of cancer in women with regard to incidence and prevalence. Several risk factors interact to increase the probability of breast cancer development. Biological environmental contaminants such as infectious agents play a significant role in tumor development, and helminths have been recognized as cancer enhancers or inducers due to their ability to regulate the host immune response. *Toxocara canis* is a zoonotic and cosmopolite nematode with immuno-regulatory abilities. *T. canis* infection has been related to T helper type-2 cell (Th2 or type 2) and regulatory responses. Type 2 and regulatory immune responses may favor the development of comorbidities that are usually controlled or eliminated through a type 1 response such as cancer. The aim of this study was to determine whether *T. canis* infection alters mammary tumor growth through modulation of the immune response. Infected mice developed larger tumors. Tumor immune cell milieu analysis revealed that infection reduced the proportions of $CD8^+$ lymphocytes and increased the proportions of $F4/80^+$ macrophages and $CD19^+$ B cells. These changes were accompanied by a type 2 local response represented by increased amounts of IL-4 and VEGF and a regulatory microenvironment associated with higher IL-10 levels. Thus, this study demonstrates that *T. canis* infection enhances tumor development and suggests that this is through modulation of the tumor immune microenvironment.

Keywords: oncoimmunology, immune regulation, tumor microenvironment, breast cancer, risk factor, infection

INTRODUCTION

Breast cancer is the most prevalent cancer in women and their leading cause of cancer death (1). There are several risk factors associated with breast tumor development. First and foremost is gender; women present with breast cancer more frequently than men (1). Risk factors such as alcohol intake, smoking, and hormone replacement treatment, among others, have been linked to breast cancer development (2). Nevertheless, other environmental factors also play a prominent role in breast tumor development. Environmental contaminants, including physical, chemical, and biological agents, have been associated with tumor development (3). In fact, 15% of different cancer types are linked to viral, bacterial, or parasite infections (4). In this sense, some helminthic infections play an important role in cancer progression. The helminths are ubiquitous parasites that cause chronic infections in human, livestock, and domestic animals; they include platyhelminths (flatworms) and nematodes (roundworms) (5, 6). Most of the parasite species from the phylum Platyhelminths are cestodes (tapeworms) and trematodes (flukes), while the phylum Nematoda contains ascarides and strongylids among other roundworms (5, 6). For example, some trematodes are considered to cause bladder cancer (*Schistosoma haematobium*) and cholangiocarcinoma (*Chlonorchis sinensis* and *Opisthorchis viverrini*) (7, 8). Nematode infections are also reported as colon cancer enhancers (*Heligmosomoides polygyrus*) (9).

Helminths may promote tumor growth through different mechanisms that are related to chronic infection and long-lasting inflammation (7, 8). Chronic inflammation is mediated by helminth excretory-secretory (ES) products that modify the host immune response to the parasite and diminish tissue damage in the host (10). These processes allow helminth survival and may favor the development of other diseases.

In this regard, Treg expansion is stimulated by nematode infections (9, 11). It is known that Treg cells exert immune suppression through secretion of tolerogenic cytokines such as IL-10 and the dysfunction of cytotoxic T $CD8^+$ cell activity (12, 13). Aside from Treg lymphocyte generation, nematodes also induce the generation of other regulatory cells and soluble factors associated with the promotion of tumor growth, thereby worsening prognosis by promoting metastasis (14). Among these are alternatively activated macrophages (AAMs), Breg lymphocytes, and IL-10 (10). AAMs are involved in wound healing and humoral response and produce IL-4, IL-10, VEGF, and other soluble factors (15, 16).

Macrophages are also linked to tumor development, as tumor-associated macrophages (TAMs). An AAM phenotype and a higher-density infiltration of these cells in breast tumors are associated with a worse prognosis (14). Another soluble factor produced by AAMs is VEGF, which is involved in angiogenesis promotion by increasing the sprouting and infiltration of new blood vessels in the tumor, leading to higher oxygen and nutrient levels, which enhance tumor cell proliferation (17).

The importance of helminth infection is not only related to the regulatory functions of these parasites but also to their rates of infection and their geographic distribution. A helminth that possesses immuno-regulatory properties and infects several hosts, including humans, worldwide is *Toxocara canis* (18).

T. canis has a wide range of hosts, including definitive (canids) and paratenic hosts such as humans, cats, lambs, pigs, cows, mice, rats, cockroaches, and flies (19–23). In paratenic hosts, *T. canis* larvae never develop into the adult form but migrate through different organs, including lungs, liver, heart, skeletal muscles, brain, and eyes (24). This migration induces a broad spectrum of signs and symptoms, which are characterized in humans as visceral, ocular, covert larva migrans, and neurotoxocariasis depending on the place where the larvae lodges and induces damage (24, 25). Although positive human sera to *T. canis* is reported worldwide, with serological frequencies in humans as high as 86.75% (26), an accurate incidence rate per country has not been established; therefore, national surveys are needed to determine the actual infection risk in humans due to the elevated rate of *T. canis*-infected dogs that excrete *T. canis* eggs in feces and contaminate the environment (27). Thus, the lack of information about the real incidence of this disease is hazardous *per se* because *T. canis* infection is an important neglected disease that could potentially affect the development of other pathologies.

The host immune response is induced by the *T. canis* larvae excretory-secretory (TES) products, and the evasion of this response allows the nematode to survive for many years in different host tissues (18). The mouse immune response to *T. canis* chronic infection has been reported as a type 2 response and a regulatory one (28). This is characterized by an increased proportion of $F4/80^+$ macrophages, $CD19^+$ lymphocytes, and $CD4^+Foxp3^+$ Treg cells in the spleen, as well as higher splenic and serum levels of IL-4, IL-10, and VEGF (28). For the abovementioned reasons, *T. canis* could regulate the host immune response, and in turn, favor tumor growth (29).

Consequently, we aimed to elucidate the role of *T. canis* infection in the development of mammary tumors and the associated local and systemic immune response.

METHODS

Ethics Statement

The experimental procedures and animal care were performed at the Instituto de Investigaciones Biomédicas (IIB), Universidad Nacional Autónoma de México (UNAM), in the Biological Models Unit (Unidad de Modelos Biológicos, or UMB). These procedures were evaluated and approved by the Institutional Care and Animal Use Committee (CICUAL) (permit number 2017–208), in accordance with Mexican regulation (NOM-062-ZOO-1999) and with the Guide for the Care and Use of Laboratory Animals of the National Institute of Health (NIH) of the United States of America.

Blood samples were collected by cardiac puncture in deeply anesthetized animals (Sevofluorane 5%, Abbot, Mexico). Anesthetized mice were euthanized through cervical dislocation. Sera were obtained by blood centrifugation and were stored at −70°C until use.

Animals

Twenty female mice, BALB/c AnN (MGI Cat# 5654849, RRID:MGI:5654849), 8–9 weeks old, were obtained from Envigo México (Facultad de Química, UNAM, México). They were maintained under standard conditions: controlled temperature (22°C), 12-h light-dark cycles, ad libitum water, and Envigo LabDiet 5015 (Cat# 0001328 Purina, St. Louis, MO) delivered in sterile conditions.

Mice were randomized into two experimental groups: 4T1 (tumor induction) and 4T1+*T. canis* (infection and tumor induction), each one with 10 animals. Infection was performed for 4T1+*T. canis*; meanwhile, the 4T1 group was administered phosphate-buffered saline solution (PBS, pH 7.4). Twenty-one days post-infection (dpi), a tumor was induced in both groups. Tumor growth was observed for 28 days.

Toxocara canis Infection

Adult *T. canis* specimens were obtained from dog feces and washed 3 times with PBS and PBS/2% formaldehyde solution. The uteri were excised from adult *T. canis* females through cuticle incision in the anterior section. Eggs were extracted and filtrated through a fine mesh to eliminate debris, and then the suspension was centrifuged at 3250 g/5 min (HERMLE Z400K) and resuspended in PBS. The resulting suspension was maintained at room temperature. Larvae development was supervised every week.

When 80–90% of the eggs were larvated, the suspension was ready to induce the infection. This was performed in overnight fasted mice by administering 500 larvated eggs, which were inoculated *per os* with an oral feeding needle.

Cell Culture and Mammary Tumor Induction

The 4T1 mammary mouse carcinoma cell line (ATCC Cat# CRL-2539, RRID:CVCL_0125) was grown in supplemented RMPI 1640 medium (Sigma, St. Louis, MO) with 10% FBS (ByProducts, Guadalajara, México), 1.0 mM sodium pyruvate, 100 U/ml penicillin, and 100 mg /ml streptomycin. The cells were harvested after a second subculture at 80% of confluency, resuspended in sterile 0.9% NaCl solution (250,000 cells/ml), and maintained in ice until inoculation.

The mice were anesthetized (Sevofluorane 5%, Abbot, Mexico), the abdominal area was aseptically prepared, and 10^4 4T1 cells were injected subcutaneously into the fat pad under the second last right nipple. Mouse recovery was supervised.

Toxocara canis Larvae Cultures and Collection of TES Products

TES products were obtained based on methods by De Savigny (30) and Bowman (31), with modifications. Briefly, larvated egg suspension was centrifuged at 3250 g/5 min. To disaggregate the outer egg layer, 1 ml of sodium hypochlorite was added. After 10 min in continuous gentle agitation, the eggs were washed with 10 ml of bi-distillate sterile water, centrifuged at 3250 g/5 min, and washed three times with PBS. The eggs were resuspended in RPMI 1640 (Sigma, St. Louis, MO) with 1% antibiotic-antimycotic (GIBCO). Larva hatching was stimulated with a magnetic stirrer for 20 min, and the egg suspension was maintained at 37°C in a humidified atmosphere containing 5% (v/v) CO_2 overnight. The larvae were cleaned from eggshells through a modified Baermann technique and maintained at a concentration of 10^4 larvae/ml. The supernatant was recollected weekly and filtered with 0.22 μm syringe filter (Millipore); the medium was replaced. Protein was precipitated with acetone (Herschi Trading, high purity, 99.5%) at −20°C, resuspended in PBS, and stored at −20°C until use. Protein concentration was calculated with the Bradford Protein Assay Bio Rad® technique.

Anti-*Toxocara canis* IgG Detection

Coated polystyrene wells (96-well plate, MaxiSorp Nunc Cat# NNC#442404) with 50 μl of TES/bicarbonate buffer (pH 9.6) suspension (1 μg/ml) were incubated at 4°C overnight. The plate was washed (PBS/Tween 20 0.05%) and blocked with 200 μl of 3% bovine serum albumin (BSA) and SIGMA washing solution for 30 min at 37°C. After the plate had been washed three times, 50 μl of sera from the mice was added (1:200 in PBS 1% BSA, 0.05%Tween 20) in duplicate and incubated for 1 h at room temperature. The plate was washed, and 50 μl of peroxidase goat anti-mouse IgG (Jackson, RRID:AB_2338511) at 1:10,000 dilution was added, followed by standing for 90 min at room temperature. An enzyme-substrate reaction was developed by the addition of 50 μl of freshly prepared substrate solution (0.05% o-phenylenediamine/0.01% H_2O_2/0.1 M sodium citrate/0.1 M citric acid) and stopped after 10 min with 50 μl 2N sulfuric acid. The plate was read at a wavelength of 492 nm in a Stat Fax 4200 microplate reader (Awareness Technology).

Flow Cytometry

The left and right peripheral (inguinal) lymph nodes (PLNs) and the spleen were excised and mechanically disaggregated through a 50-μm nylon mesh with PBS. Tumors were excised and minced with a scalpel. After the PBS wash, the lymph node cells were resuspended in FACS buffer (PBS, 2% FBS, 0.02% NaN_3). Erythrocytes in splenic suspension were lysed for 10 min with ACK buffer (150 mM NH_4Cl, 10 mM $KHCO_3$, 0.1 mM Na_2 EDTA, pH 7.3), washed with PBS and resuspended in FACS buffer. The minced tumors were incubated in digestion medium (RPMI 1640, 10 U/ml DNase, Roche, Mannheim, Germany; 0.5 mg/ml type IV Collagenase, Sigma, St. Louis, MO) for 20 min, and 50 μl FBS was added to stop digestion. Mechanical disruption in a 50-μm nylon mesh was performed. After the PBS wash, the cells were resuspended in FACS buffer. Approximately 1×10^6 cells were incubated (20 min at 4°C) with anti-CD16/CD32 (TruStain®, Cat# 101319, Clone 93, RRID:AB_1574973, BioLegend, San Diego, CA) and washed. Then, they were stained with the following panels. For T lymphocyte: AlexaFluor®488-conjugated anti-CD3ε (Cat# 100321, Clone 145-2C11, RRID:AB_389301) 1:100, PE-conjugated anti-CD4 (Cat# 100407, Clone GK1.5, RRID:AB_2075573) 1:300, PerCP-conjugated anti-CD8 (Cat# 100732, Clone 53-6.7, RRID:AB_893423) 1:100, and AlexaFluor®647-conjugated anti-Foxp3 (Cat# 320013, Clone 150D, RRID:AB_439750) 1:100. For macrophage and NK: AlexaFluor® 647-conjugated anti-F4/80 (Cat# 123122, Clone

BM8, RRID:AB_893492) and PE-conjugated anti-NKp46 (Cat# 137604, Clone 29A1.4, RRID:AB_2235755). For B lymphocyte: PE-conjugated anti-CD19 (Cat# 115507, Clone 6D5, RRID:AB_313642), 1:200. Antibodies from BioLegend, San Diego, CA, and the Foxp3/Transcription Factor Staining Buffer kit (Cat# TNB-0607-KIT, Tonbo Biosciences, San Diego, CA) were used for intracellular Foxp3 staining, according to the manufacturer's protocol.

Cell analysis was performed with a BD FACSCalibur™ (BD Biosciences) flow cytometer. The data were analyzed with FlowJo software (Treestar Inc.). Compensation was assessed in BD FACSCalibur™ and FlowJo software with unstained samples, single stain controls, and FMO for $Foxp3^+$ ($CD3^+/CD4^+$; $CD3^+/CD8^+$).

Cytokine Determination

The tumors and spleens from the mice were stored in TRIzol™ reagent (Cat# 15596026, Invitrogen) at −70°C until use. Protein isolation was performed according to the procedural guidelines for TRIzol® reagent use. Protein quantification was done with a NanoDrop 1000 spectrophotometer (Thermo Scientific). An amount of 10 μg of protein was used to determine cytokine tissue levels.

Sera, splenic, and tumor cytokines were measured with ABTS ELISA kits (PeproTech) with the following antibodies: TNF-α (Cat# 500-P64bt, RRID:AB_147984), IFN-γ (Cat# 500-P119bt, RRID:AB_148087), IL-4 (Cat# 500-P54bt, RRID:AB_147636), IL-5 (Cat# 500-P55), and IL-10 (Cat# 500-P60, RRID:AB_147978), and unconjugated antibodies were used for cytokine capture, according to the manufacturer's instructions, with modifications. Briefly, coated plates (96-well plate, MaxiSorp Nunc Cat# NNC#442404) with 50 μl (2 μg/ml) of different antibodies were incubated overnight. After 3 washes (wash buffer, PeproTech), the plates were blocked (block buffer: PeproTech) and then washed again. Next, 50 μl of sera (1:2 dilution) or tissue protein (10 μg) was added in duplicate (in diluent solution, PeproTech), maintained at 4°C for 2 h, and washed three times. An enzyme-substrate reaction was developed with ABTS liquid substrate (PeproTech). All solutions were from the ABTS ELISA buffer kit (Cat# 900-K00). The plates were read at a wavelength of 405 nm with wavelength correction set at 650 nm at different time points in a Stat Fax 4,200 microplate reader (Awareness Technology).

VEGF Quantification

Polystyrene wells (96-well plate, MaxiSorp Nunc Cat# NNC#442404) were coated with 50 μl of splenic protein (10 μg), sera (dilution 1:2), or standard curve (0.001-1 ng) with VEGF mBA-165 (Cat# sc-4571, Santa Cruz Biotechnology) in bicarbonate buffer (pH 9.6) per duplicate and incubated at 4°C overnight. The plate was washed and blocked with 200 μl of PBS/BSA 1%/Tween 20 0.05% for 1 h at 4°C. After washing, 50 μl of anti-VEGF/C-1 antibody (Cat# sc-7269, RRID:AB_628430, Santa Cruz Biotechnology) in a 1:200 dilution was added, followed by incubation for 1 h at 4°C. After washing, 50 μl of m-IgGκ/BP-HRP (Cat# sc-516102, RRID:AB_2687626, Santa Cruz Biotechnology) (1:400) was added and maintained for 2 h at room temperature. An enzyme-substrate reaction was developed with 50 μl of substrate solution and stopped after 15 min with 50 μl 2N sulfuric acid. The plates were read at a wavelength of 492 nm in a Stat Fax 4,200 microplate reader (Awareness Technology). Cytokine and VEGF concentrations were calculated by interpolation from a standard curve.

Cytokine and antibody determination were performed after proper ELISA standardization.

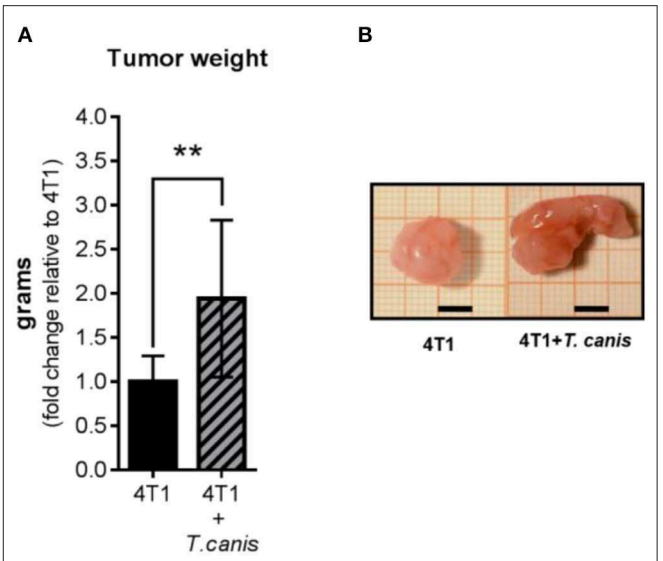

FIGURE 1 | Tumor growth. **(A)** Tumor weight from control (4T1) and infected animals (4T1-*T. canis*). **(B)** Representative images of tumors from both groups (4T1 and 4T1+*T. canis*). Millimetric grid as a background; black bar = 0.5 cm. Graphs represent the mean ± SD of the data from two experiments (4T1, $n = 10$; 4T1+*T. canis*, $n = 10$). Statistical significance was calculated using a *t*-test (**$p \leq 0.01$).

Statistical Analysis

Data were charted as mean ± SD. To compare the differences between intact and infected animals, a Student's *t*-test was used. A Welch's correction was applied in the groups in which the variances were different, as determined by an *F*-test. The differences were considered significant when $p \leq 0.05$. All the analyses were calculated with Prism 6® software (GraphPad Sofware Inc.).

RESULTS

Toxocara canis Infection Increases Tumor Size and Weight

After 28 days of 4T1 cell inoculation, higher tumor enlargement was observed in *T. canis*-infected animals compared to tumors from the 4T1 mice group. This was quantified by measuring tumor mass, which was greater in the 4T1+*T. canis* group ($p = 0.0035$) (**Figures 1A,B**) than in the 4T1 group. In these infected mice, the mean tumor mass was almost doubled (91% increase) in mean weight compared to the group without infection.

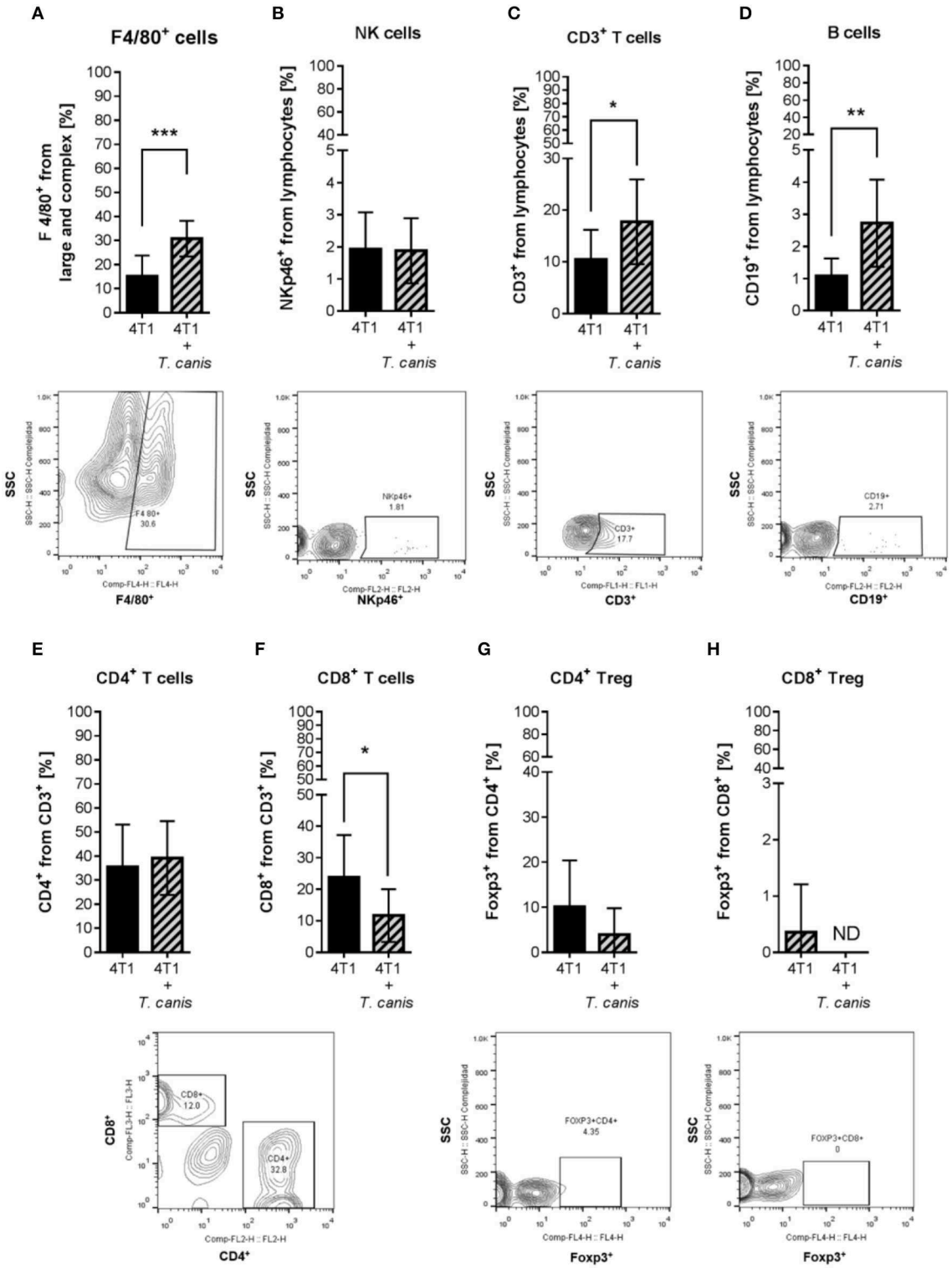

FIGURE 2 | Innate and adaptive immune cells in the tumor microenvironment. Determination of innate immune subpopulations by flow cytometry. **(A)** F4/80$^+$ macrophages. **(B)** NKp46$^+$ cells. Flow cytometry analysis of adaptive immune cells within the tumor. **(C)** T CD3$^+$. **(D)** CD19$^+$ B lymphocytes. **(E)** CD4$^+$ T helper lymphocytes. **(F)** CD8$^+$ T cytotoxic lymphocytes. **(G)** CD4$^+$/Foxp3$^+$ T lymphocytes. **(H)** CD8$^+$/Foxp3$^+$ T lymphocytes. Graphs represent the mean ± SD of the data from two independent experiments (4T1, $n = 10$; 4T1+*T. canis*, $n = 10$). Representative contour plots of the cytometric analysis of the corresponding population (below). Gate from 10,000 cells was collected. Statistical significance was calculated using a *t*-test (*$p \leq 0.05$; **$p \leq 0.01$, ***$p \leq 0.001$).

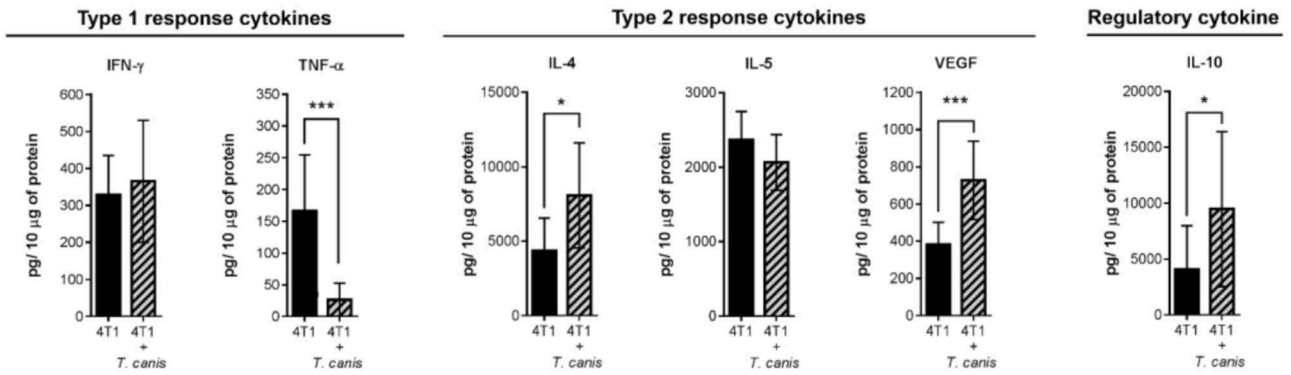

FIGURE 3 | Expression of soluble factors in the tumor microenvironment. Analysis of type 1 (IFN-γ and TNF-α), type 2 (IL-4, IL-5, and VEGF), and regulatory (IL-10) cytokines. Graphs indicate data from tumor proteins obtained from two independent experiments (4T1, $n = 10$; 4T1+*T. canis*, $n = 10$). Bars represent the mean ± SD of cytokine levels (pg/10 μg of tumor protein). Statistical significance was calculated using a *t*-test (*$p \leq 0.05$; ***$p \leq 0.001$).

Increased Tumor Growth Is Associated With Changes in the Tumor Microenvironment

Because *T. canis* infection modifies the mouse's immune systemic response toward type 2 and regulatory responses (28), we wondered whether this change may reach the tumor microenvironment. To determine if tumor enlargement was associated with tumor microenvironment changes in innate ($F4/80^+$ macrophages and NK cells) and adaptive (T, T helper, T cytotoxic, Treg, and B lymphocytes) cell proportions, we performed a flow cytometry evaluation. The percentage of $F4/80^+$ macrophages was higher ($p = 0.0004$) in the 4T1+*T. canis* group (**Figure 2A**) compared to the 4T1 group. NK cells were present in a low percentage in tumors from both groups, and no change was observed in the proportions of this population (**Figure 2B**).

As for the adaptive populations in the tumor milieu, statistically, differences were observed in T lymphocyte $CD3^+$, B cells $CD19^+$, and T cytotoxic $CD8^+$, but not in T helper ($CD4^+$) or Treg (**Figure 2**) cells. In *T. canis*-infected mice, there were increased proportions of $CD3^+$ ($p = 0.0334$) and $CD19^+$ ($p = 0.0042$) lymphocytes (**Figures 2C,D**) and a decreased percentage of $CD8^+$ cells ($p = 0.0279$) in the tumors (**Figure 2F**).

On the other hand, soluble factors in the tumor microenvironment are also important drivers of the local immune response. Therefore, we determined tumor cytokine expression of type 1 (TNF-α and IFN-γ), type 2 (IL-4 and IL-5), and regulatory (IL-10) cytokines. In the present study, the cytokine tumor milieu from 4T1+*T. canis* is polarized toward a type 2 and regulatory response. This is evidenced by the reduced amount of TNF-α ($p = 0.0006$) and the higher amounts of IL-4 ($p = 0.0111$), VEGF ($p = 0.0003$), and IL-10 ($p = 0.0456$) (**Figure 3**).

Systemic Humoral *T. canis* Response Is Preserved in Tumor-Bearing Mice

Characteristic *T. canis* infection-associated splenomegaly was detected in the 4T1+*T. canis* group (**Figures 4A,B**). In these mice, the splenic weight was higher than the splenic weight in the control animals from the 4T1 group ($p < 0.0001$) (**Figure 4A**). In addition, the anti-*T. canis* IgG level (**Figure 4C**) was higher in infected mice than in tumor-bearing uninfected mice ($p < 0.0001$). There was an increased percentage of B cells in the spleen ($p = 0.0002$), but in the lymph nodes, there was no statistically significant increase in this subpopulation (**Figures 4D,E**).

Systemic Immune Response to *T. canis* Is Modified by Tumor Induction

As mentioned before, *T. canis* infection modifies the systemic immune response in secondary lymphoid organs. In order to assess whether these modifications in splenic and lymph node immune cell proportions are present in infected tumor-bearing mice, innate and adaptive immune cells were analyzed. The splenic innate and adaptive cellular compositions were similar in the two groups (**Figure 5**).

Although no changes were observed in splenic immune cells (**Figure 5A1-7**), in PLNs from infected mice, the $CD4^+Foxp3^+$ lymphocyte proportion was increased ($p = 0.0162$) compared to the 4T1 control group (**Figure 5B.5**). Although the increase in $CD8^+$ T cells from PLN was linked to the *T. canis* infection (28), when the tumor was induced, the $CD8^+$ T lymphocyte proportion in PLNs was decreased ($p = 0.0137$) in comparison to the 4T1 control group (**Figure 5B.6**).

Expression of systemic soluble factors was performed to determine whether the changes in the tumor microenvironment were related to the systemic response (**Figures 6A–L**). In the spleen, type 1 response cytokine TNF-α was decreased ($p = 0.0311$) in infected mice from the 4T1+*T. canis* group (**Figure 6B**). Although the type 2 cytokine IL-4 and the regulatory IL-10 (**Figure 6C,F**) were augmented in the spleen, these differences were not statistically significant. However, there was a reduction in splenic IL-5 ($p = 0.0002$) and a higher amount of VEGF ($p < 0.0001$) (**Figures 6D,E**).

Soluble factors measured in sera (**Figures 6G–L**) were mostly similar in the 4T1 and 4T1+*T.canis* groups, with the exception of an increased level of VEGF ($p = 0.0030$) in 4T1+*T. canis* mice (**Figure 6K**).

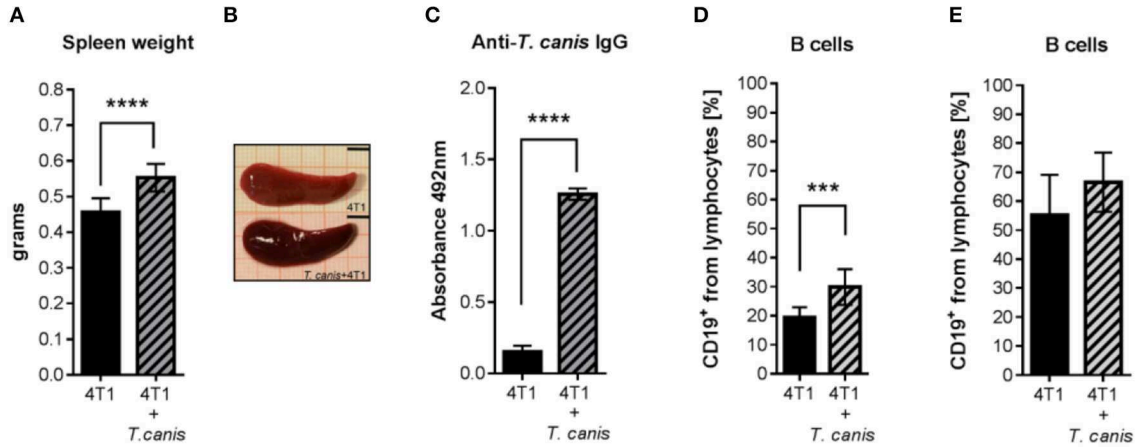

FIGURE 4 | Humoral response to *T. canis* infection in BALB/c mice. **(A)** Splenic weight. **(B)** Representative images of a spleen from a mouse with tumors (4T1 group) and of a spleen from a mouse with tumors and infection (4T1+*T. canis*). Millimetric grid as a background. Black bar = 0.5 cm. **(C)** Anti-*T. canis* IgG serum levels measured by indirect ELISA. **(D)** Frequencies of $CD19^+$ B lymphocytes in the spleen. **(E)**. Frequencies of $CD19^+$ B lymphocytes in PLNs. Graphs represent the mean ± SD of the data from two experiments (4T1, $n = 10$; 4T1+*T. canis*, $n = 10$). Statistical significance was calculated using a *t*-test (***$p \leq 0.001$; ****$p < 0.0001$).

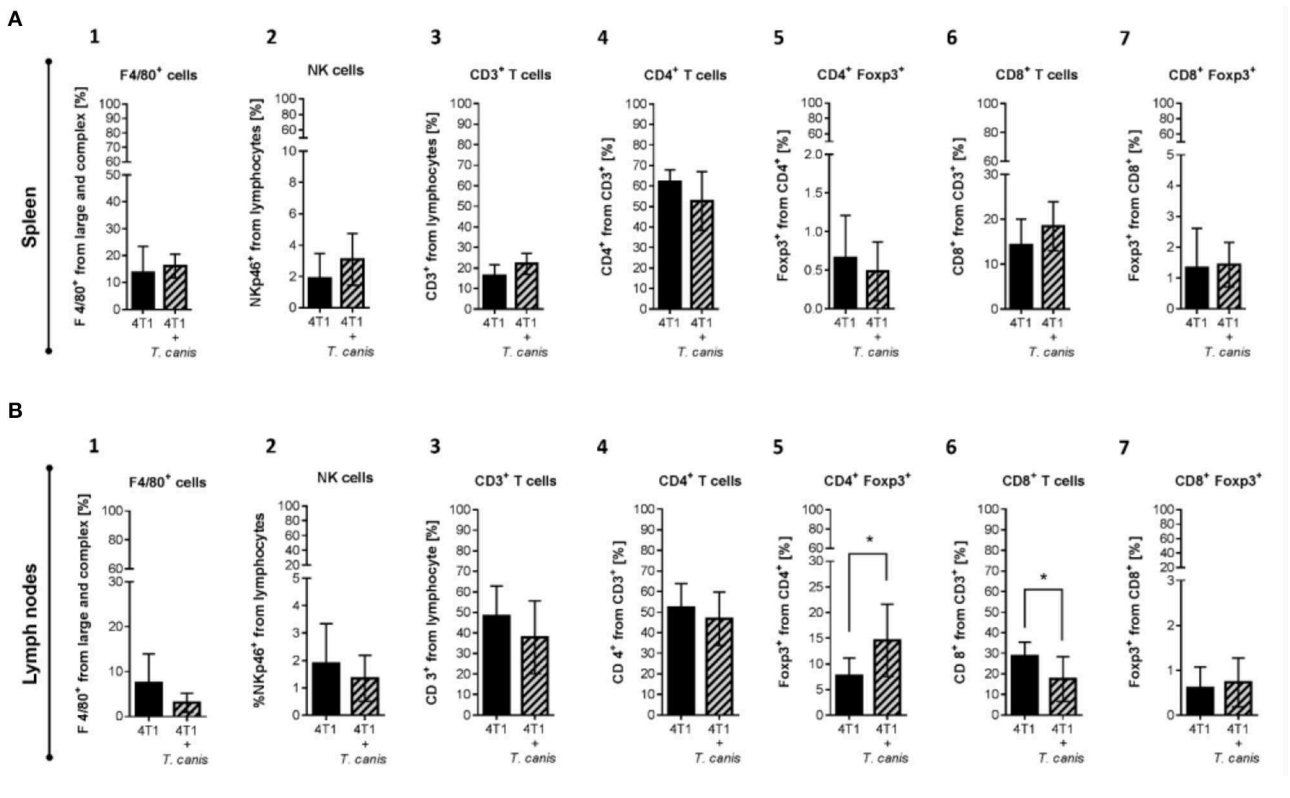

FIGURE 5 | Innate and adaptive immune cells in secondary lymphoid organs. **(A)** Cells from the spleen: 1. $F4/80^+$ macrophages. 2. $NKp46^+$ cells. 3. T $CD3^+$. 4. $CD4^+$ T helper lymphocytes. 5. $CD4^+/Foxp3^+$ T lymphocytes. 6. $CD8^+$ T cytotoxic lymphocytes. 7. $CD8^+/Foxp3^+$ T lymphocytes. **(B)** Immune cells from NLPs: 1. $F4/80^+$ macrophages. 2. $NKp46^+$ cells. 3. T $CD3^+$. 4. $CD4^+$ T helper lymphocytes. 5. $CD4^+/Foxp3^+$ T lymphocytes. 6. $CD8^+$ T cytotoxic lymphocytes. 7. $CD8^+/Foxp3^+$ T lymphocytes. **(B)** Graphs represent the mean ± SD of the data from two independent experiments (4T1, $n = 10$; 4T1+*T. canis*, $n = 10$). Gate from 10,000 cells was collected. Statistical significance was calculated using a t-test (*$p \leq 0.05$).

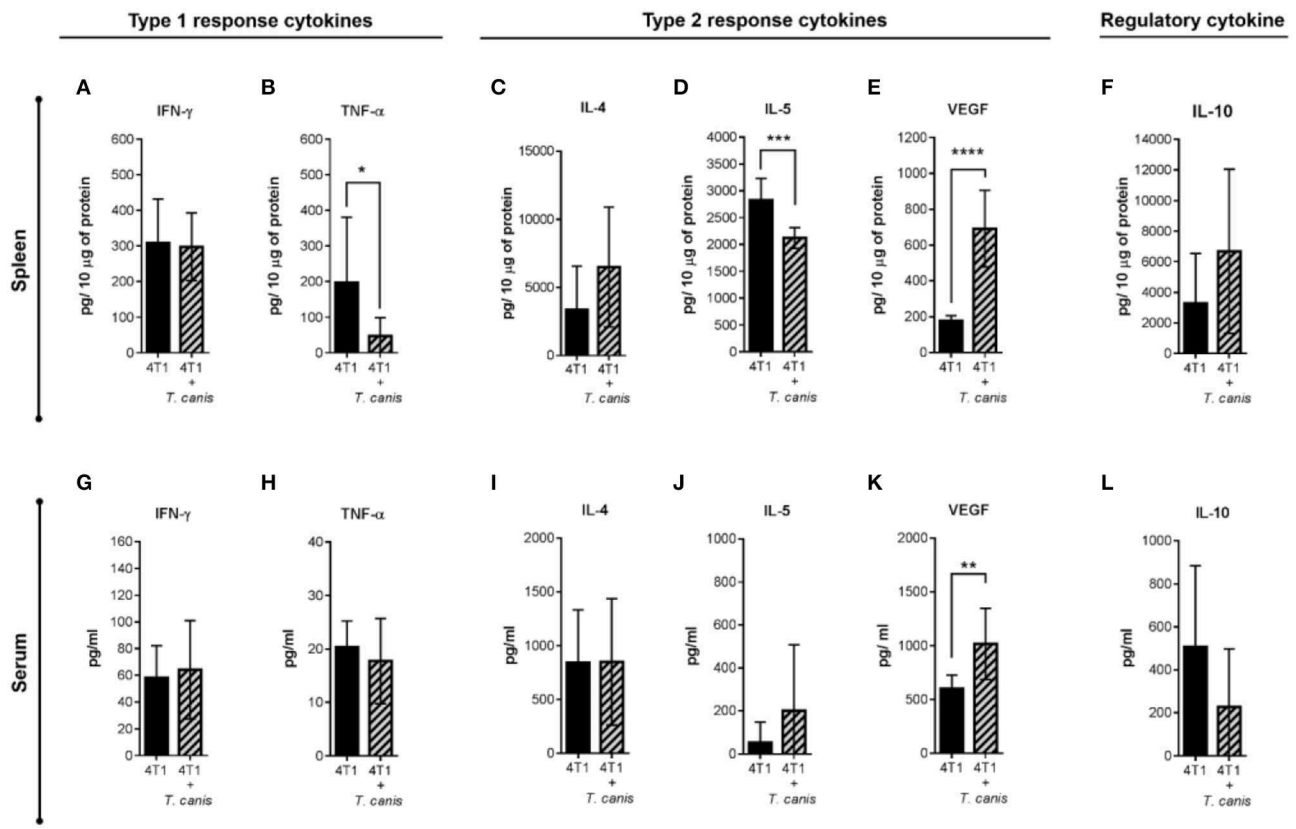

FIGURE 6 | Analysis of systemic soluble factor expression in spleen and serum. Determination by sandwich ELISA of the splenic type 1 response cytokines. **(A)** IFN-γ. **(B)** TNF-α; the type 2 cytokines: **(C)** IL-4, **(D)** IL-5, **(E)** VEGF; and the regulatory cytokine. **(F)** IL-10. Analysis of soluble factors in serum. **(G)** IFN-γ. **(H)** TNF-α. **(I)** IL-4. **(J)** IL-5. **(K)** VEGF. **(L)** IL-10. Graphs indicate data from splenic proteins and sera obtained from two independent experiments (4T1, $n = 10$; 4T1+*T. canis*, $n = 10$). Bars represent the mean ± SD of cytokine levels (pg/10 μg of splenic proteins or pg/ml of sera). Statistical significance was calculated using a *t*-test (*$p \leq 0.05$; **$p \leq 0.01$; ***$p \leq 0.001$; ****$p < 0.0001$).

DISCUSSION

For many years, cancer research has been focused on a cell-central approach based on cancer cell signaling pathways and DNA changes (32), with the main goal of finding a cancer cure. This type of research has made some advances in cancer cell biology and treatment, but it has also neglected some cancer risk factors related to the interactions among cells, the tumor microenvironment, and infectious agents. Besides cell-cell interactions, the interaction with infectious agents is another important factor to consider in this sense. In particular, helminths are well-known as regulators of the host immune response through the generation of AAMs, Tregs, and B regulatory cells, mediated by helminth SE products (29).

In our study, we observed the effect of *T. canis* infection in the development of 4T1 mammary tumor model in BALB/c mice because we do not need any modification to the immune system of these animals to allow tumor growth and so we were able to assess the local and systemic reactions. Notably, after 28 days of 4T1 cell inoculation, enhanced tumor promotion was observed in *T. canis*-infected mice. Furthermore, the tumor microenvironment was modified, explaining the larger tumor size.

There is evidence that some helminths are inductors of different types of tumors (8), and the coexistence of diseases caused by helminths and enhancement of tumor growth has also been described. In a tumor model of colitis-associated colon cancer in mice, an intestinal infection with the nematode *H. polygyrus* promoted tumor growth (9). In another colon cancer model, the intestinal infection with the nematode *Trichuris muris* accelerated the progress of spontaneously developed intestinal adenomas in APC min/+ mice (33). In both studies, the nematode and the tumor are in the same anatomical location, but, *T. canis* larvae migrate through different organs (24), and the regulatory immune response induced by the parasite is widespread throughout different body compartments, which, in the 4T1 model, promotes the size of the mammary tumor.

Contrary to our initial hypothesis, tumor enlargement was not associated with an increase in the local proportion of T regulatory cells ($CD4^+/Foxp3^+$ and/or $CD8^+/Foxp3^+$). Although the tumor Treg proportion was not increased due to the infection in the PLN from infected mice, we detected a higher proportion

of $CD4^+$/$Foxp3^+$ Treg cells in the PLNs of both *T. canis*-infected mice and the 4T1+*T. canis* group. Treg induction in tumors may be less frequent than Treg production in tumor-draining lymph nodes (TDLNs), perhaps because the conversion is more active in lymph nodes than in tumors (34).

The microenvironment in TDLNs is important in the progression of the tumor immune response (35). For example, $Foxp3^+$ Treg cells in TDLNs modulate T lymphocyte function by suppressing IFN-γ secretion in $CD8^+$ cells (35). Another mechanism by which Treg cells regulate $CD8^+$ T lymphocyte expansion and modify differentiation is by competing for IL-2; at the same time, this cytokine may promote Treg functions (36). This may explain the increased proportion of $CD4^+$/$Foxp3^+$ Treg in PLNs, accompanied by a decreased proportion of $CD8^+$ T lymphocytes in PLNs and the tumor infiltrate, from *T. canis* infected mice.

$CD8^+$ anti-tumor function depends on its differentiation and infiltration into the tumor microenvironment (37). Differentiation progresses to $CD8^+$ T cell cytotoxic function, which may induce tumor cell apoptosis through IFN-γ secretion (38). Although, in the present study, the percentage of $CD8^+$ T cells was lower in tumors from 4T1+*T. canis* mice, the IFN-γ levels were unchanged with respect to non-infected mice. This may be because other hematopoietic cells, such as NK and $CD4^+$ T cells, also produce IFN-γ within the tumor (39). The larger tumor size in the *T. canis* group could be related to the reduction in $CD8^+$ T cell infiltration into the tumor, associated with deficient local recruitment. There could also be an impairment in the cytotoxic function of the recruited $CD8^+$ cells. As mentioned previously, Treg cells play an important role in the suppression of IFN-γ secretion by $CD8^+$ lymphocytes (35), but in our study, the Treg percentage was inferior in tumors of *T. canis*-infected mice. Therefore, Treg may not exert an important effect in $CD8^+$ cell recruitment and function, but another population such as TAMs, through IL-10 secretion or tumor cell direct contact, could promote $CD8^+$ cell impairment (40).

A Type 1 response linked to cell-mediated immunity usually prevents tumor growth because of a CTL response (41). Type 2 polarization promotes tumor development through the regulation of the host immune response and is associated with solid tumors (41, 42). This polarization is associated partially with cytokines in the tumor milieu (43), so we determined Type 1 and Type 2 cytokine expression of tumor extracts. Among the cells that promote the secretion of type 2 cytokines in the tumor microenvironment are the TAMs (42). This Type 2 polarization has been described in 4T1 BALB/c mouse tumors and is characterized by the presence of IL-4, VEGF, $F4/80^+$ macrophages, and $CD4^+$/$Foxp3^+$ Treg cells (43). In the present study, these cytokines and cells were present in the 4T1 tumors, and in the 4T1+*T. canis* group, the cytokine milieu was enriched by the increase of IL-4, VEGF, and IL-10 and the decreased amount of the Type 1 cytokine TNF-α.

This microenvironment suggests that the intra-tumoral cell populations may be polarized as a Type 2 and/or regulatory phenotype. Thus, although we need to further characterize the $F4/80^+$ macrophages and $CD19^+$ B lymphocytes phenotype, these cells possibly display local Type 2 and regulatory functions. This polarization is reported in an *in vitro* experiment where macrophages obtained from *T. canis*-infected mice secreted higher amounts of IL-10 and lower quantities of TNF-α as compared to macrophages from uninfected mice (44). Furthermore, splenic Breg lymphocytes ($CD19^+$) also secrete IL-10, which suppresses $CD4^+$ and $CD8^+$ T cells (45).

Type 2 response, solid tumor growth, and angiogenesis are also related (46). Angiogenesis plays an important role in tumor development and the spread of tumor cells through blood vessels (47), and as mentioned before, VEGF promotes angiogenesis (17). Thus, systemic and local VEGF increase in tumors from *T. canis*-infected mice is associated with the Type 2 response in the tumor microenvironment and promotes tumor growth.

The humoral response is related to *T. canis* infection, and antibody detection is the basis for immunological diagnostic tests (18). In the present study,the level of IgG at 49 d.p.i was very similar to that in *T. canis*-infected mice with tumors and B lymphocyte expansion in the spleen was also found (28). Thus, the systemic response to infection was evidenced by the specific humoral response.

In regard to splenomegaly, *T. canis* infection induced spleen enlargement (48), but also, the 4T1 tumor induction increased the spleen size (49) and induced splenic Treg depletion (3). Both abnormalities are associated with a leukemoid response and extramedullary (splenic) hematopoiesis in 4T1 tumor-bearing mice, in which an increased proportion of granulocytes diminishes the proportion of lymphocytes (50). This response may mask the expected modifications in immune cell proportions in the secondary lymphoid organs from the 4T1+T. canis mice.

Although IL-5 serum levels in infected tumor-bearing mice were not increased enough to be statistically significant, we observed an increase in this cytokine associated with the infection. Splenic IL-5 level in 4T1+*T. canis* animals were very similar compared to infected mice without tumor (28).

Higher proportions of immune cells found in the tumor microenvironment (**Figure 7A**) were $F4/80^+$ macrophages and $CD19^+$ B cells, which could contribute to tumor enlargement. For example, macrophages such as AAMs produce IL-4, IL-10, and VEGF (15) (**Figures 7B–D**). These soluble factors act on other cell populations. For instance, IL-4 (**Figure 7B**) may inhibit Th1 polarization and, therefore, the production of TNF-α and IFN-γ (41) (**Figure 7E**), which stimulates $CD8^+$ cytotoxicity (45). IL-4 also promotes Th2 polarization and thereby the secretion of IL-4, IL-10, and IL-5 (41) (**Figure 7F**), a typical cytokine of *T. canis* systemic immune response (28). Another AAM related-cytokine is IL-10 (15) (**Figure 7G**), which stimulates LB to Breg switch (51) (**Figure 7H**). Together, Treg and Breg produce and enrich an IL-10 milieu (**Figure 7I**). IL-10 inhibits cytotoxicity activity and proliferation of LT $CD8^+$ cells (52) (**Figure 7J**). Meanwhile, local increase of VEGF (**Figure 7A**) enhances the blood vessel formation that nourishes the tumor and promotes metastasis to distant organs such as lungs and liver (17) (**Figure 7K**). This tumor VEGF was accompanied by systemic augmentation levels of this soluble factor in serum

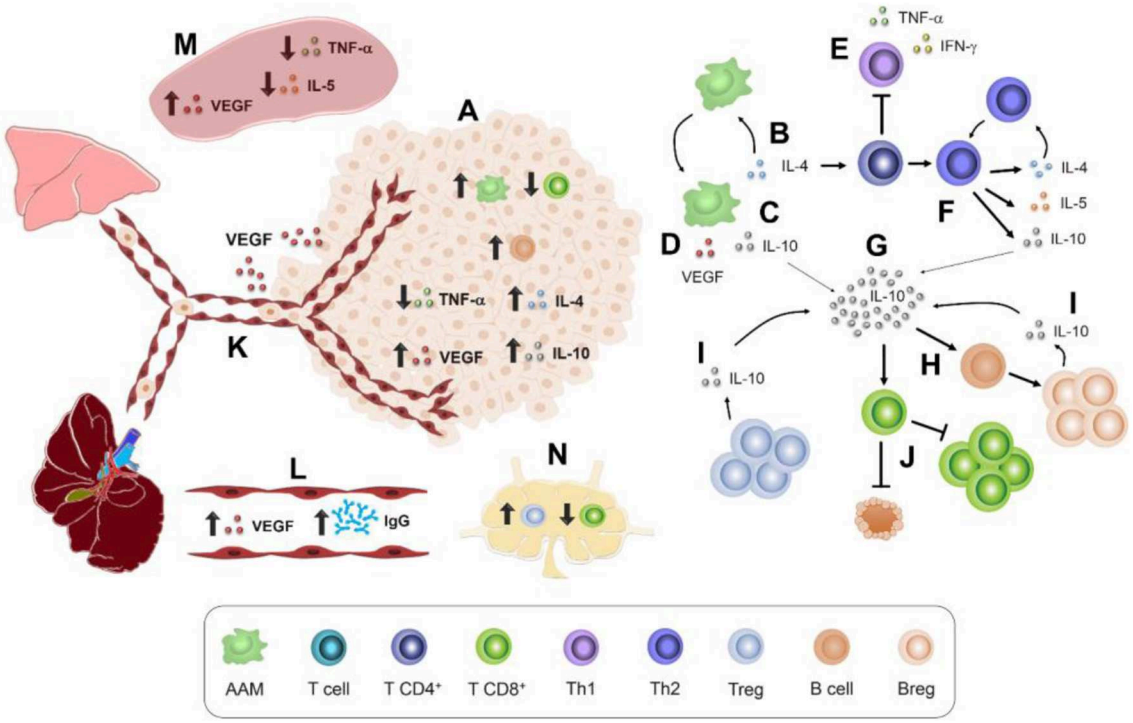

FIGURE 7 | Immune interactions in 4T1 tumor-bearing mice chronically infected with *T. canis*. **(A)** Tumor immune microenvironment. AAM secretion of: **(B)** IL-4. **(C)** IL-10. **(D)** VEGF. **(E)** Th1 polarization inhibition. **(F)** Th2 polarization promotion by IL-4. **(G)** IL-10 production and stimulus in different immune cells. **(H)** B lymphocyte conversion to Breg lymphocytes. **(I)** IL-10-secretory Breg cells. **(J)** Inhibitory effect of IL-10 on T CD8$^+$ proliferation and cytotoxic activity. **(K)** VEGF promotes angiogenesis and pulmonary and liver metastasis. **(L)** Higher levels of anti-*T. canis* IgG and VEGF in serum. **(M)** Splenic immune microenvironment. **(N)** PLN immune cell milieu.

(**Figure 7L**) and spleen (**Figure 7M**). Additionally, CD8$^+$ T cytotoxic cells may eliminate tumor cells (38), and a reduced proportion within the tumor in *T. canis*-infected mice could allow a larger tumor size (**Figure 7A**). Together with a lower CD8$^+$ cell percentage in tumor, in PLN, the decrease in this population in infected animals could be associated with the increased proportion of Treg (36) (**Figure 7N**). On a systemic level, higher serum *T. canis*-IgG levels were sustained in tumor-bearing mice (**Figure 7L**). With regard to splenic changes associated with *T. canis* infection, TNF-α and IL-5 decrease were detected (**Figure 7M**).

This study showed that immune system modulation caused by *T. canis* infection leads to a different anti-tumor response and triggers tumor growth. This modulation was mainly associated with a tumor microenvironment characterized by a Type 2, regulatory immune, and angiogenic milieu.

Augmented tumor growth associated with *T. canis* infection is the result of complex interactions among the immune system, tumor cells, and the nematode larvae. In this intricate network, the immune response must act against two different etiologies that usually occur in everyday life and in all kinds of organisms. Therefore, the identification of risk factors that promote tumor progression by regulating the immune response is important for making decisions about lifestyle options and seeking medical attention. In this sense, *T. canis* infection prevention should be an important issue not only for the clinical disease itself but also because of an increased susceptibility to develop larger mammary tumors. Prevention is essential given the limited treatment efficacy against *T. canis* larvae encapsulated in tissues (27). Nevertheless, in human breast cancer patients or even in companion animals such as dogs and cats with mammary tumors, the screening of anti-*T. canis* antibodies to identify the infection is recommended to treat them and try to restrict the continuous promotion of a regulatory and angiogenic host immune response due to *T. canis*.

DATA AVAILABILITY STATEMENT

The data used in this study are available from the corresponding author upon reasonable request.

ETHICS STATEMENT

The protocol used in this study was approved by the Committee on Ethics and Use in Animal Experimentation of the Instituto de Investigaciones Biomédicas, UNAM. The study was performed following the guidelines of Mexican regulations (NOM-062-ZOO-1999) and the Guide for the Care and Use of Laboratory Animals of the National Institute of Health, 8th Edition to

ensure compliance with the established international regulations and guidelines.

AUTHOR CONTRIBUTIONS

JM-M, conceived and designed the study. RR-M, MP-A, RH-C, and VD developed the methodology. JM-M and KN-C acquired the data (provided animals, provided facilities, etc.). RR-M, PO-S, SM-C, and JM-M analyzed and interpreted data. JM-M, RR-M, PO-S, KN-C, SM-C, and VD wrote and/or reviewed the manuscript. RR-M, MP-A, and KN-C provided administrative, technical, or material support (i.e., reporting or organizing data, constructing databases). JM-M supervised the study.

FUNDING

This study was supported by grants from Programa de Apoyo a Proyectos de Investigación e Innovación Tecnológica (PAPIIT), Dirección General de Asuntos del Personal Académico (DGAPA), Universidad Nacional Autónoma de México (UNAM), grant/award number IN-209719, and from Fronteras en la Ciencia, Consejo Nacional de Ciencia y Tecnología (CONACYT), Grant No FC 2016 2125, both to JM-M. Grants from PAPIIT, DGAPA, UNAM, and IA 20219 were awarded to KN-C.

ACKNOWLEDGMENTS

RR-M and RH-C are students from the Programa de Doctorado en Ciencias Biomédicas, Universidad Nacional Autónoma de México (U.N.A.M.), and are recipients of CONACyT Ph.D. scholarships, numbers 421443 (RARM) and 293845 (RHC), respectively. MP-A has a postdoctoral fellowship from D.G.A.P.A., U.N.A.M. The authors wish to thank Juan Pablo Martínez Labat, from Facultad de Estudios Superiores Cuautitlán, U.N.A.M., for providing *Toxocara canis* eggs.

REFERENCES

1. GLOBOCAN 2018. Global Cancer Observatory. *Int Agency Res Cancer*. (2019) Available online at: http://gco.iarc.fr/
2. Barnard ME, Boeke CE, Tamimi RM. Established breast cancer risk factors and risk of intrinsic tumor subtypes. *Biochim Biophys Acta*. (2015) 1856:73–85. doi: 10.1016/j.bbcan.2015.06.002
3. Palacios-Arreola MI, Nava-Castro KE, Río-Araiza VH Del, Pérez-Sánchez NY, Morales-Montor J. A single neonatal administration of Bisphenol A induces higher tumour weight associated withassociated with changes in tumour microenvironment in the adulthood. *Sci Rep*. (2017) 7:1–11. doi: 10.1038/s41598-017-10135-1
4. Plummer M, de Martel C, Vignat J, Ferlay J, Bray F, Franceschi S. Global burden of cancers attributable to infections in 2012: a synthetic analysis. *Lancet Glob Heal.* (2016) 4:e609–16. doi: 10.1016/S2214-109X(16)30143-7
5. Consortium IHG. Comparative genomics of the major parasitic worms. *Nat Genet.* (2019) 51:163–74. doi: 10.1038/s41588-018-0262-1
6. Northrop-Clewes CA, Shaw C. Parasites. *Brithish Med Bull.* (2000) 56:193–208. doi: 10.1258/0007142001902897
7. Botelho MC, Veiga I, Oliveira PA, Lopes C, Teixeira M, da Costa JMC, et al. Carcinogenic ability of Schistosoma haematobium possibly through oncogenic mutation of KRAS gene. *Adv cancer Res Treat.* (2013) 2013:1–8. doi: 10.5171/2013.876585
8. Machicado C, Marcos LA. Carcinogenesis associated with parasites other than Schistosoma, Opisthorchis and Clonorchis: a systematic review. *Int J Cancer*. (2016) 138:2915–21. doi: 10.1002/ijc.30028
9. Pastille E, Frede A, McSorley HJ, Gräb J, Adamczyk A, Kollenda S, et al. Intestinal helminth infection drives carcinogenesis in colitis-associated colon cancer. *PLoS Pathog.* (2017) 13:e1006649. doi: 10.1371/journal.ppat.1006649
10. Nutman TB. Looking beyond the induction of Th2 responses to explain immunomodulation by helminths. *Parasite Immunol.* (2015) 37:304–13. doi: 10.1111/pim.12194
11. Othman AA, El-Shourbagy SH, Soliman RH. Kinetics of Foxp3-expressing regulatory cells in experimental Toxocara canis infection. *Exp Parasitol.* (2011) 127:454–9. doi: 10.1016/j.exppara.2010.10.005
12. Khor B. Regulatory T cells: central concepts from ontogeny to therapy. *Transfus Med Rev.* (2017) 31:36–44. doi: 10.1016/j.tmrv.2016.07.003
13. Vignali DAA, Collison LW, Workman CJ. How regulatory T cells work. *Nat Rev Immunol.* (2008) 8:523–32. doi: 10.1038/nri2343
14. Zhao X, Qu J, Sun Y, Wang J, Liu X, Wang F, et al. Prognostic significance of tumor-associated macrophages in breast cancer: a meta-analysis of the literature. *Oncotarget*. (2017) 8:30576–86. doi: 10.18632/oncotarget.15736
15. Qian BZ, Pollard JW. Macrophage diversity enhances tumor progression and metastasis. *Cell.* (2010) 141:39–51. doi: 10.1016/j.cell.2010.03.014
16. La Flamme AC, Kharkrang M, Stone S, Mirmoeini S, Chuluundorj D, Kyle R. Type II-activated murine macrophages Produce IL-4. *PLoS ONE.* (2012) 7:e46989. doi: 10.1371/journal.pone.0046989
17. Alameddine RS, Otrock ZK, Awada A, Shamseddine A. Crosstalk between HER2 signaling and angiogenesis in breast cancer: molecular basis, clinical applications and challenges. *Curr Opin Oncol.* (2013) 25:313–324. doi: 10.1097/CCO.0b013e32835ff362
18. Maizels RM. Toxocara canis: Molecular basis of immune recognition and evasion. *Vet Parasitol.* (2013) 193:365–74. doi: 10.1016/j.vetpar.2012.12.032
19. Strube C, Heuer L, Janecek E. Toxocara spp. infections in paratenic hosts. *Vet Parasitol.* (2013) 193:375–89. doi: 10.1016/j.vetpar.2012.12.033
20. Parsons JC, Bowman DD, Grieve RB. Pathological and haematological responses of cats experimentally infected with Toxocara canis larvae. *Int J Parasitol.* (1989) 19:479–88. doi: 10.1016/0020-7519(89)90077-5
21. Lopes Rassier G, Borsuk S, Pappen F, Scaini CJ, Gallina T, Villela MM, et al. Toxocara spp. seroprevalence in sheep from southern Brazil. *Parasitol Res.* (2013) 112:3181–6. doi: 10.1007/s00436-013-3499-8
22. de Oliveira VC, de Mello RP, D'Almeida JM. Muscoid dipterans as helminth eggs mechanical vectors at the zoological garden, Brazil. *Rev Saude Publica.* (2002) 36:614–20. doi: 10.1590/S0034-89102002000600011
23. González-García T, Muñoz-Guzmán MA, Sánchez-Arroyo H, Prado-Ochoa MG, Cuéllar-Ordaz JA, Alba-Hurtado F. Experimental transmission of Toxocara canis from Blattella germanica and Periplaneta americana cockroaches to a paratenic host. *Vet Parasitol.* (2017) 246:5–10. doi: 10.1016/j.vetpar.2017.08.025
24. Schnieder T, Laabs EM, Welz C. Larval development of Toxocara canis in dogs. *Vet Parasitol.* (2011) 175:193–206. doi: 10.1016/j.vetpar.2010.10.027
25. Beaver PC. Visceral and cutaneous larva migrans. *Public Heal Rep.* (1959) 74:328–32. doi: 10.2307/4590442
26. Fu CJ, Chuang TW, Lin HS, Wu CH, Liu YC, Langinlur MK, et al. Seroepidemiology of Toxocara canis infection among primary schoolchildren in the capital area of the Republic of the Marshall Islands. *BMC Infect Dis.* (2014) 14:261. doi: 10.1186/1471-2334-14-261
27. Ma G, Holland C V., Wang T, Hofmann A, Fan CK, Maizels RM, et al. Human toxocariasis. *Lancet Infect Dis.* (2018) 18:e14–24. doi: 10.1016/S1473-3099(17)30331-6
28. Ruiz-Manzano RA, Hernández-Cervantes R, Río-Araiza VH Del, Palacios-Arreola MI, Nava-Castro KE, Morales-Montor J. Immune response to chronic Toxocara canis infection in a mice model. *Parasite Immunol.* (2019) 11:e12672. doi: 10.1111/pim.12672

29. McSorley HJ, Maizels RM. Helminth infections and host immune regulation. *Clin Microbiol Rev.* (2012) 25:585–608. doi: 10.1128/CMR.05040-11
30. De Savigny H. *In vitro* maintenance of Toxocara canis larvae and a simple method for the production of Toxocara ES antigen for use in serodiagnostic tests for visceral larva migrans. *J Parasitol.* (1975) 61:781–2. doi: 10.2307/3279492
31. Bowman DD, Mika-Grieve M, Grieve RB. Circulating excretory-secretory antigen levels and specific antibody responses in mice infected with toxocara canis. *Am J Trop Med Hyg.* (1987) 36:75–82. doi: 10.4269/ajtmh.1987.36.75
32. Law AMK, Lim E, Ormandy CJ, Gallego-Ortega D. The innate and adaptive infiltrating immune systems as targets for breast cancer immunotherapy. *Endocr Relat Cancer.* (2017) 24:R123–44. doi: 10.1530/ERC-16-0404
33. Hayes KS, Cliffe LJ, Bancroft AJ, Forman SP, Thompson S, Booth C, et al. Chronic Trichuris muris infection causes neoplastic change in the intestine and exacerbates tumour formation in APC min /+ mice. *PLoS Negl Trop Dis.* (2017) 11:e0005708. doi: 10.1371/journal.pntd.0005708
34. Wang C, Lee JH, Kim CH. Optimal population of Foxp3+ T cells in tumors requires an antigen priming-dependent trafficking receptor switch. *PLoS ONE.* (2012) 7:e30793. doi: 10.1371/journal.pone.0030793
35. Deng L, Zhang H, Luan Y, Zhang J, Xing Q, Dong S. Accumulation of Foxp3+ T regulatory cells in draining lymph nodes correlates with disease progression and immune suppression in colorectal cancer patients. *Clin Cancer Res.* (2010) 16:4105–12. doi: 10.1158/1078-0432.CCR-10-1073
36. Mcnally A, Hill GR, Sparwasser T, Thomas R, Steptoe RJ. CD4+CD25+ regulatory T cells control CD8+ T-cell effector differentiation by modulating IL-2 homeostasis. *PNAS.* (2011) 108:7529–34. doi: 10.1073/pnas.1103782108
37. Nolz JC. Molecular mechanisms of CD8+ T cell trafficking and localization. *Cell Mol Life Sci.* (2015) 72:2461–73. doi: 10.1007/s00018-015-1835-0
38. Yang SX, Wei WS, Ouyan QW, Jiang QH, Zou YF, Qu W, et al. Interleukin-12 activated CD8+T cells induces apoptosis in breast cancer cells and reduces tumor growth. *Biomed Pharmacother.* (2016) 84:1466–71. doi: 10.1016/j.biopha.2016.10.046
39. Resende M, Cardoso MS, Ribeiro AR, Flórido M, Borges M, Castro AG, et al. Innate IFN-γ- producing cells developing in the absence of IL-2 receptor common γ-chain. *J Immunol.* (2017) 1429–39. doi: 10.4049/jimmunol.1601701
40. Resegofetse N, Liu S, Zhang Y. Fates of CD8 + T cells in tumor microenvironment. *Comput Struct Biotechnol J.* (2019) 17:1–13. doi: 10.1016/j.csbj.2018.11.004
41. Kidd P. Th1/Th2 balance: the hypothesis, its limitations, and implications for health and disease. *Altern Med Rev.* (2003) 8:223–246.
42. Colotta F, Allavena P, Sica A, Garlanda C, Mantovani A. Cancer-related inflammation, the seventh hallmark of cancer: links to genetic instability. *Carcinogenesis.* (2009) 30:1073–81. doi: 10.1093/carcin/bgp127
43. Liao D, Luo Y, Markowitz D, Xiang R, Reisfeld RA. Cancer associated fibroblasts promote tumor growth and metastasis by modulating the tumor immune microenvironment in a 4T1 murine breast cancer model. *PLoS ONE.* (2009) 4:e7965. doi: 10.1371/journal.pone.0007965
44. Kuroda E, Yoshida Y, Shan BE, Yamashita U. Suppression of macrophage interleukin-12 and tumour necrosis factor-alpha production in mice infected with. *Parasite Immunol.* (2001) 23:305–11. doi: 10.1046/j.1365-3024.2001.00387.x
45. Rosser EC, Mauri C. Perspective regulatory B cells : origin, phenotype, and function. *Immunity.* (2015) 42:607–12. doi: 10.1016/j.immuni.2015.04.005
46. Hanahan D, Weinberg RA. The Hallmarks of Cancer Review. *Cell.* (2000) 100:57–70. doi: 10.1016/S0092-8674(00)81683-9
47. Joyce JA, Pollard JW. Microenvironmental regulation of metastasis. *Nat Rev Cancer.* (2009) 9:239–52. doi: 10.1038/nrc2618
48. Kayes SG, Omholt PE, Grieve RB. Immune Responses of CBA / J Mice to Graded Infections with T. *canis*. *Infect Immun.* (1985) 48:697–703. doi: 10.1128/IAI.48.3.697-703.1985
49. Gregório AC, Fonseca NA, Moura V, Lacerda M, Figueiredo P, Simões S, et al. Inoculated cell density as a determinant factor of the growth dynamics and metastatic efficiency of a breast cancer murine model. *PLoS ONE.* (2016) 11:e0165817. doi: 10.1371/journal.pone.0165817
50. DuPre SA, Hunter KW. Murine mammary carcinoma 4T1 induces a leukemoid reaction with splenomegaly: association with tumor-derived growth factors. *Exp Mol Pathol.* (2007) 82:12–24. doi: 10.1016/j.yexmp.2006.06.007
51. Kim HS, Lee JH, Han HD, Kim A, Nam ST, Kim HW, et al. Autocrine stimulation of IL-10 is critical to the enrichment of IL-10-producing CD40hi CD5+ regulatory B cells *in vitro* and *in vivo*. *BMB Rep.* (2015) 48:54–59. doi: 10.5483/BMBRep.2015.48.1.213
52. Carter NA, Rosser EC, Mauri C. Interleukin-10 produced by B cells is crucial for the suppression of Th17/Th1 responses, induction of T regulatory type 1 cells and reduction of collagen-induced arthritis. *Arthritis Res Ther.* (2012) 14:R32. doi: 10.1186/ar3736

Conflict of Interest: The authors declare that the research was conducted in the absence of any commercial or financial relationships that could be construed as a potential conflict of interest.

8.3 Artículo original relacionado con el tema de Tesis (tumores mamarios)

Ruiz-Manzano Rocío Alejandra, Palacios-Arreola Margarita Isabel, Hernández-Cervantes Rosalía, Del Río-Araiza Víctor Hugo, Segovia-Mendoza Mariana, Nava-Castro Karen Elizabeth, and Morales-Montor Jorge. (2020). Novel *in situ* treatment with androstene-3beta, 17alpha-diol for mammary tumor in a mice model. En proceso de envío.

Novel *in situ* treatment with 5-Androstene-3β, 17α-diol for mammary tumor in a mice model.

Rocío Alejandra Ruiz-Manzano[1], Margarita Isabel Palacios-Arreola[2], Rosalía Hernández-Cervantes[1], Víctor Hugo Del Río-Araiza[3], Mariana Segovia-Mendoza[4], Karen Elizabeth Nava- Castro[2], Jorge Morales-Montor[1]*

[1]Departamento de Inmunología, Instituto de Investigaciones Biomédicas, Universidad Nacional Autónoma de México, Ciudad de México, México.
[2]Departamento de Genotoxicología y Mutagénesis Ambiental, Centro de Ciencias de la Atmósfera, Universidad Nacional Autónoma de México, Ciudad de México, México.
[3]Laboratorio de Inmunología y Biología Molecular de Parásitos, Facultad de Medicina Veterinaria y Zootecnia, Departamento de Parasitología, Universidad Nacional Autónoma de México, Ciudad de México, México.
[4]Departamento de Farmacología, Facultad de Medicina, Universidad Nacional Autónoma de México, 04510. Ciudad de México, México

*** Correspondence:**
Jorge Morales-Montor
jmontor66@biomedicas.unam.mx

Keywords: Mammary tumor, treatment, alpha-androstenediol

Abstract

Breast cancer treatment-failure is related to low compliance rates, high costs, and long-term toxicities. Thus, to find less toxic and cheaper treatments is necessary. In this sense, dehydroepiandrosterone (DHEA) analog, the androstene-3beta, 17alpha-diol (α-AED), has been proven to inhibit breast tumor cell proliferation *in vitro* independently of either the alpha estrogen or the androgen receptors presence, thus it results an ideal candidate to treat mammary tumors. The aim of this study was to evaluate the *in situ* effect of α-AED on tumor

mammary growth. First, we obtained half-maximal inhibitory concentration (IC50) for α-AED, which was 1x10-4.035 Molar (~100 μM). Thereafter, 4T1 tumors with 14 days of growth were injected with IC50 (100 μM) and double this concentration (200 μM). In both groups there were a reduction in size and average tumor weight. NK, plasmatic ($CD138^+$) and plasmablast cells ($CD19^+/CD138^+$) percentages were higher in tumors injected with α-AED 100 μM ($p \leq 0.05$, $p=0.01$ and $p=0.001$, respectively). Meanwhile tumors injected with α-AED 200 μM contained an elevated proportion of plasmablast and B cells ($CD19^+$) ($p \leq 0.05$). Of noticed, VEGF level in all α-AED-treated tumors were lower than the Vh group average level. The tumoral *in situ* response was reflected systemically by the increase of anti-4T1 IgG in serum from α-AED mice, but no other associated systemic change was detected. In sum, the reduction in tumor size for to the local injection of α-AED, is produced by the anti-proliferative effect of this hormone, could be associated to the of tumor VEGF reduction and to an increase of antibody-dependent cellular cytotoxicity (ADCC) linked to the intratumoral rise of NK and plasmatic cells, specific antibodies in serum. In conclusion, because of the astonishing tumor size reduction of α-AED treated mass further studies are needed to prove it as a viable mammary tumor treatment.

Background

There is a broad range of accepted therapeutic approaches to treat breast cancer to this day. These treatments have as an objective to reduce tumor size and risk of metastasis development (Waks and P, 2019). Among these therapies, the estrogen antagonist, tamoxifen, and aromatase inhibitors are commonly used as an adjuvant to treat hormone receptor-positive breast cancer despite that toxicity associated to these treatments is related to low compliance rates and long-term toxicities (van Hellemond et al., 2018). Additionally, patients with triple-negative breast cancer (TNBC) do not benefit from anti-estrogenic therapy (Wahba and El-hadaad, 2015).

Aside from estrogenic antagonists, other steroid compounds such as dehydroepiandrosterone (DHEA) have been proven to inhibit the proliferation and migration of breast cancer cell lines *in vitro*, and to prevent the development of breast cancer after mutagen administration(López-Marure et al., 2011; Mccormick et al., 1996). Another steroid

that possess a potent anti-proliferative effect, is the DHEA-analogue named 5-Androstene-3β, 17α-diol (α-AED). This hormone is demonstrated to be more effective in the inhibition of MCF-7 and MDA-MB231 breast cancer cell lines (Graf et al., 2012; López-Marure et al., 2011). In regard to α-AED, its antiproliferative effect is independent of either the α estrogen or the androgen receptors (Huynh et al., 2000).

The androstene α-AED is an epimer of 5-Androstene-3β, 17β-diol (β-AED), which has been shown to upregulate immune activity (Loria, 2002). Both steroids occur naturally, being α-AED found to be secreted in the spermatic vein of human testes (Dehennin, 1993; Huynh and Loria, 1997). This steroid is aldo been found in amniotic fluid and fetal-placenta circulation of normal pregancies and low levels were related to pathological pregnancies linked to diabetes, toxemia an placental insufficiency (Mancuso et al., 1980).

Despite the fact that androstenes are related to immune-regulation, the main effect of α-AED is on the proliferation of tumor cells, and the study of the immune system, and the development of tumor cells has been done independently, and mainly *in vitro,* thus, the resulting interaction between both remains unknown. This interaction is relevant knowing that immune cells influence the microenvironment of the tumor and can determinant in tumor development halts or progresses (Emens et al., 2012; Zitvogel et al., 2006).

In addition to immune cells proportions and phenotypes, another important drivers in the tumor microenvironment are the soluble factors that play an important role in immune tumor milieu. In this sense, angiogenesis is associated with tumor nutrient supply and metastasis and is importantly drive through the secretion of Vascular Endothelial Growth Factor (VEGF) by tumor and immune cells in response to hypoxia (Bohn et al., 2017). Hence, elevated levels of VEGF correlate with lymph node metastasis augmentation and worse prognosis in patients with breast tumors (Konecny et al., 2004).

All thing considered, it is possible to directly modify tumor microenvironment by direct administration of pharmacological agents (Kim et al., 2016). Thus, to address the local microenvironmental modifications of tumor and immune cells by α-AED, this compound was administered directly into mice tumors induced by 4T1 mammary tumor cells.

Methods

Materials

The α-AED was supplied by Dr. Roger Loria (Virginia Commonwealth University). All additional reagents used were acquired as described below. All procedures were performed at the Instituto de Investigaciones Biomédicas (IIB) from the Universidad Nacional Autónoma de México (UNAM).

Ethic statement

All the experimental procedures and animal studies were performed within the standards stablished by the Institutional Care and Animal Use Committee (CICUAL) (permit number 2017-208), in accordance with Mexican regulation (NOM-062-ZOO-1999) and with the Guide for the Care and Use of Laboratory Animals of the National Institute of Health (NIH) of the United States of America. Animal procedures were performed at the IIB, UNAM, in the Biological Models Unit (Unidad de Modelos Biológicos, UMB).

Animals

Female BALB/c AnN mice (MGI Cat# 5654849, RRID: MGI:5654849) of 8 to 9 weeks old, were obtained from Envigo México (Facultad de Química, UNAM, México). The animals were housed 4-5 per with 12 hours of alternating light at 22 °. Food (Envigo LabDiet 5015 - Cat# 0001328 Purina, St. Louis, MO-) and water were delivered *ad libitum* in sterile conditions.

Cell culture

The 4T1 murine mammary carcinoma cell line (ATCC Cat# CRL-2539, RRID: CVCL_0125) was cultured in RMPI 1640 medium (Sigma, St. Louis, MO) supplemented with 10% fetal bovine serum (FBS) (ByProducts, Guadalajara, Mexico), 1.0 mM sodium pyruvate, 100 units⁄mL penicillin, and 100 mg⁄ml streptomycin. 4T1 cells were maintained at 37°C, 5% CO_2 atmosphere, and 95% humidity.

Cell viability assay

For the Sulforhodamine B (SRB) assay (Sigma, St. Louis MO), 4T1 cells were seeded in 96-well culture plates ($1x10^3$ cells per well) in media supplemented with 10% heat-inactivated and charcoal treated-FBS, 100 units/mL penicillin plus 100 µg/mL streptomycin and maintained with a 5% atmosphere of CO_2 at 37°C and 95% humidity. After 24 hours after seeding, cells were treated with vehicle (0.1 % v/v EtOH) or with increasing concentrations of α-AED and incubated for 72 hours. Next, cell viability was obtained using SRB assay that determines cell density by measuring protein content, performed according to Vichai and Kirtikara, 2006, with modifications. In brief, cells were fixed with 100 µl of cold trichloroacetic acid (10%) for 1 hour, washed 3 times with water and air-drier overnight. Afterwards, cells were stained with 100 µl of SRB 0.057% in 1% acetic acid during 30 min, washed with 150 µl of acetic acid (1%), and air dried for 2 hours. Next, 100 µl of 10 mM Tris Base solution (pH 10) were aggregated, to solubilize the protein-bound dye, and the plates were agitated during 30 min. Plates were read at 492 nm in a Stat Fax 4200 microplate reader (Awareness Technology). Data were normalized to run between 0-100% and 0-1 as follows: Cell viability= optical density (OD) 492 in treatment wells/OD492 in control wells x 100 and x1, respectively. Experiments were performed in triplicate at 3 different occasions. The values of the IC50 were calculated with Prism 6® software (GraphPad Sofware Inc.).

Cell proliferation assay

To quantify 4T1 cell proliferation, we determined the Bromodeoxyuridine (BrdU) incorporation during DNA synthesis. This assay was performed in cells maintained in the same culture conditions that the ones for SRB assay and treated with vehicle, 100 µM, and 200 µM, during 72 hours. Procedures were performed according to the manufacturer's protocol (BD Apoptosis, DNA Damage and Cell Proliferation Kit, Cat 15821759, Thermo Fischer Scientific) with PerCP-Cy5.5 Mouse Anti-BrdU. Cell analysis was performed with BD FACSCalibur™ (BD Biosciences) flow cytometer and the data was analyzed with FlowJo software (Treestar Inc.). Compensation was assessed in BD FACSCalibur™ and FlowJo software with unstained samples.

Orthotropic tumor cell induction

After a second subculture at 80% of confluency, 4T1 cells were harvested and suspended in sterile 0.9% NaCl solution in a concentration of 250,000 cells/ml and conserved in ice until inoculation.

For mammary tumor induction, mice were anesthetized with Sevofluorane 5% (Abbot, Mexico), the abdominal area was cleaned with EtOH 70%, and in the fat pad under the second last right nipple were injected subcutaneously 4T1 cells 10^4. Mice recovery was supervised.

Tumor model and α-AED treatment

To test the intratumoral effect of α-AED on tumor growth, female mice were randomized into four experimental groups: 1) 4T1 group of animals with untreated tumors (12); 2) Vh group with tumors injected with 40 μl of corn oil-vehicle (14); 3) AED 100 μM group of mice with intratumoral injection of 580 ng of α-AED in 40 μl of corn oil (15), and 4) AED 200 μM: intratumoral injection of 1160 ng of α-AED (12), 40 μl. Tumor growth was observed for 28 days, and the tumor weight was obtained at the moment of the euthanization at day 28 post-inoculation.

Flow cytometry

The left and right peripheral (inguinal) lymph nodes (PLNs) and the spleen were excised and mechanically disaggregated through a 50 μm nylon mesh with PBS. Tumors were excised and minced with a scalpel. After the PBS wash, the lymph node cells were resuspended in FACS buffer (PBS, 2% FBS, 0.02% NaN_3). Erythrocytes in splenic suspension were lysed for 10 minutes with ACK buffer (150 mM NH_4Cl, 10 mM $KHCO_3$, 0.1 mM Na_2 EDTA, pH 7.3), washed with PBS and resuspended in FACS buffer. The minced tumors were incubated in digestion medium (RPMI 1640, 10 U/ml DNase, Roche, Mannheim, Germany; 0.5 mg/ml type IV Collagenase, Sigma, St. Louis, MO) for 20 minutes, and 50 μl FBS was added to stop digestion. Mechanical disruption in a 50 μm nylon mesh was performed. After the PBS wash, the cells were resuspended in FACS buffer. Approximately $1x10^6$ cells were incubated (20 minutes at 4°C) with anti-CD16/CD32 (TruStain®, Cat# 101319, Clone 93, RRID:AB_1574973, BioLegend, San Diego, CA) and washed. Then, they were stained with the following panels. For T lymphocyte:

AlexaFluor®488-conjugated anti-CD3ε (Cat# 100321, Clone 145-2C11, RRID:AB_389301) 1:100, PE-conjugated anti-CD4 (Cat# 100407, Clone GK1.5, RRID:AB_2075573) 1:300, PerCP-conjugated anti-CD8 (Cat# 100732, Clone 53-6.7, RRID:AB_893423) 1:100, and AlexaFluor®647-conjugated anti-Foxp3 (Cat# 320013, Clone 150D, RRID:AB_439750) 1:100. For macrophage and NK: AlexaFluor® 647-conjugated anti-F4/80 (Cat# 123122, Clone BM8, RRID:AB_893492) and PE-conjugated anti-NKp46 (Cat# 137604, Clone 29A1.4, RRID:AB_2235755). To B lymphocyte: PE-conjugated anti-CD19 (Cat# 115507, Clone 6D5, RRID:AB_313642), 1:200, plasmatic cells: Brilliant Violet 421™ anti-mouse CD138 (Syndecan-1) (Cat# 142507, Clone 281-2, RRID: AB_2565621). Antibodies from BioLegend, San Diego, CA, and the Foxp3/Transcription Factor Staining Buffer kit (Cat# TNB-0607-KIT, Tonbo Biosciences, San Diego, CA) were used for intracellular Foxp3 staining, according to the manufacturer's protocol.

Cell analysis was performed with a BD FACSCalibur™ (BD Biosciences) flow cytometer. The data was analyzed with FlowJo software (Treestar Inc.). Compensation was assessed in BD FACSCalibur™ and FlowJo software with unstained samples, single stain controls, and FMO for Foxp3$^+$ (CD3$^+$/CD4$^+$; CD3$^+$/CD8$^+$).

Cytokine determination

The tumors from the mice were stored in TRIzol™ reagent (Cat# 15596026, Invitrogen) at -70°C until use. Protein isolation was performed according to the procedural guidelines for TRIzol® reagent use. Protein quantification was done with a NanoDrop 1000 spectrophotometer (Thermo Scientific). An amount of 10 µg of protein was used to determine cytokine tissue levels.

Tumor cytokines were measured with ABTS ELISA kits (PeproTech) with the following antibodies: TNF-α (Cat# 500-P64bt, RRID:AB_147984), IFN-γ (Cat# 500-P119bt, RRID:AB_148087), IL-4 (Cat# 500-P54bt, RRID:AB_147636), IL-5 (Cat# 500-P55), and IL-10 (Cat# 500-P60, RRID:AB_147978), and unconjugated antibodies were used for cytokine capture, according to the manufacturer´s instructions, with modifications. Briefly, coated plates (96-well plate, MaxiSorp Nunc Cat# NNC#442404) with 50 µl (2 µg/ml) of different antibodies were incubated overnight. After 3 washes (wash buffer, PeproTech), the plates were blocked (block buffer: PeproTech) and then washed again. 50 µl of sera (1:2 dilution)

or tissue protein (10 µg) was added in duplicate (in diluent solution, PeproTech), maintained at 4°C for 2 h, and washed three times. An enzyme-substrate reaction was developed with ABTS liquid substrate (PeproTech). All solutions were from ABTS ELISA buffer kit (Cat# 900-K00). The plates were read at a wavelength of 405 nm with a wavelength correction set at 650 nm at different time points in a Stat Fax 4200 microplate reader (Awareness Technology).

VEGF quantification

Polystyrene wells (96-well plate, MaxiSorp Nunc Cat# NNC#442404) were coated with 50 µl of tumor protein (10 µg) or standard curve (0.001-1 ng) with VEGF mBA-165 (Cat# sc-4571, Santa Cruz Biotechnology) in bicarbonate buffer (pH 9.6) per duplicate and incubated at 4°C overnight. The plate was washed and blocked with 200 µl of PBS/BSA 1%/Tween 20 0.05% for 1 hour at 4°C. After washing, 50 µl of anti-VEGF/C-1 antibody (Cat# sc-7269, RRID:AB_628430, Santa Cruz Biotechnology) in a 1:200 dilution was added and incubated for 1 h at 4°C. After washing, 50 µl of m-IgGκ/BP-HRP (Cat# sc-516102, RRID:AB_2687626, Santa Cruz Biotechnology) (1:400) was added and maintained for 2 hours at room temperature. An enzyme-substrate reaction was developed with 50 µl of substrate solution and stopped after 15 minutes with 50 µl 2N sulfuric acid. The plates were read at a wavelength of 492 nm in a Stat Fax 4200 microplate reader (Awareness Technology). Cytokine and VEGF concentrations were calculated by interpolation from a standard curve.

IgG detection

Coated polystyrene wells (96-well plate, MaxiSorp Nunc Cat# NNC#442404) with 50 µl of mice sera/bicarbonate buffer (pH 9.6) suspension (1:1000) or with 1 µg/1ml of 4T1 crude extract, overnight at 4°C. The plate was washed three times with (PBS/Tween 20 0.05%) and blocked with 200 µl of 3% bovine serum albumin (BSA) and washing solution, for 30 minutes at room temperature. The plate was washed as mentioned. For the anti-4T1 IgG determination plates were incubated with mice sera (1:200) during 2 hours at room temperature and washed. In both cases were added 50 µl of peroxidase goat anti-mouse IgG (Jackson, RRID:AB_2338511) at 1:10,000 dilution was added during 90 min at room temperature. An enzyme-substrate reaction was developed by the addition of 50 µl of freshly prepared substrate solution (0.05% o-phenylenediamine/0.01% H_2O_2/0.1 M sodium

citrate/0.1 M citric acid) and stopped after 10 min with 50 µl 2N sulfuric acid. The plate was read at a wavelength of 492 nm in a Stat Fax 4200 microplate reader (Awareness Technology).

Cytokine, VEGF and antibody determination were performed after proper ELISA standardization.

Statistical analysis

Data were charted as mean±SD. To compare the differences between a non-parametrical Kruskall-Wallis test and Dunn test for multiple comparison were used. The differences were considered significant when $p \leq 0.05$. All the analyses were calculated with Prism 6® software (GraphPad Sofware Inc.).

Results

Elevated concentrations of α-AED reduce the viability of mammary tumor 4T1 cells *in vitro*

To obtain α-AED IC50 we measured the viability of 4T1 cell line after the *in vitro* exposition to increasing concentrations of α-AED (1x10-12 to 1x10-3.3 Molar) during 72 hours (Fig. 1A). SRB assay was used to quantify the cell density through the determination of cellular protein content. IC50 value was determinate at 1x10-4.035 with an interval of 1x10-4.253 to 1x10-3.817. Of notice, low concentrations of α-AED (1x10-12 to 1x10-8 Molar) slightly increased 4T1 cell density, meanwhile, high doses (1x10-6 to 1x10-3.3 Molar) reduced the quantity of 4T1 cells (Fig. 1A, B). This reduction was 3.2 (p 0.01), 2.4 ($p \leq 0.05$), and 2.8 (p 0.01) times lower than the vehicle, with 1x10-4 (100 µM), 1x10-3.7 (200 µM) and 1x10-3.3 (500 µM) concentrations, respectively (Figure 1B).

In order to assess the α-AED anti-proliferative effect, we measure BrdU incorporation in 4T1 proliferating cells treated with vehicle (EtOH 0.2%), α-AED 1x10-4 Molar (100 µM) and twice this concentration (1x10-3.7 Molar or 200 µM). Average BrdU positive-cells was 9-fold lower

when treated with α-AED 1x10-4 Molar (100 μM) and 4-fold inferior with 1x10-3.3 Molar (200 μM) (p 0.01 and p ≤ 0.05, respectively), compared with vehicle-treated cells.

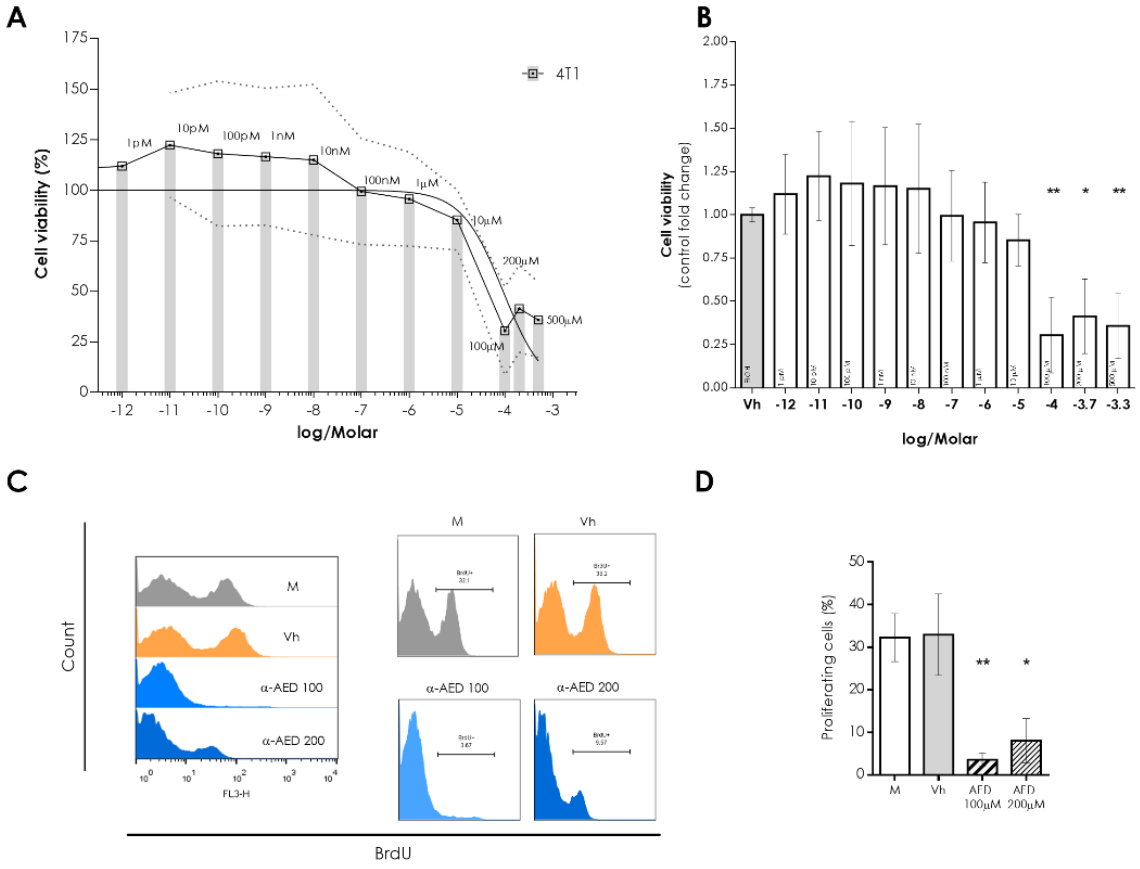

Figure 1. Effect of α-AED in 4T1 cells. The 4T1 cell line was exposed to vehicle (EtOH 0.2%) and α-AED 1x10-12 to 1x10-3.3 Molar for 72 hours. Cell density was measured through SRB assay. A. Cell viability adjusted as a percentage to obtain half-maximal inhibitory concentration (IC50). B. Cell density adjusted to vehicle (Vh). Graph represent the mean ± SD of the data from three experiments in triplicate. C. BrdU incorporation was determined in proliferative cells: offset histogram (left) and separated histograms of untreated 4T1 cells (M, Medium), treated with vehicle (Vh), α-AED 100 μM and 200 μM (1x10-4-and 1x10-3.3). D. Percentage of proliferating cells. Graph represent the mean ± SD of the data from four experiments (Medium, n = 6; Vh, n 6; AED 100 μM, n = 4; AED 100 μM, n = 4). Statistical significance was calculated using Kruskal-Wallis test (*, p ≤ 0.05; **, p ≤ 0.01).

Intratumoral injection with α–AED reduces tumor size and weight

After 28 days from 4T1 cell inoculation and 14 days after intratumoral injection, the mean weight of tumors treated with α-AED was smaller than the untreated (4T1) and the vehicle (Vh) injected tumors (Fig. 2A). As observed *in vitro* (Fig. 1), average weight of tumors treated with α-AED 100 μM (1x10-4) was smaller than the treated with twice this dose (200 μM=1x10-3.3) (Fig. 2A). Tumor mass weight was 65% and 50% smaller than α-AED treated-groups (α-AED 100= p 0.0001, α-AED 200=p ≤ 0.05), when compared with Vh group.

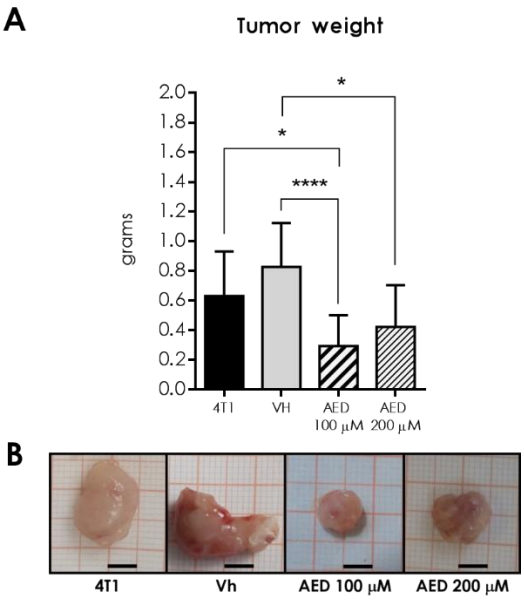

Figure 2. Effect of α-AED in 4T1 tumor growth in BALB/c mice. After 14 days of growth tumors were injected with vehicle -corn oil 40 μl- (Vh), α-AED 100 μM (1x10-4) and 200 μM (1x10-3.3), and excised after 28 days of tumor development. A. Tumor weight from intact tumors (4T1), Vh, α-AED 100 μM and α-AED 200 μM groups. (B) Representative images of tumors from all groups. Millimetric grid as a background; black bar = 0.5 cm. Graphs represent the mean±SD of the data from three experiments. Statistical significance was calculated using Kruskal-Wallis test (*, p ≤ 0.05; ****, p ≤ 0.0001).

Decreased tumor growth is associated with minor changes in tumor microenvironment

Androstene steroids has been linked to immune response regulation (Urban et al., 2008), therefore, we determined some cells populations of innate (macrophages and NK cells) and adaptive (T and B lymphocytes) immune response within the tumor.

Mean percentages of F4/80$^+$ macrophages and T cells (CD3$^+$, CD4$^+$, CD8$^+$, CD4$^+$Foxp3$^+$) intratumoral cells, remains without statistically difference (Fig. 3). Meanwhile, percentage of NK cells was higher (p 0.01) in tumors, when treated with 100 μM (Fig. 3A).

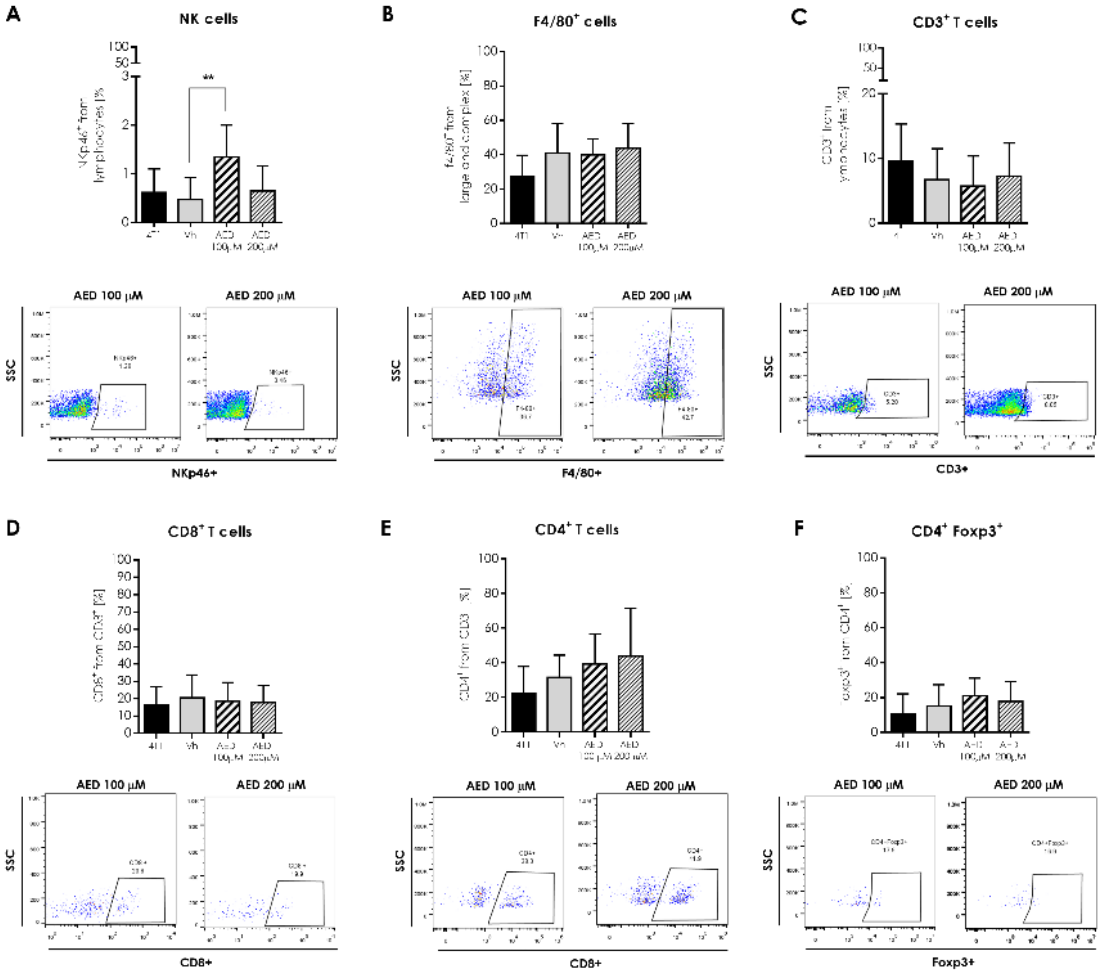

Figure 3. Effect of intratumoral α-AED treatment on immune cell infiltration in the 4T1 tumor model**.** Innate and adaptive immune cells in the tumor microenvironment. Determination of innate and adaptive immune subpopulations by flow cytometry within the tumor. A. NKp46$^+$ cells. B. F4/80$^+$ macrophages. C. T CD3$^+$. D. CD8$^+$ T cytotoxic lymphocytes. E. CD4$^+$ T

helper lymphocytes. F. CD4^{+}/Foxp3^{+} T lymphocytes. Graphs represent the mean±SD of the data from three independent experiments. Representative dot plots of the cytometric analysis of the corresponding population tumor cells (below). Gate from 10,000 cells was collected. Statistical significance was calculated using a Kruskal-Wallis test (**p ≤ 0.01).

Aside NK cell proportion rise, some changes were also noticed in regard to the mean proportion of humoral-related cells inside the tumor (Fig. 4). The first of these changes was the elevated percentage (p ≤ 0.05) of plasmatic cells (CD138^{+}) in α-AED 100 μM treated group (Fig. 4A), the second was the increase of B lymphocytes (CD19^{+}) proportion (p ≤ 0.05) in α-AED 200 μM (Fig. 4C), and the third was associated to plasmablast cells (CD19^{+}/CD138^{+}) that had different proportions when treated with α-AED, but this population is very scarce inside 4T1 tumors (Fig. 4B).

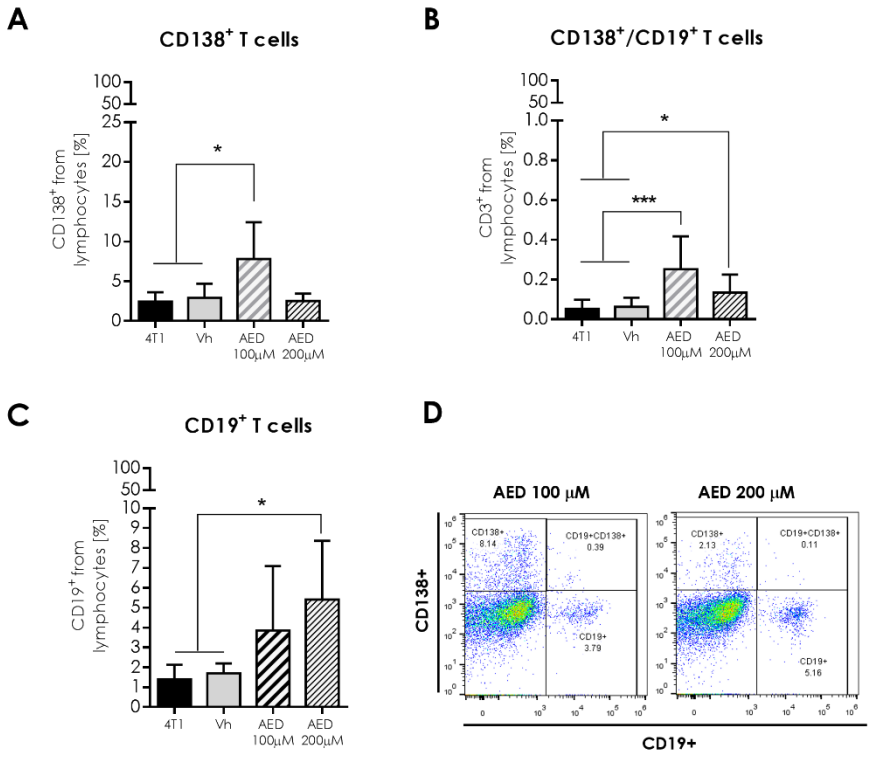

Figure 4. Effect of α-AED local injection on the humoral-related cell infiltration in the 4T1 tumor model**.** Humoral-related cells subpopulations by flow cytometry of the tumor. A. Plasmatic cells (CD138^{+}). B. Plasmablasts (CD138^{+}/CD19^{+}). C. B cells (CD19^{+}). D. Representative dot plots of the cytometric analysis of the corresponding population tumor

cells. Graphs represent the mean±SD of the data from three independent experiments. Gate from 10,000 cells was collected. Statistical significance was calculated using a Kruskal-Wallis test (*, $p \leq 0.05$; ***, $p \leq 0.001$).

Because of the importance of cell microenvironment communication, additionally to immune cells proportions, we search for another way by which α-AED could be intermediating the reduction of tumor size, thus we determine tumor VEGF concentration. Notably, VEGF levels in α-AED-treated tumors were lower (100 μM=p 0.01, 200 μM=p 0.0001) than the Vh group (Fig. 5).

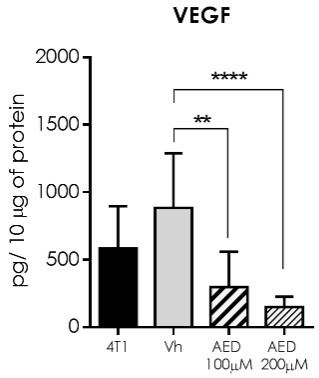

Figure 5. Analysis of the VEGF expression in the tumor microenvironment. Graph show data from tumor proteins obtained from two independent experiments. Bars represent the mean±SD of cytokines levels (pg/10 μg of tumor protein). Statistical significance was calculated using a Kruskal-Wallis test (**$p \leq 0.01$; ****$p \leq 0.0001$).

Since local treatment with α-AED 200 μM did not had the same effect on the reduction of tumor size compared with 100 μM intratumoral administration, we chose to measure some representative interleukins in the tumor of Vh and α-AED 100 μM only (Fig. 6). We determined Type 1 (TNF-α, IFN-γ)), Type 2 (IL-4 and IL-5), and regulatory (IL-10), cytokines. No changes were observed in these interleukins within the tumor (Fig. 6A-E).

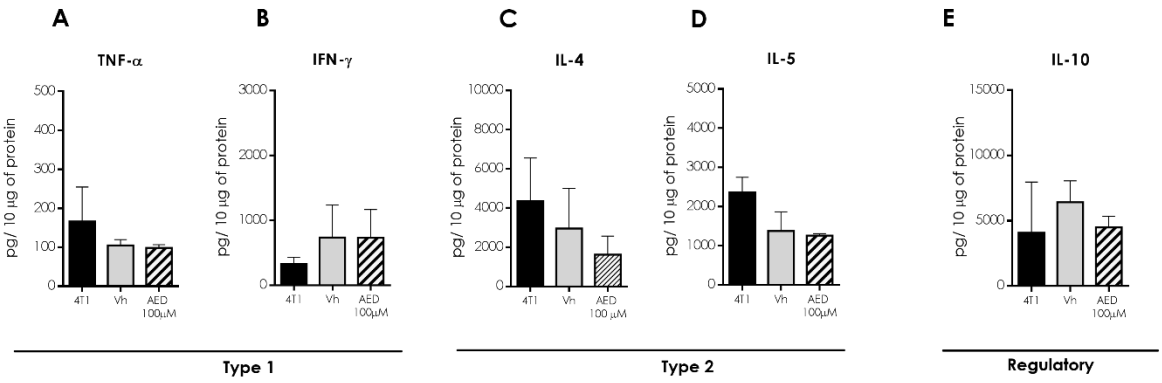

Figure 6. Expression of soluble factors in the tumor microenvironment. Analysis of type 1 (IFN-γ and TNF-α), type 2 (IL-4, IL-5), and regulatory (IL-10) cytokines. Graphs indicate data of tumor proteins obtained from two independent experiments. Bars represent the mean±SD of cytokine levels (pg/10 µg of tumor protein).

Systemic innate and adaptive immune response is preserve in tumor-bearing mice treated with α-AED

Because the injection of α-AED was performed inside the tumor, and we want to find out if this local treatment could reach a systemic level, we analyzed the effect of this local treatment in the systemic immune response in secondary lymphoid organs. In order to assess whether these modifications in splenic and PLN immune cell proportions were different in treated and untreated mice (Fig 7). Innate and adaptive cells obtained from these secondary lymphoid organs from mice treated with α-AED, conserved their proportions when compared with Vh group, with exception of $CD4^+/Foxp3^+$ T cells. The proportion of this regulatory population was augmented in spleen of tumor-bearing mice treated with α-AED 100 µM (p 0.001) and α-AED 200 µM ($p \leq 0.05$).

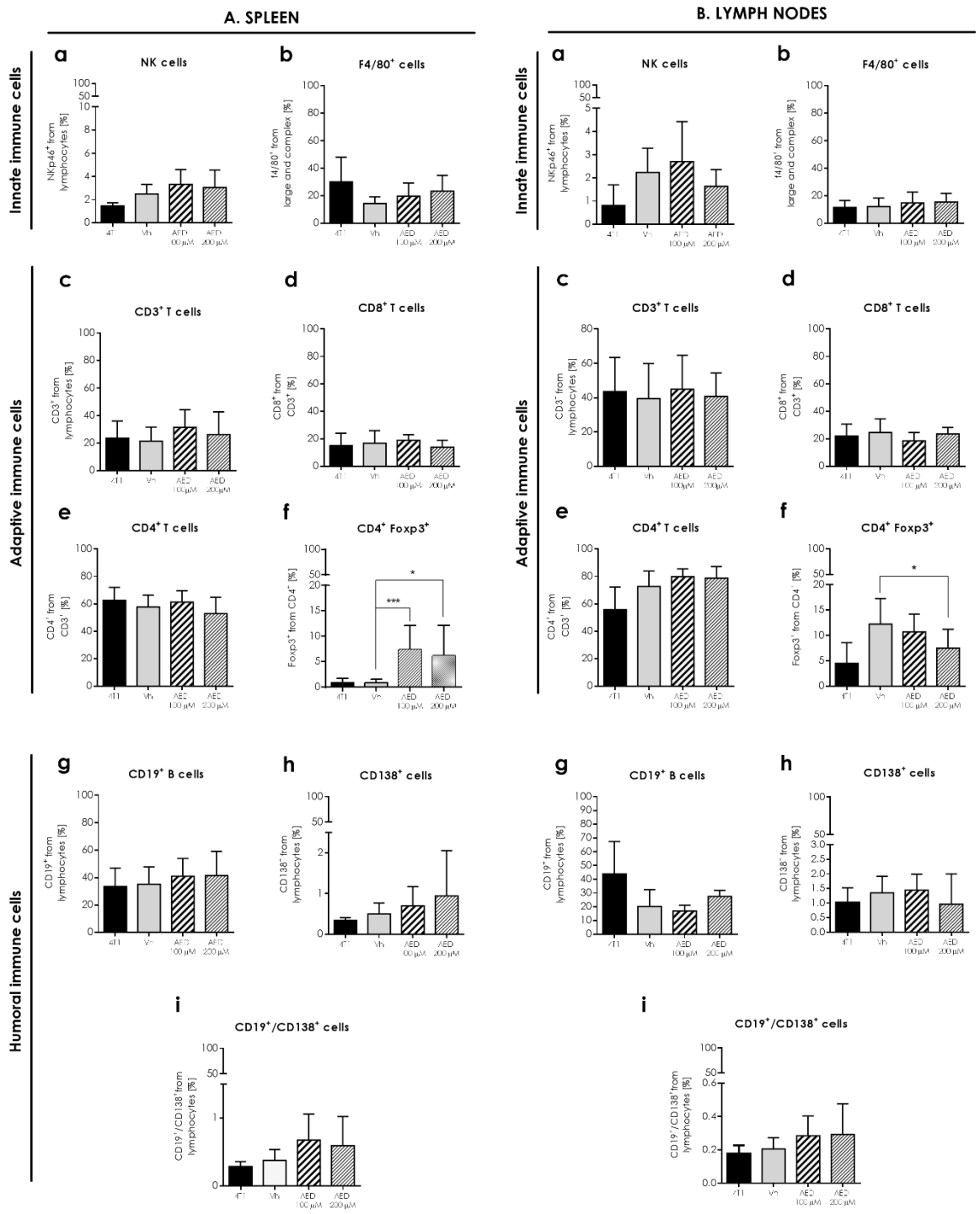

Figure 7. Effect of intratumoral α-AED treatment in the immune cell infiltration of secondary lymphoid organs, in the 4T1 tumor model**.** Determination of innate and adaptive immune subpopulations by flow cytometry in the (A) spleen (left panel) and (B) lymph nodes (right panel). a. NKp46$^+$ cells. b. F4/80$^+$ macrophages. c. T lymphocytes CD3$^+$. d. CD8$^+$ T cytotoxic lymphocytes. e. CD4$^+$ T helper lymphocytes. f. CD4$^+$/Foxp3$^+$ T lymphocytes. g. CD19$^+$ B

lymphocytes. h. Plasmatic cells ($CD138^+$). i. Plasmablasts ($CD138^+/CD19^+$). Graphs represent the mean±SD of the data from three independent experiments. Gate from 10,000 cells was collected. Statistical significance was calculated using a Kruskal-Wallis test (*, $p \leq 0.05$; ***, $p \leq 0.001$).

Specific humoral response against 4T1 cells is enhanced in mice treated with α-AED

As part of the systemic immune response analysis in tumor-bearing mice, we determined the percentage of B ($CD19^+$), plasmatic ($CD138^+$) and plasmacytoid cells ($CD19^+/CD138^+$) from the spleen (Fig. 7A g, h, i) and PNL (Fig. 7B g, h, i). Additionally we obtained the IgG and anti-4T1 IgG serum levels. None of these three humoral-related cell proportions were different, neither unspecific levels of IgG, in response to α-AED treatment. Nevertheless, anti 4T1-IgG from serum of α-AED-treated mice were higher with intratumoral injection of 100 μM (p 0.001) and 200 μM ($p \leq 0.05$).

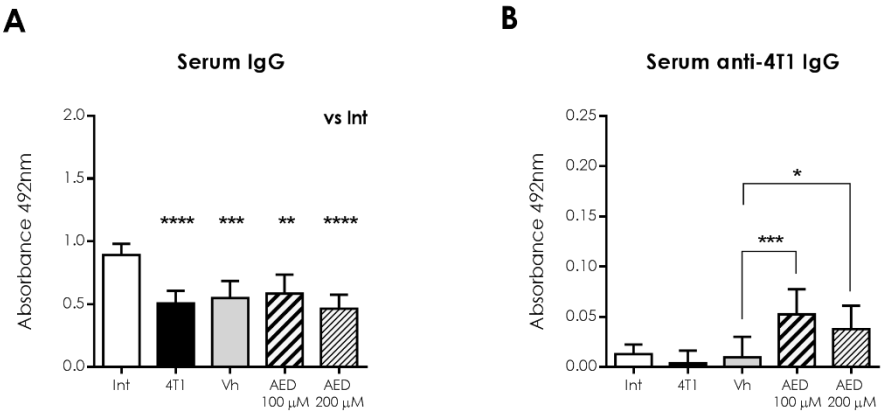

Figure 8. Systemic humoral response to intratumoral α-AED treatment in BALB/c mice. A. IgG and B. IgG anti-4T1 levels, in sera from intact (Int), tumor bearing mice with no treatment (4T1), and sera from mice injected into the tumor with vehicle (corn oil 40 μl), α-AED 100 μM or α-200 μM. Graphs represent the mean ± SD of data from two experiments. Statistical significance was calculated using Kruskal-Wallis test (*, $p \leq 0.05$; **P ≤ .01; ***P ≤ .001; ****P ≤ .0001)

Discussion

The neurosteroid α-AED has been widely proved as a proliferation inhibitor in different cancer cell lines and depending on the type of these, its IC50 is different. For instance, IC50 for glioma cells from human origin, ranges from 8.5±1.30 μM to 22.35 μM; for rat glioma cells F98 and RT-2 are 13.65±1.55 μM and 18.05±0.25 μM, respectively. Lastly the IC50 of the murine glioma cell line GL261 is 17.25±1.05 (Loria and Graf, 2012). In regard to the murine 4T1 cell line, the IC50 was 100.875 μM (1x10-4.035 Molar). This concentration was higher than the one reported for glioma cell lines, but as mention before α-AED IC50 varies among cell lines. In addition to the inhibitory effect of α-AED on glioma cells growth, this epimer also, inhibited the proliferation of breast cancer cell lines *in vitro*. Examples include breast adenocarcinoma (MCF-7, MDA-MB231), and mammary ductal carcinoma (T47D and TTU-1) (Graf et al., 2012). Despite, IC50 was not assessed in these cell lines, but lethal dose (LD)50 was stablished between 8 - 15μM (Graf et al., 2012).

On the other hand, the proliferation and viability increase of cells treated with concentrations lower than 10 nM has also been observed in murine macrophage-like cell line RAW 264.7 (concentration lower than 6.25 nM) cultured for 48h, and in human breast ductal carcinoma cells ZR75-1, as well as, MDA-MB231 breast tumor cells (lower than 12.5 nM) cultured during 6 days (Loria, 2002).

In line with the reduction of 4T1 cell density treated with α-AED 100 μM (1x10-4) and 200 μM (1x10-3.7) concentrations (p 0.01 and $p \leq 0.05$) (Fig. 1A, B), we assessed if this effect was associated to the inhibition of the proliferation through the BrdU incorporation in proliferating cells. After 72 hours of treatment with 100 μM and 200 μM we observed a dramatic reduction in the percentage of proliferating cells $BrdU^+$ (p 0.01 and $p \leq 0.05$, respectively) (Fig. 1C, D). These results suggest that the reduction in cell density detected through SRB assay was associated to a diminution in the proliferation of 4T1cells treated with α-AED, this last one, a phenomena reported in ZR75-1 and MDA-MB231 breast cancer cells (Huynh et al.,2000).

As mention before, IC50 variability among the different cancer cell lines, this is why although we determined IC50 of α-AED as 100 μM (1x10-4), treated 4T1 stablished tumors with this and twice this dose (α-AED 200 μM -1x10-3.3-), in order to determine if the *in vitro* effect of these two concentrations was preserved *in vivo*. Indeed, intratumoral injection with α-AED 100 μM and α-AED 200 μM reduced dramatically the weight and size (Fig. 2A, B) of the 4T1 tumors, but this effect was not dose-dependent, as we observed *in vitro*. Despite double dose (200 μM) reduced 50% ($p \leq 0.05$) their tumor size, the average weight of tumors treated with 100 μM diminished 65% (p 0.0001).

After we assessed the size reduction of tumors treated with α-AED 100 μM and 200 μM, we determined the effect of intratumoral treatment on immune cell infiltration in the 4T1 tumor model. Accordingly to Loria 2002, immune regulation is associated to β-AED, which is chemically identical to α-AED, and the anti-tumoral effect is linked to α-AED (Graf et al., 2009; Loria, 2002). But, because the structural similaritires among androstenediol α and β, and the lack of information associated to the immune tumor cells microenvironment, we search for some immune components of this milieu in order to determine if α-AED intratumoral treatment exert local immune changes.

For instance, NK cells proportion was augmented within the tumors treated with α-AED 100 μM (Fig. 3A). NK cells are known as a cytotoxic cells of innate response, and in tumors are effectors of cancer immunoediting by recognizing and destroying tumor cells directly through the exocytosis of granules with perforin and granzyme, apoptosis mediated by death receptors (FasL, TRAIL and TNF) and IFN-γ secretion (Gross et al., 2013; Smyth et al., 2005; Zitvogel et al., 2006). Another way by which NK cells exert their cytotoxic effect in solid tumors is by antibody dependent cell-mediated cytotoxicity, activated by antibodies linked to target cells (Nigro et al., 2019).

In order with this findings in the present study we also search for humoral-response components in tumor milieu as we described as follows. In treated tumors, plasmatic $CD138^+$ and plasmablast cells $CD19^+/CD138^+$ percentages were higher in tumors injected with α-AED 100 μM ($p \leq 0.05$ and p 0.001, respectively) (Fig. 5A, B). Meanwhile the tumors

injected with α-AED 200 μM contained an elevated proportion of plasmablast and B cells $CD19^+$ ($p \leq 0.05$) (Fig. 4B, C). To our knowledge, there is no report of the effect of α-AED on humoral-related response, thus this findings are the beginning of a further investigation, nevertheless, the presence of naïve or mature B cells within different types of breast tumors, is related to a positive prognostic effect in 54 cohorts studies (Wouters and Nelson, 2018). Also, the presence of B lymphocytes $CD19^+$ is associated to a favorable prognostic in overall survival of patients with tongue squamous cell carcinoma (Lao et al 2016). In a similar case, elevated plasma cell density is linked to a longer time to relapse in triple negative breast cancer tumors (TNBC) (Yeong et al., 2018).

Consequently to this knowledge and the increased proportions of B and plasmatic cells in millieau of α-AED treated-tumors, we determined the systemic humoral response of these tumor-bearing mice. Neither of the populations changes observed in tumor were detected in the spleen or PLN (Fig. 7)

Additionally to immune cells proportions, we search for another way by which α-AED was mediated the reduction of tumor size, thus we determine tumor soluble factors, that included angiogenic (VEGF), Type 1 response (TNF-α, IFN-γ), Type 2 response(IL-4, IL-5) and regulatory (IL-10) soluble factors. Notably, VEGF levels in α-AED-treated tumors were lower (100 μM=p 0.01) than the Vh group (Fig. 6.F). As previously mentioned, VEGF is related to vessel growth, nutrient supply and tumor cell dispersion to other tissues, thus its decrease within the tumor may lead to the reduction of tumor growth and metastasis (Bohn et al., 2017). The diminished concentration of VEGF in α-AED 100 μM treated tumors may be associated to a direct production inhibition of the tumor milieu cells, or linked to other microenvironmental factors. The VEGF expression is modify by hypoxia, free radicals, pH imbalance and nutrient deficiency, that increase at the same time that the tumor grow, therefore, the inhibition of the 4T1 cells proliferation mediated by α-AED, could reduce these pro-angiogenic factors within the treated tumors and in consequence the VEGF production (Wang et al., 2013). Further studies to unveil these mechanisms are needed.

Since local treatment with α-AED 200 μM did not had the same effect on the reduction of tumor size compared with α-AED 100 μM intratumoral administration, we chose to exclude this group of this determination (Fig. 6). None of the Type 1, Type 2 and regulatory response interleukins were different in α-AED injected tumors (Fig 6 A-E).

Intratumoral drug delivery is not a common practice in breast cancer patients, being the intravenous systemic chemotherapy the most common administration route. But only a small fraction of the anticancer drug reach the tumor, therefore high doses of the medicament have to be administrated, which in turn increase the undesirable side effects of chemotherapeutic compounds that affects healthy tissues (Weinberg et al., 2008). A leading objective in cancer research is to avoid or reduce the toxicity of the conventional cytotoxic treatment, and a promising method is the local delivery of the anticancer drug (Wolinsky et al., 2012), which may be used as a neoadjuvant therapy before tumor removal. In this study, we injected locally the anti-proliferative neuroesteroid α-AED and besides local changes, we look for its immune systemic effect in secondary lymphoid organs such as spleen and PLN. Innate (NK cells and macrophages) and adaptive (T and B lymphocytes) components of immune response remain with no changes, with exception of T regulatory cells ($CD3^+/CD4^+/Foxp3^+$). A previous study reported that 4T1 tumor induction decreased dramatically the percentage of splenic $Foxp3^+$ Treg cells (Palacios-Arreola et al., 2017), thus the increase in $CD3^+/CD4^+/Foxp3^+$ cells percentage from α-AED 100 μM and 200 μM treated mice (p 0.001 and $p \leq 0.05$, respectively) (Fig. 7), was tending to the normal proportion of these cells in the spleen. Additionally to splenic Treg change, we also detected a reduction of this population percentage in PLN of α-AED 200 μM injected tumors, when compared to the Vh group, but this was because of the increase induced by the injection of the vehicle.

Following the previous findings, the reduction in tumor size accompanied with changes in humoral-related response within the neoplasias treated with α-AED, suggest a role of this cells in tumor growth control. This could be explained because in tumor microenvironment, the B lymphocytes promote T-cell responses through the production of cytokines and chemokines, they also differentiate into producing-antibodies plasmatic cells (Wouters and

Nelson, 2018). Specific antibodies may be able to recognize tumor associated antigens and act directly on target proteins or through their Fc receptor trigger the ADCC, and in turn improve antigen presentation and activation of T cells (Wouters and Nelson, 2018). Thus, to improve our understanding in humoral-related mechanisms in 4T1 tumor mice model treated with α-AED, we determined the levels of unspecific IgG and anti-4T1 IgG in mice serum. As well as B, plasmatic and plasmablasts cells, we found no-changes in unspecific antibodies (IgG). In contrast 4T1-specific IgG was elevated in mice treated with 100 μM and 200 μM (Fig. 8).

To sum up, exceptional effect of the intratumoral injection of α-AED is most likely associated to the tumor cell anti-proliferative effect of this neurosteroid and linked to the immunomodulation associated to an ADCC response, leading by NK cells, plasmatic cells, B cells and anti-4T1 antibodies. Although this study showed some advances in the effect and possible mechanisms of α-AED in tumor growth further studies are needed to define its effect in other types of tumors, to use as a neoadjuvant and adjuvant treatment, to extrapolate these remarkable effects in human and animal companion cancer treatment.

References

Bohn, K.A., Adkins, C.E., Nounou, M.I., Lockman, P.R., 2017. Inhibition of VEGF and angiopoietin-2 to reduce brain metastases of breast cancer burden. Front. Pharmacol. 8, 1–10. https://doi.org/10.3389/fphar.2017.00193

Dehennin, L., 1993. Secretion by the human testis of epitestosterone, with its sulfoconjugate and precursor androgen 5-androstene-3 beta,17 alpha-diol. J. Steroid Biochem. Mol. Biol. 44, 171–177. https://doi.org/10.1016/0960-0760(93)90025-r

Emens, L.A., Silverstein, S.C., Khleif, S., Marincola, F.M., Galon, J., 2012. Toward integrative cancer immunotherapy: targeting the tumor microenvironment. J.Transl.Med. 10, 70. https://doi.org/10.1186/1479-5876-10-70

Graf, M.R., Jia, W., Marvin, L., Loria, R.M., 2009. The Anti-tumor Effects of Androstene Steroids Exhibit a Strict Structure – Activity Relationship Dependent upon the Orientation of the Hydroxyl Group on Carbon-17 625–629. https://doi.org/10.1111/j.1747-0285.2009.00900.x

Graf, M.R., Jia, W., Powell, T., Loria, R.M., 2012. Human Breast Cancer Cells and Enhances

Radiation Cytotoxicity. J. Cancer Ther. Res. 1–10. https://doi.org/10.7243/2049-7962-1-25

Gross, E., Sunwoo, J.B., Bui, J.D., 2013. Cancer immunosurveillance and immunoediting by natural killer cells. Cancer J. 19, 483–9. https://doi.org/10.1097/PPO.0000000000000005

Huynh, P.N., Carter, W.H.J., Loria, R.M., 2000. 17 alpha androstenediol inhibition of breast tumor cell proliferation in estrogen receptor-positive and -negative cell lines. Cancer Detect. Prev. 24, 435–444.

Huynh, P.N., Loria, R.M., 1997. Contrasting of a- and myeloid on oncogenic cell lines in vitro. J. Leukoc. Biol. 62, 258–267.

Kim, D.Y., Kwon, D.Y., Kwon, J.S., Park, J.H., Park, S.H., Oh, H.J., Kim, J.H., Min, B.H., Park, K., Kim, M.S., 2016. Synergistic anti-tumor activity through combinational intratumoral injection of an in-situ injectable drug depot. Biomaterials 85, 232–245. https://doi.org/https://doi.org/10.1016/j.biomaterials.2016.02.001

Konecny, G.E., Meng, Y.G., Untch, M., Wang, H., Bauerfeind, I., Epstein, M., Stieber, P., Vernes, J., Gutierrez, J., Hong, K., Beryt, M., Hepp, H., Slamon, D.J., Pegram, M.D., 2004. Association between HER-2 / neu and Vascular Endothelial Growth Factor Expression Predicts Clinical Outcome in Primary Breast Cancer Patients. Clin. Cancer Res. 10, 1706–1716.

López-Marure, R., Contreras, P.G., Dillon, J.S., 2011. Effects of dehydroepiandrosterone on proliferation, migration, and death of breast cancer cells. Eur. J. Pharmacol. 660, 268–274. https://doi.org/10.1016/j.ejphar.2011.03.040

Loria, R.M., 2002. Immune up-regulation and tumor apoptosis by androstene steroids. Steroids 67, 953–966.

Loria, R.M., Graf, M.R., 2012. 17??-Androstenediol-Mediated Oncophagy of Tumor Cells By Different Mechanisms Is Determined By the Target Tumor. Ann. N. Y. Acad. Sci. 1262, 127–133. https://doi.org/10.1111/j.1749-6632.2012.06602.x

Mancuso, S., Bellante, F.P., Angelini, A., Marana, R., 1980. Amniotic 5-androstene-3 beta, 17 alpha-diol in high risk pregnancy. J. Steroid Biochem. 12, 95–96. https://doi.org/10.1016/0022-4731(80)90256-3

Mccormick, D.L., Rao, K.V.N., Johnson, W.D., Bowman-gram, T.A., Steele, V.E., Lubet, R.A., Kelloff, G.J., 1996. Advances in Brief Exceptional Chemopreventive Activity of

Low-Dose Dehydroepiandrosterone in the Rat Mammary Gland. Cancer Res. 56, 1724–1726.

Nigro, C. Lo, Macagno, M., Sangiolo, D., Bertolaccini, L., Aglietta, M., Merlano, M.C., 2019. NK-mediated antibody-dependent cell-mediated cytotoxicity in solid tumors : biological evidence and clinical perspectives 7, 1–12. https://doi.org/10.21037/atm.2019.01.42

Palacios-Arreola, M.I., Nava-Castro, K.E., Río-Araiza, V.H. Del, Pérez-Sánchez, N.Y., Morales-Montor, J., 2017. A single neonatal administration of Bisphenol A induces higher tumour weight associated to changes in tumour microenvironment in the adulthood. Sci. Rep. 7, 1–11.

Smyth, M.J., Cretney, E., Kelly, J.M., Westwood, J.A., Street, S.E.A., Yagita, H., Takeda, K., van Dommelen, S.L.H., Degli-Esposti, M.A., Hayakawa, Y., 2005. Activation of NK cell cytotoxicity. Mol. Immunol. 42, 501–510. https://doi.org/10.1016/j.molimm.2004.07.034

Urban, N.H., Chamberlin, B., Ramage, S., Roberts, Z., Loria, R.M., Beckman, M.J., 2008. Effects of α/β-androstenediol immune regulating hormones on bone remodeling and apoptosis in osteoblasts. J. Steroid Biochem. Mol. Biol. 110, 223–229. https://doi.org/10.1016/j.jsbmb.2008.04.005

van Hellemond, I.E.G., Geurts, S.M.E., Tjan-heijnen, V.C.G., 2018. Current Status of Extended Adjuvant Endocrine Therapy in Early Stage Breast Cancer. Curr. Treat. optons Oncol. 19, 1–18. https://doi.org/10.1007/s11864-018-0541-1

Vichai, V., Kirtikara, K., 2006. Sulforhodamine B colorimetric assay for cytotoxicity screening. Nat. Protoc. 1, 1112–1116. https://doi.org/10.1038/nprot.2006.179

Wahba, H.A., El-hadaad, H.A., 2015. Current approaches in treatment of triple-negative breast cancer Treatment modalities of TNBC. Cancer Biol Med 12, 106–116. https://doi.org/10.7497/j.issn.2095-3941.2015.0030

Waks, A.G., P, W.E., 2019. Breast Cancer Treatment A Review. Clin. Rev. Educ. 321, 288–300. https://doi.org/10.1001/jama.2018.19323

Wang, F., Xu, P., Xie, K.C., Chen, X.I.A.F., Li, C.Y., Huang, Q., 2013. Effects of tumor microenviromental factors on VEGF expression 539–544. https://doi.org/10.3892/br.2013.115

Weinberg, B.D., Blanco, E., Gao, J., 2008. Polymer implants for intratumoral drug delivery and cancer therapy. J. Pharm. Sci. 97, 1681–1702. https://doi.org/10.1002/jps.21038

Wolinsky, J.B., Colson, Y.L., Grinstaff, M.W., 2012. Local Drug Delivery Strategies for Cancer Treatment: Gels, Nanoparticles, Polymeric Films, Rods, and Wafers. J. Control Release 159, 1–34. https://doi.org/10.1016/j.jconrel.2011.11.031.Local

Wouters, M.C.A., Nelson, B.H., 2018. Prognostic Signi fi cance of Tumor-In fi ltrating B Cells and Plasma Cells in Human Cancer 6125–6136. https://doi.org/10.1158/1078-0432.CCR-18-1481

Yeong, J., Chun, J., Lim, T., Lee, B., Li, H., Chia, N., 2018. High Densities of Tumor-Associated Plasma Cells Predict Improved Prognosis in Triple Negative Breast Cancer 9, 2–11. https://doi.org/10.3389/fimmu.2018.01209

Zitvogel, L., Tesniere, A., Kroemer, G., 2006. Cancer despite immunosurveillance: immunoselection and immunosubversion. Nat. Rev. Immunol. 6, 715–727. https://doi.org/10.1038/nri1936

8.4 Artículo de revisión relacionado al tema de la Tesis (tumores de mama).

Méndez-García Lucía Angélica, Nava-Castro Karen Elizabeth, Ochoa-Mercado Tania de Lourdes, Palacios-Arreola Margarita Isabel, **Ruiz-Manzano Rocío Alejandra**, Segovia-Mendoza Mariana, Solleiro-Villavicencio Helena, Cázares-Martínez Cinthia, and Morales-Montor Jorge. (2019). Breast Cancer Metastasis: Are Cytokines Important Players During Its Development and Progression? Journal of Interferon & Cytokine Research, 39: 1. DOI: 10.1089/jir.2018.0024

JOURNAL OF INTERFERON & CYTOKINE RESEARCH
Volume 39, Number 1, 2019

DOI: 10.1089/jir.2018.0024

Breast Cancer Metastasis: Are Cytokines Important Players During Its Development and Progression?

Lucía Angélica Méndez-García,[1,*] Karen Elizabeth Nava-Castro,[2,*] Tania de Lourdes Ochoa-Mercado,[3,*] Margarita Isabel Palacios-Arreola,[2,*] Rocío Alejandra Ruiz-Manzano,[3,*] Mariana Segovia-Mendoza,[3,*] Helena Solleiro-Villavicencio,[4,*] Cinthia Cázarez-Martínez,[2] and Jorge Morales-Montor[3]

In breast cancer, an uncontrolled cell proliferation leads to tumor formation and development of a multifactorial disease. Metastasis is a complex process that involves tumor spread to distant parts of the body from its original site. Metastatic dissemination represents the main physiopathology of cancer. Inter- and intracellular communication in all systems in vertebrates is mediated by cytokines, which are highly inducible, secretory proteins, produced not only by immune system cells, but also by endocrine and nervous system cells. It has become clear in recent years that cytokines, as well as their receptors are produced in the organisms under physiological and pathological conditions; recently, they have been closely related to breast cancer metastasis. The exact initiation process of breast cancer metastasis is unknown, although several hypotheses have emerged. In this study, we thoroughly reviewed the role of several cytokines in breast cancer metastasis. Data reviewed suggest that cytokines and growth factors are key players in the breast cancer metastasis induction. This knowledge must be considered with the aim to development of new therapeutic approaches to counter breast cancer metastasis.

Keywords: metastasis, breast cancer, cytokines, metastasis development, metastasis progression

Introduction

In breast cancer an uncontrolled cell proliferation leads to tumor formation and the development of a multifactorial disease. Breast cancer tumors may grow in different breast areas, such as lobules, ducts, and connective tissue, being ductal cancer the most common of all (Nava-Castro and others 2014). However, the hallmark of cancer pathology is not the tumor itself, but the migration of transformed cells to different tissues of the tumor origin. In breast cancer, a patient with a primary tumor has a 5-year survival rate of 99%, whereas when metastasic tumors are present, this rate decreases to up to 23% (Siegel 2012). In this process, named metastasis, immunological factors, particularly cytokines, have a fundamental role. There are numerous risk factors linked to breast cancer tumorigenesis. The principal is the gender. According to World Health Organization (WHO), breast cancer is the most frequent women malignancy in incidence and mortality (GLOBOCAN 2012). Other aspects such as genetic background or breast cancer familial history, age, ethnic group, and higher mass index and nulliparity are other risk factors (Nava-Castro and others 2014). Of note, pregnancy reduces breast cancer risk, through breast cell maturation and diminishing the estrogen exposure during gestation (Russo and others 2005). Additional factors that enhance the estrogen exposure are an early beginning of menstrual cycle, a delayed menopause, and estradiol ingestion as hormone replacement (Nava-Castro and others 2014).

Metastasis in breast cancer

Metastasis is a complex process that involves tumor spread to distant parts of the body from its original site. To successfully colonize a distant organ in the organism, a

[1]Unidad de Medicina Experimental, Hospital General de México ''Dr. Eduardo Liceaga'', México DF, México.
[2]Laboratorio de Genotoxicología y Medicina Ambientales, Departamento de Ciencias Ambientales, Centro de Ciencias de la Atmósfera, Universidad Nacional Autónoma de México, México DF, México.
[3]Departamento de Inmunología, Instituto de Investigaciones Biomédicas, Universidad Nacional Autónoma de México, Ciudad de México, México.
[4]Departamento de Fisiología, Facultad de Medicina, Universidad Nacional Autónoma de México, Ciudad Universitaria, México DF, Mexico.
*These authors contributed equally to this work.

cancer cell must complete a series of steps before it becomes a clinically detectable lesion. Cancer cells use 2 main dissemination pathways: the lymphatic pathway, leading to the invasion of the lymph nodes draining the organs where the tumor evolves; and the blood pathway that leads to the invasion of distant organs. In breast cancer, metastasis preferentially is targeted to the bones, lung, liver, and brain. The molecular mechanisms that promote the preferential migration to these organs are described extensively.

Different signaling pathways are involved in metastasis, such as the integrin pathway, the transforming growth factor beta (TGF-β) pathway, and different cytokine pathways among others. These pathways allow the possibility of therapeutic targeting, thanks to monoclonal antibodies or small molecules inhibiting the kinases involved in these signaling pathways. It is important to mention that, until now there is not a single antimetastatic drug for breast cancer, or any other type of cancer metastasis therapy.

The metastatic process

Metastasis is a complex phenomenon that comprises several processes which cancer cells must undergo, to transport themselves from the primary tumor to a distant organ. Briefly, we have categorized these processes into 3 stages, namely local invasion, migration, and colonization.

Initially, cancer cells reside within a well-defined primary tumor delimited by the adjacent stromal extracellular matrix, which separates it from the surrounding tissues, the lymphatic, and blood vessels. During local invasion, cancer cells undergo phenotypic changes toward more mobile ones, through a process known as epithelial–mesenchymal transition (EMT). EMT was initially involved in embryonic development in different animal species, in which mesenchymal cells acquire characteristics that allow them to migrate to different areas in the organ formation process (Thiery 2002).

There are 3 EMT subtypes based on biological processes (Kalluri and Weinberg 2009). Type I EMT is related with embryogenesis, embryo implantation, and initial placenta development, also with mesoderm and endoderm formation (epiblast–mesoderm transition) and the generation of mobile neural crest cells (Duband and Thiery 1982; Hay 1995; Vicovac and Aplin, 1996). Meanwhile, Type II EMT is associated with organ fibrosis mediated through the release of inflammatory factors and collagen, laminin, elastin, and tenancin (EMC components) by inflammatory cells and fibroblasts, for tissue reparation (Kalluri and Weinberg 2009). Finally, Type III EMT is related with tumor progression and metastasis. During this Type III EMT, polarized epithelial cells attached to basement membrane are transformed into mobile cells with the capacity of secrete ECM components and migrate to other tissues (Kalluri and Weinberg 2009; Wendt and others 2009).

In this context, Type III EMT is closely related to the development of metastasis and the transformation of mesenchymal cells by 3 different mechanisms: (1) morphology changes; (2) deregulation of epithelial markers [E-cadherin and cytokeratins 8 and 18 (CK-8 and 18)] and upregulation of mesenchymal markers (N-cadherin, vimentin, fibronectin, and SMA), which in turn, reduces intercellular adhesion; and (3) secretion of protein-dissolving enzymes that degrade extracellular matrix facilitating invasion and metastasis (Xu and others 2015). Since it allows cancer cells to become motile, Type III EMT contributes to metastasis favoring the dissemination of cancer cells to distant locations (Chang 2016). This process is highly promoted by angiogenesis, since it increases the number of available vessels (Baluk and others 2003).

Those cells (or cell clusters) that successfully survive to this process can then extravasate to a new organ parenchyma, where they will need to survive, adapt, and proliferate to generate a new tumor. This last process, called colonization, is favored in cells with a stem-like phenotype, known as cancer stem cells (CSCs), particularly breast cancer stem cells (BCSC's) (Al-Hajj and others 2003). These cells express CD44 but not CD24, which is consistent with a stem-like phenotype with multipotent differentiation ability. Other markers include EpCAM, CD47, and MET, which are usually found in metastasic lung, liver, and bone marrow tumors (Bacelli 2013). This kind of cells posess the gene expression signature Ras or HER2 overexpression, claudin-low, which is related to an increased Type IIIEMT potential (Geng 2014). It has been described that BCSC expresses the chemokine receptor CXCR4; whereas its ligand, the chemokine CXCL-12 is predominantly expressed in lymph nodes, lung, liver, and skeletal muscle–the common sites of metastasic tumors-(Muller 2001).

Another important condition that favors the breast cancer metastasis is angiogenesis, by which tumor promotes the formation of abnormal vasculature to provide the tumor with oxygen and nutrients. Among these proangiogenic factors are genetic mutations, mechanical stress, inflammation, the expression of angiogenic factors by tumor cells and of importance, hypoxia. This a vicious cycle since, in response to low oxygen levels, there is an induction of the expression of a series of factors related to proliferation, metabolism, angiogenesis, pH regulation, invasion, and metastasis and maintenance of CSC phenotype. The family of hypoxia-inducible factors, such as TGF-α, vascular endothelial growth factor (VEGF), insulin-like growth factor (IGF)-2, and IGF-Bp2 (Favaro and others 2011) are the cause of all these processes.

In the present review, we will thoroughly discuss the roles that known cytokines have during breast cancer metastasis. To do this in an organized manner, we have listed all cytokines and their role on metastasis by numerical order.

Interleukin-1

Interleukin 1 (IL-1) is a pleiotropic cytokine involved in inflammatory processes. In different studies, elevated levels of this cytokine have been observed in breast cancer tumors and it has been proposed as a factor that promotes metastasis (Elaraj and others 2006). IL-1α and IL-1β are the main agonist proteins of the IL-1 family. In addition to being pleiotropic proteins, they bind to the same receptors and appear to have the same biological function. However, they are activated differently. Whereas IL-1β is only activated in its secreted form, IL-1α is activated intracellularly or bound to the plasma membrane and very little is secreted. Therefore, it has been proposed that IL-1β secreted into the tumor microenvironment activates inflammation and promotes invasion processes; whereas IL-1α is expressed inside tumor cells and it stimulates an antitumor immune response (Apte and others 2006). On the other hand, IL-1β has been associated

with the induction of metalloproteinase expression (Fig. 1), such as the matrix metalloproteinase-1 (MMP-1) in BC-8701 breast cancer cells and fibroblasts (Rutter and others 1997) and the induction of the matrix metalloproteinase-9 (MMP-9) in the human breast cancer cell line MCF-7. Thereby, it has been proposed that the overexpression of these metalloproteinases mediated by IL-1β could favor the invasion ability of these tumor cells (Wang and others 2005). The group of Soria and *col*. suggests that the expression of IL-1β and tumor necrosis factor-α (TNF-α) has a role related to progression in breast cancer, since a greater amount of these proinflammatory cytokines were found in patients with invasive ductal carcinoma with relapse compared with samples of patients with ductal carcinoma *in situ*, and patients with ductal carcinoma without relapse. In addition, the continuous expression of these 2 cytokines led to Type III EMT in tumor cells, which could be favoring the observed relapse (Soria and others 2011).

Different studies have shown that autocrine or paracrine activation of the cytokine family of IL-1 and its receptors in human breast cancer could favor mechanisms that lead to the expression of pro-tumorogenic cytokines such as IL-8, and thus initiate a process of angiogenesis, tumor proliferation and invasion (Pantschenko and others 2003). Although IL-1β has been associated with the promotion of tumor cell invasion in breast cancer, IL-1α has been shown to play an important role in the expression of pro-metastatic genes in breast cancer cells and in stromal cells. Studies where an antibody against IL-1α has been used, showed a reduction of pro-inflammatory cytokines, such as IL-6 and IL-8 in breast cancer cells and metalloproteinase-3 protein (MMP-3) in fibroblasts, which could inhibit the invasion and metastasis of these tumor cells (Nozaki and others 2000) (Fig. 1). Although the main source of IL-1 is activated macrophages, it has been observed that a subpopulation of $CD44^{+}/CD24^{-}$ breast cancer cells express invasion-related genes such as *IL-1α*, *IL6*, and *IL8* (Sheridan and others 2006). Studies in animals have shown that the inhibition of IL-1β by the IL-1 receptor antagonist (IL-1Ra) reduces both metastasis and tumor size, therefore, the use of monoclonal antibodies neutralizing the IL-1 pathway has been proposed as a complementary therapy to block both angiogenesis and metastasis (Dinarello 2010).

Interleukin-4

IL-4 is a cytokine produced mainly by innate immune system cells and Th2 cells; it plays an important role in the humoral immune response against parasites and allergic antigens. However, it has also been shown to be involved in tumor growth mediating increased proliferation and

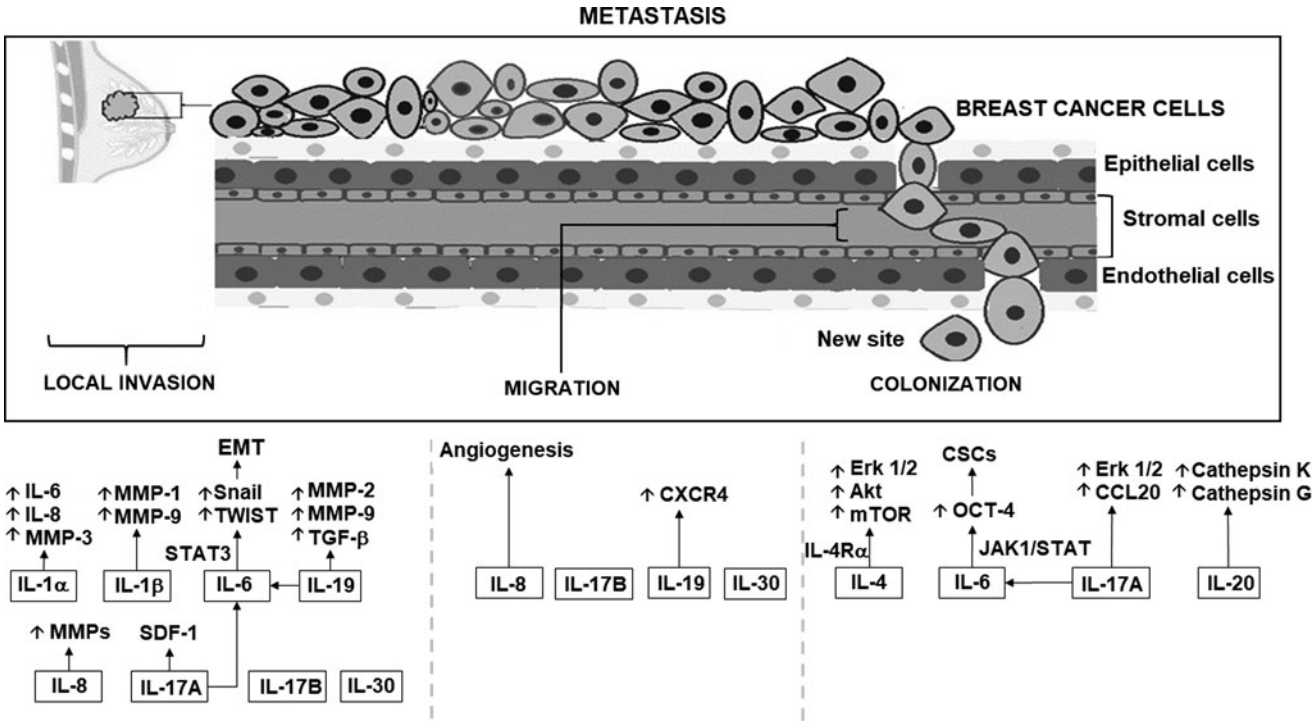

FIG. 1. Regulation of cytokines that favor metastasis in breast cancer. The figure shows how interleukins 1, 4, 6, 8, 17, 19, 20, 25, and 30 regulate different signaling pathways that contribute to the process of metastasis in breast cancer cells, as well as the generalized pattern of migration of tumor cells to a secondary site. In this metastasis process, cytokines regulate the activation of metalloproteinases, kinases, chemokines, cellular processes, such as apoptosis, as well as the activation of other cytokines that are considered proinflammatory. MMP1,2,3,9,12,14, matrix metalloproteinase 1,2,3,9,12,14; IL-1Ra, interleukin 1 receptor antagonist; IL-4Rα, interleukin 4 receptor antagonist; Erk1/2, extracellular signal-regulated kinase; AKT, AKT serine/threonine kinase 1; mTOR, mechanistic target of rapamycin kinase; non-CSCs, nonstem cancer cells; CSCs, stem cancer cells; Jak1, janus kinase 1; Stat1,3, signal transducer and activator of transcription1,3; Oct-4, octamer-binding protein 4; Type III EMT, III epithelial–mesenchymal transition; HER2, human epidermal growth factor receptor 2; ER, estrogen receptor; SDF-1, stromal cell-derived factor 1; CXCR4, C-X-C motif chemokine receptor 4; TGF-β, transforming growth factor beta; KISS-1, KiSS-1 metastasis-suppressor; VEGF-A, vascular endothelial growth factor A; CXCL-10/IP10, C-X-C Motif Chemokine Ligand 10; CD11b, CD11 antigen-like family member B; Grl, glucocorticoid receptor.

survival. On the other hand, this cytokine promotes differentiation of tumor-associated macrophages (TAM) toward a phenotype M2-like, thus increasing metastasis by activating epidermal growth factor receptor (EGFR) expressed in epithelial mammary cancer cells, in the presence of colony-stimulating factor-1 (CSF-1) (DeNardo and others 2009).

IL-4 binding to IL-4Rα (its surface cell receptor) promotes breast cancer colonization to metastasis sites such as lungs. This phenomenon occurs through the activation of extracellular signal-regulated kinases (Erk) 1/2, Akt, and mammalian target of rapamycin (mTOR) pathway (Fig. 1). Conversely, IL-4Rα knockout experimental models have shown a decrease in lung and liver metastasis (Venmar and others 2014). In the same way, neutralized IL-4 and IL-4Rα, in breast cancer experimental models, reduce metastatic foci in lungs (DeNardo and others 2009). Moreover, STAT6 activation by IL-4 is associated with proliferation (Hallett and others 2012). Alternatively, there are other ways in which IL-4 promotes tumor growth; one of them is related to glucose and glutamine metabolism (Venmar and others 2015).

Thus, interaction of IL4–IL-4Rα, promotes metastasis and tumor growth, its blockade could be a factor that decreases proliferation, metastasis, colonization, and survival in breast cancer cells.

Interleukin-6

IL-6 is a pleiotropic cytokine involved in inflammatory responses and hematopoiesis (Tanaka and others 2014). Also, IL-6 has an important role on many other physiological processes, such as steroidogenesis and neurotransmission. This cytokine signals through a receptor comprised by 2 chains, the IL-6-binding chain and a signal-transducing glycoprotein gp130 (Tanaka and Kishimoto 2014). The binding of IL-6 to its receptor induces the activation of the Janus kinases (JAK), JAK1, JAK2, and Tyk2. JAK-phosphorylation of gp130 allows further downstream signaling through the signal transducer and activator of transcription 1 and 3 (STAT1 and STAT3), SHP2, and phosphatidylinositol 3-kinase (PI3K) pathways (Fisher and others 2014).

One of the first described roles for IL-6 was the differentiation of activated B cells into plasma cells, but it also induces differentiation of $CD4^+$ T lymphocytes into some effector T helper subsets. Together with TGF-β, IL-6 promotes differentiation into Th17 phenotype, while inhibiting the regulatory (Treg) phenotype usually endorsed by TGF-β (Tanaka and Kishimoto 2014). In addition, IL-6 induces the differentiation of $CD8^+$ T lymphocytes into cytotoxic lymphocytes (Tanaka and others 2014). Furthermore, IL-6 also stimulates the production of acute-phase proteins (C-reactive protein, serum amyloid A, fibrinogen, hepcidin, and α1-antichymotrypsin) in the liver (Tanaka and Kishimoto 2014).

In breast cancer, several studies have shown a positive relationship between serum IL-6 levels and disease progression, suggesting a role as a negative prognostic marker (Knüpfer and Preiss 2007; Sullivan and others 2009). Particularly, IL-6 can promote metastasis by aberrantly activating STAT3 pathway, promoting Type III EMT and supporting CSCs (Fig. 1).

The activation of the IL-6/JAK/STAT3 pathway has been implicated in breast cancer progression. In the tumor milieu immune cells, adipocytes and fibroblasts secrete IL-6 as part of the inflammatory and wound-healing processes, but cancer cells have been shown not only to take advantage of it, but also to secrete and use this cytokine in an autocrine fashion to the point that they experience a constitutive activation of the STAT3 pathway (Dethlefsen and others 2013). The former gains relevance when looking at some of the STAT3 target genes, which control proliferation (*Bcl-2*, *Bcl-xL*, *BIRC5*, *CCND1*, *c-Myc*, *Mcl-1*), angiogenesis (*HIF-1α*, *VEGF*), and Type III EMT *(VIM*, *Snail*, *TWIST*, *MMP-7*, *MMP-2*, *MMP-9*) (Castellana and others 2015; Banerjee and Resat 2016). MMPs play a key role in the metastatic process; these enzymes facilitate the degradation of extracellular matrix, allowing cells to detach from the primary tumor. Furthermore, IL-6 activates STAT3 pathway leading to the transcription of Snail and *TWIST*, which are both repressors of E-cadherin. In this way, IL-6 has been shown to induce Type III EMT of cancer cells (Sullivan and others 2009; Huang and others 2011).

Although CSCs comprise a very small population within tumors, it has been proposed that nonstem cancer cells (non-CSCs) can become CSCs to maintain equilibrium. In that regard, it has been demonstrated that IL-6 is able to convert non-CSCs into CSCs in several breast cancer lines (Iliopoulos and others 2011). This is possible since secreted IL-6 from non-CSCs activates JAK1/STAT pathway, upregulating *OCT-4* gene expression, which is one of the key genes involved in pluripotency (Kim and others 2013).

As it has been exposed, IL-6 is a critical factor in the development of breast cancer metastasis; in this sense, this cytokine could be considered as a prognostic marker as well as a therapeutic target for this disease.

Interleukin-8

Another interleukin that has an important role in tumor proliferation, angiogenesis, and metastasis is IL-8, also known as CXCL8. This interleukin is expressed in humans, but not in mice; its receptors are CXCR1 (IL-8RA) and CXCR2 (IL-8RB), and is secreted by fibroblasts, tumor, stromal, and endothelial cells (Zlotnik and others 2006; Todorovic-Rakovic and Milovanovic 2013).

Overexpression of this cytokine has been recently considered a cancer prognostic marker, especially in breast cancer, because of the coexpression of IL-8, human epidermal growth factor receptor 2 (HER2), and the lack of expression of estrogen receptor (ER), are correlated with a worse prognosis (Fig. 1) (Todorovic-Rakovic and Milovanovic 2013). It has been found that both ER-negative human breast cancer tumors and breast cancer cell lines express higher levels of IL-8 compared with breast cancer cell lines positive for the hormone receptor. In this regard, higher levels of IL-8 were found in sera of patients with lymph node metastasis and/or ER^- and $HER2^+$ breast tumors (Ma and others 2017).

Originally, IL-8 was described as a chemoattractant for neutrophils that produced proangiogenic factors that enhanced tumor vascular neoformation and growth. Nowadays, it is known that IL-8 is *per se*, a proangiogenic factor with autocrine and paracrine functions. For instance, the stimulation with IL-8 of endothelial proliferation and capillary development *in vitro* model enhanced production of MMP-2 (Li and others 2005). Also, the stimulation with IL-8 in another *in vitro* cancer model leads to the increase of

VEGF and VEGF receptor expression (Martin and others 2009), suggesting that if this protein is present in breast cancer microenvirontment, it can contribute in the metastatic process of this cancer type.

IL-8 enhanced invasiveness of ER^- breast cancer cells, but not their proliferation (Freund and others 2003). This IL-8 feature can be related to late stages, in which the expression of ER is suppressed and the cancer invasiveness is increased. According to this observation, in an *in vitro* study, IL-8 did not increase cancer cell proliferation; however, the IL-8 treatment enhanced endothelial cell proliferation and survival (Li and others 2003) indicating that it can modulate the tumor microenvironment.

As mentioned before, IL-8 receptors are expressed in epithelial and tumor cells (Miller and others 1998; Murdoch and others 1999). In a report, all breast cancer samples expressed CXCR1 and CXCR2, but only a half of normal breast tissues expressed CXCR1 or CXCR2 (Miller and others 1998). Also, CXCR1 expression is higher in breast CSCs (Sheridan and others 2006), and *in vitro* assays using antibodies anti-CXCR1, induced apoptosis (Ginestier and others 2010). Thus, the 3 most important features related to cancer metastasis, namely tumor vascularization, migration, and invasion are characteristics promoted directly by IL-8. As we have reviewed in this section, vascularization, migration, invasion, and metastasis are promoted by IL-8. In fact, its expression is closely related to metastasis in breast cancer patients, whereby, its molecular mechanisms should be deeply studied in the near future.

Interleukin-10

IL-10 is an immunoregulatory cytokine that inhibits the activity of proinflammatory helper T subsets, cytotoxic T cells, macrophages, and NK cells. This immune regulation can influx immune response toward a more permissive microenvironment but can also reduce the tissue damage associated to inflammation (Couper and others 2018).

This cytokine plays a fundamental role within the tumor microenvironment, but its role regarding the metastatic process particularly in breast cancer remains unclear. In the 90's, Kundu and collaborators transfected murine mammary tumor cell lines to stably express IL-10 and found that not only the transfected cells grew more slowly than the parental ones, but also the metastasis was almost abolished (Kundu and others 1996). Later, another group reported similar results in a melanoma model, finding that IL-10 diminished neovascularization of the tumors and decreased MMP-9 expression, thus inhibiting the metastatic dissemination (Huang and others 1999).

More recently, human cohort studies have reported dissimilar results regarding IL-10 role in metastasis. One group, focusing in invasive ductal carcinoma, found that higher IL-10 expression within the tumor was associated with lower risk of distant metastasis (Li and others 2014), whereas another group, focused in inflammatory breast cancer, reported that IL-10 stimulates carboxypeptidase B2 expression, which in turn is positively correlated with lymphovascular invasion (Mohamed and others 2018). The later result seems to be in agreement with Woo's report of higher IL-10 expression in sentinel lymph nodes of breast cancer patients (Woo and others 2007), but still, it is not clear whether IL-10 directly plays a role in cancer cell's lymphatic dissemination.

Interleukin-17

The cytokine IL-17 is a proinflammatory cytokine that is secreted primarily by Th17 cells, but it can also be produced by $CD8^+$ T cells, γδ T cells, natural killer T (NKT), and lymph tissue inducer cells (LTi) (Ma and others 2014). IL-17A binds to and signals through IL-17 receptor A (IL-17RA), which is ubiquitously expressed in hematopoietic tissues, various myeloid cells, epithelial cells, fibroblasts, and endothelial cells. The linkage of IL-17A to its receptor induces the release of proinflammatory cytokines, chemokines, and MMPs that positively feedback the inflammatory cascade.

IL-17A has been found increased in many types of human cancers and murine models of tumors; however, its role in tumor development is controversial. Some studies have found antitumoral effects, whereas some others associate this cytokine to protumoral functions. Given the controversial results, several researchers agree that the effects of IL-17A depend on the context and the anatomical site where the tumor develops.

Some research groups have studied the role of IL-17A in invasive breast tumor pathogenesis. In this sense, it has been demonstrated mainly that IL-17A comes from different cell lines and exerts protumoral actions. For example, in a model of mammary tumors in mice, it was observed that IL-17A expression from γδ T cells, results in G-CSF-dependent expansion and polarization of neutrophils, suppressing cytotoxic T lymphocytes, which limit the establishment of metastasis (Coffelt and others 2015). Macrophages have also been identified as a major cellular source of IL-17 in breast tumors and have been shown to directly promote breast cancer cell invasion *in vitro* (Zhu and others 2008).

The ability of IL-17A to favor breast cancer metastasis may be related to the fact that this cytokine can also induce IL-6 and the chemokine (C-C motif) ligand 20 (CCL20) production in metastatic tumor cells, favoring the recruitment and differentiation of Th17 cells (Benevides and others 2015). On the other hand, IL-17A has the ability to modify the gene-expression profile and the behavior of nonmetastatic tumor cells, causing tumor growth *in vivo*. The molecular mechanisms by which IL-17A induces the secretion of prometastatic factors have not been fully described. However, it is probable that they occur in a mitogen-activated protein kinase (MAPK) pathway-dependent manner, since it has been observed that recombinant IL-17A upregulates ERK1/2 in human breast cancer cell lines (Fig. 1). Thereby, IL-17A promotes proliferation and resistance to conventional chemotherapeutic agents such as docetaxel (Cochaud and others 2013). Other possible mechanism might be related to the apoptotic pathways, as it has been observed that IL-17A suppresses apoptosis of several tumor cell lines *in vitro* (Nam and others 2008). Consistent with this result, a knockdown of the IL-17 receptor in 4T1 mouse mammary cancer cells enhanced apoptosis and decreased tumor growth *in vivo*.

Several studies have confirmed that the neutralization of IL-17A in breast cancer reduces the development of metastasis. Coffelt and others (2015) observed that the neutralization of IL-17A in the absence of γδ T cells prevents

neutrophil accumulation and downregulates the T cell-suppressive phenotype of neutrophils. On the other hand, Roy and cols. demonstrated that breast cancer-associated secondary metastasis is significantly increased in proarthritic and arthritic conditions, and that blocking the IL-17A and cyclooxygenase-2 (COX-2) pathways may significantly reduce the rate of metastasis (Roy and others 2009). Finally, in 2 immune competent arthritic mouse models, in which the animals develop spontaneous breast cancer-associated bone and lung metastasis, it was observed that the systemic neutralization of IL-17A can block the C-X-C chemokine receptor type 4 (CXCR4)/stromal cell-derived factor (SDF)-1 signaling pathway. This phenomenon occurs as a result of the reduction of the expression of SDF-1 in the metastatic niches (Roy and others 2014).

More research is necessary to delve into the molecular mechanisms that allow IL-17A to be a factor that favors metastasis, since with the evidences exposed in the previous paragraphs suggest that the IL-17A axis represents an attractive target of potential prognostic or have a therapeutic value.

Interleukin-19, Interleukin-20, Interleukin-22, Interleukin-25, Interleukin-30, and Interleukin 17B

There are other cytokines that have been related to the process of metastasis in breast cancer as shown in Fig 1.

IL-19 is part of the IL-10 family, expressed in different types of tumor cells. In breast cancer, it has been expressed in advanced stages of the tumor, and it has also been observed to be involved in an increase in mitosis and in a significant increase in metastasis, which leads to a worse prognosis (Hsing and others 2012; Chen and others 2013). IL-19 is able to upregulate CXCR4, MMP-2, MMP-9, TGF-β, IL-1β, and IL-6, all factors that induce the migration of breast cancer cells (e.g., Hs578T and 4T1), and it has been involved in breast tumor metastastasis. Hsing and others (2012), have shown that overexpression of IL-19 in 67NR cells (which usually have low endogenous IL-19 levels), and also in MCF-7 cells, stimulates their proliferation and migration, enabling them to form larger tumors and metastastic micronodules in the lung.

Another cytokine that has been related to metastasis in breast cancer is IL-20. *In vitro,* treatment with IL-20 upregulates MMP-9, MMP-12, cathepsin K, and cathepsin G, thus enhancing proliferation and migration of breast cancer cells. Interestingly, IL-20 is highly expressed in breast cancer bone metastasis (Hsu and others 2012).

IL-22, which belongs to the family of IL-10, has also been shown to be overexpressed in breast cancer. This cytokine is secreted by $CD4^+$ effector T cells, such as TH1, TH17, TH22, and innate lymphoid cells (Lanfranca and others 2016). Both pro- and antitumor roles have been reported for this cytokine (Kim and others 2014). However, it has recently been shown that overregulation of IL-22 is associated with a worse prognosis in patients with breast cancer since it correlates with the expression of HER-2 in invasive ductal carcinomas (Zhang and Liu 2017). Additionally, the upregulation of this cytokine in parallel with the overexpression of a long noncoding RNA seems to favor growth, migration, and invasion through the PI3K/AKT signaling pathway in breast cancer patients (Riu and others 2017). More studies are needed on the role of IL-22 in the tumor microenvironment, however, it is proposed as a cytokine whose deregulation can function as cancer immunotherapy (Markota and others 2018).

Regarding IL-25 (also called IL-17E), the inhibition of its expression in an aggressive spontaneous breast tumor model (MMTV-PyMT), reduced the metastasis to the lung (Jiang and others 2017). However, other studies, in tumor-associated fibroblasts in a breast cancer model induced by transformed 4T1 cell injection, authors showed that the activity of IL-25 induced by a phytochemical (Q2-3) can provide antitumorigenic activities (Yin and others 2016).

Interleukin-30 (IL-30) is commonly expressed in breast cancer specimens; it has been associated with recurrence and with advanced stages of the disease. *In vitro* studies showed that IL-30 contributes to the overexpression of a pro-oncogenic program and in triple negative breast cancer cells, triggers a program of proliferation, invasive migration, and inflammation (Airoldi and others 2016).

Finally, another cytokine, named IL-17B promotes breast cancer cell migration (Molloy and others 2009; Goldstein and others 2010; De Luca and others 2012). Mesenchymal stem cells (MSCs) produce factors such as VEGF and IL-6 that, in addition to promoting angiogenesis, induce breast cancer cell migration and invasion, (Beckermann and others 2008; De Luca and others 2011, 2012). VEGF stimulates the invasion of breast cancer cells by activating MAPK and PI3K/AKT signaling (Price and others 2001).

Tumor Necrosis Factor Alpha

The TNF-α is a multifunctional proinflammatory cytokine that regulates different processes, such as inflammation, cellular apoptosis, coagulation, metabolism, tumor growth, and invasion, and also has vascular functions (Ji and others 2014). TNF-α plays an important role on the innate inflammatory responses by promoting the expression of cytokines, chemokines, adhesion, extravasation, attraction, and activation of the leukocytes at the site of the infection (Varfolomeev and Ashkenazi 2004). TNF-α induces its cellular effects by signaling through 2 receptors: TNFR1 (p55 or CD120a) that binds the soluble ligand and TNFR2 (p75 or CD120b), which binds mainly to the transmembrane form [5]. Both receptors have been found in hematopoietic cells, but TNFR1 has a wider distribution than TNFR2. In general, TNF-α may activate intracellular pathways leading to 2 different responses: cell survival, proliferation, and gene transcription or cell death. TNF-α is a two-edged sword molecule to tumors. It can induce tumor apoptosis (Donato 2004), but it can also induce tumor development (Balkwill 2006). As for cancer, TNF-α promotes breast tumor cell invasion as evidenced by *in vitro* experiments, upregulating several genes that are associated with proliferation, invasion, and metastasis. In this work, coculture of MCF-7 breast cancer cells with macrophages increases MCF-7 invasiveness. Microarray analysis of these cells demonstrated the enhanced expression of 39 genes, including *MMP-9* and 13–related to Type III EMT; CD44–a marker of BCSC's; and CXCR-4 and its ligand CXCL-12–involved in tumor migration. Interestingly, KiSS1–a protein identified as a tumor suppressor was downregulated after TNF-α treatment (Yin and others 2009).

In addition, it has been shown that exposure of tumor cells to TGF-β and TNF-α induce Type III EMT, generating

a BCSC phenotype characterized by the downregulation of claudins 3, 4, and 7 and cytokeratin 18 (Asiedu 2011). TNF and TNFR1 may be involved in type III EMT and metastasis, by the activation of the PI3K/AKT signaling pathway by 2 signaling cascades: (1) the activation of the Ras/Raf/MEK1/ERK pathway; in which Ras may also directly activate PI3K, allowing the activation of AKT and increased expression of the NF-kB p65 subunit (Downward 2003); and (2) by inducing GSK-3β ubiquitination and degradation, which in turn, impairs Snail degradation, inducing the phosphorylation of AKT (Wang and others 2013). In both cases, the final target is the stabilization of the Type III EMT-related transcription factor, Snail.

Finally, TNF-α-TNFR1-activated inflammatory macrophages produce high levels of VEGF-C to coordinately activate VEGFR3. TNF-α-stimulated lymphangiogenesis was completely abrogated in *Tnfr1*$^{-/-}$ mice (Ji and others 2014). Even when there is no described evidence for breast cancer metastasis; it may be an important factor during the inital steps of tumor cell migration.

Growth Factors Involved in Metastasis

Colony-stimulating factor 1

It has been shown that colony-stimulating factor 1 (CSF-1) in breast tumors could mediate the recruitment of macrophages (Lin and others 2001). Interestingly, the proto-oncogene c-fos is the only gene that encodes to the only known CSF-1 receptor, (CSF-1R) (Sherr and others 1985; Dai and others 2002). Moreover, in neoplastic epithelial breast cancer cells, the expression of CSF-1 and its receptor correlated well with a poor prognosis, and it is predictive of ipsilateral recurrence (Scholl and others 1994; Maher and others 1998; Kluger and others 2004). CSF-1 promotes metastasis, stimulates angiogenesis, and participates in a paracrine loop with EGF to spur tumor cell invasion in mouse models (Lin and others 2001; Aharinejad and others 2002, 2004; Wyckoff and others 2004). Furthermore, it has been consistenly found that breast cancer cell lines express CSF-1 and CSF-1R, which sustains the proliferation of breast cancer cells (SK-BR-3 and MDA-MB-468) through ERK1/2 activation, stimulating c-Jun and upregulating c-myc and cyclin D1.

With the given background, we conclude that the role of the CSF-1R/CSF-1 system in breast cancer metastais is complex and requires further investigation as a therapeutic target.

Tumor Growth Factor Beta

The human TGF-β is a highly conserved superfamily of cytokines that are involved in controling the mammal development, a fact that may explain why their dysregulation has a close relation with tumorigenesis (Massague 2008).

TGF-β regulates innate and adaptative immune cell functions, and it is known that, depending on the tumor microenvironment, and thereby tumor stage, it performs suppressor or protumoral functions (Chen and Ten Dijke 2016). On the one hand, in early tumor development, TGF-β suppresses cell proliferation even when is mediated by ERα (Ewan and others 2005). Meanwhile, in late stages owing to abnormalities on TGF-β signaling, the cells lose their sensibility to antiproliferative signals. This event, along with the TGF-β ability to induce Type III EMT, leads to progression and dissemination of breast cancer (Wendt and others 2009; Esquivel-Velázquez and others 2015).

All members of TGF-β superfamily share structurally related membrane receptors type I (TRβI), type II (TRβII), and type III (TRβIII). These receptors transduce principally through Smad intracellular proteins, and by noncanonical signaling pathways (Massague 2008; Imamura and others 2012; Zarzynska 2014). In breast tissue, TRβI and TRβII are normally expressed, but this expression is decreased during carcinoma *in situ*, and increased in invasive carcinoma. This may be due to the initial losing of TGF-β sensibility signals in early tumor stages, and the turnover in advanced stages, associated with Type III EMT induction and metastasis (Hachim and others 2016).

With regard to the TGF-β role in metastasis, this cytokine supports tumor cell release and organ colonization. The releasing of tumor cells is mainly promoted by Type III EMT induction and its effects of adherent and tight junction gene downregulation such as (*E-Cadherine*, *CDH1*), the upregulation of motility genes' expression and the loss polarity in epithelial cells, thus promoting a mesenchymal invasive phenotype (Wendt and others 2009). Besides, TGF-β and the invasive potential of breast cancer cell lines, correlates with junctional adhesion molecule-A (JAM-A) decreased expression (Naik and others 2008), associated with TGF-β/Smad and TGF-β/p54 JNK pathways, promoting breast cancer cell release and further invasion (Wang and Lui 2012).

TGF-β has a main role in tumor progression when cells arrive to a metastatic niche. Despite the original conception that colonizing cancer cells retain their mesenchymal state in metastasis sites after Type III EMT, clinical evidence shows that cells undergo a mesenchymal-to-epithelial (MET)-type regression, revealed by the presence of tumor cells with epithelial morphology in metastatic sites (Thiery 2002; Tarin 2005). This EMT–MET change may be helpful in the colonization process, when cells proliferate in the metastatic tumor site (Stankic and others 2013). TGF-β induced MET mediated by *Id1* gene in lung colonization breast cancer cells, but only in the ones that first underwent Type III EMT, a feature that might enhance local settlement (Yang and others 2008).

In a low-oxygen-level condition, MSCs produce cytokines and growth factors, such as TGF-β1, TGF-β2, and TGF-β3, which enhance proliferation and invasiveness of breast cancer cells (Hung and others 2012a, 2012b). TGF-β in a hypoxic microenvironment (through HIF-1α) regulates different gene expressions (*CTGF*, *OPN*, *MMP-1*, *IL-6*, and *IL-8*) to promote bone metastasis and increases VEGF and CXCR4 expression (Dunn and others 2009). Also, in spheroid assays, TGF-β promotes the invasiveness in MCF-10A1 (M1) (noncarcinogenic epithelial cells) and M1-derived MCF-10AneoT (M2) (RAS-transformed cells) (Naber and others 2011).

Meanwhile, in bone metastasis, TGF-β is released from bone matrix by osteoclastic activity, promoted by cancer cells, and in turn, this TGF-β stimulates the release of osteoclastic cytokines by tumor cells, forming a loop of bone matrix degradation (Kingsley and others 2007).

Therefore, either by eliciting Type III EMT–MET of cancer cells, by enhancing angiogenesis, or by its immunosuppressive effects, TGF-β is a crucial cytokine involved

not only in tumor development and proliferation, but also in cell release, migration, and survival in metastasic sites.

Vascular Endothelial Growth Factor

In breast cancer, a key regulator in the metastasis is VEGF, which has been related to the neovascularization process, one of the first steps for metastasis. VEGF is a glycoprotein, member of the platelet-derived growth factor family (Ferrara and Davis-Smyth 1997). There are several subtypes of VEGF (VEGF A-F), all of them related to angiogenesis (Shibuya 2011). VEGFs exert their angiogenic functions throughout the binding of their specific tyrosine kinase receptors VEGFR-1 (Flt-1), VEGFR-2 (Flk-1/KDR), and VEGFR-3 (Flt-4), which are mainly expressed in endothelial cells (Ferrara and Davis-Smyth 1997). It has been described that the angiogenesis, lymphangiogenesis, migration, and invasion processes in breast cancer are mainly driven by VEGF-A and VEGFR-C (Mandriota and others 2001; Alitalo and Carmeliet 2002). In this sense, it was observed that VEGFR-3 and their ligands, VEGF-C, are overexpressed in human aggressive breast cancer tumor tissues, and their coexpression correlates with poor prognosis (Su and others 2006). Furthermore, the expression of VEGF-C in plasma has been correlated with the expression of HER2-positive breast cancer patients (Yang and others 2002; Hoar and others 2003). In addition, elevated plasma concentrations of VEGF-A have also been found in hormonal positive breast cancer patients that are in remission, and with metastatic disease instead of in patients with local tumors. On the other hand, an interesting interaction between VEGF and chemokine receptors has been described. VEGF throughout the binding of a nonclassical receptor that lacks canonical signaling sites, neuropilin-1 (NRP-1), activates invasion and migration actions in breast cancer. This ligand–receptor interaction has also been linked to the protein upregulation of chemokine receptor CXCR4 and its ligand, SDF-1, driving the migration of breast cancer cells to secondary sites (Bachelder and others 2002).

The coexpression of VEGF/NRP-1 was found in a large number of mammary tumors and they were associated positively with lymph node metastasis. This interaction was associated with the enhancement of the Type III EMT process and the modulation of the transcription factor NF-κB, β-catenin, and glycogen synthase kinase-3 (GSK-3β) signaling. It is worth mentioning that the knockdown of both proteins (VEGF/NRP-1) induced apoptosis and the re-expression of adhesion proteins such as E-cadherin in aggressive breast cancer cells. Additionally, this knockdown inhibited the development of liver metastatic nodules in a mice model (Luo and others 2016). Thus, VEGF/NRP-1 axis may be a valuable target for the design of antimetastatic therapies in breast cancer.

Another biointeraction that favors the metastasis in breast cancer is the interplay between tumor suppressor genes and VEGF modulation. Recently, loss of expression of p16 gene suppressor was reported in human primary breast carcinomas (Silva and others 2003). This protein is important because it can downregulate *VEGF* gene and protein expression, resulting in the suppression of angiogenesis and metastasis in breast cancer. The pathway by which this suppressor gene acts in breast cancer cells is through the change of localization from nuclear to cytoplasm of HIF-1α, preventing the transactivation of VEGF promoter (Zhang and others 2007). Thus, the reactivation of the p16 activity will be an innovative approach to counteract the metastasis in breast cancer.

HIF-1α is a transcription factor that controls the expression of VEGF (Krock and others 2011). In this sense, a specific drug known as 2-benzoyl-3-phenyl-6,7-dichloroquinoxaline 1,4-dioxide (DCQ) that reduces the low oxygen microenvironment was able to block the metastatic process in breast cancer cell lines through the inhibition of 2 target genes of HIF-1α implicated in angiogenesis and Type III EMT, *VEGF*, and *TWIST*, respectively (Ghattass and others 2014). These findings open the possibility for the search of new drugs that not only inhibit proteins involved in the metastasis process, but also drugs that counteract the tumor microenvironment.

Notch pathway has been related to multiple processes such as cell–cell communication, cell differentiation, and angiogenesis through VEGF (Kofler and others 2011; Benedito and others 2012; Garcia and Kandel 2012; Hernandez and others 2013). Besides, aberrant Notch pathway activity is involved in breast cancer progression (Reedijk 2012). Interestingly, a feedback between VEGF and one ligand of Notch pathway, delta-like 4 ligand (ΔII4), has been described. In this sense, VEGF can increase the expression of ΔII4. This protein can also be stimulated by hypoxic conditions and in this way it can stimulate at the same time the VEGF expression (Patel and others 2005). However, little is known about this feedback regulation in breast cancer, leaving the possibility of new research to inhibit both pathways.

A close relationship between VEGF expression and MMP-9 was found in breast cancer tumors (Dore-Savard and others 2016), highlighting their interaction to promote tumor metastasis. Furthermore, this detailed work found the presence of 23 cytokines related with angiogenic/metastatic processes in the tumor interstitial fluid of breast cancer xenografts termed as ''angiogenic secretome,'' proposing the collection of this fluid instead of plasma from patients with aggressive cancers with the aim to design effective personalized treatments (Dore-Savard and others 2016).

Moreover, it has been described as a ''metastatic signature'' driven by VEGF in a human orthotopic model of ER-positive and -negative breast cancer cells (Pathak and others 2013). VEGF has a narrow interaction in the extracellular matrix remodeling, driving the metastasis toward the lung and lymph nodes mediated by its participation as activator of fibrin degradation and promoter of extracellular proteolysis (Pathak and others 2013). VEGF also was able to increase breast cancer cell invasion mediated by its association with MMPs, and by the activation of MAPK and PI3K pathways with the consequent activation of the proto-oncogene c-Fos (Miralem and others 2001; Chen and others 2017a). In relation to the works mentioned above, it is clear that not only VEGF is responsible for the ''metastatic phenotype,'' but there are also several targets that need to be taken into account to improve the therapies and even predict the ability of tumors to have metastasis.

Also, in ER- and HER2-negative breast cancer, it has been described that a group of cytokines, such as VEGF-A and VEGF-C, forms a paracrine loop to promote metastasis in breast cancer (Lee and others 2014a, 2014b). A more recent work complemented this information in different

breast cancer tumor sample subtypes. This work described a blend of prometastatic factors, where VEGF ligands and its receptors are involved (VEGF-A, VEGF-C, VEGFR-2, VEGFR-3, NRP-1, and NRP-2) (Fertig and others 2015). The overall conclusion of this research is that VEGF-A and VEGF-C mRNA are overexpressed in both ER/HER2-negative and HER2-positive breast cancer more than ER-positive subtype (Fertig and others 2015). This is partly because there is a crosstalk between EGFR and angiogenesis signaling in breast cancer (Alameddine and others 2013).

Broadening the previous crosstalk, heregulin-1β (HRG-1β), a ligand of the EGFR family, upregulates the VEGF-C gene and protein expression throughout the p38 MAPK and NF-κB signaling pathways in human breast cancer cells (Xiong and others 2001; Tsai and others 2003). Additionally, HRG-1β has also been shown to upregulate the expression of VEGF-A in breast cancer cells, inducing the neovascularization process (Yen and others 2000). Overall, this protein modulation panel is involved in lymphangiogenesis, metastasis, and drug resistance, pointing out NF-κB as an important therapeutic target in this pathology (Godwin and others 2013). On the other hand, the alterations in HRG-1β expression, impact on the invasive and metastatic process in breast cancer, since this protein has shown to regulate the expression of proteins implicated in Type III EMT, such as MMP-9 (Yao and others 2001). In summary, the cooperation between EGFR family ligands and VEGF signaling confers an enhanced metastatic potential (Fig. 2), which eventually may result in a poor prognostic condition in breast cancer patients.

The overexpression of SIX1, a transcription factor, has been associated with lymph node positivity and poor prognosis in breast cancer (Iwanaga and others 2012). Moreover, this protein is involved in the regulation of multiple protumorigenic genes (Yu and others 2006; McCoy and others 2009; Micalizzi and others 2009). In fact, its expression has been closely related to later stages of breast cancer metastasis through the upregulation of TGF-β signaling (Micalizzi and others 2010). In this sense, the promoting activity of SIX1 upon VEGF-C/VEGR3 lymphangiogenesis and lymphatic metastasis actions has been demonstrated (Wang and others 2012). SIX1 could become a diagnostic protein for breast cancer patients as a preventive metastatic process.

In addition, another transcription factor, STAT3, has been correlated with VEGF-C, VEGF-D, and VEGFR-3 expression in lymph node metastasis in breast cancer tissues. Thereby, this suggests that STAT3 may be an important molecular marker for predicting metastasis to axillary lymph nodes in breast cancer, which is associated also with cancer recurrence and poor prognosis (Chen and others 2017b). Moreover, a clear interaction among STAT-3/VEGF-C/VEGFR-3 expressions was established with lymphangiogenesis, whereas STAT-3/

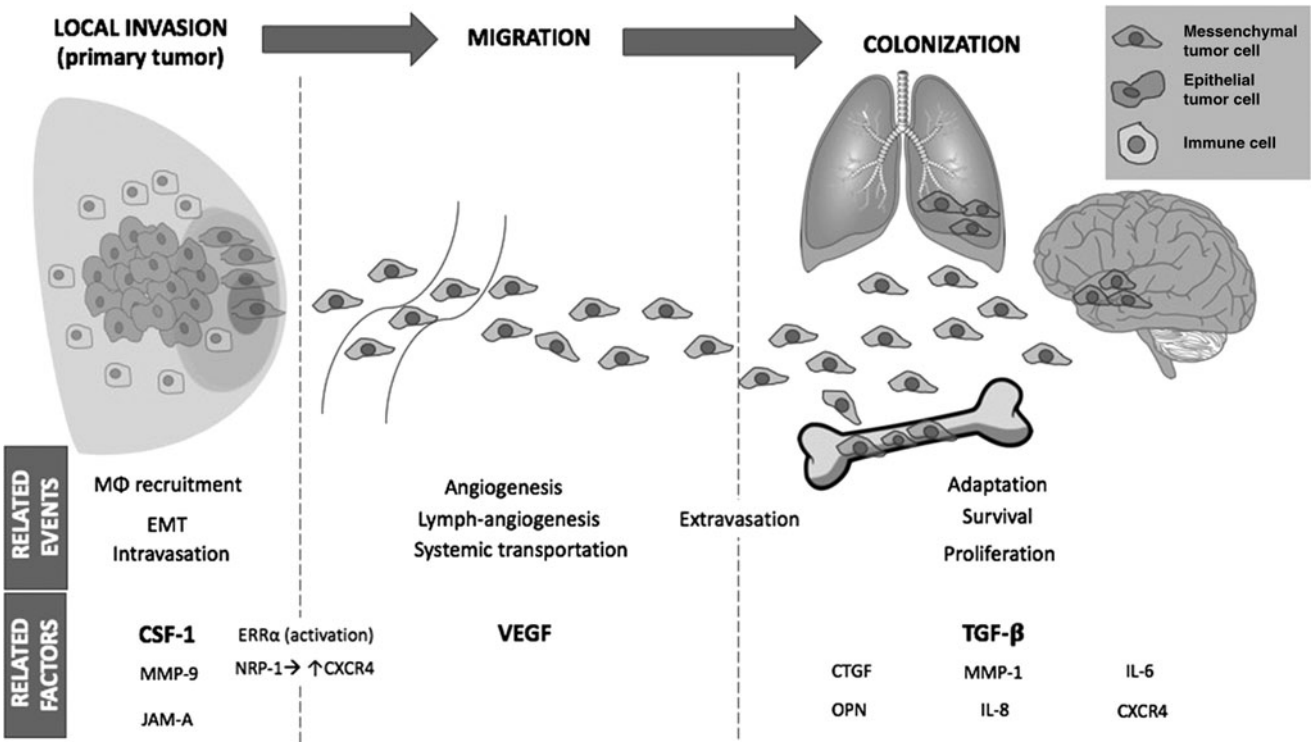

FIG. 2. Growth factors involved in the development of breast cancer metastasis. The figure shows how VEGF, CSF-1, and TGF-β regulate different signaling pathways that contribute to the development of breast cancer cell metastasis. This process is evolving starting from epithelial tumor cells in the breast tumor (primary tumor), the Type III EMT and the intravastion, extravasation, and colonization of other organs as mesenchymal tumor cells. VEGF, vascular endothelial growth factor; CSF-1, colony-stimulating factor 1; TGF-βR, transforming growth factor beta receptor; MØ, macrophage; ERK, extracellular signal-regulated kinase; MAPK, mitogen-activated protein kinase; PI3K, phosphatidylinositol-4,5-bisphosphate 3-kinase; NRP-1, neuropilin 1; NFkB, nuclear factor kappa-light-chain-enhancer of activated B cells; HIF1α, hypoxia-inducible factor 1 alpha subunit; GSK-3β, glycogen synthase kinase 3 Beta; III EMT, type III epithelial–mesenchymal transition; CTGF, connective tissue growth factor; OPN, osteopontin; ERRα, estrogen-related receptor alpha; CXCR4, C-X-C Motif Chemokine Receptor 4; JAM-A, junctional adhesion molecule-A; JNK, c-Jun N-terminal kinase.

Table 1. Role of Cytokines in Breast Cancer Metastasis

Cytokine	*Effects upon breast cancer metastasis*	*Reference*
IL-1α, IL-1β	Induction of MMP-1 and MMP-9 expression	
	Contribution to the secretion of proinflammatory cytokines such as TNF-α, IL-8, and IL-6	(Rutter and others 1997) (Wang and others 2005)
	Favoring the EMT	(Soria and others 2011)
	Expression of other protumorigenic cytokines such as IL-6 and IL-8	(Pantschenko and others 2003) (Nozaki and others 2000) (Sheridan and others 2006)
IL-4	Promotion of TAMS and favoring their M2 phenotype	
	Induction of growth factor receptors such as EGFR	(DeNardo and others 2009)
	Activation of proliferation and survival pathways, Erk1/2, Akt, and STAT6, and promotion of lung metastasis	(Venmar and others 2014) (Hallett and others 2012)
	Alteration of cell glucose and glutamine metabolism	(Venmar and others 2015)
IL-6	Induction of Th17 phenotype	
	Activation of STAT3 pathway–apoptosis evasion through activation of antiapoptotic genes	(Dethlefsen and others 2013) (Banerjee and Resat 2016)
	Induction of VEGF and MMPs–sustained angiogenesis	(Castellana and others 2015)
	Promotion of EMT	(Huang and others 2011)
	Support of CSC phenotype	(Sullivan and others 2009)
	Induction of pluripotency	(Iliopoulos and others 2011) (Kim and others 2013)
IL-8	Related with lymph node metastasis	
	Neutrophil recruitment toward the tumor	(Ma and others 2017)
	Stimulation of endothelial proliferation (VEGF and VEGFR)	(Li and others 2005)
	Induction of MMP-2	(Martin and others 2009)
	Association with loss of ER expression	(Freund and others 2003)
	Potentiation of cancer stem cell phenotype through activation of its receptors	(Ginestier and others 2010)
IL-17A	Modulation of infiltrating immune population–Neutrophil	
	polarization and infiltration into the tumors and suppression of TCD8+ lymphocytes	(Coffelt and others 2015) (Zhu and others 2008)
	Induction of MMPs	(Benevides and others 2015)
	Neutrophil polarization and infiltration into the tumors	(Cochaud and others 2013)
	Promotion of cell invasion	(Roy and others 2014)
	Induction of IL-6 expression and recruitment of Th17 toward tumor	
	Activation of MAPK pathway related with therapy resistance	
	Association with lung metastasis	
IL-19	Induction of cell migration by interaction with CXCR4, MMP-2, MMP-9, TGF-β, IL-1β, and IL-6	(Chen and others 2013) (Hsing and others 2012)
IL-20	Upregulation of MM-9 and MMP-12 activity	
	Enhancement of cell proliferation and migration through cathepsin K, and cathepsin G	(Hsu and others 2012)
IL-25/ IL17E	Promotion of BCLM	
	Participates in antitumorogenic activities	(Jiang and others 2017) (Yin and others 2016)
IL-30	Promotion of pro-oncogenic factors	(Airoldi and others 2016)
MCP-1/ CCL2	Promotion of cell migration	
	Interaction with VEGR, MAPK, and PI3K signaling pathways	(Molloy and others 2009) (Goldstein and others 2010) (De Luca and others 2012) (Price and others 2001)
CSF-1	Macrophage recruitment	
	Favors the angiogenic process	(Lin and others 2001)
	Interaction with growth factors such as EGFR	(Aharinejad and others 2002) (Aharinejad and others 2004) (Wyckoff and others 2004)
TNF-α	Promotion of inflammatory microenvironment	
	Upregulation of proliferation, invasion, and metastasis process	(Varfolomeev and Ashkenazi 2004)
	Increase the expression of oncogenes, such as MMPs, IL-8, CXCR, VEGF, and MCP-1 Activation of several pathways such as NF-κB, PI3K/AKT, Ras/Raf/MEK1/ERK, GSK-3β	(Yin and others 2009) (Baumgarten and Frasor 2012) (Zhu and others 2014)
	Stabilization of EMT process through Snail protein	(Tanaka and others 2014)

(*continued*)

Table 1. (Continued)

Cytokine	*Effects upon breast cancer metastasis*	*Reference*
		(Downward 2003)
		(Wang and others 2013)
TGF-β	Associated in late stages of breast cancer	
	Promotion of EMT	(Esquivel-Velázquez and others 2015)
	Increase in the mamosphere formation	
	Association with HER2	(Wendt and others 2009)
	Enhances cancer invasiveness	(Mani and others 2008)
	Allows the BCBoM and the expression of prometastasic factors such as VEGF and CXCR4	(Gupta and Srivastava 2014) (Hung and others 2012a, 2012b)
	Inhibition of adhesion proteins such as JAM-A through activation of Smad and JNK pathways	(Dunn and others, 2009) (Arteaga and others 1988)
	Organ colonization support through deregulation of E-cadherine	(Koli and Arteaga 1997)
	Increase of lung metastasis	(Naik and others 2008)
	Osteoclastic cytokines and bone matrix degradation	(Wang and Lui 2012) (Wendt and others 2009) (Yang and others 2008) (Kingsley and others 2007) (Donovan and others 1997)
VEGF	Induction of HER2	
	Upregulation of CXCR4 and SDF-1 signaling	(Hoar and others 2003)
	Maintenance of EMT	(Yang and others 2002)
	Activation of NF-κB, β-catenin, GSK-3β, Notch, PI3K, and MAPK signaling pathways	(Bachelder and others 2002) (Luo and others 2016)
	Downregulation of tumor suppressor genes such as p16	(Zhang and others 2007)
	Induction of MMP-9	(Patel and others 2005)
	Activation of proto-oncogenes such as c-fos	(Dore-Savard and others 2016)
	Overexpression of transcription factors such SIX1 and STAT3	(Chen and others 2017a)
	Interaction with other cytokines such as IL-8	(Miralem and others 2001)
	Promotion of BCBrM through other growth factors such as angiopoietin-2	(Wang and others 2012) (Bohn and others 2017)
	Promotion of BCBoM and recurrence through ERRα signaling	(Fradet and others 2011)
	Promotion of BCLiM–activation of MAPK and NF-κB	(Chen and others 2017a)
	Promotion of BCLuM through MAMs phenotype	(Tsai and others 2003) (Qian and others 2015)

BCBoM, breast cancer bone metastasis; BCBrM, breast cancer brain metastasis; BCLiM, breast cancer liver metastasis; BCLuM, breast lung metastasis; CAFs, cancer-associated fibroblasts; CSC, cancer stem cell phenotype; CXCR, chemokine receptors; CSF-1, colony-stimulating factor 1; MCP-1/CCL2, derived monocyte chemotactic protein-1; EMT, epithelial–mesenchymal transition; ERK1/2, extracellular signal-regulated protein kinases 1 and 2; GSK-3β, glycogen synthase kinase-3; HER2, human epidermal growth factor receptor 2; IL, interleukin; JAM-A, junctional adhesion molecule-A; MMP, metalloproteinase; MAMs, metastasis-associated macrophages; MAPK, mitogen-activated protein kinase; miR, microRNA; MCP-1, monocyte chemotactic protein 1; NF-κB, nuclear Factor-Kappa B; ERRα, orphan estrogen-related receptor alpha; PI3K, phosphatidylinositol 3-kinase; AKT, protein kinase B; STAT, signal transducer and activator of transcription; SDF-1, stromal-derived factor-1; TAMS, tumor-associated macrophages; TNF-α, tumor necrosis factor alpha; TGF-β, transforming growth factor beta; VEGF, vascular endothelial growth factor.

VEGF-D/VEGFR-2 expression was associated with carcinogenesis in breast cancer (Chen and others 2017b). The main cross of these pathways is that STAT3 can bind to one of the binding sites of VEGF, upregulating its expression (Niu and others 2002).

In addition, a coexpression of 2 growth factors, VEGF and angiopoietin-2, was related to breast cancer brain metastasis, development, and progression, in a mice model where hypoxic conditions are critical for the maintenance and stimulation of the secretion of angiogenic factors. Further works should be driven to determine if simultaneous blocking of these proteins can be effective to reduce breast cancer brain metastasis (Bohn and others 2017).

VEGF was also associated with breast cancer bone metastasis through the activation of the orphan estrogen-related receptor alpha (ERRα) (Fradet and others 2011). This protein is increased in breast cancer cells and it is associated with its recurrence (Ariazi and others 2002; Suzuki and others 2004). The mRNA expression of target genes of ERRα, such as VEGF, MMP-1, and MMP-13 was increased in breast cancer biopsies that contained elevated ERRα expression. Therefore, the mechanism by which ERRα favors bone metastasis processes is through the modulation of proteins involved in angiogenesis and invasion (Fradet and others 2011). This orphan receptor represents a novel guide for breast cancer treatment.

Regarding breast cancer liver metastasis, the main pathways suggested that govern this process are MAPK, NF-κB, and VEGF. This genetic network was clarified with different databases. Interestingly, these proteins are associated with distinct stages of breast cancer liver metastasis (Tsai and others 2003; Chen and others 2017a). The best molecular understanding of this condition is important because breast cancer liver metastasis is a disease that once detected, it only allows a short survival time (Adam and others 2006).

Recently, in a breast cancer lung metastasis mice model, an interesting relationship between VEGFR-1 and a population of metastasis-associated macrophages (MAMs) was

identified (Qian and others 2015). These cells have shown to stimulate tumor extravasation and they also sustained distal metastasis (Qian and others 2009). Moreover, MAMs express VEGR-1 in their surface, and it acts as a chemotactic molecule and vascular permeability enhancer. It was also associated with the inflammatory signaling through stimulation of a key regulator of macrophage lineage-specific growth, the CSF-1 (Murakami and others 2008; Qian and others 2015), which in turn stimulates the VEGF expression in macrophages (Curry and others 2008). Of note, VEGFR-1 expression in MAMs was extremely remarkable, whereas in lung resident macrophages this expression was not found. Significantly, VEGFR-1 ablation resulted in a decrease of breast cancer lung metastasis (Qian and others 2015). This angiogenic/immunological modulation invites to extend the cancer therapy options not only to breast cancer cells and VEGF signaling but also to their immune cell counterpart.

In Table 1, we sumarize the available information regarding the role of different cytokines involved in breast cancer metastatic process.

Concluding Remarks

Metastasis is the major cancer pathophysiology and there are a lot of interactions of different signaling pathways that lead to the possibility of developing specific therapeutic target drugs. To counteract breast cancer metastasis, in this study, we described different molecular targets that should be blocked together, with the aim to offer a promisig antimetastatic drug regardless of the expression of hormonal receptors. We also want to highlight that not only cancer cells must be taken into account but also the modification of the tumor microenvironment and the surrounding cell metabolism play a key role in attacking the metastatic breast cancer process and it would result in a better patient clinical outcome. In addition, the immune cells and cytokines are key factors whose modulation would be important as an adjuvant drug option in breast cancer metastasis.

Acknowledgments

Financial support: Grant IN208715 from Programa de Apoyo a Proyectos de Innovación Tecnológica, Dirección General de Asuntos del Personal Académico, Universidad Nacional Autónoma de México to J. Morales-Montor. Rocío Alejandra Ruìz-Manzano is a PhD student at Programa de Doctorado en Ciencias Biomédicas, Universidad Nacional Autónoma de México and received a fellowship from CONACyT. Margarita I Palacios-Arreola and Mariana Segovia-Mendoza, both are Postdoctoral fellows from Dirección General de Asuntos del Personal Académico (DGAPA), from Universidad Nacional Autónoma de México (UNAM), and receive a fellowship from DGAPA. Lucía Angélica Méndez-García is a CONACyT Postdoctoral fellow.

Author Disclosure Statement

Authors declare that no competing financial interests exist.

References

Adam R, Aloia T, Krissat J, Bralet MP, Paule B, Giacchetti S, Delvart V, Azoulay D, Bismuth H, Castaing D. 2006. Is liver resection justified for patients with hepatic metastases from breast cancer? Ann Surg 244(6):897–907; Discussion 907–908.

Aharinejad S, Abraham D, Paulus P, Abri H, Hofmann M, Grossschmidt K, Hofbauer R. 2002. Colony-stimulating factor-1 antisense treatment suppresses growth of human tumor xenografts in mice. Cancer Res 62(18):5317–5324.

Aharinejad S, Paulus P, Sioud M, Hofmann M, Zins K, Schäfer R, Abraham D. 2004. Colony-stimulating factor-1 blockade by antisense oligonucleotides and small interfering RNAs suppresses growth of human mammary tumor xenografts in mice. Cancer Res 64(15):5378–5384.

Airoldi I, Cocco C, Sorrentino C, Angelucci D, Di Meo S, Manzoli L, Esposito S, Ribatti D, Bertolotto M, Iezzi L, Natoli C, Di Carlo E. 2016. Interleukin-30 Promotes Breast Cancer Growth and Progression. Cancer Res 76(21):6218–6229.

Alameddine RS, Otrock ZK, Awada A, Shamseddine A. 2013. Crosstalk between HER2 signaling and angiogenesis in breast cancer: molecular basis, clinical applications and challenges. Curr Opin Oncol 25(3):313–324.

Alitalo K, Carmeliet P. 2002. Molecular mechanisms of lymphangiogenesis in health and disease. Cancer Cell 1(3):219–227.

Apte RN, Dotan S, Elkabets M, White MR, Reich E, Carmi Y, Voronov E. 2006. The involvement of IL-1 in tumorigenesis, tumor invasiveness, metastasis and tumor-host interactions. Cancer Metastasis Rev 25(3):387–408.

Ariazi EA, Clark GM, Mertz JE. 2002. Estrogen-related receptor alpha and estrogen-related receptor gamma associate with unfavorable and favorable biomarkers, respectively, in human breast cancer. Cancer Res 62(22):6510–6518.

Arteaga CL, Tandon AK, Von Hoff DD, Osborne CK. 1988. Transforming growth factor beta: potential autocrine growth inhibitor of estrogen receptor-negative human breast cancer cells. Cancer Res 48(14):3898–3904.

Asiedu MK, Ingle JN, Behrens MD, Radisky DC, Knutson KL. 2011. TGFβ/TNFα-mediated epithelial-mesenchymal transition generates breast cancer stem cells with a claudin-low phenotype. Cancer Res 71(13):4707–4719.

Baccelli I, Schneeweiss A, Riethdorf S, Stenzinger A, Schillert A, Vogel V, Klein C, Saini M, Bäuerle T, Wallwiener M, Holland-Letz T, Höfner T, Sprick M, Scharppf M, Marmé F, Sinn HP, Pantel K, Weichert W, Trumpp A. 2013. Identification of a population of blood circulating tumor cells from breast cancer patients that initiates metastasis in a xenograft assay. Nat Biotechnol 31(6):539–544.

Bachelder RE, Wendt MA, Mercurio AM. 2002. Vascular endothelial growth factor promotes breast carcinoma invasion in an autocrine manner by regulating the chemokine receptor CXCR4. Cancer Res 62(24):7203–7206.

Balkwill F. 2006. TNF-α in promotion and progression of cancer. Cancer Metastasis Rev 25(3):409–416.

Banerjee K, Resat H. 2016. Constitutive activation of STAT3 in breast cancer cells: a review. Int J Cancer 138(11):2570–2578.

Baumgarten SC, Frasor J. 2012. Minireview: inflammation: an instigator of more aggressive estrogen receptor (ER) positive breast cancers. Mol Endocrinol 26(3):360–371.

Beckermann BM, Kallifatidis G, Groth A, Frommhold D, Apel A, Mattern J, Herr I. 2008. VEGF expression by mesenchymal stem cells contributes to angiogenesis in pancreatic carcinoma. Br J Cancer 99(4):622–631.

Benedito R, Rocha SF, Woeste M, Zamykal M, Radtke F, Casanovas O, Duarte A, Pytowski B, Adams RH. 2012. Notch-dependent VEGFR3 upregulation allows angiogenesis

without VEGF-VEGFR2 signalling. Nature 484(7392):110–114.

Benevides L, da Fonseca DM, Donate PB, Tiezzi DG, De Carvalho DD, de Andrade JM, Martins GA, Sila JS. 2015. IL17 promotes mammary tumor progression by changing the behavior of tumor cells and eliciting tumorigenic neutrophils recruitment. Cancer Res 75(18):3788–3799.

Bohn KA, Adkins CE, Nounou MI, Lockman PR. 2017. Inhibition of VEGF and Angiopoietin-2 to reduce brain metastases of breast cancer burden. Front Pharmacol 8:193.

Calon A, Tauriello DVF, Batlle E. 2014. TGF-beta in CAF-mediated tumor growth and metastasis. Semin Cancer Biol 25:15–22.

Castellana B, Aasen T, Moreno-Bueno G, Dunn SE, Ramón y Cajal S. 2015. Interplay between YB-1 and IL-6 promotes the metastatic phenotype in breast cancer cells. Oncotarget 6(35): 38239–38256.

Chang JC. 2016. Cancer stem cells: role in tumor growth, recurrence, metastasis, and treatment resistance. Medicine 95(1 Suppl 1):S20–S25.

Chen W, ten Dijke P. 2016. Immunoregulation by members of the TGFβ superfamily. Nat Rev Immunol 16:723–740.

Chen X, Zheng Z, Chen L, Zheng H. 2017a. MAPK, NFkappaB, and VEGF signaling pathways regulate breast cancer liver metastasis. Oncotarget 8(60):101452–101460.

Chen Y, Liu Y, Wang Y, Li W, Wang X, Liu X, Ouyang C, Wang J. 2017b. Quantification of STAT3 and VEGF expression for molecular diagnosis of lymph node metastasis in breast cancer. Medicine (Baltimore) 96(45):e8488.

Chen YY, Li CF, Yeh CH, Chang MS, Hsing CH. 2013. Interleukin-19 in Breast Cancer. Clin Dev Immunol 2013: 294320.

Cochaud S, Giustiniani J, Thomas C, Laprevotte E, Garbar C, Savoye, AM, Curé H, Mascaux C, Alberici G, Bonnefoy N, Eliaou JF, Bensussan A, Bastid J. 2013. IL-17A is produced by breast cancer TILs and promotes chemoresistance and proliferation through ERK1/2. Sci Rep 3:3456.

Coffelt SB, Kersten K, Doornebal CW, Weiden J, Vrijland K, Hau CS, Verstegen NJM, Ciampricotti M, Hawinkels LJAC, Jonkers J, de Visser KE. 2015. IL17-producing γδ T cells and neutrophils conspire to promote breast cancer metastasis. Nature 522(7556):345–348.

Couper KN, Blount DG, Riley EM. 2008. IL-10: the master regulator of immunity to infection. J Immunol 180(9):5771–5777.

Curry JM, Eubank TD, Roberts RD, Wang Y, Pore N, Maity A, Marsh CB. 2008. M-CSF signals through the MAPK/ERK pathway via Sp1 to induce VEGF production and induces angiogenesis in vivo. PLoS One 3(10):e3405.

Dai X-M, Ryan GR, Hapel AJ, Dominguez MG, Russell RG, Kapp S, Stanley ER. 2002. Targeted disruption of the mouse colony-stimulating factor 1 receptor gene results in osteopetrosis, mononuclear phagocyte deficiency, increased primitive progenitor cell frequencies, and reproductive defects. Blood 99(1):111–120.

De Luca A, Gallo M, Aldinucci D, Ribatti D, Lamura L, D'Alessio A, Normanno N. 2011. Role of the EGFR ligand/receptor system in the secretion of angiogenic factors in mesenchymal stem cells. J Cell Physiol 226(8):2131–2138.

De Luca A, Lamura L, Gallo M, Maffia V, Normanno N. 2012. Mesenchymal stem cell-derived interleukin-6 and vascular endothelial growth factor promote breast cancer cell migration. J Cell Biochem 113(11):3363–3370.

DeNardo DG, Barreto JB, Andreu P, Vasquez L, Tawfik D, Kolhatkar N, Coussens LM. 2009. CD4+ T cells regulate pulmonary metastasis of mammary carcinomas by enhancing protumor properties of macrophages. Cancer Cell 16(2):91–102.

Dethlefsen C, Højfeldt G, Hojman P. 2013. The role of intratumoral and systemic IL-6 in breast cancer. Breast Cancer Res Treat 138(3):657–664.

Dinarello CA. 2010. Why not treat human cancer with interleukin-1 blockade?. Cancer Metastasis Rev 29(2):317–329.

Donato NJ, Klostergaard J. 2004. Distinct stress and cell destruction pathways are engaged by TNF and ceramide during apoptosis of MCF-7 cells. Exp Cell Res 294(2):523–533.

Donovan D, Harmey JH, Toomey D, Osborne DH, Redmond HP, Bouchier-Hayes DJ. 1997. TGF beta-1 regulation of VEGF production by breast cancer cells. Ann Surg Oncol 4(8):621–627.

Dore-Savard L, Lee E, Kakkad S, Popel AS, Bhujwalla ZM. 2016. The Angiogenic Secretome in VEGF overexpressing Breast Cancer Xenografts. Sci Rep 6:39460.

Downward J. 2003. Targeting RAS signalling pathways in cancer therapy. Nat Rev Cancer 3(1):11–22.

Duband JL, Thiery JP. 1982. Distribution of fibronectin in the early phase of avian cephalic neural crest cell migration. Dev Biol 93(2):308–323.

Dunn LK, Mohammad KS, Fournier PGJ, McKenna CR, Davis HW, Niewolna M, Guise TA. 2009. Hypoxia and TGF-beta drive breast cancer bone metastases through parallel signaling pathways in tumor cells and the bone microenvironment. PLoS One 4(9):e6896.

Elaraj DM, Weinreich DM, Varghese S, Puhlmann M, Hewitt, SM, Carroll NM, Alexander HR. 2006. The role of interleukin 1 in growth and metastasis of human cancer xenografts. Clin Cancer Res 12(4):1088–1096.

Esquivel-Velázquez M, Ostoa-Saloma P, Palacios-Arreola MI, Nava-Castro KE, Castro JI, Morales-Montor J. 2015. The Role of Cytokines in Breast Cancer Development and Progression. J Interferon Cytokine Res 35(1):1–16.

Ewan KBR, Oketch-rabah HA, Moses HL, Barcellos-hoff MH. 2005. Proliferation of estrogen receptor-α-positive mammary epithelial cells is restrained by transforming growth factor-β1 in adult mice. Am J Patho 167(2):409–417.

Favaro E, Lord S, Harris AL, Buffa FM. 2011. Gene expression and hypoxia in breast cancer. Genome Med 3(8):55.

Ferrara N, Davis-Smyth T. 1997. The biology of vascular endothelial growth factor. Endocr Rev 18(1):4–25.

Fertig EJ, Lee E, Pandey NB, Popel AS. 2015. Analysis of gene expression of secreted factors associated with breast cancer metastases in breast cancer subtypes. Sci Rep 5(1): 12133.

Fisher DT, Appenheimer MM, Evans SS. 2014. The two faces of IL-6 in the tumor microenvironment. Semin Immunol 26(1):38–47.

Fradet A, Sorel H, Bouazza L, Goehrig D, Depalle B, Bellahcene A, Castronovo V, Follet H, Descotes F, Aubin JE, Clezardin P, Bonnelye E. 2011. Dual function of ERRalpha in breast cancer and bone metastasis formation: implication of VEGF and osteoprotegerin. Cancer Res 71(17):5728–5738.

Freund A, Chauveau C, Brouillet JP, Lucas A, Lacroix M, Licznar A, Vignon F, Lazennec G. 2003. IL-8 expression and its possible relationship with estrogen-receptor-negative status of breast cancer cells. Oncogene 22(2):256–265.

Garcia A, Kandel JJ. 2012. Notch: a key regulator of tumor angiogenesis and metastasis. Histol Histopathol 27(2):151–156.

Geng SQ, Alexandrou AT, Li JJ. 2014. Breast cancer stem cells: Multiple capacities in tumor metastasis. Cancer Lett 349(1):1–7.

Ghattass K, El-Sitt S, Zibara K, Rayes S, Haddadin MJ, El-Sabban M, Gali-Muhtasib H. 2014. The quinoxaline di-N-oxide DCQ blocks breast cancer metastasis in vitro and in vivo by targeting the hypoxia inducible factor-1 pathway. Mol Cancer 13:12.

Ginestier C, Liu S, Diebel ME, Korkaya H, Luo M, Brown M, Wicinski J, Cabaud O, Charafe-Jauffret E, Bimbaum D, Guan JL, Dontu G, Wicha MS. 2010. CXCR1 blockade selectively targets human breast cancer stem cells in vitro and in xenografts. J Clin Invest 120(2):485–497.

GLOBOCAN 2012: Estimated cancer incidence, mortality and prevalence worldwide in 2012. International Agency for Research on Cancer. World Health Organization. Available at http://globocan.iarc.fr/Pages/fact_sheets_cancer.aspx Consulted January, 2018.

Godwin P, Baird AM, Heavey S, Barr MP, O'Byrne KJ, Gately K. 2013. Targeting nuclear factor-kappa B to overcome resistance to chemotherapy. Front Oncol 3:120.

Goldstein RH, Reagan MR, Anderson K, Kaplan DL, Rosenblatt M. 2010. Human bone marrow-derived MSCs can home to orthotopic breast cancer tumors and promote bone metastasis. Cancer Res 70(24):10044–10050.

Gupta P, Srivastava SK. 2014. HER2 mediated de novo production of TGFβ leads to SNAIL driven epithelial-to-mesenchymal transition and metastasis of breast cancer. Mol Oncol 8(8):1532–1547.

Hachim IY, Hachim MY, López-Ozuna VM, Ali S, Lebrun JJ. 2016. A dual prognostic role for the TGFβ receptors in human breast cancer. Hum Pathol 57:140–151.

Hallett MA, Venmar KT, Fingleton B. 2012. Cytokine stimulation of epithelial cancer cells: the similar and divergent functions of IL-4 and IL-13. Cancer Res 72(24):6338–43.

Hay ED. 1995. An overview of epithelio-mesenchymal transformation. Acta Anat (Basel) 154(1):8–20.

Hernandez SL, Banerjee D, Garcia A, Kangsamaksin T, Cheng WY, Anastassiou D, Funahashi Y, Kadenhe-Chiweshe A, Shawber CJ, Kitajewski JK, Kandel JJ, Yamashiro DJ. 2013. Notch and VEGF pathways play distinct but complementary roles in tumor angiogenesis. Vasc Cell 5(1):17.

Hoar FJ, Chaudhri S, Wadley MS, Stonelake PS. 2003. Co-expression of vascular endothelial growth factor C (VEGF-C) and c-erbB2 in human breast carcinoma. Eur J Cancer 39(12): 1698–1703.

Hsing CH, Cheng HC, Hsu YS, Chan CH, Yeh CH, Li CF, Chang MS. 2012. Upregulated IL-19 in breast cancer promotes tumor progression and affects clinical outcome. Clin Cancer Res 18(3):713–725.

Hsu YH, Hsing CH, Li CF, Chan CH, Chang M-C, Yan JJ, Chang MS. 2012. Anti-IL-20 monoclonal antibody suppresses breast cancer progression and bone osteolysis in murine models. J Immunol 188(4):1981–1991.

Huang C, Yang G, Jiang T, Zhu G, Li H, Qiu Z. 2011. The effects and mechanisms of blockage of STAT3 signaling pathway on IL-6 inducing EMT in human pancreatic cancer cells in vitro. Neoplasma 58(5):396–405.

Huang S, Ullrich SE, Bar-Eli M. (1999). Regulation of tumor growth and metastasis by interleukin-10: the melanoma experience. J Interferon Cytokine Res 19(7):697–703.

Hung S-P, Ho JH, Shih Y-R, Lo T, Lee OK. 2012a. Hypoxia promotes proliferation and osteogenic differentiation potentials of human mesenchymal stem cells. J Orthop Res 30(2): 260–266.

Hung S-P, Yang M-H, Tseng K-F, Lee OK. 2012b. Hypoxia induced secretion of TGF-beta 1 in mesenchymal stem cell promotes breast cancer cell progression. Cell Transplant 22(10):1869–1882.

Iliopoulos D, Hirsch HA, Wang G, Struhl K. 2011. Inducible formation of breast cancer stem cells and their dynamic equilibrium with non-stem cancer cells via IL6 secretion. Proc Natl Acad Sci USA 108(4):1397–1402.

Imamura T, Hikita A, Inoue Y. 2012. The roles of TGF-β signaling in carcinogenesis and breast cancer metastasis. Breast Cancer 19:118–124.

Iwanaga R, Wang CA, Micalizzi DS, Harrell JC, Jedlicka P, Sartorius CA, Kabos P, Farabaugh SM, Bradford AP, Ford HL. 2012. Expression of Six1 in luminal breast cancers predicts poor prognosis and promotes increases in tumor initiating cells by activation of extracellular signal-regulated kinase and transforming growth factor-beta signaling pathways. Breast Cancer Res 14(4):R100.

Ji H, Cao R, Yang Y, Zhang Y, Iwamoto H, Lim S, Nakamura M, Andersson P, Wang J, Sun Y, Dissing S, He X, Yang X, Cao Y. 2014. TNFR1 mediates TNF-α-induced tumour lymphangiogenesis and metastasis by modulating VEGF-C-VEGFR3 signalling. Nat Commun 5:4944.

Jiang Z, Chen J, Du X, Cheng H, Wang X, Dong C. 2017. IL-25 blockade inhibits metastasis in breast cancer. Protein Cell 8(3):191–201.

Kalluri R, Weinberg RA. 2009. The basics of epithelial-mesenchymal transition. J Clin Invest 119(6):1420–1428.

Kim K, Kim G, Kim JY, Yun HJ, Lim SC, Choi HS. 2014. Interleukin-22 promotes epithelial cell transformation and breast tumorigenesis via MAP3K8 activation. Carcinogenesis 35(6):1352–1361.

Kim SY, Kang JW, Song X, Kim BK, Yoo YD, Kwon YT, Lee YJ. 2013. Role of the IL-6-JAK1-STAT3-Oct-4 pathway in the conversion of non-stem cancer cells into cancer stem-like cells. Cell Signal 25(4):961–969.

Kingsley LA, Fournier PGJ, Chirgwin JM, Guise TA. 2007. Molecular Biology of Bone Metastasis. Mol Cancer Ther 6: 2609–2617.

Kluger HM, Dolled-Filhart M, Rodov S, Kacinski BM, Camp RL, Rimm DL. 2004. Macrophage colony-stimulating factor-1 receptor expression is associated with poor outcome in breast cancer by large cohort tissue microarray analysis. Clin Cancer Res 10(1 Pt 1):173–177.

Knüpfer H, Preiss R. 2007. Significance of interleukin-6 (IL-6) in breast cancer (review). Breast Cancer Res Treat 102(2): 129–35.

Kofler NM, Shawber CJ, Kangsamaksin T, Reed HO, Galatioto J, Kitajewski J. 2011. Notch signaling in developmental and tumor angiogenesis. Genes Cancer 2(12):1106–1116.

Koli KM, Arteaga CL. 1997. Predominant cytosolic localization of type II transforming growth factor beta receptors in human breast carcinoma cells. Cancer Res 57(5):970–977.

Krock BL, Skuli N, Simon MC. 2011. Hypoxia-induced angiogenesis: good and evil. Genes Cancer 2(12):1117–1133.

Kundu N, Beaty TL, Jackson MJ, Fulton AM. 1996. Antimetastatic and antitumor activities of interleukin 10 in a murine model of breast cancer. J Natl Cancer Inst 88(8):536–41.

Lanfranca MP, Lin Y, Fang J, Zou W, Frankel T. 2016. Biological and pathological activities of interleukin-22. J Mol Med 94(5):523–534.

Larue L, Bellacosa A. 2005. Epithelial–mesenchymal transition in development and cancer: role of phosphatidylinositol 3′ kinase/AKT pathways. Oncogene 24(50):7443–7454.

Lee E, Fertig EJ, Jin K, Sukumar S, Pandey NB, Popel AS. 2014a. Breast cancer cells condition lymphatic endothelial

cells within pre-metastatic niches to promote metastasis. Nat Commun 5:4715.
Lee E, Pandey NB, Popel AS. 2014b. Lymphatic endothelial cells support tumor growth in breast cancer. Sci Rep 4: 5853.
Li A, Dubey S, Varney ML, Dave BJ, Singh RK. 2003. IL-8 directly enhanced endothelial cell survival, proliferation, and matrix metalloproteinases production and regulated angiogenesis. J Immunol 170(6):3369–3376.
Li A, Varney ML, Valasek J, Godfrey M, Dave BJ, Singh RK. 2005. Autocrine role of interleukin-8 in induction of endothelial cell proliferation, survival, migration and MMP-2 production and angiogenesis. Angiogenesis 8(1):63–71.
Li Y, Gao P, Yang J, Yu H, Zhu Y, Si W. 2014. Relationship between IL-10 expression and prognosis in patients with primary breast cancer. Tumor Biol 35(11):11533–11540.
Lin EY, Nguyen AV, Russell RG, Pollard JW. 2001. Colony-stimulating factor 1 promotes progression of mammary tumors to malignancy. J Exp Med 193(6):727–740.
Luo M, Hou L, Li J, Shao S, Huang S, Meng D, Liu L, Feng L, Xia P, Qin T, Zhao X. 2016. VEGF/NRP-1axis promotes progression of breast cancer via enhancement of epithelial-mesenchymal transition and activation of NF-kappaB and beta-catenin. Cancer Lett 373(1):1–11.
Ma S, Cheng Q, Cai Y, Gong H, Wu Y, Yu X, Shi L, Wu D, Dong C, Liu H. 2014. IL-17A produced by γδ T cells promotes tumor growth in hepatocellular carcinoma. Cancer Res 74(7):1969–1982.
Ma Y, Ren Y, Dai ZJ, Wu CJ, Ji YH, Xu J. 2017. IL-6, IL-8 and TNF-α levels correlate with disease stage in breast cancer patients. Adv Clin Exp Med 26(3):421–426.
Maher MG, Sapi E, Turner B, Gumbs A, Perrotta PL, Carter D, Haffty BG. 1998. Prognostic significance of colony-stimulating factor receptor expression in ipsilateral breast cancer recurrence. Clin Cancer Res 4(8):1851–1856.
Malik ST, Naylor MS, East N, Oliff A, Balkwill FR 1990. Cells secreting tumour necrosis factor show enhanced metastasis in nude mice. Eur J Cancer 26(10):1031–1034.
Mandriota SJ, Jussila L, Jeltsch M, Compagni A, Baetens D, Prevo R, Banerji S, Huarte J, Montesano R, Jackson DG, Orci L, Alitalo K, Christofori G, Pepper MS. 2001. Vascular endothelial growth factor-C-mediated lymphangiogenesis promotes tumour metastasis. EMBO J 20(4):672–682.
Mani SA, Guo W, Liao MJ, Eaton EN, Ayyanan A, Zhou AY, Brooks M, Reinhard F, Zhang CC, Shipitsin M, Campbell LL, Polyak K, Brisken C, Yang J, Weinberg RA. 2008. The epithelial-mesenchymal transition generates cells with properties of stem cells. Cell 133(4):704–715.
Markota A, Endres S, Kobold S. 2018. Targeting interleukin-22 for cancer therapy. Hum Vaccin Immunother 4: 1–4.
Martin D, Galisteo R, Gutkind JS. 2009. CXCL8/IL8 stimulates vascular endothelial growth factor (VEGF) expression and the autocrine activation of VEGFR2 in endothelial cells by activating NFkappaB through the CBM (Carma3/Bcl10/Malt1) complex. J Biol Chem 284(10):6038–6042.
Massague J. 2008. TGFβ in cancer. Cell 134(2):215–230.
McCoy EL, Iwanaga R, Jedlicka P, Abbey NS, Chodosh LA, Heichman KA, Welm AL, Ford HL. 2009. Six1 expands the mouse mammary epithelial stem/progenitor cell pool and induces mammary tumors that undergo epithelial-mesenchymal transition. J Clin Invest 119(9):2663–2677.
Micalizzi DS, Christensen KL, Jedlicka P, Coletta RD, Baron AE, Harrell JC, Horwitz KB, Billheimer D, Heichman KA, Welm AL, Schiemann WP, Ford HL. 2009. The Six1 homeoprotein induces human mammary carcinoma cells to undergo epithelial-mesenchymal transition and metastasis in mice through increasing TGF-beta signaling. J Clin Invest 119(9):2678–2690.
Micalizzi DS, Wang CA, Farabaugh SM, Schiemann WP, Ford HL. 2010. Homeoprotein Six1 increases TGF-beta type I receptor and converts TGF-beta signaling from suppressive to supportive for tumor growth. Cancer Res 70(24):10371–10380.
Miller LJ, Kurtzman SH, Wang Y, Anderson KH, Lindquist RR, Kreutzer DL. 1998. Expression of interleukin-8 receptors on tumor cells and vascular endothelial cells in human breast cancer tissue. Anticancer Res 18(1A):77–81.
Miralem T, Steinberg R, Price D, Avraham H. 2001. VEGF (165) requires extracellular matrix components to induce mitogenic effects and migratory response in breast cancer cells. Oncogene 20(39):5511–5524.
Mohamed HT, El-Husseiny N, El-Ghonaimy EA, Ibrahim SA, Bazzi ZA, Cavallo-Medved D, Mohamed MM. 2018. IL-10 correlates with the expression of carboxypeptidase B2 and lymphovascular invasion in inflammatory breast cancer: the potential role of tumor infiltrated macrophages. Curr Probl Cancer 42(2):215–230.
Molloy AP, Martin FT, Dwyer RM, Griffin TP, Murphy M, Barry FP, Kerin MJ. 2009. Mesenchymal stem cell secretion of chemokines during differentiation into osteoblasts, and their potential role in mediating interactions with breast cancer cells. Int J Cancer 124(2):326–332.
Morandi A, Barbetti V, Riverso M, Dello Sbarba P, Rovida E. 2011. The colony-stimulating factor-1 (CSF-1) receptor sustains ERK1/2 activation and proliferation in breast cancer cell lines. PLoS One 6(11):e27450.
Müller A, Homey B, Soto H, Ge N, Catron, D, Buchanan ME, Murphy E, Yuan W, Wagner S, Barrera JL, Mohar A, Verástegui E, Zlotnik A. 2001. Involvement of chemokine receptors in breast cancer metastasis. Nature 410(6824):50–56.
Murakami M, Zheng Y, Hirashima M, Suda T, Morita Y, Ooehara J, Ema H, Fong GH, Shibuya M. 2008. VEGFR1 tyrosine kinase signaling promotes lymphangiogenesis as well as angiogenesis indirectly via macrophage recruitment. Arterioscler Thromb Vasc Biol 28(4):658–664.
Murdoch C, Monk PN, Finn A. 1999. CXC chemokine receptor expression on human endothelial cells. Cytokine 11(9):704–712.
Naber HPH, Wiercinska E, Ten Dijke P, van Laar T. 2011. Spheroid assay to measure TGF-b-induced invasion. J Vis Exp (57):1–7.
Naik MU, Naik TU, Suckow AT, Duncan MK, Naik UP. 2008. Attenuation of junctional adhesion molecule-A is a contributing factor for breast cancer cell invasion. Cancer Res 68(7): 2194–2203.
Nam JS, Terabe M, Kang MJ, Chae H, Voong N, Yang YA, Laurence A, Michalowska A, Mamura M, Lonning S, Berzofsky JA, Wakefield LM. 2008. Transforming growth factor β subverts the immune system into directly promoting tumor growth through interleukin-17. Cancer Res 68(10):3915–3923.
Nava-Castro KE, Palacios-Arreola MI, Ostoa-Saloma P, Muñiz-Hernandez S, Cerbon MA, Gomez-Icazbalceta G, Muñoz-Cruz S, Aguilar-Díaz, Pavón L, Castro-Romero JI, Morales-Montor J. 2014. The Immunoendocrine Network in Breast Cancer. Adv Neuroimmune Biol 5:109–131.
Niu G, Wright KL, Huang M, Song L, Haura E, Turkson J, Zhang S, Wang T, Sinibaldi D, Coppola D, Heller R, Ellis LM, Karras J, Bromberg J, Pardoll D, Jove R, Yu H. 2002. Constitutive Stat3 activity up-regulates VEGF expression and tumor angiogenesis. Oncogene 21(13):2000–2008.
Nozaki S, Sledge GW, Nakshatri H. 2000. Cancer cell-derived interleukin 1α contributes to autocrine and paracrine induc-

tion of pro-metastatic genes in breast cancer. Biochem Biophys Res Commun 275(1):60–62.
Orosz P, Krüger A, Hubbe M, Rüschoff J, Von Hoegen P, Männel DN. 1995. Promotion of experimental liver metastasis by tumor necrosis factor. Int J Cancer 60(6):867–871.
Pantschenko AG, Pushkar I, Anderson KH, Wang Y, Miller LJ, Kurtzman SH, Kreutzer DL. 2003. The interleukin-1 family of cytokines and receptors in human breast cancer: implications for tumor progression. Int J Oncol 23(2):269–284.
Patel NS, Li JL, Generali D, Poulsom R, Cranston DW, Harris AL. 2005. Up-regulation of delta-like 4 ligand in human tumor vasculature and the role of basal expression in endothelial cell function. Cancer Res 65(19):8690–8697.
Pathak AP, McNutt S, Shah T, Wildes F, Raman V, Bhujwalla ZM. 2013. In vivo ''MRI phenotyping'' reveals changes in extracellular matrix transport and vascularization that mediate VEGF-driven increase in breast cancer metastasis. PLoS One 8(5):e63146.
Price DJ, Miralem T, Jiang S, Steinberg R, Avraham H. 2001. Role of vascular endothelial growth factor in the stimulation of cellular invasion and signaling of breast cancer cells. Cell Growth Differ 12(3):129–135.
Qian B, Deng Y, Im JH, Muschel RJ, Zou Y, Li J, Lang RA, Pollard JW. 2009. A distinct macrophage population mediates metastatic breast cancer cell extravasation, establishment and growth. PLoS One 4(8):e6562.
Qian BZ, Zhang H, Li J, He T, Yeo EJ, Soong DY, Carragher NO, Munro A, Chang A, Bresnick AR, Lang RA, Pollard JW. 2015. FLT1 signaling in metastasis-associated macrophages activates an inflammatory signature that promotes breast cancer metastasis. J Exp Med 212(9):1433–1448.
Reedijk M. 2012. Notch signaling and breast cancer. Adv Exp Med Biol 727:241–257.
Roy DL, Pathangey LB, Tinder TL, Schettini JL, Gruber HE, Mukherjee P. 2009. Breast cancer-associated metastasis is significantly increased in a model of autoimmune arthritis. Breast Cancer Res 11(4):R56.
Roy LD, Sahraei M, Schettini JL, Gruber HE, Besmer DM, Mukherjee P. 2014. Systemic neutralization of IL-17A significantly reduces breast cancer associated metastasis in arthritic mice by reducing CXCL12/SDF-1 expression in the metastatic niches. BMC Cancer 14(1):225.
Rui J, Chunming Z, Binbin G, Na S, Shengxi W, Wei S. (2017). IL-22 promotes the progression of breast cancer through regulating HOXB-AS5. Oncotarget 8(61):103601.
Russo J, Moral R, Balogh GA, Mailo D, Russo IH. 2005. The protective role of pregnancy in breast cancer. Breast Cancer Res 7(3):131–142.
Rutter JL, Benbow U, Coon CI, Brinckerhoff CE. 1997. Cell-type specific regulation of human interstitial collagenase-1 gene expression by interleukin-1β (IL-1β) in human fibroblasts and BC-8701 breast cancer cells. J Cell Biochem 66(3):322–336.
Scholl SM, Pallud C, Beuvon F, Hacene K, Stanley ER, Rohrschneider L, Lidereau R. 1994. Anti-colony-stimulating factor-1 antibody staining in primary breast adenocarcinomas correlates with marked inflammatory cell infiltrates and prognosis. J Natl Cancer Inst 86(2):120–126.
Sheridan C, Kishimot H, Fuchs RK, Mehrotra S, Bhat-Nakshatri P, Turner CH, Nakshatri H. 2006. CD44+/CD24-breast cancer cells exhibit enhanced invasive properties: an early step necessary for metastasis. Breast Cancer Res 8(5):R59.
Sherr CJ, Rettenmier CW, Sacca R, Roussel MF, Look AT, Stanley ER. 1985. The c-fms proto-oncogene product is related to the receptor for the mononuclear phagocyte growth factor, CSF-1. Cell 41(3):665676.
Shibuya M. 2011. Vascular Endothelial Growth Factor (VEGF) and Its Receptor (VEGFR) Signaling in Angiogenesis: a Crucial Target for Anti- and Pro-Angiogenic Therapies. Genes Cancer 2(12):1097–1105.
Shiozawa Y, Nie B, Pienta KJ, Morgan TM, Taichman RS. 2013. Cancer stem cells and their role in metastasis. Pharmacol Ther 138(2):285–93.
Siegel R, DeSantis C, Virgo K, Stein K, Mariotto A, Smith T, Cooper D, Gansler T, Lerro C, Fedewa S, Lin C, Leach C, Spillers R, Cho H, Scoppa S, Hachey M, Kirch R, Jemal A, Ward E. 2012. Cancer treatment and survivorship statistics, 2012. CA Cancer J Clin 62(4):220–241.
Silva J, Silva JM, Dominguez G, Garcia JM, Cantos B, Rodriguez R, Larrondo FJ, Provencio M, Espana P, Bonilla F. 2003. Concomitant expression of p16INK4a and p14ARF in primary breast cancer and analysis of inactivation mechanisms. J Pathol 199(3):289–297.
Soria G, Ofri-Shahak M, Haas I, Yaal-Hahoshen N, Leider-Trejo L, Leibovich-Rivkin T, Ben-Baruch A. 2011. Inflammatory mediators in breast cancer: coordinated expression of TNFα & IL-1β with CCL2 & CCL5 and effects on epithelial-to-mesenchymal transition. BMC Cancer 11(1): 130.
Stankic M, Pavlovic S, Chin Y, Brogi E, Padua E, Norton L, Massague J, Benezra R. 2013. TGF-β-Id1 signaling opposes twist1 and promotes metastatic colonization via a mesenchymal-to-epithelial transition. Cell Rep 5(5):1228–1242.
Su JL, Yang PC, Shih JY, Yang CY, Wei LH, Hsieh CY, Chou CH, Jeng YM, Wang MY, Chang KJ, Hung MC, Kuo ML. 2006. The VEGF-C/Flt-4 axis promotes invasion and metastasis of cancer cells. Cancer Cell 9(3):209–223.
Sullivan NJ, Sasser AK, Axel AE, Vesuna F, Raman V, Ramirez N, Oberyszyn TM, Hall, BM. 2009. Interleukin-6 induces an epithelial-mesenchymal transition phenotype in human breast cancer cells. Oncogene 28(33):2940–7.
Suzuki T, Miki Y, Moriya T, Shimada N, Ishida T, Hirakawa H, Ohuchi N, Sasano H. 2004. Estrogen-related receptor alpha in human breast carcinoma as a potent prognostic factor. Cancer Res 64(13):4670–4676.
Tanaka T, Kishimoto T. 2014. The biology and medical implications of interleukin-6. Cancer Immunol Res 2(4):288–94.
Tanaka T, Narazaki M, Kishimoto T. 2014. Il-6 in inflammation, immunity, and disease. Cold Spring Har Perspect Biol 6(10):a016295.
Tarin D. 2005. The fallacy of epithelial mesenchymal transition in neoplasia the fallacy of epithelial mesenchymal transition in neoplasia. Cancer Res 65(14):5996–6001.
Thiery JP. 2002. Epithelial–mesenchymal transitions in tumour progression. Nat Rev Cancer 2(6):442–454.
Todorovic-Rakovic N, Milovanovic J. 2013. Interleukin-8 in Breast Cancer Progression. J Interferon Cytokine Res 33(10): 563–70.
Tsai PW, Shiah SG, Lin MT, Wu CW, Kuo ML. 2003. Up-regulation of vascular endothelial growth factor C in breast cancer cells by heregulin-beta 1. A critical role of p38/nuclear factor-kappa B signaling pathway. J Biol Chem 278(8): 5750–5759.
Varfolomeev EE, Ashkenazi A. 2004. Tumor necrosis factor: an apoptosis JuNKie? Cell 116(4):491–497.
Venmar KT, Carter KJ, Hwang DG, Dozier EA, Fingleton B. 2014. IL4 receptor ILR4α regulates metastatic colonization by mammary tumors through multiple signaling pathways. Cancer Res 74(16):4329–4340.

Venmar KT, Kimmel DW, Cliffel DE, Fingleton B. 2015. IL4 receptor α mediates enhanced glucose and glutamine metabolism to support breast cancer growth. Biochim Biophys Acta 1853(5):1219–1228.

Vićovac L, Aplin JD. 1996. Epithelial-mesenchymal transition during trophoblast differentiation. Acta Anat (Basel) 156(3): 202–216.

Wang CA, Jedlicka P, Patrick AN, Micalizzi DS, Lemmer KC, Deitsch E, CÃsas-Selves M, Harrell JC, Ford HL. 2012. SIX1 induces lymphangiogenesis and metastasis via upregulation of VEGF-C in mouse models of breast cancer. J Clin Invest 122(5):1895–1906.

Wang FM, Liu HQ, Liu SR, Tang SP, Yang L, Feng GS. 2005. SHP-2 promoting migration and metastasis of MCF-7 with loss of E-cadherin, dephosphorylation of FAK and secretion of MMP-9 induced by IL-1 β *in vivo* and *in vitro*. Breast Cancer Res Treat 89(1):5–14.

Wang H, Wang HS, Zhou BH, Li CL, Zhang F, Wang XF, Zhang G, Bu XZ, Cai SH, Du J. 2013. Epithelial-mesenchymal transition (EMT) induced by TNF-α requires AKT/GSK-3β-mediated stabilization of snail in colorectal cancer. PloS One 8(2):e56664.

Wang Y, Lui W-Y. 2012. Transforming growth factor-b1 attenuates junctional adhesion molecule-A and contributes to breast cancer cell invasion. Eur J Cancer 48(18):3475–3487.

Wendt MK, Allington TM, Schiemann WP. 2009. Mechanisms of epithelial-mesenchymal transition by TGF-β. Futur Oncol 5:1145–1168.

Woo SU, Bae JW, Yang J-H, Kim JH, Nam SJ, Shin YK. (2007). Overexpression of interleukin-10 in sentinel lymph node with breast cancer. Ann Surg Oncol 14(11): 3268–3273.

Wyckoff J, Wang W, Lin EY, Wang Y, Pixley F, Stanley ER, Condeelis J. 2004. A paracrine loop between tumor cells and macrophages is required for tumor cell migration in mammary tumors. Cancer Res 64(19):7022–7029.

Xiong S, Grijalva R, Zhang L, Nguyen NT, Pisters PW, Pollock RE, Yu D. 2001. Up-regulation of vascular endothelial growth factor in breast cancer cells by the heregulin-beta1-activated p38 signaling pathway enhances endothelial cell migration. Cancer Res 61(4):1727–1732.

Xu W, Yang Z, Lu N. 2015. A new role for the PI3K/Akt signaling pathway in the epithelial-mesenchymal transition. Cell Adh Migr 9(4):317–324.

Yang L, Huang J, Ren X, Gorska AE, Chytil A, Aakre M, Carbone DP, Matrisian LP, Richmond A, Lin PC, Moses HL. 2008. Abrogation of TGFβ signaling in mammary carcinomas recruits Gr-1+CD11b+ myeloid cells that promote metastasis. Cancer Cell 13(1):23–35.

Yang W, Klos K, Yang Y, Smith TL, Shi D, Yu D. 2002. ErbB2 overexpression correlates with increased expression of vascular endothelial growth factors A, C, and D in human breast carcinoma. Cancer 94(11):2855–2861.

Yao J, Xiong S, Klos K, Nguyen N, Grijalva R, Li P, Yu D. 2001. Multiple signaling pathways involved in activation of matrix metalloproteinase-9 (MMP-9) by heregulin-beta1 in human breast cancer cells. Oncogene 20(56): 8066–8074.

Yen L, You XL, Al Moustafa AE, Batist G, Hynes NE, Mader S, Meloche S, Alaoui-Jamali MA. 2000. Heregulin selectively upregulates vascular endothelial growth factor secretion in cancer cells and stimulates angiogenesis. Oncogene 19(31):3460–3469.

Yin SY, Jian FY, Chen YH, Chien SC, Hsieh MC, Hsiao PW, Lee WH, Kuo YH, Yang NS. 2016. Induction of IL-25 secretion from tumourassociated fibroblasts suppresses mammary tumour metastasis. Nat Commun 3(7):11909.

Yin Y, Chen X, Shu Y. 2009. Gene expression of the invasive phenotype of TNF-alpha-treated MCF-7 cells. Biomed Pharmacother 63(6):421–428.

Yu Y, Davicioni E, Triche TJ, Merlino G. 2006. The homeoprotein six1 transcriptionally activates multiple protumorigenic genes but requires ezrin to promote metastasis. Cancer Res 66(4):1982–1989.

Zarzynska JM. 2014. Two faces of TGF-beta1 in breast cancer. Mediators Inflamm 2014:141747.

Zhang J, Lu A, Beech D, Jiang B, Lu Y. 2007. Suppression of breast cancer metastasis through the inhibition of VEGF-mediated tumor angiogenesis. Cancer Ther 5:273–286.

Zhang X, Liu Y. (2017). Association of Interleukin-22 expression with HER-2 amplification in patients with breast cancer. Breast 32(Suppl 1):S109.

Zhu G, Du Q, Wang X, Tang N, She F, Chen Y. 2014. TNF-α promotes gallbladder cancer cell growth and invasion through autocrine mechanisms. Int J Mol Med 33(6):1431–1440.

Zhu X, Mulcahy LA, Mohammed RA, Lee AH, Franks HA, Kilpatrick L, Yilmazer A, Paish EC, Ellis IO, Patel PM, Jackson AM. 2008. IL-17 expression by breast-cancer-associated macrophages: IL-17 promotes invasiveness of breast cancer cell lines. Breast Cancer Res 10(6):R95.

Zlotnik A, Yoshie O, Nomiyama H. 2006. The chemokine and chemokine receptor superfamilies and their molecular evolution. Genome Biol 7(12):243.

Address correspondence to:
Dr. Jorge Morales-Montor
Departamento de Inmunología
Instituto de Investigaciones Biomédicas
Universidad Nacional Autónoma de México
AP 70228
Ciudad de México 04510
México

E-mail: jmontor66@biomedicas.unam.mx;
jmontor66@hotmail.com

Received 17 February 2018/Accepted 31 July 2018

8.5 Capítulo de libro relacionado al tema de la Tesis (tumores de mama).

Ruiz-Manzano Rocío Alejandra, Ochoa-Mercado Tania de Lourdes, Segovia-Mendoza Mariana, Nava-Castro Karen Elizabeth, Palacios-Arreola Margarita Isabel, and Morales-Montor Jorge. (2019). Neuroimmunoendocrine Interactions in Tumorigenesis and Breast Cancer. Intech Open. 1-32.
DOI: http://dx.doi.org/10.5772/intechopen.88128

Chapter

Neuroimmunoendocrine Interactions in Tumorigenesis and Breast Cancer

Rocío Alejandra Ruiz-Manzano, Tania de Lourdes Ochoa-Mercado, Mariana Segovia-Mendoza, Karen Elizabeth Nava-Castro, Margarita Isabel Palacios-Arreola and Jorge Morales-Montor

Abstract

Organism homeostasis is regulated through the tri-directional relationships between immune, endocrine, and nervous systems. These relationships are established by a complex network of chemokines, cytokines, hormones (peptide and non-peptide), neurotransmitters, and neurohormones that act onto its target cells, through common receptors. Despite initial attribution of the exclusive action of each molecule group (neurotransmitters, hormones, and cytokines), to the function of one specific system (nervous, endocrine, and immune, respectively), ligand and receptor pleiotropy and redundancy showed the multidirectional communication between systems. Cancer and metabolic and autoimmune diseases get established when homeostasis is disrupted. These interactions act in different disease levels, in cancer, since initial immunosurveillance phase, until immunosubversion and metastasis, in all cases is crucial for tumor development, cancer outcome, and patient prognosis.

Keywords: neuroimmunoendocrine network, breast cancer, neuroimmunoregulation, endocrinoimmune regulation, tumor, cytokines, steroids, neurotransmitters

1. Introduction

Cancer is one of the most common health issues worldwide. According to the World Health Organization (WHO), in 2018 18,078,957 new cases and 9,555,027 related deaths were reported. Breast cancer is the second leading cancer, after lung cancer, but is the first in women incidence and prevalence [1]. An estimation made in 2009 calculated that one out of eight American women could develop breast cancer in their life course [2].

There are several risk factors associated with breast cancer. The first and most important is gender; as mentioned before, women get breast cancer more often than males. Other risk factors are early menarche, first terminal pregnancy after 30 years old, late menopause, nulliparity, no breastfeeding, overweight or obesity, family or personal history of breast cancer, alcohol abuse, consumption of hormone oral

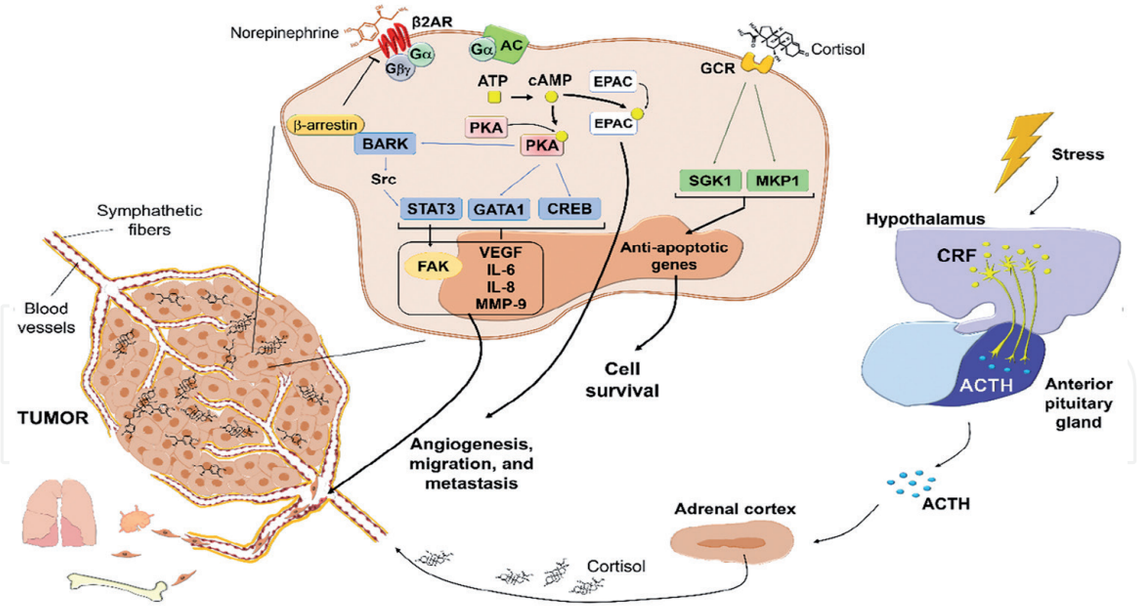

Figure 1.
Nervous regulation during breast tumor growth and metastasis. Sympathetic fibers and blood vessels infiltrate tumor and are responsible for tumor communication with the nervous system. Sympathetic fibers release norepinephrine in tumor, which binds to β_2-adrenergic receptor in the tumor cell membrane and activates adenylate cyclase through G-protein-coupled receptor subunit α. AC promotes ATP-cAMP conversion, and cAMP activates protein kinase A and exchange protein activated by adenylyl cyclase. PKA phosphorylates β-adrenergic receptor kinase, CREB, and GATA1 transcription factors. BARK recruits β-arrestin, inhibits β-adrenergic signal, and activates Src kinase, which in turn activates STAT3 and downstream focal adhesion kinase. FAK enhances migration. CREB, GATA1, and STAT3 promote VEGF, IL-6, IL-8, and MMP-9 expression, enhancing angiogenesis, migration, and invasion. In the other pathway activated through cAMP, EPAC also promotes cell migration. Stress stimulates hypothalamic-pituitary-adrenocortical axis, and the hypothalamus secretes corticotropin-releasing factor (CRF) that stimulates the adrenocorticotropic hormone (ACTH) secretion into blood vessels and systemic circulation. ACTH in adrenal gland cortex stimulates cortisol release. In tumor, cortisol binds to glucocorticoid receptor (GCR) in breast cancer cells and promotes the expression of MAPK phosphatase-1 (MKP1) and serine/threonine protein kinase 1 (SGK1) and other genes related to cell survival and apoptosis protection.

contraceptives or menopausal hormone therapy, and environmental pollution with compounds such as bisphenols and phthalates, among others [3–5].

To classify breast cancer, the actualized TNM anatomical staging system categorizes primary tumor (T), regional lymph node invasion (N), and distant metastases (M), to determine the actual stage group of breast cancer. This classification is very useful, not only for diagnosis and prognosis but also for treatment. In addition to the anatomical staging system, factor-based prognostic stage groups that include tumor grade (histological), hormone receptor status, and a multigene panel status (when is available) were added in the 2017 TNM meeting [2, 3, 6].

Hormone receptor status takes into account the presence of estrogen receptor (ER), progesterone receptor (PR), and human epidermal growth factor receptor 2 (HER-2) in tumor mammary cells. There are some characteristics that determine the status of the tumor, such as anatomical localization, tumor grade, hormone receptor status, and, with it, the prognostic and treatment of breast cancer [6].

A normal breast is composed of mammary glands (lobules and ducts), fibrous connective and adipose tissues, blood and lymph vessels, lymph nodes, nerves, and ligaments [7]. Duct branches form each mammary gland epithelium whose caliber is decreased until it forms ductules that flow into lobes [7, 8]. The epithelium is formed by luminal epithelial cells and basal epithelial cells, also known as myoepithelial cells, adjacent to the basement membrane [9]. Proliferation and apoptosis of mammary epithelia are regulated by the extracellular matrix (ECM) signals [10]. Either lobules or ducts can become dysplastic and eventually neoplastic, a phenomenon also regulated by ECM, and adjacent cell interactions, including stromal,

vascular, fibroblasts, and immune cells, may favor the transformation and uncontrolled proliferation of cells in the breast tissue.

In breast cancer progression, there are three phases: benign disease and noninvasive and invasive cancer (**Figure 1**). By definition, benign disease and noninvasive cancer share the same condition, where transformed cells do not trespass the basal membrane but are differentiated by histological grade. An example of this is the lobular carcinoma in situ, classified as a benign tumor, with associated risk in developing carcinoma [6]. On the other hand, in the invasive cancer, cells migrate through basal membrane to stromal breast and/or adjacent tissues and organs [11].

Several interactions determine different outcomes in tumor development, including the interactions among nervous, immune, and endocrine systems with the tumor. Next, we described the overall function of these systems in breast cancer and finally the interactions between them.

2. System interactions in breast cancer

2.1 The role of the nervous system on tumor growth and metastasis

Nervous regulation during cancer is mainly mediated through the sympathetic nervous system (SNS) and the hypothalamic-pituitary-adrenocortical (HPA) axis [12].

2.1.1 Sympathetic nervous system

The sympathetic nervous system regulates the organism's vital involuntary functions and is in charge of the "fight-or-flight" response in danger and stressful situations and modulates the connection between the central nervous system and immune system [13].

SNS nerve fibers emerge from the thoracolumbar spinal cord, innervate different tissues, and produce norepinephrine [12, 14]. Nowadays, it is known that sympathetic nerve fibers innervate the bone marrow, thymus (primary lymphoid organs), spleen and lymph nodes (secondary lymphoid organs), and mucosa- (MALT), bronchus- (BALT), and gut- (GALT) associated lymphoid tissues [15–17]. Epinephrine arrives to the target tissue through blood circulation after being produced in the adrenal gland. Both norepinephrine and epinephrine bind with different affinities to adrenergic receptors α (α_1/α_2) and β ($\beta_1/\beta_2/\beta_3$) in target cells in different tissues and organs, such as the heart, brain, adipose tissue, mammary gland, ovaries, prostate, lymphoid tissue, bones, and different types of cancer cells [13, 14].

These adrenergic receptors are expressed differentially. In smooth muscles α_1AR and α_2AR can be found, although the latter also is expressed in platelets and neurons [14]. Regarding β receptors, of which noradrenaline is the main ligand, β_1AR can be found in the adipose tissue and cardiac muscle. And β_2-adrenergic receptors (β_2ARs) are expressed in tumor and immune cells, in the heart, lung tissue, and smooth muscle. At least, β_3AR can be found in the adipose tissue. Either β_1AR, β_2AR, or β_3AR activates cAMP and in turn stimulates protein kinase A (PKA) [14].

2.1.2 Adrenergic signaling in tumors

β_2AR expression has been detected in breast cancer cell lines, with different densities among them [18], and also in human breast tumor biopsies [19, 20]. Therefore, β_2AR expression should be considered if a β_2AR agonist treatment is going to be performed [21].

It is known that β_2AR signaling regulates proliferation and tumor cell invasion; this is evidenced with β_2AR blockers and the associated beneficial effect in breast cancer recurrence and bone, lung, and brain metastasis [13, 22]. Interestingly, primary TN tumor cells expressed lesser β_2AR mRNA and protein than TN brain metastatic cells from primary breast tumor; these metastatic cells exhibited increased proliferation and migration. In vivo and in vitro, invasive and metastatic potential of these cells was diminished when treated with propranolol [22].

There have been different mechanisms described that regulate invasion and metastasis through β_2AR signaling in tumor cells. Norepinephrine, epinephrine, or agonists bind β_2AR and activate adenylate cyclase (AC) through G-protein-coupled receptor subunit α ($G\alpha_s$). AC activation promotes ATP-cAMP conversion (**Figure 1**) and Ca^{2+} intracellular increase [23]. In highly metastatic breast tumor cells (MDA-MB-231HM), another G-protein subunit, Gβγ, also promotes intracellular Ca^{2+} augmentation through β_2AR signaling. Either through Gβγ or $G\alpha_s$, cAMP activates effector PKA and exchange protein activated by adenylyl cyclase (EPAC) and inhibits pERK1/pERK2; therefore, cell proliferation is mediated independently by ERK phosphorylation [23]. PKA phosphorylates CREB/ATF, GATA1 transcription factors, and β-adrenergic receptor kinase (BARK). BARK recruits β-arrestin which activates Src kinase, and this activates STAT3 [24]. Focal adhesion kinase (FAK) activated by STAT3 enhances migration and apoptosis resistance. CREB/ATF, GATA1, and STAT3 promote VEGF, IL-6, IL-8, and MMP-9 expression and enhance angiogenesis, migration, and invasion (**Figure 1**) [24]. Meanwhile, in breast tumor cells (MCF-7 and MDA-MB-231) treated with an EPAC inhibitor (ESI-09), migration inhibition was found associated with mislocalization of the A-kinase anchoring protein 9 (AKAP9); therefore, EPAC also promotes cell migration [25].

Another way in which β_2AR signaling stimulates tumor growth is through promoting DNA damage and p53-associated apoptosis suppression [26].

2.1.3 Tumor innervation

During tumor initial innervation, nearby healthy tissue provides sympathetic fibers that infiltrate the periphery of the growing tumor [27], in response to neurotropic factors secreted by tumor cells, such as neurotrophic growth factor (NGF) [28] and brain-derived neurotrophic factor (BDNF) [29]. These factors increase nerve fiber growth and thereby tumor innervation [28]. Tumor innervation is associated with vasculature; therefore, together with nerve fibers, blood vessels go through the tumor mass [30] (**Figure 1**). Sympathetic innervation in tumor is the main catecholamine source [30, 31]; this is evidenced because its local concentration is higher than plasma [31]. In this sense, innervation is a feature of tumor microenvironment associated with tumor aggressiveness [28].

Therefore, β-receptor antagonists could have an important role in the development of new therapies that diminish metastasis risk and promote a slow tumor progression.

2.1.4 HPA axis

The HPA axis also plays an important role in stress response in mammals. In the hypothalamus, the paraventricular nucleus neurons secrete corticotropin-releasing factor into hypophyseal portal blood. CRF stimulates the release of adrenocorticotropic hormone by the anterior pituitary gland, to the blood vessels and systemic circulation. When ACTH reaches adrenal glands, the cortex stimulates the corticosterone production (in rodents) or cortisol (humans) (**Figure 1**) [32].

Cortisol and corticosterone (glucocorticoids) exert their effects through glucocorticoid receptor. Different immune and breast cancer cells express this receptor, and glucocorticoids exert different effects in these cells.

GCR in breast cancer cells, especially in triple-negative lines (MDA-MB-231), promotes the expression of genes related to cell survival and apoptosis protection, for example, MAPK phosphatase-1 and serine/threonine protein kinase 1 (**Figure 1**) [33, 34]. In addition, the activation of the GCR induces the expression of genes related to cell survival, adhesion, and EMT in a premalignant breast [35]. Correspondingly, in xenograft MDA-MB-231 breast tumors in mice pre-treated with systemic dexamethasone, the paclitaxel treatment effect was inhibited [36]. Therefore, glucocorticoids protect breast cancer cells from apoptosis and enhance their survival capabilities, favoring tumor growth.

2.1.5 Stress and tumor growth

Stress is largely linked to cancer development. Stressor exposition and SNS activation promote noradrenaline release into the tumor that regulates tumor progression [30]. In animals under social isolation (a stress experimental model), there is an increased tumor size and reduced survival [37]. Also in other stress models, increased tumor progression and metastasis have been observed [38, 39].

During metastatic establishment, β_2AR overexpression enhances cell proliferation and invasion, to ensure metastatic establishment, and, maybe, that is why in primary tumor resection, the surgery induces stress and releases norepinephrine and epinephrine that enhance tumor metastasis. Thus, the use of treatments that antagonize the effect of these neurotransmitters may reduce metastasis [22].

Thus, nervous control of tumor growth is regulated by the sympathetic and HPA systems. The sympathetic regulation is via tumor innervation with sympathetic fibers and the adrenergic signaling in tumor, through local and peripheral catecholamine (epinephrine and norepinephrine) production and the β_2AR expression in tumor and immune cells. Meanwhile, HPA system regulates glucocorticoid production, which enhances tumor cell survival and downmodulates inflammatory response, thus enhancing tumor growth and metastasis (**Figure 1**).

3. Immune response in mammary tumors

Tumorigenesis usually courses a slow development during years, and the immune response depends on the different stages of the disease and the tumor microenvironment [40].

Every day, immune cells detect and destroy transformed cells, in a phenomenon called immunosurveillance. But, when transformed cells evade elimination mechanisms (immunoescape), survive and proliferate. At this point, tumor can remain in a state of dormancy, partially by the action of immune cells, but when the balance between stromal, immune, and tumor cells with their secretory products leads to local immunosuppression, the immunosubversion is established, and the tumor grows (**Figure 2**) [41, 42].

3.1 Immune innate cells in mammary tumors

3.1.1 Dendritic cells

Dendritic cells are antigen-presenting cells (APCs) that recognize, uptake, process, and present antigens to different cells including T cells. In the immunosurveillance

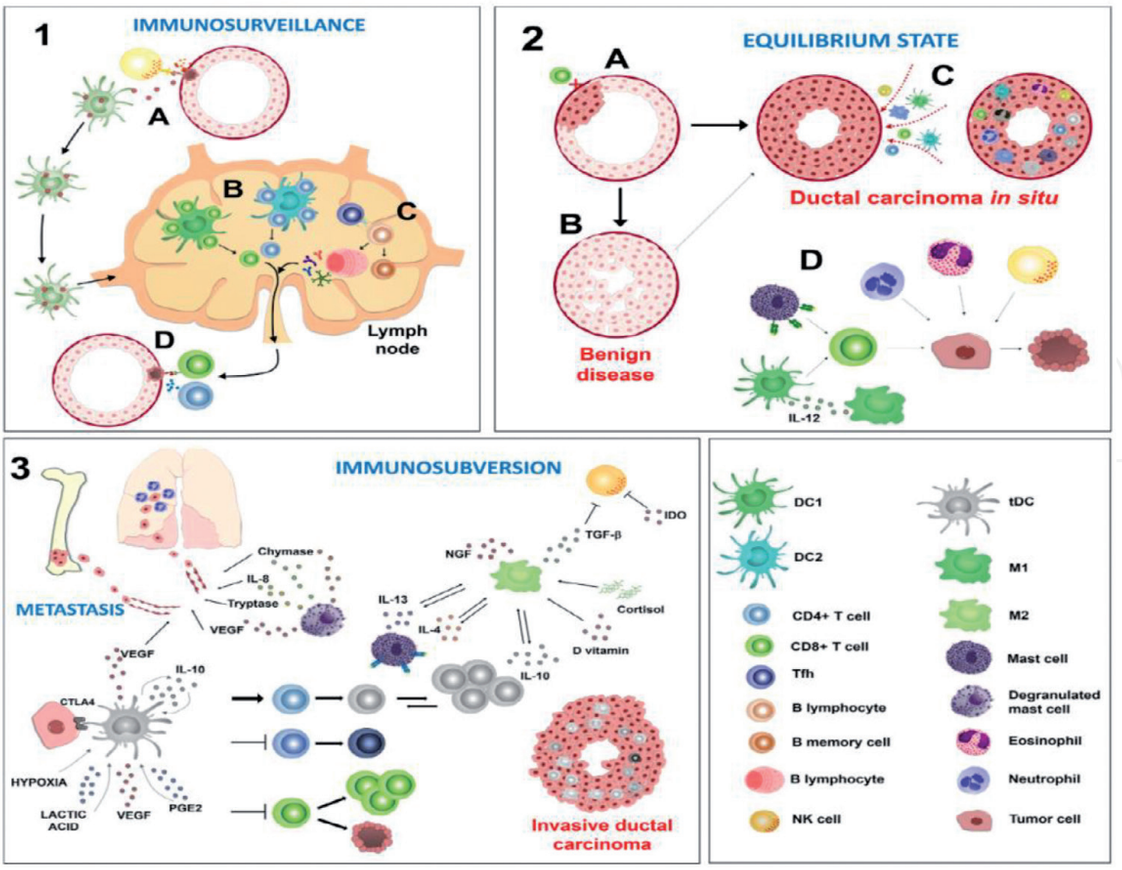

Figure 2.
Immune response in breast tumor development. (1) In immunosurveillance, breast tissue-resident conventional dendritic cells (cDC) capture antigens released by transformed cell after recognition and destruction by cytotoxic cells (NK cells). cDC migrate to peripheric lymph node and as DC type 1 (DC1) or DC type 2 (DC2) present antigens to $CD8^+$ T cells or $CD4^+$ T cells, respectively. In lymph nodes T follicular cells activate B lymphocytes into plasma (antibody producer) or B memory cells. After the activation and subsequent proliferation, $CD8^+$ T cytotoxic and $CD4^+$ T helper cells migrate. Cytotoxic cells induce apoptosis to transformed cells, and T helper cells produce cytokines and chemokines to enhance cytotoxic effect. (2) In the equilibrium state, transformed cells evade immune recognition and proliferate to hyperplasia (benign disease) and eventually to ductal carcinoma in situ (DCIS). In these phases immune cells are recluted, and cytotoxic cells ($CD8^+$, neutrophils, and eosinophils) may eliminate transformed cells in an equilibrium phase. Indirectly, other cells enhance cytotoxic response, for example, M1 macrophages produce IL-12 that enhances dendritic cell antigen presentation to $CD8^+$ cells. Also mast cells MHC-I^+ stimulate $CD8^+$ T-cell proliferation. (3) In immunosubversion and metastasis, when invasive ductal carcinoma is established, tumor dendritic cells (tDC) are induced through IL-10, vascular endothelial factor (VEGF), prostaglandin E2 (PGE2), hypoxia, and lactic acid and by direct contact with tumor $CTLA4^+$. tDC produce IL-10, which in turn induces their own expansion as well as T regulatory cell (Tregs) proliferation and the inhibition of effector $CD4^+$ and $CD8^+$ T cells, Th1 differentiation, and $CD8^+$ T cells function. Also, IL-10, D vitamin, and cortisol activate M2. M2 macrophages produce IL-4, IL-10, IL-13 (that feedback M2 generation), NGF, and TGF-β that with IDO inhibit cytotoxic NK function. Mast cells secrete VEGF, tryptase, chymase, and IL-8 that enhance metastasis to different organs (lung and bone). Neutrophils may enhance metastasis because they form premetastatic niches that promote tumor cell migration and metastasis establishment.

phase, dendritic cells resident in the breast tissue sense and capture different antigens released by transformed cells and then migrate to draining lymph nodes, where, as a mature cell, antigens to naïve T cells are present [43–45]. After the activation and subsequent proliferation, the $CD8^+$ T and $CD4^+$ T cells migrate to the site where transformed neoplastic cells reside. The cytotoxic response is carried out mainly by $CD8^+$ T cells and NK cells, which detect and induce apoptosis to transformed cells; meanwhile, $CD4^+$ T helper cells produce cytokines and chemokines that modulate the immune response and recruit other immune cells (**Figure 2**).

Two lineages of dendritic cells are responsible for T-cell priming. The first are DC1s that express chemokine receptor CXR1 and present antigens through MHC-I

preferentially to $CD8^+$ T cells. The second are the DC2s that express CD172a and MHC-II (high), to activate $CD4^+$ T cells [43]. DC1s can be lymphoid-resident DC1s (CD8α in mice) or migratory DC1s ($CD103^+$ in mice), being the latter mentioned as the main subset of DC that can induce a strong cytotoxic response against tumor through the activation of $CD8^+$ T cells [46]. Meanwhile, DC2s ($CD11^+$ in mouse) seem to fail in tumor antigen presentation to $CD4^+$ T cells in lymph nodes, but it is unclear why. A possibility is an inadequate process of antigen or the nature of tumor antigen. These DC2s cells can be tolerogenic, because they cannot generate an adequate activation and stimulation [43].

Three features lead to the induction of suppressive or tumor phenotype DC. The first is the presence of tumor cell neoantigens that leads eventually to immunoescape and the failure of immunosurveillance. The second is the degree of DC maturation, in which immature DC acquire a tolerogenic phenotype and generate regulatory T cells. And the third is related to the immune suppression in the tumor microenvironment mediated by other cells and soluble factors. The balance of stimulatory and suppressive signals determines tumor progression and is related to cell tumor phenotype and the interaction among cells [43].

There are many tumor microenvironment factors that suppress DC activation in vitro, for example, IL-10, vascular endothelial factor, prostaglandin E2, hypoxia, and lactic acid [47]. Another important interaction is when breast tumor and DC are in contact. Chen et al. showed a decreased expression of CD40, CD80, CD86 (costimulatory molecules), HLA-DR, and CD83 and a reduced production of IFN-γ, TNF-α, IL-1β, IL-2, IL-6, and IL-12, in lipopolysaccharide (LPS)-stimulated human DC, when co-cultured with $CTLA4^+$ breast cancer cells. These suppressive DC inhibit $CD4^+$ and $CD8^+$ T-cell proliferation, Th1 differentiation, and cytotoxic lymphocyte (CTL) function (**Figure 2**) [48].

When a transformed cell escapes of the immune recognition and destruction, and starts proliferating, it recruits different immune cells and promotes a protumoral and suppressor microenvironment. Among these tumor-recruited cells are DCs, which migrate to local lymph nodes and present tumor antigens to lymphocytes. Meanwhile some recruited DC go to lymph nodes, and another subset of DC remains in tumor and developed suppressor functions through the direct inhibition of the local activation of $CD4^+$ and $CD8^+$ T cells or through suppressive cytokine production (IL-10) (**Figure 2**) [43, 49]. These DC may have an important role in lymphocyte priming in tumor, associated with the presence of tertiary lymphoid structures (TLS) in breast tumors, specially placed in stroma and with naïve T cells in tumors that are activated in situ [50, 51].

3.1.2 Neutrophils

Neutrophils are polymorphonuclear (PMN) cells and the most abundant leukocyte in human. These cells are responsible for host defense to bacterial, fungal, and viral infections and support wound healing [52]. Neutrophils can phagocyte, form neutrophil extracellular traps (NETs) to eliminate invasive microorganisms, and synthesize and store in cytoplasmic granules neutrophil elastase, cathepsin G, proteinase 3, neutrophil collagenase (MMP-8), gelatinase B (MMP-9), reactive oxygen species (ROS), and antimicrobial peptides [53–55]. Through chemotactic stimuli, neutrophils arrive to the inflammation site and phagocyte the invading microorganism. Thereafter, cytoplasmic granules in the neutrophil get fused with the phagolysosome where the microorganism is destroyed [52]. Under adverse circumstances, neutrophil can release proteinases through microbursts, to the extracellular space, or produce NETs to fix the microorganisms, stop their migration, and concentrate on toxic factors [56].

Some authors mentioned a neutrophil polarization similar to classical activated macrophages (M1) and alternative activated macrophages (M2), named N1 and N2; also, neutrophils present different degrees of activation, and according to it, there are four types of PMN: naïve circulating, mildly activated, activated (acute inflammation), and highly activated (sepsis, unsuccessful phagocytosis). Among mildly activated neutrophils are tumor-associated neutrophils (TANs) that in mice express $CD11b^{+}$ and $Ly\text{-}6G^{hi}$ markers [52, 57].

Cellular cytotoxic role in cancer is traditionally associated with cytotoxic T cells, NK cells, and macrophages, and little attention is focused on neutrophils, but nowadays, reports are linking neutrophils to different stages of cancer [56]. Naïve neutrophils are recruited to the tumor, mainly by macrophages, and display the same repertory to kill a microorganism for the destruction of a tumor cell, and eventually a pro-host or pro-tumoral effect in situ is developed (**Figure 2**) [52].

The presence or absence and quantity of neutrophils within the tumor, associated with tumor type, determine the prognostic of the disease [57]. In an orthotopic murine model of breast cancer with 4T1 (metastatic cells) and 4T07 (nonmetastatic cells), more neutrophils within 4T1 tumors in comparison to 4T07 tumors were detected. Also in 4T1 tumors, higher mRNA expression of CXCL1, a neutrophil-recruiting chemokine, was detected [58]. For example, a pre-metastatic niche has been reported in remote organs, where neutrophils come together and shape a microenvironment that favored the migration of tumor cells (**Figure 2**) [59]. One of the mechanisms that shape a pre-metastatic niche could be mediated by NETs, as has been demonstrated in an experiment where neutrophils were co-cultured with 4T1 cells in a transwell chamber assay and produced more NETs than neutrophils co-cultured with 4T07 cells. In the same report, authors proved the presence of NET structures located next to 4T1 cells, which was assumed to contribute to support metastasis [58].

3.1.3 Eosinophils

Eosinophils are granulocyte cells that can be found in the spleen, lymph nodes, thymus, and gastrointestinal tract [60] and are able to phagocyte and act as antigen-presenting cell in lymph nodes, through the expression of major compatibility complex and costimulatory molecules (CD40, CD80, CD86) [61]. Furthermore, eosinophils produce cytokines, chemokines, growth factors, lipid mediators, and cytotoxic granules (**Table 1**).

Eosinophils are usually related to parasitic infections, especially helminthiases, in which eosinophilia is a characteristic feature. But recently their role in cancer has become relevant. Depending on its cytokine profile production, a new classification of eosinophils has been proposed; the eosinophils that secrete Th1 cytokines (IL-8, TNF-α, and IFN-γ) are called E1, and the ones that produce Th2 cytokines (IL-4, IL-5, and IL-13) are E2. Despite this classification, in breast cancer it is unknown if the eosinophils secrete any of those cytokines, although blood eosinophilia is related to a good or poor prognostic of the disease, depending on the cancer type [79]. Related to eosinophil infiltration into the breast cancer tumor, the presence of eosinophils is one indicator of increased survival, maybe because these cells participate in host-tumor interactions and because of their cytotoxic activity [83].

3.1.4 Mast cells

Mast cells originate in bone marrow, then circulate and migrate to tissues, and in nearby blood vessels mature into effector cells, in which along with DC and macrophages, are the first cells to recognize and interact with pathogens or allergens [84, 85]. Inside mast cells there are granules with preformed substances that included histamine

		General functions	Cancer-related features
Cytokines	IL-8	Supports endothelial cell proliferation and survival [62]	Breast cancer tissue expresses higher concentrations of IL-8 than normal tissue[63]
	TNF-α	Pro-inflammatory cytokine	Chronic expression sustains breast tumor growth [64]
	IL-4	Promotes a Th2 profile, B-cell differentiation, and IgE isotype switch	
	IL-5	Stimulates proliferation, differentiation, recruitment, and activation of eosinophils [65]	
	IL-13	Regulates IgE synthesis and mucus production [66]	A higher tumor stage correlates with higher serum levels and lymph node metastasis [67]
Chemokines	CCL3, CCL5, CCL11, CCL24; CXCL8, CCL7	Chemoattractant for eosinophils	Recruitment of eosinophils to tumor
	CCL3, CCL5, CCL11, CCL17, CCL22, CCL23; CXCL1, CXCL5, CXCL8, CXCL9, CXCL10, CXCL11	Chemokines secreted by eosinophils to recruit other immune cells	Recruitment of immune cells to tumor
Growth factors	TGF-α		In mammary mouse tissue, overexpression of TGF-α induces hyperplasia and proliferation [68]
	TGF-β	Regulates cellular differentiation, proliferation, apoptosis, and migration [69]	In early stages suppresses tumor progression but in late stages favors tumor growth [69]
	VEGF	Promotes angiogenesis	Promotes tumor angiogenesis
Lipid mediators	Leukotrienes	Pro-inflammatory	Elevated levels in colon, pancreatic, and prostate cancer [70]
	Prostaglandin E2	Shifts Th2 response and downregulates $CD8^+$ T-cell activity and tumor cell antigen presentation [71]	Promotes tumor growth in breast cancer Is associated with poor prognosis [72]
	Thromboxanes		Overexpression is associated with poor prognosis in urothelial cancer [73]
	Lipoxins (lipoxin A4)		Suppressing the polarization of B regulatory cells [74]

		General functions	Cancer-related features
Cytotoxic granules	Eosinophil cationic protein	Tissue remodeling, suppression of T-cell proliferation, mast cell degranulation, and secretion of airway mucus [75]	Proliferation inhibition in colorectal carcinoma and oral squamous cell carcinoma cell lines, via osmotic lysis [76, 77]
	Major basic protein	Tissue damage	Cytotoxic effect in human cancer cell lines [78]
	Eosinophil-derived neurotoxin	Cytotoxic activity and chemoattractant of DC, monocytes, neutrophils, mast cells, and T cells [79]	Cytotoxic activity in colorectal carcinoma cell line [80]
	Eosinophil peroxidase	Related to inflammatory tissue injury [81]	Absent in normal breast tissue but present in breast cancer tumor stroma [82]

CCL5 or RANTES, regulated on activation normal T expressed and secreted; CCL3 or MIP-1α, macrophage inflammatory protein; CCL7 or MCP-3, monocyte-specific chemokine protein; TGF-α, transforming growth factor α; TGF-β, transforming growth factor β; VEGF, vascular endothelial cell growth factor; GM-CSF, granulocyte macrophage colony-stimulating factor

Table 1.
Functions and related cancer features of cytokines and chemokines.

(vasodilator), heparin (anticoagulant), serotonin, dopamine, tryptase, and chymase. The mast cell activation stimulates the production of leukotrienes and cytokines (e.g., TNF-α) and the cell degranulation [86].

Mast cells may perform both immunosuppressive and inflammatory functions depending on the interaction with the effector or regulatory immune cells [85]. For example, the expression of MHC-II in mast cells can be induced by the exposure of LPS and IFN-γ, and the interaction of MHC-II-expressing mast cells with effector T cells induces the expansion of Treg cells; meanwhile, mast cells expressing MHC-I can enhance the proliferation of $CD8^+$ T cells [87, 88]. Besides direct contact with T cell, an alternative activation mechanism could be the mast cell production of IFN. This cytokine enhances the proliferation of T cells, depending on the number of mast cells within the microenvironment, for example, at low numbers proliferation is enhanced, but in higher numbers proliferation is inhibited, in a mechanism mediated by the H1 histamine receptor [89, 90].

On the other hand, for naïve B-cell survival and activation and for plasma cell proliferation and differentiation, mast cells interact with B cell through superficial CD40L. Also for the B-cell synthesis of IgE, the secretion of IL-4 and IL-13, among others, by mast cells is necessary [85].

Despite mast cells releasing angiogenic factors, as VEGF, chymase, tryptase, heparin, fibroblast growth factor-2 (FGF-2), IL-8, TGF-β, and nerve growth factor, the inhibition of mast cell degranulation did not change the mammary tumor vascularization, but that does not mean that degranulation may enhance angiogenesis [91]. In this regard, a study informed that tryptase did not stimulate the proliferation of MDA-MB-231 breast cancer cells but indeed enhances its migration and invasion [92]. In malignant breast carcinomas, there are more tryptase-containing mast cells detected through immunohistochemistry assay than that in benign lesions [93]. Given the prominent angiogenic character of mast cells, to date, their presence has not been strongly associated with the enhancement of the tumor

vascularization, and it is not clear if comorbidities favoring increased quantities of mast cells may improve tumor vascularization and metastasis.

3.1.5 Macrophages

Macrophages are mononuclear phagocytic cells that according to environment signals turn into different phenotypes. One of these phenotypes is the classically activated macrophages or M1, induced by Toll-like receptors (TLR) and IFN-γ. These cells are characterized by the expression of IL-12, the major histocompatibility complex class II (MHC-II) and TNF-α, and ROS and nitric oxide (NO) production and are associated with microorganisms and cell destruction [94]. The second phenotype is the "alternatively or selectively" activated macrophages, which are characterized by the secretion of IL-4, IL-10, IL-13, and TGF-β and the expression of arginase-1 and VEGF and are related to wound healing and humoral response [94, 95].

Macrophages, monocytes, and DC can be found in tumor microenvironment, being the macrophages the most abundant phagocytic population. Tumor-associated macrophages (TAMs) are characterized by the cell surface expression of CD68 and have been related to invasion and migration of cancer cells, being a prognostic factor in cancer [95, 96]. Some reports have shown that the density of TAMs in breast cancer samples is related to hormone receptor status, lymph node metastasis, stage, and prognosis. Higher concentrations of TAMs are associated with a poor prognosis, and the worse prognostic group is the one with a high proportion of CD163 and CD206 (M2 markers) [95].

TAMs are related to immunosuppressive features, for example, low antigen-presenting capability, low tissue remodeling activity, and low toxicity functions that promote tumor growth and metastasis [97]. These immunosuppressive TAMs function as M2 macrophages and are activated by IL-4, IL-10, IL-13, glucocorticoids, and vitamin D_3 [98].

3.1.6 NK cells

The innate immune system recognizes and kills infected and transformed cells; NK cells are responsible for this task, through granzyme b-perforin system, TNF-related apoptosis-inducing ligand (TRAIL), and the expression of CD95 ligand [99]. NK cells produce IFN-γ, granulocyte/macrophage colony-stimulating factor (GM-CSF), and TNF [100] and are one of the main cells in antitumoral response.

Depending on the signals that NK cells receive, activation or inhibition receptors or coreceptors are expressed [101, 102].

NK cell cytotoxicity is activated by different ligands upregulated during cellular stress, also with the recognition of antibodies in the antibody-dependent cellular toxicity (ADCC) through the expression of CD16 (Fc immunoglobulin fragment low-affinity receptor) and with the detection of cells that underexpressed HLA-class I molecules [101, 103]. In immunosurveillance, tumor cells are detected and destroyed by NK cells, through these mechanisms (**Figure 2**). In immunosubversion, tumor cells evade NK cell recognition, and tumor microenvironment leads to NK cell impairment, through the inhibition of surface-activating receptor expression, such as NKp46 and NKG2D or NKp30 and NKG2D mediated by indoleamine 2,3-dioxygenase (IDO) and TGF-β1, respectively (**Figure 2**) [101, 104, 105].

In breast cancer patients, tumor NK cells possess a more prominent inhibitory phenotype than peripheral NK cells. Also depending on disease progression, for example, in late stages, NK cells lose their cytotoxic activity and express inhibitory

receptors (NKG2A); meanwhile, in early stages NK cells express activating receptors (NKp30, NKG2D, DNAM-1, and CD16). One of the stroma-derived suppressor factors that induced NK cell function impairment is TGF-β1 [101].

3.2 Immune adaptive cells in mammary tumors

3.2.1 T lymphocytes

T lymphocytes are one of the most important cell populations in cancer. The activation of T cells is performed, firstly, through TCR stimulation with its specific antigen, presented in the context of MHC, by a dendritic cell or another professional antigen-presenting cell; secondly, with the binding of "costimulatory" molecules in the dendritic cell; and, thirdly, by the cytokine milieu and soluble factors [106, 107]. In addition, antigen presentation is performed by immature DCs, resulting in a non-responsive or anergic T cells [108]. In breast cancer tertiary lymphoid structures and germinal centers were detected next to tumor in extensively infiltrated tumors. This TLS possesses a similar structure to lymph node, including a T-cell zone with $CD3^+/CD4^+$ T cells and a germinal center with B cells and T follicular helper (Tfh) cells [109].

3.2.2 T helper cells

Different factors such as the expression of transcription factors, chemokine receptors, signal transduction activators, and the chemokine and cytokine secretion regulate the effector phenotype and function of these cells [107]. Regarding human breast cancer, different effector phenotypes have been reported, for example, through flow cytometry of invasive breast tumors, Tfh, Th1, Th2, Th17, and Tregs were found [109].

3.2.3 T follicular helper (Tfh) cell

The effector phenotype Tfh cell stays in the lymph node and induces activation and differentiation of affine B cells into plasma or memory cells [110]. But, in advanced stages of invasive breast cancer, $CD4^+$ Tfh cells were detected in the T-cell zone and germinal centers of TLS. This localization is may be due to their function in tumor, because Tfh cells were localized near to B cells [111].

3.2.4 T helper 1 (Th1)

$CD4^+$ T helper 1 (Th1) cell differentiation and IFN-γ production are modulated by IL-12 produced by APCs (monocytes/macrophages, DCs, and even NK cells) and IFN-γ (**Figure 2**) [112–114]. Th1 cells express the transcription factor T-bet; secrete IFN-γ, TNF-α, and IL-2; and function as regulators of monocyte activation and T lymphocyte differentiation induction [115, 116]. Th1 cells are associated with early tumor phases, because of their IFN-γ production that activates $CD8^+$ cytotoxic T cells (**Figure 2**) [117]. Therefore, there is an association between improving survival and the infiltration of Th1 and $CD8^+$ T cells in breast tumors [118].

3.2.5 T helper 2 (Th2)

A T helper subset related to immunosubversion and tumor progression is the $CD4^+$ T helper 2 (Th2) cells, characterized by the expression of transcription factor GATA3 and the secretion of IL-4, IL-5, IL-10, and IL-13 [121]. Th2 cells are related to

nematode response, tissue repair, and antibody production. In breast cancer, Th2 cells have been found in human mammary tumors [109], and IL-13 is reported to be present also in human breast tumors, promoting tumor development (**Figure 2**) [119].

3.2.6 T helper 17 (Th17)

$CD4^+$ Th17 (T helper 17) cells are related to autoimmunity, tissue inflammation, and host defense against bacteria, fungi, viruses, and protozoa and play an important role in mucosal immunity [120]. Th17 cells produce IL-17 and IL-22 and express transcription factor RORγt [121]. Regarding Th17 cells in tumor, it is not recognized if they could be induced in tumor or be recruited from other places, but their presence has been detected in breast tumors [109]. Th17 cell tumor infiltration mediates an inflammatory microenvironment [122].

3.2.7 Regulatory T cells (Tregs)

Tregs are a subset of T helper cells that express Foxp3 transcription factor and have an important role in controlling inflammation and autoimmunity in mouse and man [123]. These cells normally are residents in the secondary lymphoid organs, lung, peripheral blood, gastrointestinal tract, liver, and skin and can be recruited to other tissues, under inflammatory conditions [124]. Tregs are $CD4^+$, $CD127^{low}$, $CD25^{hi}$, and also $CTLA^+$ and exert immune suppression through different mechanisms, for example, the production of tolerogenic cytokines (IL-10, IL-35, and TGF-β), the induction of arginine depletion that leads to T-cell dysfunction, the expression of suppressive molecules (CTLA-4, CD80/CD86), and the direct cytolysis through granzyme b-perforin system and through local consumption of IL-2 (with the constitutive expression of high-affinity receptor CD25) [125, 126].

IL-10 is a suppressive cytokine secreted by macrophages, NK cells, NKT cells, B cells, DCs, and $CD4^+$ T cell (specially Treg cells), that suppress inflammatory responses, prevent autoimmune diseases, and enhance tumor growth (**Figure 2**) [127–129].

3.2.8 T cytotoxic lymphocytes (CTLs)

$CD8^+$ cytotoxic T lymphocytes play an important role in adaptive antitumor response; therefore, when tumor immunosubversion is stablished, the cytotoxicity of $CD8^+$T cells gets compromised (**Figure 2**). During immunosurveillance, in secondary lymphoid organs (lymph nodes and spleen), APCs present tumor-associated antigens and tumor neoantigens to CTLs, which in the presence of costimulatory and cytokine signals, such as IL-12 (produced by DCs) and IFN-γ (produced by Th1 cells), undergo activation, maturation, and clonal expansion [117, 130]. After, CTLs migrate through the body, search for specific antigen, and kill the tumor antigen-specific cell through IFN-γ release and perforin and granzyme system (**Figure 2**) [117, 131, 132]. Also, through the activation of its receptor, IL-12 promotes the differentiation of effector CD8 cells and inhibits at the same time the development of memory CD8 cells [133, 134]. When effector CTL cells failed in killing target cell and are exposed to persistent antigen stimulation (in chronic infectious diseases or in tumors), CTL express inhibitory cell surface receptors, PD-1, LAG3, TIM3, TIGIT, and CTLA-4, and became exhausted $CD8^+$ T cells. During tumor immunosubversion $CD8^+$ T cell exhausted profile is generated; therefore, cytolysis or IFN-γ secretion mediated through CTLs is inhibited (**Figure 2**) [135].

Another important cytokine related to $CD8^+$ T cells is IL-2, which is described not only as a growth factor, secreted by $CD4^+$- and $CD8^+$-activated T cells, but also

as a differentiation inducer for $CD8^+$ effector cells [115]. $CD8^+$ T cells cultured with IL-2 presented an upregulation in perforin (Prf1) transcription and a suppressed expression of Bcl6 and IL-7Rα (memory $CD8^+$ markers). Meanwhile, in $CD8^+$ T cells with deficiency of IL-2 receptor (IL-2Rα or CD25), cell differentiation impairment was shown in vivo, demonstrated with granzyme B and perforin diminished expression and a poor ex vivo cytotoxicity [136].

In regard to $CD8^+$ T cell antitumor activity, an experiment in tumor from four T1 mammary gland tumor cells in syngeneic mice showed that in mice injected with IL-12, tumor growth was suppressed through an increased $CD8^+$ cell infiltration and production of IFN-γ and the induction of apoptosis of tumor cells [137]. This effect correlates with good prognosis in $CD8^+$ T cell infiltration in breast tumors in women [138]. With the time, CTLs lose their cytotoxic phenotype and acquired an exhausted phenotype that needs further characterization in breast tumors but is likely to be associated with late stages (triple-negative breast cancer).

4. Endocrine factors related to the development of breast cancer

Mammary gland epithelium is highly dynamic, characterized by proliferation, differentiation, and apoptosis cycles, regulated in part by hormones. Breast cancer is associated with an abnormal proliferation of epithelial cells, related to genetic mutations and epigenetic modifications in suppressor and DNA repair genes and oncogenes [139].

4.1 Estrogens and progesterone

During life, the mammary gland development is divided by different stages and modulated by hormones such as estrogens (17β estradiol) and progesterone. These stages are related to sexual development and includes embryonic and prepuberal phase, puberty, pregnancy, lactation, and involution. Epidermal growth factor (EGF) and estrogens that arrive through the breast stroma during puberty induce ductal elongation and branching. Meanwhile, the lobes formed by secretory epithelial cells organized in alveoli develop during gestation and probably in lactation, through the placental lactogens, progesterone, and prolactin signaling [140]. In lactation, milk secretion is promoted by the contraction of rounding epithelium smooth muscle cells mediated by oxytocin [8].

Estrogen effects are regulated through alpha and beta estrogen receptors (ERα and ERβ), both expressed in mammary normal tissue [141]. ERα signaling is responsible for ductal elongation in puberty and the stromal invasion in normal breast tissue [142].

The sharing ERα-ERβ distribution suggests that ERβ may be related to a negative ERα regulation, through antiestrogen or non-habitual effects [143]. The ERα or ERβ receptor dimerization is induced by ligand-receptor union and leads to the formation of homodimers (ERα/α, Erβ/β) or heterodimers (ERα/β). Recently, it was described that the dimer conformation is associated with their function. ERα/α is linked with proliferation induced by estrogen, and ERβ/β homodimer is linked with antiproliferative and pro-apoptotic functions; meanwhile, ERα/β effects are not elucidated as well (**Figure 3**) [144].

Proliferation in breast tumor cells is ligand-dependent in early stages and ligand-independent in late stages. In the estrogen-dependent pathway, cell proliferation is activated through cytoplasmic or membrane estrogen receptors. Intracellular signaling begins with estrogen-receptor union, their consequent translocation to nuclei, where the estrogen-receptor complex binds to specific

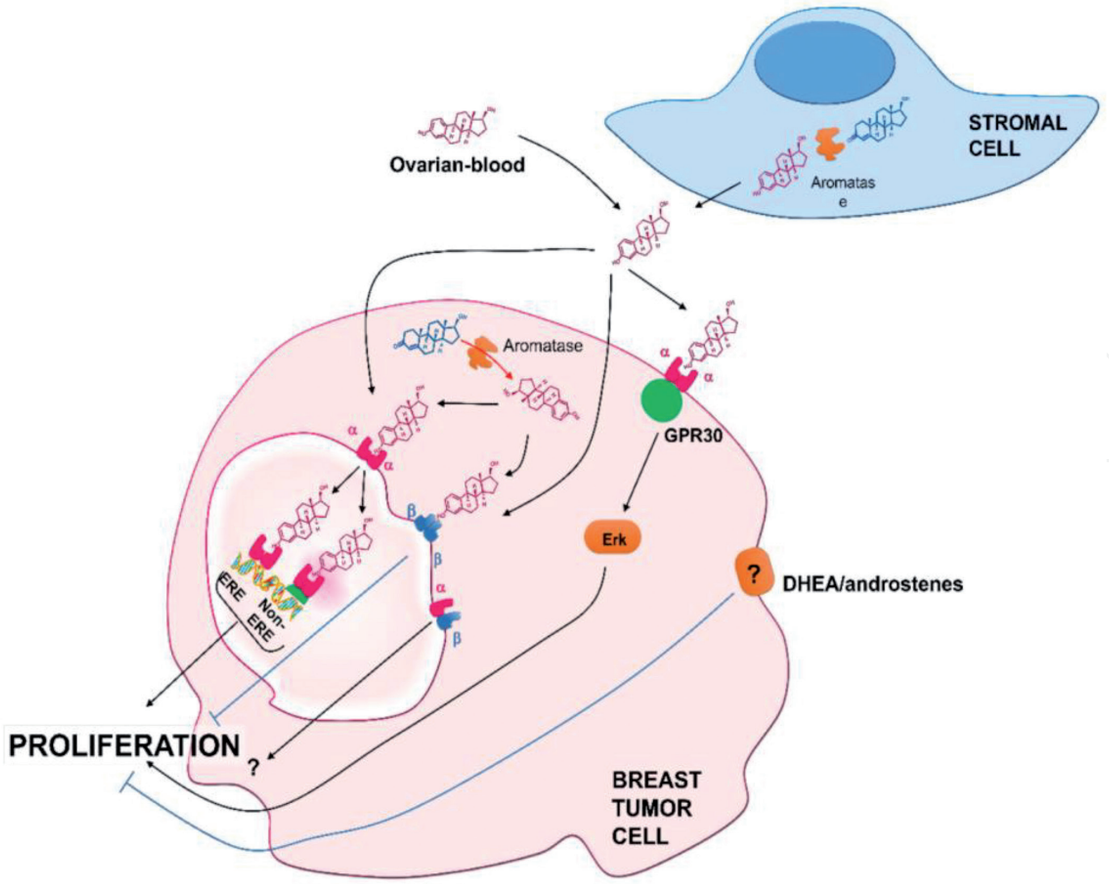

Figure 3.
Endocrine interactions in breast cancer. In the estrogen-dependent pathway, cell proliferation is activated through cytoplasmic or membrane estrogen receptors. Intracellular signaling begins with estrogen-receptor union, their consequent translocation to nuclei, where the estrogen-receptor complex binds to specific estrogen-response elements (ERE) in estrogen-responsive genes, in a non-ERE way, functioning as gene transcription co-regulator. Furthermore, estrogen-membrane ER signals through GPR30 and Erk to elicit proliferation. Estrogen sources to breast tumor cell are intracrine, endocrine (blood supply), and paracrine (stromal adjacent cells). Dehydroepiandrosterone (DHEA) and other androstenes inhibit tumor cell proliferation.

estrogen-response elements in estrogen-responsive genes or to other transcription factors, such as AP1 or Sp1, in a non-ERE way, functioning as gene transcription co-regulator [145, 146]. Furthermore, estrogen-membrane ER signals through GPR30 and Erk to elicit proliferation (**Figure 3**) [145]. Meanwhile, the estrogen-independent pathway is mediated through ligand binding and activation of growth factor receptors (GFRs), such as epithelial growth factor receptor (EGFR), insulin-like growth factor receptor (IGF), and HER-2, among others. This activation promotes ER phosphorylation and activation through PI3K/AKT and Ras/Raf/MAPK pathways [145, 147].

On the other hand, progesterone exerts its action through two receptors (PRA and PRB), both signaling and activating gene transcription [148]. ERα and PR are co-expressed in the mammary gland in 15–30% of epithelial cells [149]. Meanwhile, estradiol and progesterone drive epithelial mammary gland proliferation directly through the hormone-receptor union and have been proposing a second control mechanism in which epithelial cells sense hormone concentrations through their estrogen and progesterone receptors and, in consequence, secrete or not growth factors to promote nearby cell proliferation [148].

In breast cancer staging, ER and/or PR expression loss is associated with more aggressive tumors, with self-sufficiency of growth signals independently of estrogen or progesterone receptors. Additionally, positive ERα tumor is related to a better prognostic, as well as ERβ tumor expression [150].

Besides the receptor's presence in tumor cells, another important issue to consider is the hormone levels within the tumor. Intratumoral estradiol concentration in normal breast tissue was lower than in ductal carcinoma in situ and invasive ductal carcinoma [151].

In this regard, aromatase is an important enzyme responsible for the production of estrogens, estrone, and estradiol, through the aromatization and conversion of androstenedione and testosterone [152]. Invasive ductal carcinoma expresses a higher amount of aromatase mRNA than DCIS and normal breast tissue, and both epithelial and stromal cells expressed aromatase mRNA [151]. Therefore, tumor cells have different sources of estrogen, called endocrine (ovary), intracrine, and paracrine, which enhance cell proliferation of tumor target cells.

4.2 Androgens

Meanwhile estrogens stimulate mammary gland development, and androgens inhibit it. For example, estrogen treatment in prostate cancer patients promotes mammary gland growth and ingestion of androgens by athletes or transsexuals and produces mammary gland atrophy [153].

Androgens as testosterone (T) and dihydrotestosterone (DHT) exert their effects through the union to their androgen receptor (AR). This receptor has been colocalized with ER and PR in mammary gland epithelia, but not in adjacent stromal cells; therefore, androgen-mediated proliferation is regulated in the mammary epithelium [154]. The androgen receptor (AR) has been reported to be present in 80% of primary breast tumors, and its presence is associated with a favorable response to endocrine treatment and a better prognostic, especially if ER is also present [155].

In this sense, the union of BRCA1 gene product with AR activates AR functions; therefore, the mutation of this BRCA1 may interfere with AR antiproliferative functions and allow cell proliferation [156].

4.3 Adrenal steroids

Dehydroepiandrosterone, an estrogen and testosterone precursor [157], is an adrenal steroid which is metabolized into active metabolites, such as Δ5-androstene-3β, 17β-diol (17β-androstenediol), Δ5-androstene-3β17α-diol (17α-androstenediol), and Δ5-androstene-3β,7β,17β-triol (17β-androstenetriol) [158]. DHEA is able to activate ERα, ERβ, AR, and glucocorticoid receptor (GR); meanwhile, its metabolites showed a weaker activation [159]. All of androstene hormones (DHEA, 17β-androstenediol, 17α-androstenediol, and 17β-androstenetriol) have been shown to have an antiproliferative effect in cellular lines, including breast cancer (**Figure 3**) [160]. Only DHEA presented a protective effect in vivo, but the other androstenes have not been tested in vitro [160]; therefore, there is a promising search field around androstenes and the development of breast cancer.

5. Tumor development and neuroimmunoendocrine interactions

The relation between nervous and immune systems is importantly transduced through β_2AR and GCR localized in immune cells, such as B lymphocytes, T lymphocytes, NK cells, and macrophages, which regulate cytokine production, molecule expression, development, survival, proliferation, circulation, and cell recruitment [161]. Meanwhile, interactions among endocrine and immune or nervous systems are regulated through the hormone receptor expression (ER, PR, and AR) and the effects driving in immune and/or nervous cells (**Figure 4**).

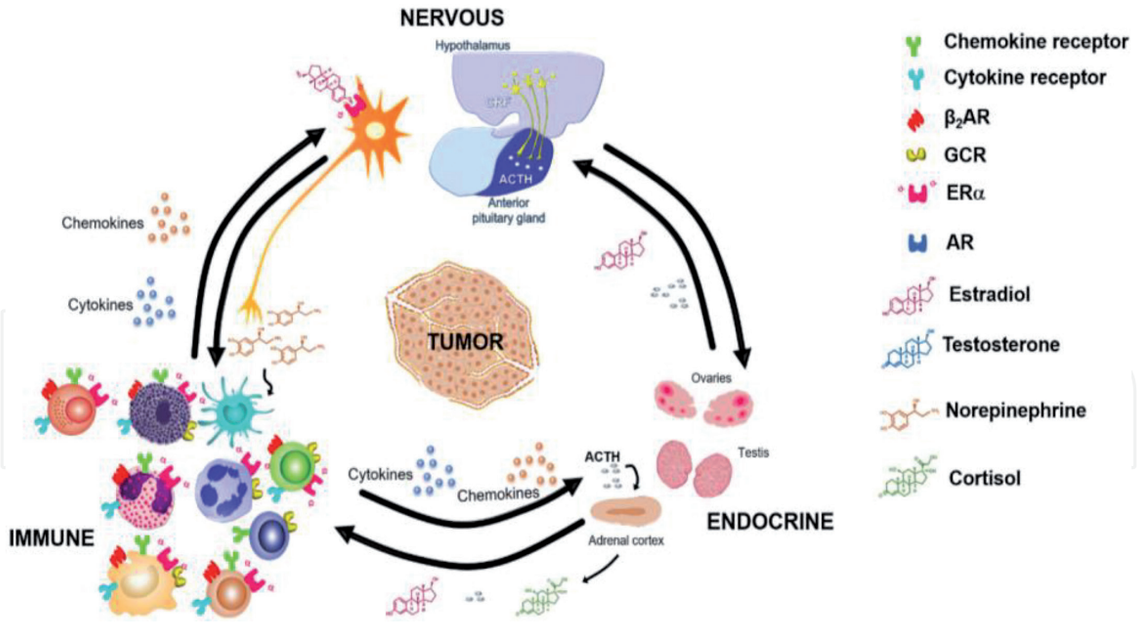

Figure 4.
Neuroimmunoendocrine interactions in breast cancer. Bidirectional interactions among nervous, immune, and endocrine systems are stablished by soluble factors and receptors in cells of the three systems.

In mice treated with selective β_2AR agonists, such as clenbuterol or salbutamol, to stimulate these receptors, the lymph node egress of $CD4^+$, $CD8^+$ T lymphocytes, and antigen-primed T cells and B cells is retarded and is associated with lymphopenia. This lymphocyte retention is mediated through CXC chemokine receptor 4 (CXCR4) in T cells and B cells and is thought to explain the reduction of T-cell-mediated inflammation and lymphopenia [161]. CXCR4 is also expressed in monocytes and dendritic cells. CXCR4 ligand is the stromal cell-derived factor 12 (CXCL12), and both are linked to breast cancer metastasis. CXCR4-CXCL12 union promotes cell migration and adhesion and angiogenesis [162].

In lymph nodes with breast cancer metastasis, an increased level of CXCR4 transcript was detected compared to nonmetastatic lymph nodes. Also, a higher mRNA expression was found in breast cancer tumor stages III–IV than in stages I–II. Interestingly, in tumor tissues with HER-2 expression, CXCR4 transcription levels are also more elevated than in HER-2-negative tumors; therefore, there is a positive correlation between CXCR4 and HER-2 expression in breast tumors [163]. This phenomenon is explained because HER-2 enhances and impedes CXCR4 degradation [164]. CXCR4-CXCL12 axis is evolved in organ-directed metastasis, mainly associated with a higher CXCL12 expression in lymph nodes and lung, liver, and bone tissues where breast cancer metastasis is very common. CXCL12 acts as a chemoattractant for breast cancer cells that express CXCR4, promoting the arrival of these cells [165, 166].

Another group of immune cells, in which β_2AR produces an inhibitory effect, is the DCs. The stimulation of β_2AR with salbutamol inhibited the NF-κB transcription [167]. This transcription factor is required for DC antigen presentation; for the expression of CD80, CD86, and CD40 (costimulatory molecules); and for IL-12 secretion [168]. Also, salmeterol (β_2AR agonist) diminishes the IL-1, IL-6, and TNF-α production, in LPS-activated DCs [169].

On the other hand, in human monocytes primed during 16 hours with IFN-γ and stimulated with LPS, the addition of salbutamol diminished the IL-12 and TNF-α secretion, but not the IL-1α, IL-1β, or IL-10 production. Also, in neonatal $CD4^+$ lymphocytes, the Th1 cell differentiation in vitro was inhibited; instead, these $CD4^+$ T cells, stimulated with β_2AR agonists, produce IL-4 (Th2 cytokine), but not

IFN-γ (Th1 cytokine) [168]. Meanwhile in rats, adrenaline or metaproterenol (β_2AR agonist) in physiologic doses inhibited NK cell activation [170].

Either by directly action on tumor or immune cells, sympathetic signals regulate tumor progression. In this regard, as mentioned before, immune cell recruitment is a crucial step in immunosurveillance and immunosubversion. Sympathetic innervation in distant organs such as bone marrow promotes noradrenaline secretion that activates bone marrow-resident cells and promotes immune cell development and trafficking [171] and the posterior cell recruitment to tumor microenvironment mediated through tumor chemokine release and chemokine receptor expression in immune cells [166]. In this sense, tumor primary macrophage recruitment [39] and tumor cells increasing cytokine pro-inflammatory expression [21] are β_2AR mediated and influencing tumor progression [37, 39].

Despite the differences in β_2AR breast tumor cell expression that as an example in MB-231 cell line is higher than in MB-231BR cell line, the treatment with a β_2AR agonist (terbutaline or norepinephrine) modulates VEGF secretion through cAMP-PKA pathway, which is diminished in MB-231 cell line and augmented in MB-231BR cell line (metastatic to mouse brain). Meanwhile, IL-6 production in both cell lines was increased, in a cAMP-dependent and PKA-independent pathway [21]. These differences in VEGF secretion are maybe associated with the brain metastatic potential of MB-231BR cell line, because VEGF enhances blood vessel neoformation for tumor growth.

As mentioned before, immunosuppressive TAM works as M2 macrophages and, in this sense, has been found that epinephrine induces M2 macrophage polarization, in RAW 264.7 cells. This polarization is regulated through β_2AR. Also, in breast tumors co-expression of $CD163^+$ (M2 macrophages human marker) and β_2AR cell has been demonstrated; thus, macrophages in tumor microenvironment are influenced by adrenergic signals [37]. The relationship between M1 or M2 macrophages and hormone receptor status in breast cancer is due to the development of the disease. Hollmen et al. reported that when a cell line positive for the estrogen receptor (ER) is co-cultured with human monocytes, they acquire an M1 phenotype; meanwhile, the co-culture of them with ER- breast cancer cell line induced an M2 phenotype. The above indicates that ER governs the changes of the macrophages phenotype [172]. ER^+ breast cancer is related with an "early" development and a better prognostic, maybe associated with a M1 acute phase inflammatory response that effectively controls tumor progression. Meanwhile, TNBC usually presents a worse prognosis, and the presence of M2 exerts an immunosuppressive intratumoral effect that allows breast tumor growth and metastasis. Therefore, the macrophage phenotype is due to microenvironmental conditions and is associated consequently with tumor staging and prognosis.

Overexpression of HER-2 is correlated with β_2AR expression levels in breast tumor samples. In this sense, in MCF-7 cells overexpressing HER-2 (MCF-7/HER-2), β_2AR expression was also elevated, in an autocrine way through MCF-7/HER-2 epinephrine secretion. Interestingly, β_2AR activation with epinephrine, with norepinephrine, or with β_2AR agonists (isoproterenol and salmeterol) induces HER-2 expression in MCF-7 breast cancer cells. These findings are important because in $HER\text{-}2^+$ breast cancer cells, the activation of this surface tyrosine kinase may improve epinephrine secretion, through ERK signaling. Epinephrine may upregulate either β_2AR expression or HER-2 [173].

Concerning to breast cancer, in more aggressive tumors (TNBC), an increased amount of $Foxp3^+$ lymphocytes can be found in than less aggressive tumors (ER^+ or HER^+ tumors); this higher Treg tumor infiltration is also related to an increased risk of recurrence and a poor prognosis [174].

Ali et al. reported that in ER^- and HER^+ breast tumors, $CD8^+$ cell infiltration in tumor was associated with a reduction (28%) of mortality risk, but if these cells were in the tumor stroma, the risk reduction was lower (21%). A similar risk reduction (27%) was found in ER^+/HER^+ breast tumors [138]. The $CD8^+$ T-cell presence in tumor is associated then with the induction of tumor cell apoptosis that improve the prognosis and in some point is still acting as an effector-killing cell rather than a memory cell.

6. Conclusion

In breast cancer development, tumor cell proliferation is extensively studied, and almost all the treatments are encouraged to diminish it. Tumor cell interactions with other immune, nervous, tumor, and stromal cells, through the production of soluble factors and the expression of receptors, are the drivers of this proliferation. These relations may be driven inside the tumor or across the organism in distant places that respond to tumor signals. Therefore, elucidating not only molecular mechanisms but interactions among cells may enhance the development of new and more effective therapies against breast cancer.

Acknowledgements

The authors are grateful for the financial support received from the following agencies: Grant IN-209719 from Programa de Apoyo a Proyectos de Innovación Tecnológica (PAPIIT), Dirección General de Asuntos del Personal Académico (DGAPA), and Universidad Nacional Autónoma de México (UNAM) and Grant 2125 from Fronteras en la Ciencia, Consejo Nacional de Ciencia y Tecnología (CONACYT), both to J. Morales-Montor. Grant IA-202919 from Programa de Apoyo a Proyectos de Innovación Tecnológica (PAPIIT), Dirección General de Asuntos del Personal Académico (DGAPA), and Universidad Nacional Autónoma de México (UNAM) to KE. Nava-Castro. Rocío Alejandra Ruiz-Manzano is a PhD student at Programa de Doctorado en Ciencias Biomédicas, Universidad Nacional Autónoma de México, and received a fellowship from CONACyT. Mariana Segovia-Mendoza and Margarita Isabel Palacios-Arreola are postdoctoral fellows from DGAPA, UNAM.

Conflict of interest

The authors declare that there is no conflict of interest.

Author details

Rocío Alejandra Ruiz-Manzano[1], Tania de Lourdes Ochoa-Mercado[1], Mariana Segovia-Mendoza[1], Karen Elizabeth Nava-Castro[2], Margarita Isabel Palacios-Arreola[2] and Jorge Morales-Montor[1]*

1 Immunology Department, Biomedical Research Institute, National Autonomous University of Mexico, Mexico City, Mexico

2 Ambiental Genotoxicity and Mutagenesis Laboratory, Environmental Sciences Department, Atmospheric Sciences Center, National Autonomous University of Mexico, Mexico City, Mexico

*Address all correspondence to: jmontor66@biomedicas.unam.mx; jmontor66@hotmail.com

References

[1] Globocan W. Breast Cancer Fact Sheet Lyon [updated]. France: WHO; 2018 Available from: http://gco.iarc.fr/today/fact-sheets-cancers

[2] Jemal A, Siegel R, Ward E, Hao Y, Xu J, Thun MJ. Cancer statistics, 2009. CA: A Cancer Journal for Clinicians. 2009;**59**(4):225-249

[3] Barnard ME, Boeke CE, Tamimi RM. Established breast cancer risk factors and risk of intrinsic tumor subtypes. BBA Reviews on Cancer. 2015;**1856**(1):73-85

[4] Nava-Castro KE, Morales-Montor J, Ortega-Hernando A, Camacho-Arroyo I. Diethylstilbestrol exposure in neonatal mice induces changes in the adulthood in the immune response to taenia crassiceps without modifications of parasite loads. BioMed Research International. 2014;**2014**:498681

[5] Palacios-Arreola MI, Nava-Castro KE, Rio-Araiza VHD, Perez-Sanchez NY, Morales-Montor J. A single neonatal administration of bisphenol a induces higher tumour weight associated to changes in tumour microenvironment in the adulthood. Scientific Reports. 2017;**7**(1):10573

[6] Giuliano AE, Connolly JL, Edge SB, Mittendorf EA, Rugo HS, Solin LJ, et al. Breast cancer-major changes in the American joint committee on cancer eighth edition cancer staging manual. CA: A Cancer Journal for Clinicians. 2017;**67**(4):291-303

[7] Macias H, Hinck L. Mammary gland development. WIREs Developmental Biology. 2012;**1**(4):533-557

[8] Hennighausen L, Robinson GW. Signaling pathways in mammary gland development. Developmental Cell. 2001;**1**(4):467-475

[9] Gusterson BA, Warburton MJ, Mitchell D, Ellison M, Munro Neville A, Rudland PS. Distribution of myoepithelial cells and basement membrane proteins in the normal breast and in benign and malignant breast diseases. Cancer Research. 1982;**42**(11):4763-4770

[10] Barcellos-Hoff MH, Aggeler J, Ram TG, Bissell MJ. Functional differentiation and alveolar morphogenesis of primary mammary cultures on reconstituted basement membrane. Development. 1989;**105**(2):223-235

[11] Hanahan D, Coussens LM. Accessories to the crime: Functions of cells recruited to the tumor microenvironment. Cancer Cell. 2012;**21**(3):309-322

[12] Hanoun M, Maryanovich M, Arnal-Estapé A, Frenette PS. Neural regulation of hematopoiesis, inflammation, and cancer. Neuron. 2015;**86**(2):360-373

[13] Elefteriou F. Chronic stress, sympathetic activation and skeletal metastasis of breast cancer cells. BoneKEy Reports. 2015;**4**:693

[14] Cole SW, Nagaraja AS, Lutgendorf SK, Green PA, Sood AK. Sympathetic nervous system regulation of the tumour microenvironment. Nature Reviews. Cancer. 2015;**15**:563

[15] Bellinger DL, Lorton D. Autonomic regulation of cellular immune function. Autonomic Neuroscience: Basic & Clinical. 2014;**182**:15-41

[16] Bellinger DL, Millar BA, Perez S, Carter J, Wood C, Thyagarajan S, et al. Sympathetic modulation of immunity: Relevance to disease. Cellular Immunology. 2008;**252**(1-2):27-56

[17] Nance DM, Sanders VM. Autonomic innervation and regulation of the immune system (1987-2007). Brain, Behavior, and Immunity. 2007;**21**(6):736-745

[18] Madden KS. Sympathetic neural-immune interactions regulate hematopoiesis, thermoregulation and inflammation in mammals. Developmental and Comparative Immunology. 2017;**66**:92-97

[19] Du YY, Zhou LH, Wang YH, Yan TT, Jiang YW, Shao ZM, et al. Association of alpha2a and beta2 adrenoceptor expression with clinical outcome in breast cancer. Current Medical Research and Opinion. 2014;**30**(7):1337-1344

[20] Powe DG, Voss MJ, Habashy HO, Zanker KS, Green AR, Ellis IO, et al. Alpha- and beta-adrenergic receptor (AR) protein expression is associated with poor clinical outcome in breast cancer: An immunohistochemical study. Breast Cancer Research and Treatment. 2011;**130**(2):457-463

[21] Madden KS, Szpunar MJ, Brown EB. Beta-adrenergic receptors (beta-AR) regulate VEGF and IL-6 production by divergent pathways in high beta-AR-expressing breast cancer cell lines. Breast Cancer Research and Treatment. 2011;**130**(3):747-758

[22] Choy C, Raytis JL, Smith DD, Duenas M, Neman J, Jandial R, et al. Inhibition of beta2-adrenergic receptor reduces triple-negative breast cancer brain metastases: The potential benefit of perioperative beta-blockade. Oncology Reports. 2016;**35**(6):3135-3142

[23] Pon CK, Lane JR, Sloan EK, Halls ML. The beta2-adrenoceptor activates a positive cAMP-calcium feedforward loop to drive breast cancer cell invasion. The FASEB Journal. 2016;**30**(3):1144-1154

[24] Cole SW, Sood AK. Molecular pathways: Beta-adrenergic signaling in cancer. Clinical Cancer Research. 2012;**18**(5):1201-1206

[25] Kumar N, Gupta S, Dabral S, Singh S, Sehrawat S. Role of exchange protein directly activated by cAMP (EPAC1) in breast cancer cell migration and apoptosis. Molecular and Cellular Biochemistry. 2017;**430**(1-2):115-125

[26] Hara MR, Kovacs JJ, Whalen EJ, Rajagopal S, Strachan RT, Grant W, et al. A stress response pathway regulates DNA damage through beta (2)-adrenoreceptors and beta-arrestin-1. Nature. 2011;**477**(7364):349-U129

[27] Ayala GE, Dai H, Powell M, Li R, Ding Y, Wheeler TM, et al. Cancer-related axonogenesis and neurogenesis in prostate cancer. Clinical Cancer Research. 2008;**14**(23):7593-7603

[28] Pundavela J, Roselli S, Faulkner S, Attia J, Scott RJ, Thorne RF, et al. Nerve fibers infiltrate the tumor microenvironment and are associated with nerve growth factor production and lymph node invasion in breast cancer. Molecular Oncology. 2015;**9**(8):1626-1635

[29] Kowalski PJ, Paulino AFG. Perineural invasion in adenoid cystic carcinoma: Its causation/promotion by brain-derived neurotrophic factor. Human Pathology. 2002;**33**(9):933-936

[30] Szpunar MJ, Belcher EK, Dawes RP, Madden KS. Sympathetic innervation, norepinephrine content, and norepinephrine turnover in orthotopic and spontaneous models of breast cancer. Brain, Behavior, and Immunity. 2016;**53**:223-233

[31] Lutgendorf SK, DeGeest K, Dahmoush L, Farley D, Penedo F, Bender D, et al. Social isolation is associated with elevated tumor

norepinephrine in ovarian carcinoma patients. Brain, Behavior, and Immunity. 2011;**25**(2):250-255

[32] Stephens MA, Wand G. Stress and the HPA axis: Role of glucocorticoids in alcohol dependence. Alcohol Research: Current Reviews. 2012;**34**(4):468-483

[33] Melhem A, Yamada SD, Fleming GF, Delgado B, Brickley DR, Wu W, et al. Administration of glucocorticoids to ovarian cancer patients is associated with expression of the anti-apoptotic genes SGK1 and MKP1/DUSP1 in ovarian tissues. Clinical Cancer Research. 2009;**15**(9):3196-3204

[34] Mikosz CA, Brickley DR, Sharkey MS, Moran TW, Conzen SD. Glucocorticoid receptor-mediated protection from apoptosis is associated with induction of the serine/threonine survival kinase gene, sgk-1. The Journal of Biological Chemistry. 2001;**276**(20):16649-16654

[35] Pan D, Kocherginsky M, Conzen SD. Activation of the glucocorticoid receptor is associated with poor prognosis in estrogen receptor-negative breast cancer. Cancer Research. 2011;**71**(20):6360-6370

[36] Pang D, Kocherginsky M, Krausz T, Kim SY, Conzen SD. Dexamethasone decreases xenograft response to paclitaxel through inhibition of tumor cell apoptosis. Cancer Biology & Therapy. 2006;**5**(8):933-940

[37] Qin JF, Jin FJ, Li N, Guan HT, Lan L, Ni H, et al. Adrenergic receptor beta2 activation by stress promotes breast cancer progression through macrophages M2 polarization in tumor microenvironment. BMB Reports. 2015;**48**(5):295-300

[38] Armaiz-Pena GN, Cole SW, Lutgendorf SK, Sood AK. Neuroendocrine influences on cancer progression. Brain, Behavior, and Immunity. 2013;**30**(Suppl):S19-S25

[39] Sloan EK, Priceman SJ, Cox BF, Yu S, Pimentel MA, Tangkanangnukul V, et al. The sympathetic nervous system induces a metastatic switch in primary breast cancer. Cancer Research. 2010;**70**(18):7042-7052

[40] Zou W, Restifo NP. T(H)17 cells in tumour immunity and immunotherapy. Nature Reviews. Immunology. 2010;**10**(4):248-256

[41] Emens LA, Silverstein SC, Khleif S, Marincola FM, Galon J. Toward integrative cancer immunotherapy: Targeting the tumor microenvironment. Journal of Translational Medicine. 2012;**10**(1):70

[42] Zitvogel L, Tesniere A, Kroemer G. Cancer despite immunosurveillance: Immunoselection and immunosubversion. Nature Reviews. Immunology. 2006;**6**(10):715-727

[43] Gardner A, Ruffell B. Dendritic cells and cancer immunity. Trends in Immunology. 2016;**37**(12):855-865

[44] Steinman RM. Decisions about dendritic cells: Past, present, and future. Annual Review of Immunology. 2012;**30**:1-22

[45] Steinman RM, Inaba K, Turley S, Pierre P, Mellman I. Antigen capture, processing, and presentation by dendritic cells: Recent cell biological studies. Human Immunology. 1999;**60**(7):562-567

[46] Segura E, Amigorena S. Cross-presentation in mouse and human dendritic cells. Advances in Immunology. 2015;**127**:1-31

[47] Gottfried E, Kreutz M, Mackensen A. Tumor-induced modulation of dendritic cell function. Cytokine & Growth Factor Reviews. 2008;**19**(1):65-77

[48] Chen X, Shao Q, Hao S, Zhao Z, Wang Y, Guo X, et al. CTLA-4 positive breast cancer cells suppress dendritic cells maturation and function. Oncotarget. 2017;**8**(8):13703-13715

[49] Ruffell B, Chang-Strachan D, Chan V, Rosenbusch A, Ho CMT, Pryer N, et al. Macrophage IL-10 blocks CD8(+) T cell-dependent responses to chemotherapy by suppressing IL-12 expression in Intratumoral dendritic cells. Cancer Cell. 2014;**26**(5):623-637

[50] Buisseret L, Desmedt C, Garaud S, Fornili M, Wang X, Van den Eyden G, et al. Reliability of tumor-infiltrating lymphocyte and tertiary lymphoid structure assessment in human breast cancer. Modern Pathology: An Official Journal of the United States and Canadian Academy of Pathology, Inc. 2017;**30**(9):1204-1212

[51] Thompson ED, Enriquez HL, Fu YX, Engelhard VH. Tumor masses support naive T cell infiltration, activation, and differentiation into effectors. The Journal of Experimental Medicine. 2010;**207**(8):1791-1804

[52] Houghton AM. The paradox of tumor-associated neutrophils fueling tumor growth with cytotoxic substances. Cell Cycle. 2010;**9**(9):1732-1737

[53] Brinkmann V, Reichard U, Goosmann C, Fauler B, Uhlemann Y, Weiss DS, et al. Neutrophil extracellular traps kill bacteria. Science. 2004;**303**(5663):1532-1535

[54] Kolaczkowska E, Kubes P. Neutrophil recruitment and function in health and inflammation. Nature Reviews. Immunology. 2013;**13**(3):159-175

[55] Pham CTN. Neutrophil serine proteases: Specific regulators of inflammation. Nature Reviews. Immunology. 2006;**6**(7):541-550

[56] Garley M, Jablonska E, Dabrowska D. NETs in cancer. Tumor Biology. 2016;**37**(11):14355-14361

[57] Treffers LW, Hiemstra IH, Kuijpers TW, van den Berg TK, Matlung HL. Neutrophils in cancer. Immunological Reviews. 2016;**273**(1):312-328

[58] Park J, Wysocki RW, Amoozgar Z, Maiorino L, Fein MR, Jorns J, et al. Cancer cells induce metastasis-supporting neutrophil extracellular DNA traps. Science Translational Medicine. 2016;**8**(361):1-21

[59] Wels J, Kaplan RN, Rafii S, Lyden D. Migratory neighbors and distant invaders: Tumor-associated niche cells. Genes & Development. 2008;**22**(5):559-574

[60] Kato M, Kephart GM, Talley NJ, Wagner JM, Sarr MG, Bonno M, et al. Eosinophil infiltration and degranulation in normal human tissue. The Anatomical Record. 1998;**252**(3):418-425

[61] Akuthota P, Wang HB, Weller PF. Eosinophils as antigen-presenting cells in allergic upper airway disease. Current Opinion in Allergy and Clinical Immunology. 2010;**10**(1):14-19

[62] Hamed EA, Zakhary MM, Maximous DW. Apoptosis, angiogenesis, inflammation, and oxidative stress: Basic interactions in patients with early and metastatic breast cancer. Journal of Cancer Research and Clinical Oncology. 2012;**138**(6):999-1009

[63] Snoussia K, Mahfoudha W, Bouaouinaac N, Ahmedd SB, Helalb AN, Chouchane L. Genetic variation in IL-8 associated with increased risk and poor prognosis of breast carcinoma. Human Immunology. 2006;**67**(1-2):13-21

[64] Kamel M, Shouman S, El-Merzebany M, Kilic G, Veenstra T, Saeed M et al. Effect of tumour necrosis factor-alpha on estrogen metabolic pathways in breast cancer cells. Journal of Cancer. 2012;**3**:310-321

[65] Sanderson CJ. Interleukin-5, eosinophils, and disease. Blood. 1992;**79**(12):3101-3109

[66] Grencis RK, Bancroft AJ. Interleukin-13—A key mediator in resistance to gastrointestinal-dwelling nematode parasites. Clinical Reviews in Allergy and Immunology. 2004;**26**(1):51-60

[67] Srabovic N, Mujagic Z, Mujanovic-Mustedanagic J, Muminovic Z, Softic A, Begic L. Interleukin 13 expression in the primary breast cancer tumour tissue. Biochemia Medica. 2011;**21**(2):131-138

[68] Humphreys RC, Hennighausen L. Transforming growth factor alpha and mouse models of human breast cancer. Oncogene. 2000;**19**(8):1085-1091

[69] Esquivel-Velazquez M, Ostoa-Saloma P, Palacios-Arreola MI, Nava-Castro KE, Castro JI, Morales-Montor J. The role of cytokines in breast cancer development and progression. Journal of Interferon and Cytokine Research. 2015;**35**(1):1-16

[70] Hennig R, Ding XZ, Tong WG, Schneider MB, Standop J, Friess H et al. 5-Lipoxygenase and leukotriene B(4) receptor are expressed in human pancreatic cancers but not in pancreatic ducts in normal tissue. The American Journal of Pathology. 2002;**161**(2):421-428

[71] Wang D, Dubois RN. Eicosanoids and cancer. Nature Reviews Cancer. 2010;**10**(3):181-193

[72] Wang D, Dubois RN. Cyclooxygenase-2: A potential target in breast cancer. Seminars in Oncology. 2004;**31**(1 Suppl 3):64-73

[73] Sobolesky PM, Halushka PV, Garrett-Mayer E, Smith MT, Moussa O. Regulation of the tumor suppressor FOXO3 by the thromboxane-A2 receptors in urothelial cancer. PLoS One. 2014;**9**(9):e107530

[74] Wang Z, Cheng Q, Tang K, Sun Y, Zhang K, Zhang Y, et al. Lipid mediator lipoxin A4 inhibits tumor growth by targeting IL-10-producing regulatory B (Breg) cells. Cancer Letters. 2015;**364**(2):118-124

[75] Rothenberg ME, Hogan SP. The eosinophil. The Annual Review of Immunology. 2006;**24**:147-174

[76] Gatault S, Legrand F, Delbeke M, Loiseau S, Capron M. Involvement of eosinophils in the anti-tumor response. Cancer Immunology, Immunotherapy. 2012;**61**(9):1527-1534

[77] De Lima PO, Dos Santos FV, Oliveira DT, De Figueredo RC, Pereira MC. Effect of eosinophil cationic protein on human oral squamous carcinoma cell viability. Molecular and Clinical Oncology. 2015;**3**(2):353-356

[78] Kubo H, Loegering DA, Adolphson CR, Gleich GJ. Cytotoxic properties of eosinophil granule major basic protein for tumor cells. International Archives of Allergy and Immunology. 1999;**118**(2-4):426-428

[79] Sakkal S, Miller S, Apostolopoulos V, Nurgali K. Eosinophils in cancer: Favourable or unfavourable? Current Medicinal Chemistry. 2016;**23**(7):650-666

[80] Davis BP, Rothenberg ME. Eosinophils and cancer. Cancer Immunology Research. 2014;**2**(1):1-8

[81] Wu W, Samoszuk MK, Comhair SA, Thomassen MJ, Farver CF, Dweik RA, et al. Eosinophils generate brominating oxidants in allergen-induced asthma. The Journal of Clinical Investigation. 2000;**105**(10):1455-1463

[82] Samoszuk M, Sholly S, Epstein AL. Eosinophil peroxidase is detectable with a monoclonal antibody in collagen bands of nodular sclerosis Hodgkin's disease. Laboratory Investigation. 1987;**56**(4):394-400

[83] Gouon-Evans V, Lin EY, Pollard JW. Requirement of macrophages and eosinophils and their cytokines/chemokines for mammary gland development. Breast Cancer Research. 2002;**4**(4):155-164

[84] Galli SJ, Borregaard N, Wynn TA. Phenotypic and functional plasticity of cells of innate immunity: Macrophages, mast cells and neutrophils. Nature Immunology. 2011;**12**(11):1035-1044

[85] Mekori YA, Hershko AY, Frossi B, Mion F, Pucillo CE. Integrating innate and adaptive immune cells: Mast cells as crossroads between regulatory and effector B and T cells. European Journal of Pharmacology. 2016;**778**:84-89

[86] Della Rovere F, Granata A, Monaco M, Basile G. Phagocytosis of cancer cells by mast cells in breast Cancer. Anticancer Research. 2009;**29**(8):3157-3161

[87] Kambayashi T, Allenspach EJ, Chang JT, Zou T, Shoag JE, Reiner SL, et al. Inducible MHC class II expression by mast cells supports effector and regulatory T cell activation. Journal of Immunology. 2009;**182**(8):4686-4695

[88] Stelekati E, Bahri R, D'Orlando O, Orinska Z, Mittrucker HW, Langenhaun R, et al. Mast cell-mediated antigen presentation regulates CD8(+) T cell effector functions. Immunity. 2009;**31**(4):665-676

[89] Khan MM, Strober S, Melmon KL. Regulatory effects of mast-cells on lymphoid-cells—The role of histamine Type-1 receptors in the interaction between mast-cells, helper T-cells and natural suppressor cells. Cellular Immunology. 1986;**103**(1):41-53

[90] Nakae S, Suto H, Kakurai M, Sedgwick JD, Tsai M, Galli SJ. Mast cells enhance T cell activation: Importance of mast cell-derived TNF. Proceedings of the National Academy of Sciences of The United States of America. 2005;**102**(18):6467-6472

[91] Faustino-Rocha AI, Gama A, Oliveira PA, Katrien VE, Saunders JH, Pires MJ, et al. Modulation of mammary tumor vascularization by mast cells: Ultrasonographic and histopathological approaches. Life Sciences. 2017;**176**:35-41

[92] Xiang M, Gu Y, Zhao F, Lu H, Chen S, Yin L. Mast cell tryptase promotes breast cancer migration and invasion. Oncology Reports. 2010;**23**(3):615-619

[93] Kankkunen JP, HArvima IT, Naukkarinen A. Quantitative analysis of tryptase and chymase containing mast cells in benign and malignant breast lesions. International Journal of Cancer. 1997;**72**(3):385-388

[94] Qian BZ, Pollard JW. Macrophage diversity enhances tumor progression and metastasis. Cell. 2010;**141**(1):39-51

[95] Zhao X, Qu J, Sun Y, Wang J, Liu X, Wang F, et al. Prognostic significance of tumor-associated macrophages in breast cancer: A meta-analysis of the literature. Oncotarget. 2017;**8**(18):30576-30586

[96] Wu P, Wu D, Zhao L, Huang L, Chen G, Shen G, et al. Inverse role of distinct subsets and distribution of macrophage in lung cancer prognosis: A meta-analysis. Oncotarget. 2016;**7**(26):40451-40460

[97] Noy R, Pollard JW. Tumor-associated macrophages: From mechanisms to therapy. Immunity. 2014;**41**(1):49-61

[98] Mantovani A, Biswas SK, Galdiero MR, Sica A, Locati M. Macrophage plasticity and polarization in tissue repair and remodelling. The Journal of Pathology. 2013;**229**(2):176-185

[99] Lodoen MB, Lanier LL. Natural killer cells as an initial defense against pathogens. Current Opinion in Immunology. 2006;**18**(4):391-398

[100] Arase H, Arase N, Saito T. Interferon gamma production by natural killer (NK) cells and NK1.1(+) T cells upon NKR-P1 cross-linking. The Journal of Experimental Medicine. 1996;**183**(5):2391-2396

[101] Mamessier E, Sylvain A, Thibult ML, Houvenaeghel G, Jacquemier J, Castellano R, et al. Human breast cancer cells enhance self tolerance by promoting evasion from NK cell antitumor immunity. The Journal of Clinical Investigation. 2011;**121**(9):3609-3622

[102] Moretta L, Moretta A. Unravelling natural killer cell function: Triggering and inhibitory human NK receptors. The EMBO Journal. 2004;**23**(2):255-259

[103] Madjd Z, Spendlove I, Pinder SE, Ellis IO, Durrant LG. Total loss of MHC class I is an independent indicator of good prognosis in breast cancer. International Journal of Cancer. 2005;**117**(2):248-255

[104] Castriconi R, Cantoni C, Della Chiesa M, Vitale M, Marcenaro E, Conte R, et al. Transforming growth factor beta 1 inhibits expression of NKp30 and NKG2D receptors: Consequences for the NK-mediated killing of dendritic cells. Proceedings of the National Academy of Sciences of the United States of America. 2003;**100**(7):4120-4125

[105] Della Chiesa M, Carlomagno S, Frumento G, Balsamo M, Cantoni C, Conte R, et al. The tryptophan catabolite L-kynurenine inhibits the surface expression of NKp46- and NKG2D-activating receptors and regulates NK-cell function. Blood. 2006;**108**(13):4118-4125

[106] Curtsinger JM, Mescher MF. Inflammatory cytokines as a third signal for T cell activation. Current Opinion in Immunology. 2010;**22**(3):333-340

[107] Kohlhapp FJ, Zloza A. $CD4^+$ T cells. In: Marshall JL, editor. Cancer Therapeutic Targets. New York, NY: Springer, New York; 2017. pp. 117-129

[108] Mescher MF, Agarwal P, Casey KA, Hammerbeck CD, Xiao Z, Curtsinger JM. Molecular basis for checkpoints in the CD8 T cell response: Tolerance versus activation. Seminars in Immunology. 2007;**19**(3):153-161

[109] Gu-Trantien C, Willard-Gallo K. Tumor-infiltrating follicular helper T cells: The new kids on the block. Oncoimmunology. 2013;**2**(10):e26066

[110] Tangye SG, Ma CS, Brink R, Deenick EK. The good, the bad and the ugly—TFH cells in human health and disease. Nature Reviews Immunology. 2013;**13**(6):412-426

[111] Gu-Trantien C, Loi S, Garaud S, Equeter C, Libin M, de Wind A et al. $CD4^+$ follicular helper T cell infiltration predicts breast cancer survival. The Journal of Clinical Investigation. 2013;**123**(7):2873-2892

[112] Gollob JA, Ritz J. CD2-CD58 interaction and the control of T-cell interleukin-12 responsiveness. Adhesion molecules link innate and acquired immunity. Annals of the New York Academy of Sciences. 1996;**795**:71-81

[113] Manetti R, Parronchi P, Giudizi MG, Piccinni MP, Maggi E, Trinchieri G, et al. Natural killer cell stimulatory factor (interleukin 12

[IL-12]) induces T helper type 1 (Th1)-specific immune responses and inhibits the development of IL-4-producing Th cells. The Journal of Experimental Medicine. 1993;**177**(4):1199-1204

[114] Trinchieri G. Interleukin-12: A cytokine produced by antigen-presenting cells with immunoregulatory functions in the generation of T-helper cells type 1 and cytotoxic lymphocytes. Blood. 1994;**84**(12):4008-4027

[115] Malek TR, Castro I. Interleukin-2 receptor signaling: At the interface between tolerance and immunity. Immunity. 2010;**33**(2):153-165

[116] Mosmann TR, Coffman RL. TH1 and TH2 cells: Different patterns of lymphokine secretion lead to different functional properties. Annual Review of Immunology. 1989;**7**:145-173

[117] Pruneri G, Vingiani A, Denkert C. Tumor infiltrating lymphocytes in early breast cancer. Breast (Edinburgh, Scotland). 2018;**37**:207-214

[118] Mahmoud S, Lee A, Ellis I, Green A. CD8(+) T lymphocytes infiltrating breast cancer: A promising new prognostic marker? Oncoimmunology. 2012;**1**(3):364-365

[119] Aspord C, Pedroza-Gonzalez A, Gallegos M, Tindle S, Burton EC, Su D, et al. Breast cancer instructs dendritic cells to prime interleukin 13-secreting $CD4^-$ T cells that facilitate tumor development. The Journal of Experimental Medicine. 2007;**204**(5):1037-1047

[120] Guglani L, Khader SA. Th17 cytokines in mucosal immunity and inflammation. Current Opinion in HIV and AIDS. 2010;**5**(2):120-127

[121] Zhu J, Paul WE. Peripheral $CD4^+$ T-cell differentiation regulated by networks of cytokines and transcription factors. Immunological Reviews. 2010;**238**(1):247-262

[122] Ye J, Livergood RS, Peng G. The role and regulation of human Th17 cells in tumor immunity. The American Journal of Pathology. 2013;**182**(1):10-20

[123] Josefowicz SZ, Lu L-F, Rudensky AY. Regulatory T cells: Mechanisms of differentiation and function. Annual Review of Immunology. 2012;**30**:531-564

[124] Sather BD, Treuting P, Perdue N, Miazgowicz M, Fontenot JD, Rudensky AY, et al. Altering the distribution of Foxp3(+) regulatory T cells results in tissue-specific inflammatory disease. The Journal of Experimental Medicine. 2007;**204**(6):1335-1347

[125] Khor B, Regulatory T. Cells: Central concepts from ontogeny to therapy. Transfusion Medicine Reviews. 2017;**31**(1):36-44

[126] Vignali DAA, Collison LW, Workman CJ. How regulatory T cells work. Nature Reviews. Immunology. 2008;**8**(7):523-532

[127] Hamidullah CB, Konwar R. Role of interleukin-10 in breast cancer. Breast Cancer Research and Treatment. 2012;**133**(1):11-21

[128] Saraiva M, O'Garra A. The regulation of IL-10 production by immune cells. Nature Reviews. Immunology. 2010;**10**(3):170-181

[129] Trandem K, Zhao J, Fleming E, Perlman S. Highly activated cytotoxic CD8 T cells express protective IL-10 at the peak of coronavirus-induced encephalitis. Journal of Immunology. 2011;**186**(6):3642-3652

[130] Curtsinger JM, Lins DC, Mescher MF. Signal 3 determines tolerance versus full activation of naive

CD8 T cells: Dissociating proliferation and development of effector function. The Journal of Experimental Medicine. 2003;**197**(9):1141-1151

[131] Varn FS, Mullins DW, Arias-Pulido H, Fiering S, Cheng C. Adaptive immunity programmes in breast cancer. Immunology. 2017;**150**(1):25-34

[132] Zhang N, Bevan MJ. CD8(+) T cells: Foot soldiers of the immune system. Immunity. 2011;**35**(2):161-168

[133] Maimela NR, Liu S, Zhang Y. Fates of $CD8^+$ T cells in tumor microenvironment. Computational and Structural Biotechnology Journal. 2019;**17**:1-13

[134] Tugues S, Burkhard SH, Ohs I, Vrohlings M, Nussbaum K, Vom Berg J, et al. New insights into IL-12-mediated tumor suppression. Cell Death and Differentiation. 2015;**22**(2):237-246

[135] Schietinger A, Greenberg PD. Tolerance and exhaustion: Defining mechanisms of T cell dysfunction. Trends in Immunology. 2014;**35**(2):51-60

[136] Pipkin ME, Sacks JA, Cruz-Guilloty F, Lichtenheld MG, Bevan MJ, Rao A. Interleukin-2 and inflammation induce distinct transcriptional programs that promote the differentiation of effector cytolytic T cells. Immunity. 2010;**32**(1):79-90

[137] Yang SX, Wei WS, Ouyan QW, Jiang QH, Zou YF, Qu W, et al. Interleukin-12 activated CD8(+) T cells induces apoptosis in breast cancer cells and reduces tumor growth. Biomedicine & pharmacotherapy = Biomedecine & Pharmacotherapie. 2016;**84**:1466-1471

[138] Ali HR, Provenzano E, Dawson SJ, Blows FM, Liu B, Shah M, et al. Association between $CD8^+$ T-cell infiltration and breast cancer survival in 12,439 patients. Annals of Oncology: Official Journal of the European Society for Medical Oncology. 2014;**25**(8):1536-1543

[139] Nava-Castro KE, Palacios-Arreola MI, Ostoa-Saloma P, Muñiz-Hernández S, Cerbón MA, Gomez-Icazbalceta G, et al. The immunoendocrine network in breast cancer. Advances in Neuroimmune Biology. 2014;**5**(2):109-131

[140] Brisken C, Park S, Vass T, Lydon JP, O'Malley BW, Weinberg RA. A paracrine role for the epithelial progesterone receptor in mammary gland development. Proceedings of the National Academy of Sciences of the United States of America. 1998;**95**(9):5076-5081

[141] Pelletier G, El-Alfy M. Immunocytochemical localization of estrogen receptors alpha and beta in the human reproductive organs. The Journal of Clinical Endocrinology and Metabolism. 2000;**85**(12):4835-4840

[142] Mallepell S, Krust A, Chambon P, Brisken C. Paracrine signaling through the epithelial estrogen receptor alpha is required for proliferation and morphogenesis in the mammary gland. Proceedings of the National Academy of Sciences of the United States of America. 2006;**103**(7):2196-2201

[143] Hall JM, McDonnell DP. The estrogen receptor beta-isoform (ERbeta) of the human estrogen receptor modulates ERalpha transcriptional activity and is a key regulator of the cellular response to estrogens and antiestrogens. Endocrinology. 1999;**140**(12):5566-5578

[144] Coriano CG, Liu F, Sievers CK, Liang M, Wang Y, Lim Y, et al. A computational-based approach to identify estrogen receptor alpha/beta heterodimer selective ligands. Molecular Pharmacology. 2018;**93**(3):197-207

[145] Khan D, Ansar AS. The immune system is a natural target for estrogen action: Opposing effects of estrogen in two prototypical autoimmune diseases. Frontiers in Immunology. 2015;**6**:635

[146] Osborne CK, Schiff R, Fuqua SA, Shou J. Estrogen receptor: Current understanding of its activation and modulation. Clinical Cancer Research. 2001;**7**(12 Suppl):4338s-4342s; discussion 411s-412s

[147] Nemere I, Pietras RJ, Blackmore PF. Membrane receptors for steroid hormones: Signal transduction and physiological significance. Journal of Cellular Biochemistry. 2003;**88**(3):438-445

[148] Scarpin KM, Graham JD, Mote PA, Clarke CL. Progesterone action in human tissues: Regulation by progesterone receptor (PR) isoform expression, nuclear positioning and coregulator expression. Nuclear Receptor Signaling. 2009;**7**:e009-e

[149] Clarke RB, Spence K, Anderson E, Howell A, Okano H, Potten CS. A putative human breast stem cell population is enriched for steroid receptor-positive cells. Developmental Biology. 2005;**277**(2):443-456

[150] Fox EM, Davis RJ, Shupnik MA. ERbeta in breast cancer—Onlooker, passive player, or active protector? Steroids. 2008;**73**(11):1039-1051

[151] Shibuya R, Suzuki T, Miki Y, Yoshida K, Moriya T, Ono K, et al. Intratumoral concentration of sex steroids and expression of sex steroid-producing enzymes in ductal carcinoma in situ of human breast. Endocrine-Related Cancer. 2008;**15**(1):113-124

[152] Sasano H, Harada N. Intratumoral aromatase in human breast, endometrial, and ovarian malignancies. Endocrine Reviews. 1998;**19**(5):593-607

[153] Dimitrakakis C, Bondy C. Androgens and the breast. Breast Cancer Research: BCR. 2009;**11**(5):212

[154] Yeh S, Hu YC, Wang PH, Xie C, Xu Q, Tsai MY, et al. Abnormal mammary gland development and growth retardation in female mice and MCF7 breast cancer cells lacking androgen receptor. The Journal of Experimental Medicine. 2003;**198**(12):1899-1908

[155] Vera-Badillo FE, Templeton AJ, de Gouveia P, Diaz-Padilla I, Bedard PL, Al-Mubarak M, et al. Androgen receptor expression and outcomes in early breast cancer: A systematic review and meta-analysis. Journal of the National Cancer Institute. 2014;**106**(1):djt319

[156] Spurdle AB, Antoniou AC, Duffy DL, Pandeya N, Kelemen L, Chen X, et al. The androgen receptor CAG repeat polymorphism and modification of breast cancer risk in BRCA1 and BRCA2 mutation carriers. Breast Cancer Research. 2005;**7**(2):R176-R183

[157] Labrie F, Belanger A, Luu-The V, Labrie C, Simard J, Cusan L, et al. DHEA and the intracrine formation of androgens and estrogens in peripheral target tissues: Its role during aging. Steroids. 1998;**63**(5-6):322-328

[158] Oberbeck R, Kobbe P. Dehydroepiandrosterone (DHEA): A steroid with multiple effects. Is there any possible option in the treatment of critical illness? Current Medicinal Chemistry. 2010;**17**(11):1039-1047

[159] Shaak TL, Wijesinghe DS, Chalfant CE, Diegelmann RF, Ward KR, Loria RM. Structural stereochemistry of androstene hormones determines interactions with human androgen, estrogen, and glucocorticoid receptors. International Journal of Medicinal Chemistry. 2013;**2013**:203606

[160] Lopez-Marure R, Contreras PG, Dillon JS. Effects of

dehydroepiandrosterone on proliferation, migration, and death of breast cancer cells. European Journal of Pharmacology. 2011;**660**(2-3):268-274

[161] Nakai A, Hayano Y, Furuta F, Noda M, Suzuki K. Control of lymphocyte egress from lymph nodes through beta2-adrenergic receptors. The Journal of Experimental Medicine. 2014;**211**(13):2583-2598

[162] Luker KE, Luker GD. Functions of CXCL12 and CXCR4 in breast cancer. Cancer Letters. 2006;**238**(1):30-41

[163] Dayer R, Babashah S, Jamshidi S, Sadeghizadeh M. Upregulation of CXC chemokine receptor 4-CXC chemokine ligand 12 axis ininvasive breast carcinoma: A potent biomarker predicting lymph node metastasis. Journal of Cancer Research and Therapeutics. 2018;**14**(2):345-350

[164] Li YM, Pan Y, Wei Y, Cheng X, Zhou BP, Tan M, et al. Upregulation of CXCR4 is essential for HER2-mediated tumor metastasis. Cancer Cell. 2004;6(5):459-469

[165] Mukherjee D, Zhao J. The role of chemokine receptor CXCR4 in breast cancer metastasis. American Journal of Cancer Research. 2013;**3**(1):46-57

[166] Palacios-Arreola MI, Nava-Castro KE, Castro JI, Garcia-Zepeda E, Carrero JC, Morales-Montor J. The role of chemokines in breast cancer pathology and its possible use as therapeutic targets. Journal of Immunology Research. 2014;**2014**:849720

[167] Herve J, Dubreil L, Tardif V, Terme M, Pogu S, Anegon I, et al. beta2-Adrenoreceptor agonist inhibits antigen cross-presentation by dendritic cells. Journal of Immunology. 2013;**190**(7):3163-3171

[168] Panina-Bordignon P, Mazzeo D, Lucia PD, D'Ambrosio D, Lang R, Fabbri L, et al. Beta2-agonists prevent Th1 development by selective inhibition of interleukin 12. The Journal of Clinical Investigation. 1997;**100**(6):1513-1519

[169] Abdi K, Singh NJ, Matzinger P. Lipopolysaccharide-activated dendritic cells: "exhausted" or alert and waiting? Journal of immunology (Baltimore, MD: 1950). 2012;**188**(12):5981-5989

[170] Ben-Eliyahu S, Shakhar G, Shakhar K, Melamed R. Timing within the oestrous cycle modulates adrenergic suppression of NK activity and resistance to metastasis: Possible clinical implications. British Journal of Cancer. 2000;**83**(12):1747-1754

[171] Scanzano A, Cosentino M. Adrenergic regulation of innate immunity: A review. Frontiers in Pharmacology. 2015;**6**:171

[172] Hollmen M, Karaman S, Schwager S, Lisibach A, Christiansen A, Maksimow M, et al. G-CSF regulates macrophage phenotype and associates with poor overall survival in human triple-negative breast cancer. Scandinavian Journal of Immunology. 2016;**83**(5):373-374

[173] Shi M, Liu D, Duan H, Qian L, Wang L, Niu L, et al. The beta2-adrenergic receptor and Her2 comprise a positive feedback loop in human breast cancer cells. Breast Cancer Research and Treatment. 2011;**125**(2):351-362

[174] Plitas G, Konopacki C, Wu K, Bos PD, Morrow M, Putintseva EV, et al. Regulatory T cells exhibit distinct features in human breast cancer. Immunity. 2016;**45**(5):1122-1134

8.6 Participación como colaboradora en otros artículos.

Del Río-Araiza Víctor H, Palacios-Arreola Margarita I., Nava-Castro Karen E, Pérez-Sánchez Nashla Y, **Ruiz-Manzano Rocío A**, Segovia-Mendoza Mariana, Girón-Pérez Manuel Iván, Navidad-Murrieta Migdalia Sarahy, and Jorge Morales-Montor. (2020). Perinatal exposure to bisphenol A increases in the adulthood of the offspring the susceptibility to the human parasite *Toxocara canis*. Environmental Research 184: 109381.

Environmental Research 184 (2020) 109381

Contents lists available at ScienceDirect

Environmental Research

journal homepage: www.elsevier.com/locate/envres

Perinatal exposure to bisphenol A increases in the adulthood of the offspring the susceptibility to the human parasite *Toxocara canis*

Víctor H. Del Río-Araiza[a], Margarita I. Palacios-Arreola[b], Karen E. Nava-Castro[b], Nashla Y. Pérez-Sánchez[c], Rocío Ruíz-Manzano[c], Mariana Segovia-Mendoza[c], Manuel Iván Girón-Pérez[d,e], Migdalia Sarahy Navidad-Murrieta[e], Jorge Morales-Montor[c,*]

[a] Departamento de Parasitología, Facultad de Medicina Veterinaria y Zootecnia, Universidad Nacional Autónoma de México, CP 04510, Ciudad de México, Mexico
[b] Departamento de Ciencias Ambientales, Laboratorio de Genotoxicología y Mutagénesis Ambientales, Centro de Ciencias de la Atmósfera, Universidad Nacional Autónoma de México, CP 04510, Ciudad de México, Mexico
[c] Departamento de Inmunología, Instituto de Investigaciones Biomédicas, Universidad Nacional Autónoma de México, CP 04510, Ciudad de México, Mexico
[d] Universidad Autónoma de Nayarit, Secretaría de Investigación y Posgrado, Laboratorio de Inmunotoxicología, Cd. de la Cultura s/n, Tepic, Nayarit, Mexico
[e] Centro Nayarita de Innovación y Transferencia de Tecnología, Unidad Especializada Laboratorio Nacional para la Investigación en Inocuidad Alimentaria (LANIIA-Unidad Nayarit), Calle Tres s/n, Tepic, Nayarit, Mexico

ARTICLE INFO

Keywords:
Bisphenol A
Perinatal exposure
Immune response
Toxocara canis
immunopathology

ABSTRACT

Bisphenol A, a very widespread environmental pollutant and endocrine disruptor compound, can interact with several steroid receptors, particularly with estrogen ones. In different studies, it has observed that the endocrine disruption during critical periods of development can trigger alterations in the immune response during the adult life. Male Wistar rats were exposed indirectly to BPA at a dose of 250 μg/kg day during the perinatal period (from day 5 of pregnancy until day 21 postnatal), At the 60 days of age, the adulthood, animals were infected with larvated eggs of the *Toxocara canis*, and were sacrificed at 7 days post-infection. Parasitic loads in the lung and in the liver were analyzed by artificial digestion. Furthermore, immune cell subpopulations (macrophages, NK cells, Tγδ, total T cells, T helper, T cytotoxic, and B lymphocytes) present in spleen, peripheral and mesenteric lymph nodes were analyzed by flow cytometry. The expression of Th1 and Th2 cytokines at the splenic level was determined by real-time quantitative PCR. Finally, the titers of specific antibodies against to the parasite were analyzed by ELISA. The BPA treatment administrated in the perinatally stage favors a significant increase of the percentage of *Toxocara canis* larvae in the lungs and liver in the adulthood. Additionally, the exposure to this compound caused a dramatically decrease in the production of specific antibodies against to this parasite, downregulating together Th2 cytokines (IL-4, IL-5 and IL-13), meanwhile upregulated Th1 cytokines (IFN-γ and TNF-α). Perinatal exposure to BPA affects the performance of the immune response during adult life, modifying both cytokines and antibodies production by these cells, which favors the susceptibility to infections, specifically toxocariosis.

1. Introduction

Communication between endocrine and immune system maintenances a bidirectional complex network through the interaction of their main soluble factors (hormones and cytokines). It has been described that both systems jointly act during an infectious process for the adequate pathogens elimination and homeostasis maintenance in the organism (Besedovsky and Del Rey, 1996). In addition, several compounds, known as Endocrine Disrupting Compounds (EDCs), present in the environment can interfere with the synthesis, metabolism, secretion, mechanism of action, and elimination of endogenous hormones (Diamanti-Kandarakis et al., 2009). Particularly, Bisphenol A (BPA) is cataloged as EDC with oestrogenic character because it can bind to nuclear estrogen receptors (ER) but with low affinity (< 1000) than the natural ligand, 17β-estradiol(E_2) (Kuiper et al., 1998; Matthews et al., 2001). In addition, it also binds to other hormone receptors such as arylhydrocarbon receptor (AhR) (Bonefeld-Jørgensen et al., 2007) thyroid hormone (ThR), among others (Zoeller et al., 2005). Moreover, due to its highly lipophilic character, BPA can be stored for prolonged periods of time in adipose tissue or it can be transfused to the fetus in a trans-placentally way or by lactogenic route (Guzmán-Arriaga and Zambrano, 2007; Ikezuki et al., 2002; Vandenberg et al., 2010). BPA is

* Corresponding author.
E-mail addresses: jmontor66@biomedicas.unam.mx, jmontor66@hotmail.com (J. Morales-Montor).

https://doi.org/10.1016/j.envres.2020.109381
Received 16 May 2019; Received in revised form 26 February 2020; Accepted 10 March 2020

commonly used in the plastics manufacture, epoxy resins and dental sealants (Amaral Mendes, 2002). The Food and Drug Administration (FDA) and the European Food Safety Agency (EFSA) calculated the tolerable daily intake of BPA at 50 μg/kg/day (Agency and Environmental Protection Agency, 2011).

Different studies have reported the BPA effects on the immune system function, however, they lack of uniformity, in other words; all of them vary depending on the *in vivo* or *in vitro* model in which they were performed, the animal species used, doses and route of administration, even, the stage of the development in which it was administrated. Of note, many *in vivo* studies have not considered that the function of the immune response must be studied under some antigenic challenge, whereby there is little information about the effects that BPA might have on the immune system during an infectious process.

On the other hand, Toxocariasis is an important medical-veterinary disease that has as definitive hosts to Canidae family members. *T. canis* can be a paratenic hosts in a large number of mammals, including humans. In addition, it is considered one of the zoonoses with a greater distribution in the world, due to the wide coexistence that the humans and domestic dogs or cats have. (Despommier, 2003). However, there are no studies that demonstrate whether environmental factors, such as BPA, might be influencing the progression of this disease.

Therefore, we decided to evaluate the effect of perinatal exposure to BPA in the immune response during adulthood using a rat model infected with *T. canis* as antigenic challenge.

2. Materials and methods

2.1. Animals and ethics statement

Male Wistar rats around 8-weeks-old, sons of female's exposed to normal water, vehicle (Vhc) or BPA were used for the experiments, they were obtained from the bioterium of the Instituto de Investigaciones Biomédicas, Universidad Nacional Autónoma de México. The animals were organized into 6 groups and allocated in polycarbonate boxes (50 cm l x 23 cm w x 21 cm h). The groups were distributed as follows: a) rats born to untreated control mothers (Unt-Ctrl $n = 6$), b) rats born to untreated infected mothers (Unt-Infx $n = 7$), c) rats born to vehicle control mothers (Vhc-Ctrl $n = 6$), d) rats born to vehicle infected mothers (Vhc-Infx $n = 6$), e) rats born to BPA control mothers (BPA-Ctrl $n = 5$) and f) rats born to BPA infected mothers (BPA-Infx $n = 5$). Animals were kept in cycles of 12 h light/darkness. Water and food were provided *ad libitum* in sterile conditions. Animal care and experiments were constantly evaluated and approved by both Institute's Animal Care and Use Committee, (Comité de Cuidado y Uso de Animales de Experimentación, CICUAL, permit number 201–2016) follow the official Mexican regulations (NOM-062-ZOO-1999), which are in accordance with the recommendations of the Guide for the Care and Use of Laboratory Animals of the National Institute of Health (NIH) of the USA, to ensure compliance with established international regulations and guidelines.

2.2. Experimental design

Female rats were placed in the presence of a one male with a separation grid for 72 h (male effect), for leading the synchronization process. Subsequently, the male was joined to the females and vaginal swabs were performed daily at mornings. Of note, once found sperms presence in the vaginal smear was considered as the first day of gestation. After that, females were administrated with Vhc or BPA, started at day 5 of gestation and continued until whole lactation (21 days). The treatments were administrated in the drinking water, on glass drinking bowls at a dose of 250 μg/kg. Previous to infection, the inoculum was washed three times to eliminate the PBS/formaldehyde solution. Eggs were then resuspended in PBS and concentrated to 1000 embryonated eggs per ml. Infection was performed by intragastric administration using a type Foley metallic probe inoculating 1000 Embryonated Eggs (EE) per rat at 8 weeks of age. The rats were euthanized at 7 days post-infection by overdose of anesthesia with sevoflurane (Sevorane®).

2.3. Perinatal BPA exposure

BPA exposure was started once the pregnant status of the females was confirmed (≈11th day of gestation). BPA was added to their drinking water in glass drinking fountains and placed for consumption by the animals until weaning. Water containers were changed every third day to administer a dose of 250 μg/weight/day. Same amount of ethanol (25 μL) was added to the drinking water of the vehicle group while control animals received just water.

2.4. Serum obtention

After rats were euthanized, blood was collected in a Vacutainer tube (Becton Dickinson). After collection of the whole blood, blood was allowed to clot by leaving it undisturbed at room temperature during 3 min. The clot was removed by centrifuging at $2000 \times g$ for 10 min in a refrigerated centrifuge. Following centrifugation, the serum was immediately transfer into a clean glass tube using a Pasteur pipette. The samples were maintained at −4 °C while handling. If the serum was not analyzed immediately, it was apportioned into 0.5 ml aliquots, and stored at −20 °C or lower. Samples never undergo freeze-thaw cycles, because this is detrimental to many serum components.

2.5. Bisphenol-A serum levels

Serum samples were obtaines as previously described. After that, we performed a simple mass organic protocol extraction from serum (Larralde et al., 1995). The Bisphenol A (BPA) serum samples were reconstituted in 500 μL metanol-HPLC grade (Sigma-Aldrich), and analyzed using a UPLC-MS/MS system Acquity serie H (Waters, Milford, USA) with a triple quadrupole mass spectrometer Xevo TQ-S (Waters, Milford, USA). Each sample was automatically injected through a Sample Manager system– FTN Acquity de Waters (Waters, Milford, USA). A column Acquity UPLC BEH C_{18} 1.7 μm, 2.1 × 50 mm was used. A s the reference compound, Bisphenol A (purity 97% of CAS number 80-50-7) was obtained from Sigma- Aldrich Company and dissolved in pure methanol HPLC-grade (Sigma-Aldrich) at a concentration of 1 mg/ml.

2.6. Harvest and processing of T. canis eggs

T. canis eggs were obtained from adult parasites donated by Centro de Control Canino de Cuautitlán, Estado de México. Worm females were separated, rinsed in tap water and placed in phosphate buffer (PBS) with a pH around 7.2–7.4. Afterwards, the uteri of them were collected through incision in the first third of the body and placed in physiological saline solution. Eggs were obtained using a fine pore filter. The ova were washed several times in PBS and centrifuged at 3250 g/5 min. Finally, the eggs from pellet were resuspended in a PBS/2% formaldehyde solution and incubated at 27 °C for 28 days to obtain the infective form (EE) of the parasite.

2.7. Larvae recovery

After euthanasia, tissue samples from lungs were taken for histopathology. Then, lungs and liver of infected animals were weighted and macerated; tissue was digested in artificial gastric juice [1% pepsin (250 units/mg, SIGMA®) and 1% HCl 37%. pH: 2.0 (10 ml of artificial gastric juice/1 gr of tissue)] for 24 h. Samples were centrifuged at 791 g/5 min, and the pellet was resuspended in 1 ml 4% paraformaldehyde. Parasite counting involved 10 counts per 20 μl sample, total number of larvae was multiplied x 50 to calculate the number of

larvae per ml and therefore the number of larvae per gram of tissue.

2.8. Histopathology

Prior to maceration, in order to obtain the number of larvae, tissue samples of (4 × 4x4 mm = 0.6 mm^3) were taken from lung and liver of all groups of infected animals. Histological sections of 4 μm thickness were performed, sections were mounted in slides previously treated with acid and alcohol and 1:10 Poly-L-lysine solution; samples were stained with hematoxylin/eosin and observed under the microscope at 20x amplification.

2.9. Flow cytometry assays

Spleen, peripheric (PLN) and mesenteric (MLN) lymphatic nodes were collected at the time of sacrifice and were disaggregated using a sterile nylon mesh (70 μm) and a syringe plunge in PBS pH at 4 °C. Cell suspension was centrifuged at 182 g/3 min, decanted and resuspended in 500 μl of erythrocyte lysis buffer (spleen only), incubated for 10 min at room temperature; 700 μl of FACS buffer was added followed by centrifugation at 182 g/3 min. Then, cells were resuspended in 500 μl FACS buffer, and a total of 25 μl was pipetted and cells were fixed with 4% paraformaldehyde for 10 min/37 °C in a 96-well plate, then centrifuged at 127 g/5 min and washed with 200 μl FACS buffer. 150 μl of absolute methanol was added and they were incubated for 10 min/4 °C. Plate was centrifuged again at 506 g/3 min, and washed with 200 μl FACS buffer; 150 μl of primary antibody solution was added to the corresponding wells and incubated for 10 min/4 °C. After incubation, following primary antibodies were selected: AF 488 anti-rat CD3 (Biolegend. Clone 1F4), PE/Cy5 Mouse anti-rat CD4 (BD bioscience. Clone Ox-35), PE Mouse anti-rat CD8α (BD bioscience. Clone Ox-8), PE anti-rat CD45RA (Biolegend. Clone Ox-33), PE anti-rat TCRγδ (Biolegend. Clone V65), AF647 anti-rat CD161 (Biolegend. Clone 10/78) and anti-rat CD11b/c-biotin (Biolegend Clone Ox-42) + PE/Cy5 Streptavidin (Biolegend). Cells were washed with 150 μl FACS buffer after incubation, resuspended in 200 μl of FACS buffer and stored at 4 °C in the dark. Data analysis was performed using the software FlowJo v10.0.

2.10. Real-time quantitative PCR

Determination of the mRNA expression levels of Th1 (IL-1β, IL-6, TNF-α and IFN-γ) and Th2 cytokines (IL-4, IL-5, IL- 9, IL-13) was performed by real-time quantitative PCR. Splenic tissue samples were frozen in TRIzol® reagent (Ambion, RNA, Carlsband CA) at the time of sacrifice. The RNA was extracted with the same reagent, following the manufacturer's protocol. Firstly, the samples were transferred to sterile glass tubes containing 500 μl of TRIzol® and homogenization of the samples was carried out in the Polytron (all this was done at 4 °C). Subsequently, the homogenate was transferred to a new tube to which 200 μl of phenol-chloroform and 200 μl of water were added with diethylpyrocarbonate (H_2O DEPC), stirred for 30 s and centrifuged at 13,000 rpm for 15 min at 4 °C. The aqueous phase was recovered (contains the RNA) and transferred to a new tube. 200 μl of cold chloroform was added for each milliliter of recovered aqueous phase, the sample was shaken again and centrifuged at 13,000 rpm for 15 min at 4 °C. Again, the aqueous phase was recovered and transferred to a new tube, where cold isopropanol was added in a 1:1 ratio. It was stirred by inversion and left at 4 °C overnight to carry out the precipitation of the RNA. In addition, next day the samples were centrifuged at 13,000 rpm for 15 min at 4 °C, the supernatant was decanted, being very careful not to remove the pellet and this was washed with 1 ml of ethanol (EtOH) at 75% cold. The sample was stirred until the pellet was removed and centrifuged at 13,000 rpm for 15 min at 4 °C, the supernatant was decanted again and centrifuged at 13,000 rpm for 1 min at 4 °C in order to remove the remaining EtOH with a pipette. Subsequently, the pellet was allowed to dry at room temperature until it took a translucent color and then it was resuspended in 30 μl of H_2O DEPC, 7 μl was taken to make the quantification of the RNA and the integrity gel. The concentration of RNA was determined by absorbance at 260 nm, and the whole was verified after electrophoresis in 1% agarose gel. The RNA samples were immediately reverse transcribed, using the reverse transcriptase enzyme MMLV-RT (Promega, Madison WI) to obtain the complementary DNA (cDNA) at a concentration of 5 μg/μl. To determine mRNA levels by real-time PCR, fluorogenic assays were performed using the LightCycler 480 SYBR Green I Master reagent (Roche Applied Scinece, Mannheim, Germany). Fluorescence was detected in the LightCycler 480 Instrument (Roche Applied Science, Mannheim, Germany, Operator's Manual Software Version 1.5). The level of expression for each gene was determined in triplicate using 113 ng of the cDNA and the pair of oligos for each gene in Optical 96 LightCycler 480 Multiwell Plates 96/384 clear well plates (Roche Applied Science, Mannheim, Germany), using 18s and cyclophilin as constitutive controls. The sequence of oligos sense and antisense that were used are presented in Table 1. For the PCR amplification the following scheme was used: 50 °C for 2 min, 95 °C for 10 min, and 45 cycles of 94 °C for 15 s followed by 60 °C for 1 min. The relative expression was evaluated in comparison with the reference genes 18s and cyclophilin, based on the following equation:

$$\frac{(Gene\ of\ interest)CT1(Conl - X)}{\sqrt{E\ Constitutive\ Gen\ 1})CT2(Ctrl - X) \times (E\ Constitutive\ Gen\ 2)CT2(Ctrl - X)}$$

Table 1
Oligonucleotide sequences used for RT-PCR. Primers were designed based on sequenced mouse genes from the Gene Databank (NCBI, NIH).

Gen	Oligo sense	Oligo antisense
IL-1β	TGCCCGTGGAGCTTCCAGGAT	CCAGCTGCAGGGTGGGTGTG
IL-6	CACTTCACAAGTCGGAGGCT	AGCACACTAGGTTTGCCGAG
TNF-α	TCCAGGCGGTGTCTGTGCCT	TCGGGGCAGCCTTGTCCCTT
IFN-γ	ACGCCGCGTCTTGGTTTTGC	TCAGCACCGACTCCTTTTCCGC
IL-4	TCCACGGATGTAACGACAGC	TCATTCACGGTGCAGCTTCT
IL-5	GAGCAATGAGACGATGAGGCT	CTCATCACGCCAAGGAACTCT
IL-9	TGCCAACGTGACCAGCTGCT	GCCTGCTGTGGTCTGGTTGCACG
IL-13	TATCGAGGAGCTGAGCAACATCA	ATAAACTGGGCTACTTCGAT

2.11. TES-Ag purification

Toxocara excretion-secretion antigens (TES-Ag) were obtained by culturing the *T. canis* larvae according to the method described by Savigny (de Savigny, 1975), and modified by Bowman (Bowman et al., 1987). Purity and integrity of excretion and secretion antigens was determined by SDS-PAGE and Coomassie staining. Protein content was quantified by Bradford method (Bradford, 1976).

2.12. Quantification of proteins by the bradford method

Different TES-Ag dilutions were performed in PBS and mixed with Bradford reagent. The protein concentration was determined by comparing the optical density (O.D.) of the sample in a standard curve (10, 20, 40, 60, 80 and 100 μg/ml) made with bovine serum albumin (SIGMA®). The concentration of total antigens obtained in the test was 282.65 μg/ml.

2.13. T. canis specific IgG determination

For the determination of specific antibodies, 96 well flat bottom polystyrene plates (Maxisorp, NUNC Labs) were sensitized with 1 μg/ml TES-Ag for 24 h at 4 °C. Subsequently, the plates were washed three times with 0.01% PBS-Tween 20, blocked with 3% bovine serum

albumin (BSA) and stored at 4 °C for 24 h. After the blocking time, the plates were washed three times with PBS-Tween 20 at 0.01% and stored at 4 °C. For each sample, 50 μl per well was used in duplicate at a 1:200 dilution of the serum with PBS, and incubated at 37 °C for 2 h. After this period, the plates were washed three times with PBS-Tween 20 at 0.01%, and 50 μl of rat IgG conjugate well dilution of 1:1000 (Peroxidase-conjugated AffiniPure Goat Anti-Rat IgG (H + L)) was added to each well and were placed in incubation at 37 °C for 1 h. The plates were washed 5 times with the same solution (PBS-Tween 20 at 0.01%) and color development was performed with 0.05% o-phenylenediamine (OPD) and 0.001% hydrogen peroxide in citrate buffer. The plates were incubated for 15 min in total darkness at 37 °C and then 50 μl per well of 0.06% orthophosphoric acid were added. The plates were read at 492 nm with 15 s of agitation in the ELISA reader (Stat Facs 4200).

2.14. Statistical analysis

Data from 2 to 3 independent experiments are charted as mean average ± standard deviation (SD). Results are presented in bar graphs, describing the mean average and standard deviation and analyzed with Prism V 7.0® software (GraphPad Software Inc). The general experimental design considers 2 independent variables: perinatal exposure (Untreated, vehicle of BPA) and infection (Control or *T.canis* infection). The data regarding parasite charges (larval recovery) only consider the infection variable. These values were evaluated by 2-way ANOVA and Bonferroni multiple comparison between all groups. A significant difference was considered when $p < 0.05$.

3. Results

3.1. Determination of BPA levels

Serum levels of BPA were measured in all the groups of animals euthanized. It was important to check on that, so we can make sure that our changes in immunity are due to BPA treatment. In Fig. 1, it is clear that, although all animals have baseline levels of BPA, only the sons of the mothers treated with BPA, have an increase of six-fold compared to control or vehicle groups in their serum levels (Fig. 1).

Serum levels of BPA by HPLC coupled to mass spectrometry in all experimental groups. The data represents the mean average (± SD). Letters (A, B) show significant differences ($p < 0.05$) due to treatment (Vhc or BPA). Ctrl: Uninfected rats, Infx: Infected rats, Unt: Untreated rats, Vhc: Rats exposed to vehicle, BPA: Rats exposed to Bisphenol A.

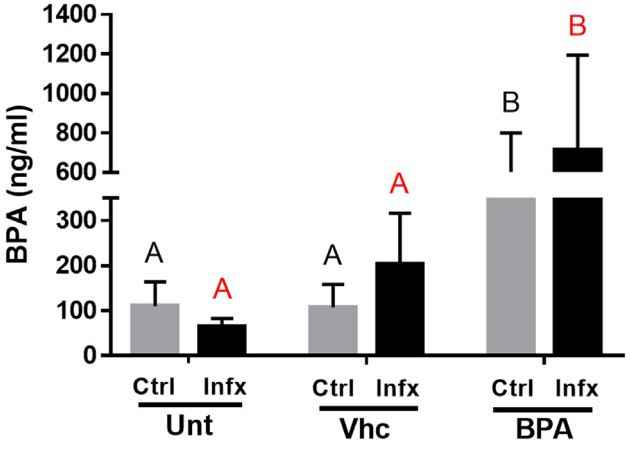

Fig. 1. BPA serum levels.

3.2. Larval recovery and inflammatory process in lung and liver

In order to determine the effect of the perinatal BPA administration in the susceptibility to *T. canis* infection, parasitic loads in the lungs and in the liver were evaluated (Fig. 2). Interestingly, animals exposed perinatally to this compound had a significantly susceptibility to develop *T. canis* infection, as it is judged by the increased number of larvae found in both organs. Accordingly, other studies have reported the migration of the eggs of this parasite to both organs, we found a greater number of larvae in both, being 31% and 24% more larvae in the lungs and in the liver, respectively as compared to Unt Infx and Vch Infx (Fig. 2. *I* and *II*).

Male rats born to untreated or vehicle or BPA treated mothers and subsequently were infected with the parasite *T. canis*. (*I*) Larvae number in the lungs, (*II*) Larvae number in the liver. Bars represent the mean ± SD of Unt Infx; Untreated infected rats, Vhc Infx; infected rats exposed to vehicle perinatally and BPA Infx; infected rats exposed to BPA perinatally ($n = 7$). ***$P < 0.001$.

On the other hand, perinatal administration of BPA caused severe and notorious gross lesions in both sites, observed at macroscopic level; this effect was barely observed in the Unt Infx and Vch Infx groups (Fig. 3A–F). In regard to changes in the lungs at the microscopic level, peribronchial and perivascular necrotic areas with an accumulation of inflammatory cells were observed in all groups due to the infection process. However, a greater presence of mononuclear cells, neutrophils, and eosinophils in the alveolar interstitium, as well as the loss of structural integrity, were mostly observed in the BPA group (Fig. 3 G-I). Moreover, at hepatic level, small foci of inflammatory infiltrate were observed at the perivascular and periportal level, being larger in size and extension in the rats exposed to BPA, compared against to control groups (Fig. 3 J-L).

Yellow arrows in lung, and yellow contour in liver indicate the presence of lesions caused by *T. canis*. (A) Untreated infected lung, (B) Vehicle infected lung, (C) BPA infected lung, (D) Untreated infected liver, (E) Vehicle infected liver, (F) BPA infected liver, (G) H-E 20X Untreated infected lung, (H) H-E 20X Vehicle infected lung, (I) H-E 20X BPA infected lung, (J) H-E 20X Untreated infected liver, (K) H-E 20X Vehicle infected liver and (L) H-E 20X BPA infected liver.

3.3. Immune cell subpopulation

3.3.1. Innate immune cells

Fig. 4 shows the percentages of the innate immunity cells analyzed (Mφ, NK and TγδL) in spleen, PLN and MLN. The analysis at the splenic level allows us to evaluate a systemic response. This analysis is important, because the larvae of the parasite migrate through the different organs and tissues. As can be seen, there is an increase in the percentage of Mφ both due to a treatment in both the Vhc Ctrl group and the BPA Ctrl ($P < 0.05$) (Fig. 4 I). In NK cells, see the same pattern, increases in treatment in the Vhc Infx and BPA Infx groups, while in animals without infection only this increase is observed in the BPA Ctrl group ($P < 0.05$) (Fig. 4 II). As for TγδL, an increase in the percentage caused by Vhc can be observed in the Ctrl and Infx groups ($P < 0.05$) (Fig. 4 III).

In the analysis of PLN and MLN, we can evaluate the immune response in a regional manner. In PLN, no significant changes were observed in the percentages of the subpopulations analyzed ($P > 0.05$) (Fig. 4 IV-VI).

Finally, in the MLN shows an increase in the percentage of Mφ due to infection ($P < 0.01$), but at the time of some of the treatments (Vhc or BPA) this increase is not significant ($P > 0.05$) (Fig. 4 VII). In NK cells, only a decrease in the percentage of treatment was observed in the BPA Infx group ($P < 0.05$) (Fig. 4 VIII). In TγδL only one difference due to infection was observed in the Vhc groups ($P < 0.05$) (Fig. 4 IX).

Flow cytometry assays were performed to determine the percentage of Mφ (CD11b/c+), NK cells (CD161+) and TγδL (TCRγδ+) in the

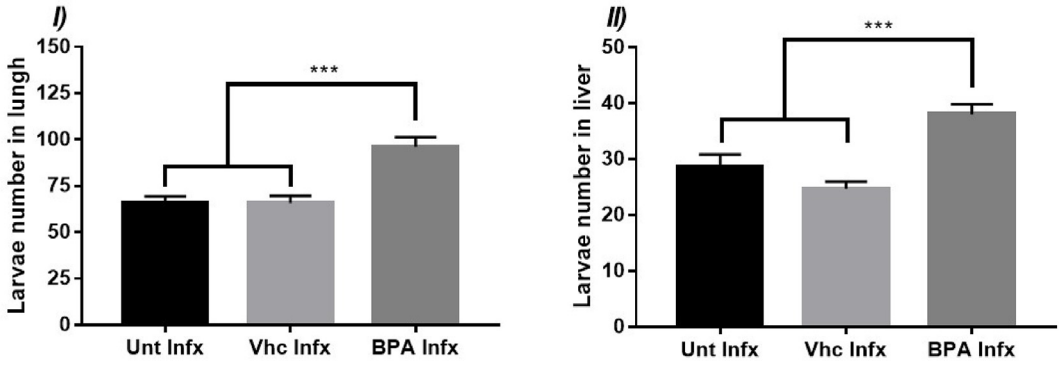

Fig. 2. Larvae number of *T. canis* in the lungs and in the liver.

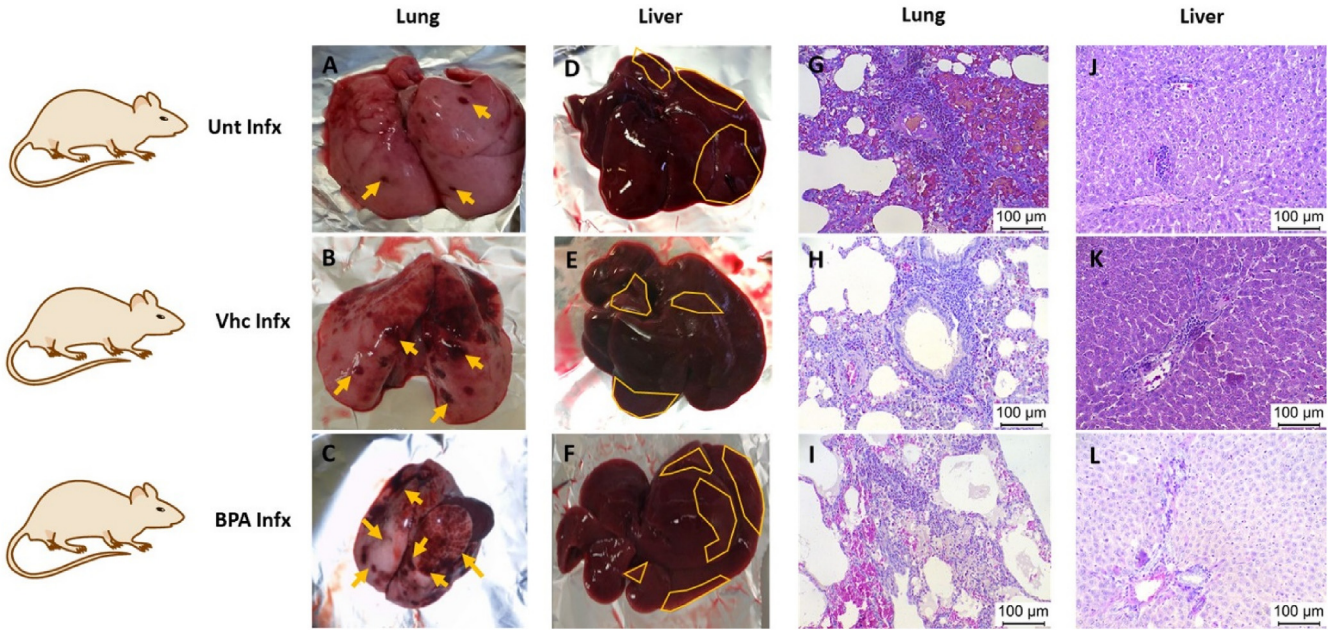

Fig. 3. Macroscopic and microscopic lesions in the lungs and in the liver of *T. canis* infected rats exposed perinatally to BPA.

spleen (*I, II, III*), Peripheric Lymph Nodes (PLN) (*IV, V, VI*) and Mesenteric Lymph Nodes (MLN) (*VII, VIII, IX*), from control and infected rats exposed perinatally to vehicle or BPA. The data represents the mean average (± SD). Significant differences due to infection status (*p < 0.05, **p < 0.01). Letters (A, B) show significant differences (p < 0.05) due to treatment (Vhc or BPA). Ctrl: Uninfected rats, Infx: Infected rats, Unt: Untreated rats, Vhc: Rats exposed to vehicle, BPA: Rats exposed to Bisphenol A.

3.3.2. Adaptative immune cells subpopulations

Fig. 5 shows the percentage of LT subpopulations (total T cells, ThL and TcL) analyzed in spleen, PLN and MLN.

In the spleen, there is an increase in the percentage of total LT due to treatment in both groups (Vhc and BPA). This increase in the percentage is independent of the infection (P < 0.05) (Fig. 5 I). In the case of the ThL and TcL, there is no difference in the percentage of these cells (P > 0.05) (Fig. 5 II, III).

In PLN, there is an increase in the percentage of total T cells due to treatment in the Vhc Ctrl and BPA Ctrl groups (P < 0.05), while within the BPA groups there is a decrease in the percentage in this subpopulation due to the infection (P < 0.05) (Fig. 5 IV). In the ThL, no significant differences were found (P > 0.05) (Fig. 5 V), while the TcL showed an increase in the percentage due to treatment in the animals exposed to BPA infected (P < 0.05) (Fig. 5 VI).

In the MLN, no differences due to infection or treatment were observed in the percentages of total T cells and ThL (P > 0.05) (Fig. 5 VII, VIII), however, in TcL there is an increase in the percentage due to infection in the Vhc groups (P < 0.001), in addition to an increase due to treatment in the Vhc Infx group compared to the Unt Infx group (P < 0.05) (Fig. 5 IX).

Finally, any change in the percentages of B Lymphocytes (BL) in all of compartments analyzed due to infection was observed (Fig. 6 *I-III*). Of note, only a decrease in the percentage of this population was observed in BPA and Ctrl group compared to the Unt Ctrl group in MLN (Fig. 6 III).

3.4. Gene expression analysis of Th1/Th2 cytokines in the spleen

Having not found a significant and direct modulation in the immune cell percentages, we proceeded to evaluate if the humoral response could be involved in the promotion of the infectious process with *T. canis* after BPA treatment. For this purpose, gene expression of Th1 (IL-1β, IL-6, TNF-α and IFN-γ) and Th2 (IL-4, IL-5, IL-9 and IL-13) cytokines at the splenic level was evaluated (Figs. 7 and 8). Regarding the expression of Th1 cytokines, it was observed that there were no changes in the gene expression of IL-1β (Fig. 7 *I*). However, the expression of IL-6 was increased due to infection in the Unt and BPA groups (Fig. 7 *II*). Besides, in the case of TNF-α, and IFN-γ expression, the results showed

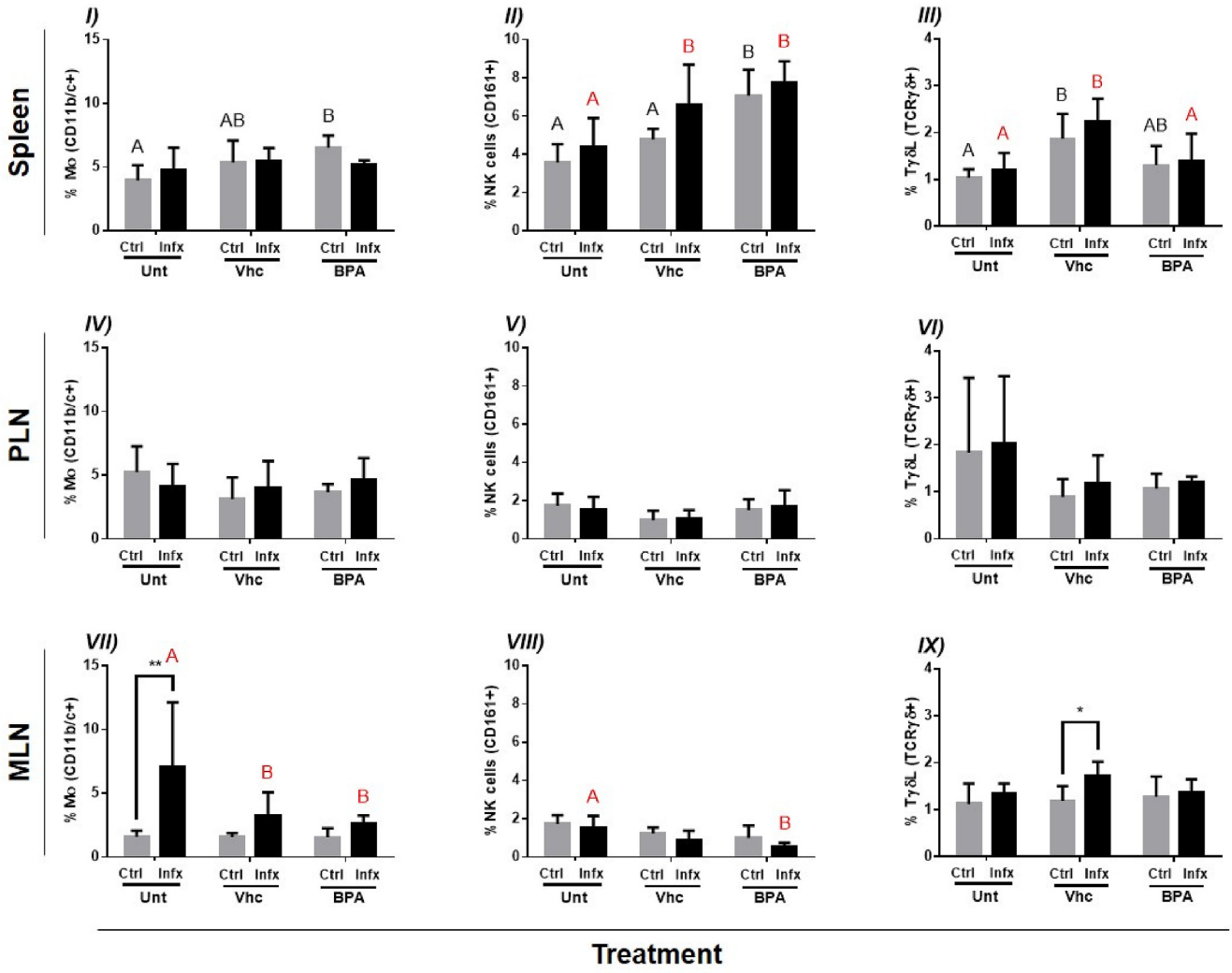

Fig. 4. Innate immune cells subpopulations.

a significant increase of both cytokines due to infection in the group exposed perinatally to BPA (Fig. 7 *III*, *IV*).

In addition, changes in Th2 cytokines expression were observed due to infection and treatment. IL-4 and IL-5 expression were upregulated due to the infection in the Unt and Vhc groups (Fig. 8 *I*, *II*). On contrast, in the BPA group, this effect was not observed. In the case of IL-13 expression, there was an increase of its levels due to the infection in the Unt and Vhc groups, and in the same way, the BPA group did not present any change of it. (Fig. 8 *III*). For IL-9 expression there were any significant difference (Fig. 8 *IV*).

3.5. Anti-T. canis antibodies production

As it is reported, the production of antibodies is essential to counteract infections caused by helminths. In this sense, the levels of specific antibodies against to *T. canis* parasite were evaluated in the serum (Fig. 9). The results show that in control experimental groups, *T. canis* infection caused an increase in the specific antibody production titers. Conversely, in the BPA group there was a dramatically decrease of antibody presence, around to 50% less than in control groups (Fig. 9).

4. Discussion

In the present work, we evaluated the effect of endocrine disruption with BPA during a critical period of development, the perinatal phase and the relationship between this disruption process and the changes on the immune response during adult life in rats infected with an important medical-veterinary parasite, *T. canis*.

It is known that during critical periods of development, formation of lymphoid organs, hematopoiesis and immune system maturation is crucial. In addition, different studies have observed that the surgical removal of the thymus of 2–4 days postnatal, as well as the treatment with ciclosporin at this age, trigger alterations in the development of LT-mediated adaptive immunity (Classen, 1998; Sakaguchi et al., 1982). Furthermore, only one study have reported that the endocrine disruption during these periods has an effect on the immune response and the susceptibility to infections during the adult stage (Guzmán et al., 2009).

As it was mentioned before, EDCs are ubiquitous compounds, their exposure occurs during the all life. However, its effects of endocrine disruption into the immune context in early stages have not been deeply studied. In line with that, the aim of this work was to indagate how BPA treatment can modulate the immune response to favor or block the susceptibility to a specific disease. For this purpose, we analyzed 3 main points: a) number of parasitic loads after BPA treatment, which reflect the susceptibility to *T. canis* infection, b) evaluation of different immune cell population at a systemic and local level, and c) evaluation of the polarization of Th1/Th2 response, as well as the humoral implications determining the antibodies production. We choose a male rat model for avoiding the estrous cycles and variation of hormones levels

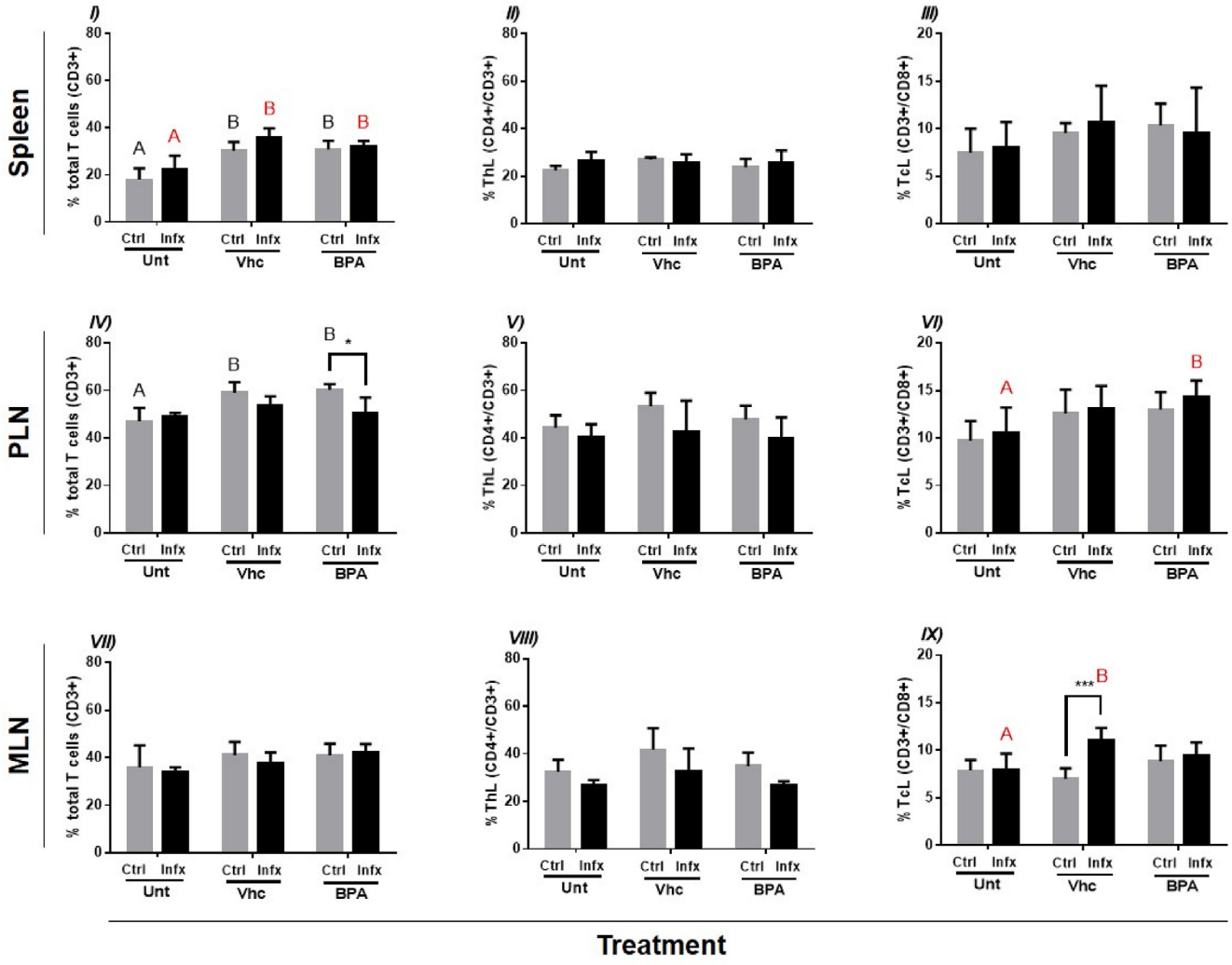

Fig. 5. Adaptive immune cells subpopulations. Flow cytometry assays corresponding of the percentage of Total T cells ($CD3^+$), ThL (CD4 + /CD3 +) and TcL (CD3 + / CD8 +) in spleen (*I, II, III*), Peripheric Lymph Nodes (PLN) (*IV, V, VI*) and Mesenteric Lymph Nodes (MLN) (*VII, VIII, IX*), from control and infected rats exposed to vehicle or BPA perinatally. The data represents the mean average (± SD). Significant differences due to infection status (*p < 0.05, ***p < 0.001). Letters (A, B) show significant differences (p < 0.05) due to treatment (Vhc or BPA). Ctrl: Uninfected rats, Infx: Infected rats, Unt: Untreated rats, Vhc: Rats exposed to vehicle, BPA: Rats exposed to Bisphenol A.

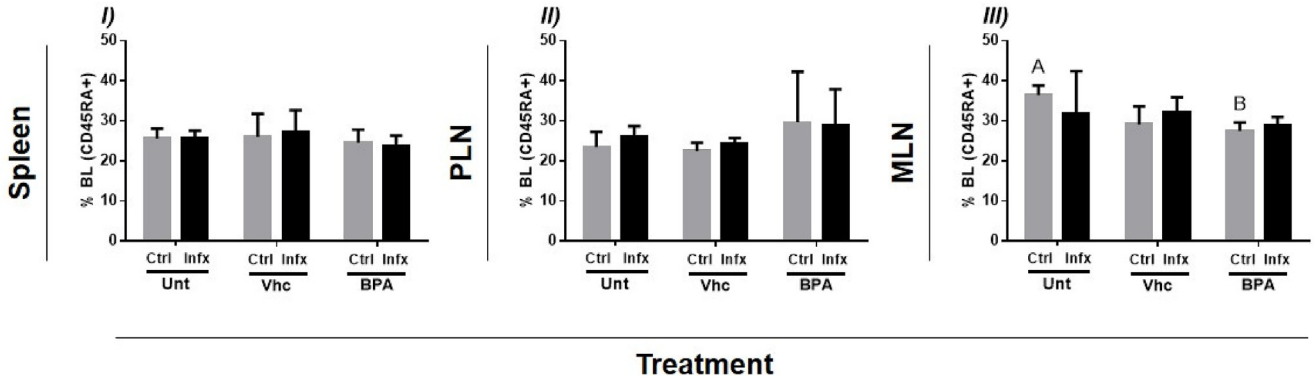

Fig. 6. Flow cytometry assay corresponding of the percentage of BL (CD45RA +) in spleen (*I*), Peripheric Lymph Nodes (PLN) (*II*) and Mesenteric Lymph Nodes (MLN) (*III*), from control and infected rats exposed to vehicle or BPA perinatally in control and infected male rats without treatment (Unt) or exposed to vehicle (Vhc) or Bisphenol A (BPA) perinatally, without infection (Ctrl) or infected (Infx) with *T. canis*. The data represents the mean average (± SD). Letters (A, B) show significant differences (p < 0.05) due to treatment (Vhc or BPA). Ctrl: Uninfected rats, Infx: Infected rats, Unt: Untreated rats, Vhc: Rats exposed to vehicle, BPA: Rats exposed to Bisphenol A. The data represents the mean average (± SD). Letters (A, B) show significant differences (p < 0.05) due to treatment (Vhc or BPA). Ctrl: Uninfected rats, Infx: Infected rats, Unt: Untreated rats, Vhc: Rats exposed to vehicle, BPA: Rats exposed to Bisphenol A.

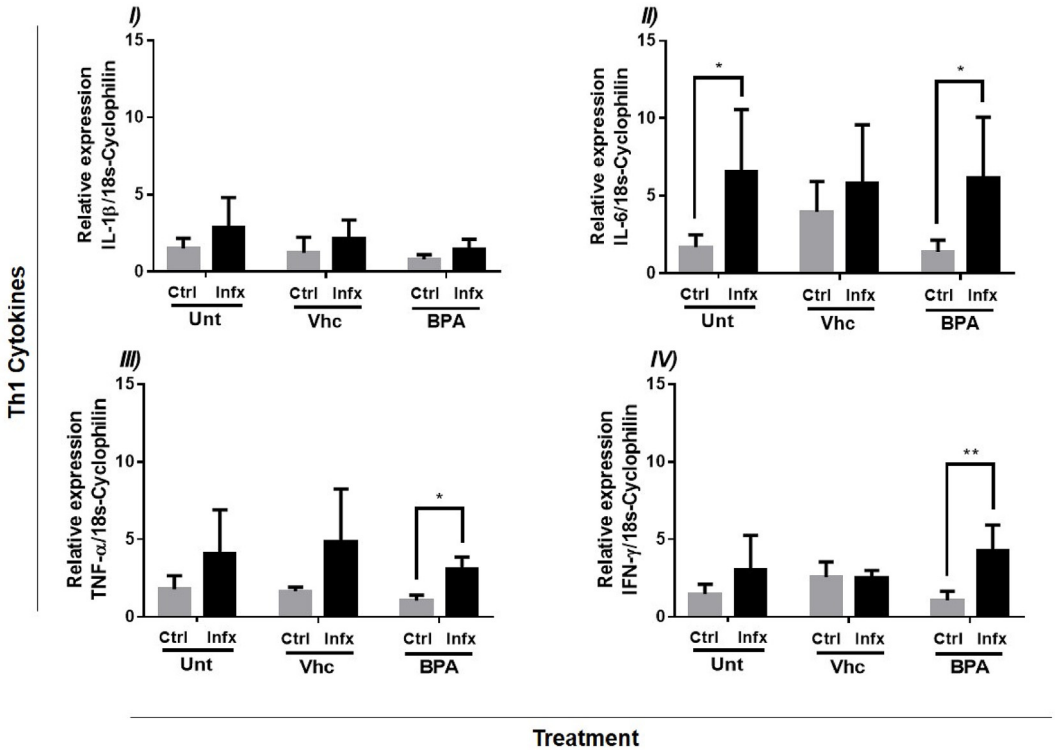

Fig. 7. Real-time PCR assay. Relative expression of Th1 cytokines in the spleen from male rats without treatment (Unt) or exposed to vehicle (Vhc) or Bisphenol A (BPA) perinatally, without infection (Ctrl) or infected (Infx) with *T. canis*. *I*) IL-1β, *II*) IL-6, *III*) TNF-α and *IV*) IFN-γ. The data represents the mean average (± SD). Significant differences due to infection status (*p < 0.05, **p < 0.01). Ctrl: Uninfected rats, Infx: Infected rats, Unt: Untreated rats, Vhc: Rats exposed to vehicle, BPA: Rats exposed to Bisphenol A.

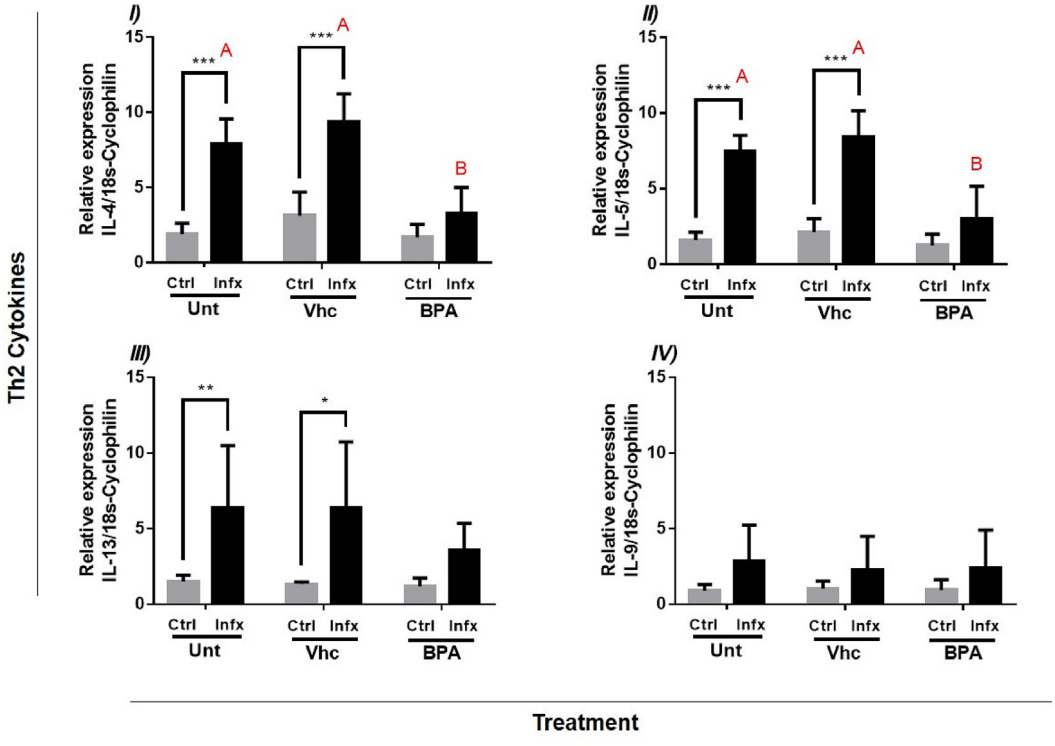

Fig. 8. Real-time PCR assay. Relative expression of Th2 cytokines in the spleen from male rats without treatment (Unt) or exposed to vehicle (Vhc) or Bisphenol A (BPA) perinatally, without infection (Ctrl) or infected (Infx) with *T. canis*. *I*) IL-4, *II*) IL-5, *III*) IL-13 and *IV*) IL-9. The data represents the mean average (± SD). Significant differences due to infection status (*p < 0.05, **p < 0.01). Letters (A, B) show significant differences (p < 0.05) due to treatment (Vhc or BPA). Ctrl: Uninfected rats, Infx: Infected rats, Unt: Untreated rats, Vhc: Rats exposed to vehicle, BPA: Rats exposed to Bisphenol A.

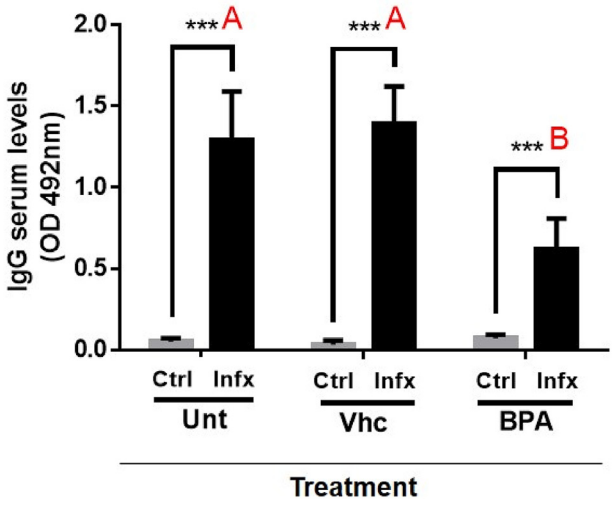

Fig. 9. Specific anti-*T. canis* antibody titration in control and infected male rats without treatment (Unt) or exposed to vehicle (Vhc) or Bisphenol A (BPA) perinatally, without infection (Ctrl) or infected (Infx) with *T. canis*. The data represents the mean average (± SD). Significant differences due to infection status (***$p < 0.001$). Letters (A, B) show significant differences ($p < 0.05$) due to treatment (Vhc or BPA). Ctrl: Uninfected rats, Infx: Infected rats, Unt: Untreated rats, Vhc: Rats exposed to vehicle, BPA: Rats exposed to Bisphenol A.

present in females.

The results showed that perinatal exposure to BPA in male rats generated a significant increase in the larvae number in the adulthood at pulmonary (31%) at a liver (24%) level as compared with non-BPA treated groups. In this respect, there are only two reports that have evaluated the perinatal exposure to BPA and the susceptibility to infections caused by helminths. Both of them differ in terms of the antigenic challenge used, the dose and scheme of BPA exposure, and the time of infection. First, our findings are similar to those reported by Menard et al., who reported an increase of *N. brasiliensis* living larvae in the intestine of the offspring of female rats perinatally administered with a low dose of BPA (5 μg/kg/day) in the water drink from day 15 of gestation, until the moment of weaning. Their scheme was performed by 25 days of age (Ménard et al., 2014). On contrary, Tian et al. reported a decrease in susceptibility to infection by *T. spiralis* at 40 days post-infection when a single dose of BPA (228μg/animal) was administered 2 h after infection in the adult life in male mice (Tian et al., 2003). However, both studies did not determine the modulation of a complete panel of different immune cells. In line with that, we decided to analyze the changes in the percentages of innate or adaptative cells in different lymphoid organs such as the spleen, the PLN and MLN, due to these sites are considered as important targets for the migration of this parasite. With respect to changes in the percentages of innate immune cells (Mφ, NK, and Tγδ lymphocytes); small differences were observed in the three proposed organs; a similar tendency was observed in the adaptive immunity cellsn (total T cells, ThL, TcL, and BL) in the animals that were exposed to BPA. Of note, the most relevant change occurred at the splenic level, where a significant increase in the percentage of total LT was found, although this effect seems to be mediated by the vehicle. Since any significant changes were observed in the immune cell percentages, functional aspects were evaluated, such as the production of different cytokines and specific antibodies.

In this sense, it has been reported that *T. canis* infection generates an immune response mediated by Th2 cells, where production of IL-4, IL-5, IL-6 and IL-13 cytokines is induced by it (Allen and Maizels, 2011; Finkelman et al., 2004; Valli et al., 2010). In addition, in murine models, an up-regulation of IFN-γ levels in plasma has been observed at 7 days post-infection with *T. canis* parasite (Pecinali et al., 2005). The above agrees with our results, where an increase in the expression of Th2 cytokines (IL-4, IL-5 and IL-13) due to *T. canis* infection was observed in control groups. However, perinatal exposure to BPA did not caused an increase in them. Moreover, TNF-α, IL-6, and IFN-γ (TH1 cytokines) also showed an increment due to the infection, nevertheless, only the last protein presented an upregulation in its gene expression in BPA group. We highlight that BPA leads the polarization of immune response into a Th1, which is permissive for the establishment of the parasite.

Finally, we decided to evaluate another mechanism for the control of helminth infections, through of production of specific antibodies against to the parasite. It is known that specific antibodies production is mediated by IL-4 cytokine, which stimulates the proliferation and maturation of BL, the isotype variation from IgM to IgE, and the production of specific IgG antibodies (Allen and Maizels, 2011). In our experiment, it was observed that *T. canis* infection generated an increase in anti-*T. canis* antibodies in control groups. However, perinatal exposure of BPA caused a dramatical reduction in it, decreasing approximately half number of them as compared to the control groups. This decrease might be mediated by IL-4 diminution since this cytokine is considered as one of the main stimuli for the differentiation of LB into plasma cells. In addition, it is worth mentioning that additional mechanism should be studied, for instance, if BPA can act an epigenetic level in different immune populations, its direct effects in the T cell polarization or in B cells differentiation into plasma cells. In addition, different immune aspects such as if BPA can modify the metabolism of the parasite through binding with different steroid receptors should be considered for different studies.

5. Conclusion

These results support the fact that perinatal BPA exposure impairs cytokines and antibody production, turning in a Th1 response in the adult life. The above impacts on the increased susceptibility to intestinal parasitic infection with *T. canis*. This emphasized that the immature immune system at perinatal period is highly sensitive BPA, altering its effector mechanisms in the adult life.

Ethic statement

Animal care and experiments were constantly evaluated and approved by both Institute's Animal Care and Use Committee, (Comité de Cuidado y Uso de Animales de Experimentación, CICUAL, permit number 201–2016) follow the official Mexican regulations (NOM-062-ZOO-1999), which are in accordance with the recommendations of the Guide for the Care and Use of Laboratory Animals of the National Institute of Health (NIH) of the USA, to ensure compliance with established international regulations and guidelines.

CRediT authorship contribution statement

Víctor H. Del Río-Araiza: Data curation, Funding acquisition, Investigation, Project administration, Resources, Software, Supervision, Validation, Visualization, Writing - review & editing, Conceptualization, Methodology, Formal analysis, Writing - original draft. **Margarita I. Palacios-Arreola:** Writing - original draft, Formal analysis, Methodology. **Karen E. Nava-Castro:** Funding acquisition, Formal analysis, Writing - original draft, Data curation, Writing - review & editing. **Nashla Y. Pérez-Sánchez:** Data curation, Investigation, Methodology, Writing - original draft. **Rocío Ruíz-Manzano:** Formal analysis, Funding acquisition, Investigation, Supervision, Validation, Visualization, Writing - review & editing, Writing - original draft. **Mariana Segovia-Mendoza:** Data curation, Investigation, Methodology, Supervision, Validation, Visualization, Formal analysis, Writing - original draft. **Manuel Iván Girón-Pérez:** Methodology, Project administration, Resources, Software, Supervision, Validation, Visualization, Writing - review & editing, Funding acquisition, Writing -

original draft. **Migdalia Sarahy Navidad-Murrieta:** Investigation, Methodology, Writing - review & editing, Writing - original draft. **Jorge Morales-Montor:** Conceptualization, Methodology, Funding acquisition, Formal analysis, Data curation, Investigation, Project administration, Resources, Software, Supervision, Validation, Visualization, Writing - original draft, Writing - review & editing.

Declaration of competing interest

The authors declare that they have no known competing financial interests or personal relationships that could have appeared to influence the work reported in this paper.

Acknowledgments

Financial support: Grant IN-209719 from Programa de Apoyo a Proyectos de Innovación Tecnológica (PAPIIT), Dirección General de Asuntos del Personal Académico (DGAPA), Universidad Nacional Autónoma de México (UNAM) and Grant FC2016-2125 from Fronteras en la Ciencia, Consejo Nacional de Ciencia y Tecnología (CONACYT), both to Jorge Morales-Montor. Grant IA 206220 to Víctor H del Río Araiza, from PAPIIT, DGAPA, UNAM. Grant IA202919 to Karen E Nava-Castro, from PAPIIT, DGAPA, UNAM. Mariana Segovia-Mendoza and Margarita I Palacios-Arreola are recipients of Post-Doctoral fellowships from DGAPA, UNAM. Rocío Ruíz Manzano is a PhD student at Programa de Doctorado en Ciencias Biomédicas, UNAM and has a scholarship from CONACYT (# 270782).

Appendix A. Supplementary data

Supplementary data to this article can be found online at https://doi.org/10.1016/j.envres.2020.109381.

References

Agency, U.S.E.P.,Environmental Protection Agency, 2011. Bisphenol A Action Plan. Environ. Health [WWW Document]. http://en.wikipedia.org/wiki/Bisphenol_A#Environmental_risk%5Cnhttp://www.epa.gov/oppt/existingchemicals/pubs/actionplans/bpa_action_plan.pdf.

Allen, J.E., Maizels, R.M., 2011. Diversity and dialogue in immunity to helminths. Nat. Rev. Immunol. 11, 375–388.

Amaral Mendes, J.J., 2002. The endocrine disrupters: a major medical challenge. Food Chem. Toxicol. 40, 781–788. https://doi.org/10.1016/S0278-6915(02)00018-2.

Besedovsky, H.O., Del Rey, A., 1996. Immune-neuro-endocrine interactions: facts and hypotheses. Endocr. Rev. 17, 64–102. https://doi.org/10.1210/edrv-17-1-64.

Bonefeld-Jørgensen, E.C., Long, M., Hofmeister, M.V., Vinggaard, A.M., 2007. Endocrine-disrupting potential of Bisphenol A, Bisphenol A dimethacrylate, 4-n-nonylphenol, and 4-n-octylphenol in vitro: new data and a brief review. Environ. Health Perspect. 115, 69–76. https://doi.org/10.1289/ehp.9368.

Bowman, D.D., Mika-Grieve, M., Grieve, R.B., 1987. Circulating excretory-secretory antigen levels and specific antibody responses in mice infected with Toxocara canis. Am. J. Trop. Med. Hyg. 36, 75–82.

Bradford, M.M., 1976. A rapid and sensitive method for the quantitation of microgram quantities of protein utilizing the principle of protein-dye binding. Anal. Biochem. 72, 248–254. https://doi.org/10.1016/0003-2697(76)90527-3.

Classen, J.B., 1998. Cyclosporine induced autoimmunity in newborns prevented by early immunization. Autoimmunity 27, 135–139.

de Savigny, D.H., 1975. In vitro maintenance of Toxocara canis larvae and a simple method for the production of Toxocara ES antigen for use in serodiagnostic tests for visceral larva migrans. J. Parasitol. 61, 781–782.

Despommier, D., 2003. Toxocariasis : clinical aspects , epidemiology , medical ecology , and molecular aspects. Society 16, 265–272.

Diamanti-Kandarakis, E., Bourguignon, J.-P., Giudice, L.C., Hauser, R., Prins, G.S., Soto, A.M., Zoeller, R.T., Gore, A.C., 2009. Endocrine-Disrupting chemicals. Endocr. Rev. 30, 293–342.

Finkelman, F.D., Shea-Donohue, T., Morris, S.C., Gildea, L., Strait, R., Madden, K.B., Schopf, L., Urban, J.F., 2004. Interleukin-4- and interleukin-13-mediated host protection against intestinal nematode parasites. Immunol. Rev. 201, 139–155.

Guzmán-Arriaga, C., Zambrano, E., 2007. Endocrine disruptor compounds and their role in the developmental programming of the reproductive axis. Rev. Investig. Clin. 59, 73–81.

Guzmán, C., Camacho-Arroyo, I., De León-Nava, M.A., Morales-Montor, J., 2009. Neonatal exposure to estradiol induces resistance to helminth infection and changes in the expression of sex steroid hormone receptors in the brain and spleen in adult mice of both sexes. Brain Behav. Immun. 23, 709–715. https://doi.org/10.1016/j.bbi.2009.02.014.

Ikezuki, Y., Tsutsumi, O., Takai, Y., Kamei, Y., Taketani, Y., 2002. Determination of bisphenol A concentrations in human biological fluids reveals significant early prenatal exposure. Hum. Reprod. 17, 2839–2841.

Kuiper, G.G., Lemmen, J.G., Carlsson, B., Corton, J.C., Safe, S.H., van der Saag, P.T., van der Burg, B., Gustafsson, J.a., 1998. Interaction of estrogenic chemicals and pytoestrogens with estrogen receptor beta. Endocrinology 139, 4252–4263. https://doi.org/10.1210/endo.139.10.6216.

Larralde, C, Morales, J, Terrazas, I, Romano, MC, 1995. Sex hormone changes induced by the parasite lead to feminization of the male host in murine Taenia crassiceps cysticercosis. Journal of Steroid Biochemistry and Molecular Biology 52 (6), 575–580. https://doi.org/10.1016/0960-0760(95)00062-5.

Matthews, J.B., Twomey, K., Zacharewski, T.R., 2001. In vitro and in vivo interactions of bisphenol A and its metabolite, bisphenol A glucuronide, with estrogen receptors α and β. Chem. Res. Toxicol. 14, 149–157. https://doi.org/10.1021/tx0001833.

Ménard, S., Guzylack-Piriou, L., Lencina, C., Leveque, M., Naturel, M., Sekkal, S., Harkat, C., Gaultier, E., Olier, M., Garcia-Villar, R., Theodorou, V., Houdeau, E., 2014. Perinatal exposure to a low dose of bisphenol a impaired systemic cellular immune response and predisposes young rats to intestinal parasitic infection. PloS One 9, 1–15. https://doi.org/10.1371/journal.pone.0112752.

Pecinali, N.R., Gomes, R.N., Amendoeira, F.C., Bastos, A.C.M.P., Martins, M.J.Q.A., Pegado, C.S., Bastos, O.M.P., Bozza, P.T., Castro-Faria-Neto, H.C., 2005. Influence of murine Toxocara canis infection on plasma and bronchoalveolar lavage fluid eosinophil numbers and its correlation with cytokine levels. Vet. Parasitol. 134, 121–130.

Sakaguchi, S., Takahashi, T., Nishizuka, Y., 1982. Study on cellular events in post-thymectomy autoimmune oophoritis in mice. I. Requirement of Lyt-1 effector cells for oocytes damage after adoptive transfer. J. Exp. Med. 156, 1565–1576.

Tian, X., Takamoto, M., Sugane, K., 2003. Bisphenol A promotes IL-4 production by Th2 cells. Int. Arch. Allergy Immunol. 132, 240–247. https://doi.org/10.1159/000074305.

Valli, J.L., Williamson, A., Sharif, S., Rice, J., Shewen, P.E., 2010. In vitro cytokine responses of peripheral blood mononuclear cells from healthy dogs to distemper virus, Malassezia and Toxocara. Vet. Immunol. Immunopathol. 134, 218–229.

Vandenberg, L.N., Chahoud, I., Heindel, J.J., Padmanabhan, V., Paumgartten, F.J.R., Schoenfelder, G., 2010. Urinary, circulating, and tissue biomonitoring studies indicate widespread exposure to bisphenol A. Environ. Health Perspect. 118, 1055–1070. https://doi.org/10.1289/ehp.0901716.

Zoeller, R.T., Bansal, R., Parris, C., 2005. Bisphenol-A, an environmental contaminant that acts as a thyroid hormone receptor antagonist in vitro, increases serum thyroxine, and alters RC3/neurogranin expression in the developing rat brain. Endocrinology 146, 607–612. https://doi.org/10.1210/en.2004-1018.